HAZELTINE CORPORATION

GREENLAWN, NEW YORK 11740

CONFIDENTIAL

AD 526585

Report 6165

OPERATIONS ANALYSIS OF A MULTISTATIC ECHO-RANGING SYSTEM (U) (FINAL REPORT)

R.A. SHADE
HAZELTINE CORPORATION
GREENLAWN, NEW YORK 11740

ONR CONTRACT N00014-71-C-0311
TASK NUMBER NR364-043/1-29-71 462

December 1972

NAVAL ANALYSIS PROGRAMS
OFFICE OF NAVAL RESEARCH
DEPARTMENT OF THE NAVY
ARLINGTON, VA., 22217

"Distribution limited to U.S. Government agencies only: Test and evaluation, 22 June 1973. Other requests for this document must be referred to Office of Naval Research (Code 462)."

"CONFIDENTIAL classified by Director, Naval Applications and Analysis Division, ONR, subject to General Declassification Schedule of Executive Order 11652, declassified 31 Dec 1978."

"NATIONAL SECURITY INFORMATION

Unauthorized disclosure subject to criminal sanctions."

354

27

HAZELTINE CORPORATION
GREENLAWN, NEW YORK 11740
CONFIDENTIAL

Report 6165

OPERATIONS ANALYSIS OF A MULTISTATIC ECHO-RANGING SYSTEM (U) (FINAL REPORT)

R.A. SHADE
HAZELTINE CORPORATION
GREENLAWN, NEW YORK 11740

ONR CONTRACT N00014-71-C-0311
TASK NUMBER NR364-043/1-29-71 462

December 1972

NAVAL ANALYSIS PROGRAMS
OFFICE OF NAVAL RESEARCH
DEPARTMENT OF THE NAVY
ARLINGTON, VA., 22217

"Distribution limited to U.S. Government agencies only: Test and evaluation, 22 June 1973. Other requests for this document must be referred to Office of Naval Research (Code 462)."

"CONFIDENTIAL classified by Director, Naval Applications and Analysis Division, ONR, subject to General Declassification Schedule of Executive Order 11652, declassified 31 Dec 1978."

"NATIONAL SECURITY INFORMATION
Unauthorized disclosure subject to criminal sanctions."

354

This Page is Unclassified
CONFIDENTIAL

Confidential

Security Classification

DOCUMENT CONTROL DATA - R & D

(Security classification of title, body of abstract and indexing annotation must be entered when the overall report is classified)

1. ORIGINATING ACTIVITY (Corporate author) Hazeltine Corporation Greenlawn, New York 11740	2a. REPORT SECURITY CLASSIFICATION CONFIDENTIAL 2b. GROUP

3. REPORT TITLE

OPERATIONS ANALYSIS OF A MULTISTATIC ECHO-RANGING SYSTEM FINAL REPORT

4. DESCRIPTIVE NOTES (Type of report and inclusive dates)

FINAL REPORT 1 June 1971 - 31 December 72

5. AUTHOR(S) (First name, middle initial, last name)

Robert A. Shade

6. REPORT DATE	7a. TOTAL NO. OF PAGES	7b. NO. OF REFS
December 1972		

8a. CONTRACT OR GRANT NO N00014-71-C-0311 b. PROJECT NO RF 018-96-01 c. NR 364-043 d.	9a. ORIGINATOR'S REPORT NUMBER(S) 6165 9b. OTHER REPORT NO(S) (Any other numbers that may be assigned this report)

10. DISTRIBUTION STATEMENT

Distribution limited to U.S. Government agencies only: Test and evaluation, 22 June 1973. Other requests for this document must be referred to Office of Naval Research (Code 462).

11. SUPPLEMENTARY NOTES	12. SPONSORING MILITARY ACTIVITY
	Naval Analysis Programs (Code 462) Office of Naval Research Arlington, Virginia 22217

13. ABSTRACT

(C) Operations analysis of a multistatic echo-ranging system consisting of the SQS-26 and remote sonobuoys demonstrates outstanding performance for scenarios of convoy screening and target prosecution in the North Atlantic and Mediterranean.

(C) The remote sonobuoy consists of a 6-element vertical line array specially designed to reduce reverberation effects. The receiver was designed using a unique bistatic acoustic computer program and did perform successfully at sea.

(C) The scenarios assume a CZ contact, and analysis utilizing an operations analysis computer model developed for this project shows that three buoys are sufficient for convoy screening and eight buoys in the Atlantic and four in the Mediterranean are sufficient for target prosecution. These buoy plants result in detection probabilities in excess of 90% and in more than half the cases, localization is possible.

(C) Highly effective ship's doctrine for convoy screening is to run a course of 45° with respect to the target datum. For target prosecution, it is best to follow a zig-zag course for environments with narrow CZ's and to head directly towards the datum for environments with wide CZ's.

(C) When a layer is present the receivers are planted at 60' and when no layer is present 1500' receivers are deployed.

(C) The system was found to have tactical advantages and to be four times more cost-effective than a CASS system with equivalent detection performance.

DD FORM 1 NOV 65 1473

Confidential

Security Classification

Unclassified

Security Classification

14 KEY WORDS	LINK A		LINK B		LINK C	
	ROLE	WT	ROLE	WT	ROLE	WT

Unclassified

Security Classification

Report 6165

This work was sponsored by ONR code 462
and performed under its technical guidance.

TABLE OF CONTENTS

LIST OF ILLUSTRATIONS

LIST OF ILLUSTRATIONS (Cont'd)

FOREWORD

The following naval activities provided assistance in the formulation of the problem:

J. Jagadzinski for discussion of helicopter parameters, Naval Air Development Center, Johnsville, Pennsylvania;

The personnel at DESDEVGRUTWO, and especially STCS E. J. A Spoonamore.

This work was sponsored by ONR Code 462 and performed under the technical guidance of R. Dickman of that office. We gratefully acknowledge his assistance during the contract and especially in the preparation of this report.

Acknowledgement is also made of the assistance given by Hazeltine personnel: T. DeFilippis, S. Ginsberg, and especially A. Novick for his technical guidance throughout this project.

Hazeltine
Corporation

SUMMARY

(C) Operations analysis of a multistatic sonar system consisting of an SQS-26 and remote sonobuoys indicates that outstanding performance can be expected for screening and target prosecution scenarios in both North Atlantic and Mediterranean environments. Consistently high target detection probabilities were obtained in all scenarios by the proper utilization of the system including buoy placement and ship's doctrine. Comparison with a CASS system which can achieve the same performance shows that the multistatic system has a four-to-one cost effectiveness advantage and a tactical advantage due to the absence of a nearby actively pinging transmitter.

(C) Recommended tactical doctrines are as follows. For environments in which the convergence zone (CZ) is narrow (3 to 5 kyds) a 45° course away from the datum for approximately 30 minutes followed by a 90° turn towards the datum with a ship speed of 15 knots is recommended. This results in a slow advancement of the CZ over the target uncertainty area and will provide the sonar with more "looks" at the target. For environments with a broad CZ, the ship should proceed directly at the datum again resulting in maximum use of the CZ coverage. Best receiver depths are 60' for environments with a layer and 1500' for environments with no layer.

(C) The sonar system consists of an SQS-26 operating in the bottom bounce search mode. In this mode, it uses three sequential 40° transmissions to cover a 120° azimuthal sector. This sonar uses 12 contiguous preformed beams to receive possible echoes. The remote bistatic receiver consists of a six element vertical line array of omnidirectional elements spaced approximately one foot apart, deployed at depths of 60 ft or 1500 ft. This type of array was designed to reduce reverberation effects and did perform successfully at sea.

(U) The study was aided by the use of two computer programs: (1) An operations analysis model used to calculate target detection probabilities as the exercise progressed with time: (2) A bistatic acoustic model used to predict buoy coverage, calculate propagation losses, and create tables of reverberation as a function of time.

(U) The study consisted of a number of exercises in various environments and scenarios. Key results of these studies are summarized below.

1. Convoy Screening in the North Atlantic

(C) This involved the problem of redetecting a target which was initially detected in the convergence zone at a range of about 70 kyds and subsequently

6165

lost. It is assumed that the submarine is attempting to penetrate a destroyer picket to attack a high value unit. An azimuthal uncertainty of $\pm 5^{\circ}$ is assumed in the initial target datum and the cumulative probabilities of detection for various target tracks are calculated spanning this uncertainty and for various target tactics.

(C) Following the initial target datum by a delay of about 10 minutes, a helicopter is launched to drop several remote sonobuoys in the vicinity of the datum. The set of drop points for these receivers was one of the parameters which was determined during this study.

(C) The final results show that the use of as few as three properly placed sonobuoys plus the shipboard sonar combined with a ship's doctrine of turning to an angle of 45° away from the target datum virtually ensure redetection of the target if it attempts to penetrate the screen. Cumulative probabilities of detection approaching unity were obtained consistently for either submarine tactic and for submarine speeds between 6-15 knots. A submarine moving faster than 15 knots should be detected passively by the sonobuoys.

2. Target Prosecution in the North Atlantic

(C) In this study, the initial datum and the system used are the same as described above, however, the target may follow a course in any direction. The goal of the ship was to redetect the submarine, with a later goal of localization and weapons drop.

(C) Analysis shows that CZ contact investigation for an SLBN submarine always results in near unity detection probabilities because of the high target strength. For other types of contacts redetection is 80-90 percent assured over a target uncertainty area of about 700 square nm (a radius of 15 nm) by using 8 sonobuoys laid down in a pattern similar to that on a playing card and using a ship's doctrine of closing directly at the datum.

(C) For a conventional submarine, after a CZ contact the probability of redetection is over 90 percent for a field of 8 sonobuoys plus the SQS-26. The best tactical doctrine here is to plant the buoys along the spiral predicted by the time late of the helicopter and for the ship to run a zig-zag track of 45° away from the datum for about 30 minutes and then turn 90° towards the datum and proceed.

(C) To examine the importance of time late on multistatic doctrine, a series of runs was made assuming rocket launched sonobuoys with delivery speed of about 1400 knots: The results show that because of the greatly reduced uncertainty area, 2 rocket launched buoys perform as well as 8 helicopter launched buoys. Best ship's doctrine in this case is to slow down to 6-10 knots and head straight at the datum.

(C) Finally, for the same environment and scenario, a comparison was made between multistatics and CASS. The results show that about twice as many bistatic buoys as CASS buoys are required to achieve the same mission effectiveness. This implies about a four times greater cost effectiveness for bistatics. In addition, bistatics has a tactical advantage over CASS in that the target can more easily avoid detection by a CASS buoy if it readjusts its track according to the location of this actively pinging buoy.

3. Target Prosecution in the Mediterranean

(C) The system was the same as described above. Because the CZ in the Mediterranean occurs at about half the range of that in the Atlantic, target prosecution was achieved with near unity detection probabilities regardless of target depth or layer depth. This was accomplished using only 4 sonobuoys plus the SQS-26 and a ship's doctrine of heading directly at the datum at a speed of 15 knots.

(C) Results show that replacing the SQS-26 by an SQS-23 will result in somewhat reduced echo-to-background levels but will still perform quite well in a multistatic operation in this environment.

(C) In all of the cases run, it appears that by intelligent operation of the system, there is a reasonable probability (about 50 percent in the North Atlantic and higher in the Mediterranean) of detecting the target simultaneously with at least two receivers and thus localization might also be achieved. This probability can of course be increased by deploying more remote sonobuoys.

4. Conclusions

(C) The results of this study substantiate that this multistatic approach significantly increases operational effectiveness for these scenarios when compared with presently used systems. It is clear that multistatic systems offer a highly useful adjunct to the Navy's existing sonar capabilities and thus merit further investigations both analytical and experimental.

LIST OF ABBREVIATIONS

AMOS	-	Acoustical, Meteorological, and Oceanographic Survey
BB	-	Bottom bounce
BB/ODT	-	Transmitter mode using 120^{o} sector formed from three contiguous 40^{o} beams
BB/TRACK	-	Transmitter mode utilizing a 40^{o} beam (SQS-26-BX) or 10^{o} beam SQS-26-AX and SQS-26-CX
BTM	-	Bottom
CASS	-	Command Active Sonobuoy System (A self-contained Xmtr/Rcvr)
CPA	-	Closest point of approach
CPD	-	Cumulative Probability of Detection
CZ	-	Convergence Zone
DP	-	Direct Path
DSL	-	Deep scattering layer
E/B	-	Echo-to-background ratio in dB
LFM	-	Linear FM
MAD	-	Magnetic anomaly detector
MGS	-	Marine Geological Survey
MTA	-	Minimum target aspect
NM	-	Nautical Mile
RCVR	-	Receiver
SL	-	Source level
SLBN	-	Nuclear missile launching submarine
VLA	-	Vertical Line Array
XMTR	-	Transmitter
41-X	-	6-element vertical line array used as buoy in this study

Hazeltine
Corporation

SECTION I (C)

INTRODUCTION

A. BACKGROUND

(C) In 1969, the technical feasibility of bistatic echo-ranging with the SQS-26 transmitter and specially designed A-size sonobuoy-type receivers was demonstrated.[1] The system concept is illustrated below. The receiver design was based on a unique bistatic analysis computer program.[2]

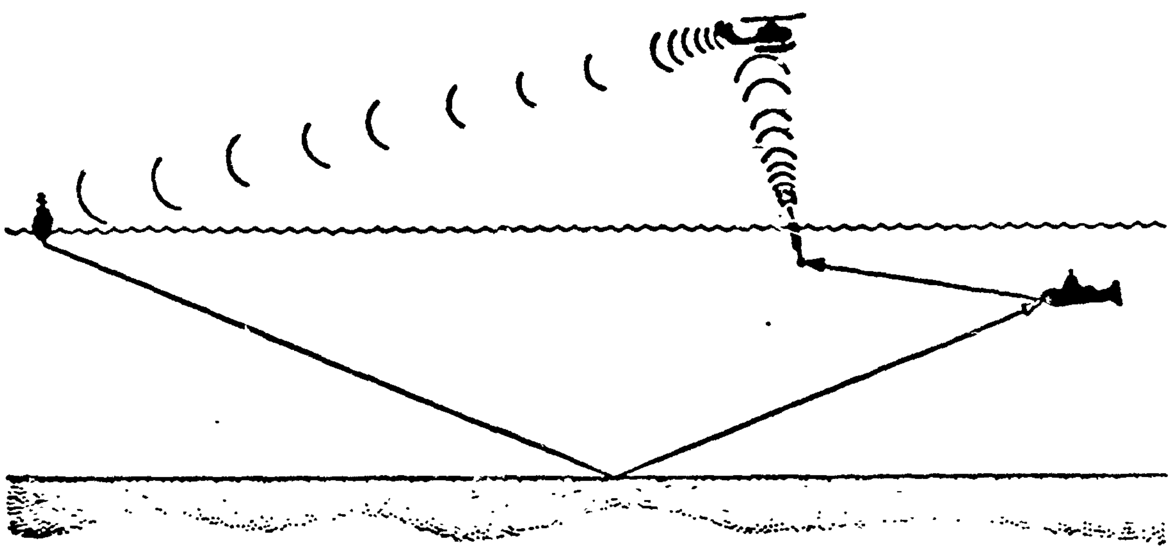

(C) The experiment was conducted during the period 1-3 October 1969 in an area 300 miles west of Bermuda. Average water depth in this area is 18,000 ft. The bottom ranges from MGS Class 2 (good) to Class 4 (poor) for bottom-bounce operation. Sea State was 2 to 3. Moderate to good surface ducts 125 to 170 ft deep existed.

(C) This sea experiment was highly successful from several points of view.

(1) Bistatic detections were achieved at transmitter-to-target ranges of 5 to 40 kyd, and at 76 kyd in the first convergence zone. For the target at periscope depth, maximum target-to-receiver ranges were 5 to 11 kyd. With a below-layer

1 Project D/S 510, "Bistatic Echo Ranging Experiment," Final Technical Report, Hazeltine Corporation, Report 7914, July 1970.

2 "Operations Analysis of Multistatic Echo-Ranging System," App. A, Interim Report, Hazeltine Corporation, Report 7984, March 1972.

target, maximum target-to-receiver ranges were up to 8.7 kyds. (These detection ranges are in good agreement with values predicted with the acoustic model in this environment.)

(2) Tests with an omnidirectional receiver showed the strong influence which reverberation has on multistatic sonar performance and pointed out the need to reduce these effects by proper hardware design.

(3) Test results showed how effective the newly designed directional sonobuoy was at suppressing the effect of this reverberation.

(4) The reverberation levels measured were in good agreement with levels predicted in advance using the bistatic acoustic computer program developed at Hazeltine. This agreement adds support to the validity of this program.

B. STUDY OBJECTIVES

(U) Once technical feasibility of this bistatic echo-ranging system was demonstrated, the next logical step was to determine the potential benefits of such a system to the Navy. The goals of the present project were to: (1) determine the effectiveness of multistatic sonar systems in several operational environments; and (2) recommend ship's doctrines to best utilize these systems. (For convenience, this bistatic sonobuoy which is similar to the SSQ-41 is designated SSQ-41-X in this report.) Other objectives of this study were to compare the effectiveness of this SQS-26/41-X multistatic system with (1) CASS, and (2) a multistatic system using the SQS-23 and remote sonobuoys.

(U) All of the scenarios analyzed in this paper are contact investigations and this study concentrates on two applications of the system: convoy screening and target prosecution.

(U) The first of these, convoy screening, involves a submarine attempting to attack a high value unit. The goal of the destroyer escort is to provide a screen with sufficient performance to detect any submarine attempting penetration.

(U) Target prosecution requires the destroyer to redetect and ultimately localize a submarine which has been alerted to the presence of the ship and is attempting to avoid detection.

(C) Two environments are considered for these scenarios: the North Atlantic and the Mediterranean Sea. Detections against both conventional and SLBN submarines were studied.

C. REPORT ORGANIZATION

(C) The remainder of this report is organized as follows: Section II gives a description of the technical approach used in this study and a brief description of the computer models used in the analysis. Section III describes the sonar equipments used in the operations analysis. Section IV presents the results for the analyses conducted in the North Atlantic; it includes the effects of time late on system performance and quantitative comparison with CASS. Section V describes the target prosecutions studies for several Mediterranean environments. Section VI summarizes the conclusions and recommendations of this study. Key figures showing detection results for various cases are included in the main body of this report. A complete summary of all computer runs is contained in Appendix A.

(U) This document is the final report of a study performed for the Office of Naval Research (Code 462) under ONR Contract N00014-71-C-0331. A comprehensive report of the work performed up to March 1972 is described in an Interim Report*; topics which are covered in detail in that report are only summarized in this report. Thus, although this document includes all work performed under the contract, some references to the Interim Report will be found in the present report.

*Referenced in the Study Summary.

SECTION II (C)

TECHNICAL ANALYSIS

(U) The method used in this project was to carry out an idealized systematic operations analysis to determine the comparative performance of monostatic and multistatic systems as a function of ship's doctrine, number of sonobuoys employed, submarine tactics (including course, speed, depth), and environment.

(U) Because of the complexity and large amount of data involved in carrying out such a task, an operations analysis computer model was written which proved to be an effective tool for comparing systems performance as the above variables were changed.

(C) Hazeltine had previously developed a unique computer program to calculate echo-to-background ratios for bistatic receivers in the presence of reverberation; computations using this program have been proved to be in good agreement with the experiment. In writing the present operations analysis computer model, full use has been taken of the contents and results of this program. (It was shown in the sea experiment that reverberation provides a limiting background for the bistatic receivers and, therefore, must be included in any accurate analysis.

(U) This section briefly describes these two models. (Additional details may be found in Appendices A and B of the Interim Report.)

A. OPERATIONS ANALYSIS COMPUTER MODEL

(U) The objective of this study project was to provide a quantitative evaluation of a multistatic sonar system concept. In order to accomplish this, it was required that the results of submarine detection schemes be analyzed. This requires knowledge of the probability of detection of a target as a function of time as both the target and the ship maneuver in the water. The first part of this project was devoted to developing a sophisticated computer model which could carry out calculations involving such complex systems as described above. The result of this effort was a versatile and efficient computer model which has been given the name SOBER (Study of Operational Bistatic Echo-Ranging).

(U) The fundamental process which the program models is a continuous cycle representing a real world time-developing physical system; actions result in new information which is used to make decisions which result in new actions. The rules which govern the system are as follows: actions are constrained by physical laws; information is governed by environment and obtained by means of sensors; and decisions are based on interpretation of information and mission objectives.

(U) A computer model which included the full implications of this cycle would be a simulation program. At present, only the action-information parts of the cycle have been programmed, deferring the addition of dynamic decision routines until a later date, if so desired.

(U) At the onset of this study, it was decided that the program should be capable of handling multiple units of all types. It rapidly became apparent, however, that such a program could require excessive amounts of computer memory storage unless it was carefully organized to avoid such problems. In order to create such a program which was both versatile and efficient, use was made of a concept which is called Unit Space. This technique gives a central role to a vehicle and then describes the environment of that vehicle in terms of its physical status and information acquired by its sensors. The importance of such a concept is that the vehicle and its environment can be described and stored independently of other vehicles. This allows the computer program to handle large numbers of vehicles since the data for each can be handled separately while all others are left in storage outside the central memory.

(U) The computer model uses a fixed time step and consists of (1) dynamics routines to move the various vehicles around in time according to predetermined tactics, (2) acoustic routines used to calculate the sound level at each target and receiver, and (3) detection routines used to calculate the probability of detection of the target at each receiver during each time step and the cumulative probability of detection for each receiver.

(U) The program includes the effects of radiated noise and specular interference carried out to paths involving 0, 1, and 2 bottom contacts. The inputs to the program consist of vehicle parameters such as speed, turn rate, tactics, etc.; equipment parameters such as sonar source level, transducer spacings, etc., and acoustical data. In the first exercises (convoy screening) the propagation losses were calculated in the operations analysis model using isovelocity ray tracing. For the remainder of the project, all propagation losses for each system and environment were input to the model in the form of tables calculated using the bistatic acoustic program and corrected for shadow zone propagation. Reverberation tables were also calculated with the bistatic program and put into the model via tables, although experimental data could be used if desired.

(U) Each exercise was set up by specifying the ship and target courses, speeds and initial locations. A fixed time step was used during which each vehicle would move (a helicopter is used to deliver the buoys to drop points assigned during input), and all acoustic signals would be transmitted, received and processed according to their occurrence during that time period. This information was used to calculate the probability of detection for that ping and the cumulative probability of detection (CPD) up to that time for each receiver.

(U) The expression used to calculate the single ping probability of detection is:

$$\exp\left((-2.3 \log_{10}(P_f) - 0.327)/(1 + SNR)\right)$$

where P_f is the probability of false alarm (typically 10^{-4}) and SNR is the echo-to-background power ratio. This result was derived by Marcum and Swerling and reported in "Transactions of the IRE," Vol IT-6, No. 2 (April 1960).

(U) The calculation of cumulative probability of detection which satisfies a rule such as M detections out of N when the total number of looks is greater than N has been solved and is incorporated in the present model.

(U) A target strength function which is dependent on target aspect is used and it is of the form of $10 + 10 \sin^2(\theta_B)$ where θ_B is the target aspect defined for bistatic receivers as shown below. (The importance of target aspect is seen in the results of the analysis.) For an SLBN submarine, the expression used is $13 + 12 \sin^2(\theta_B)$.

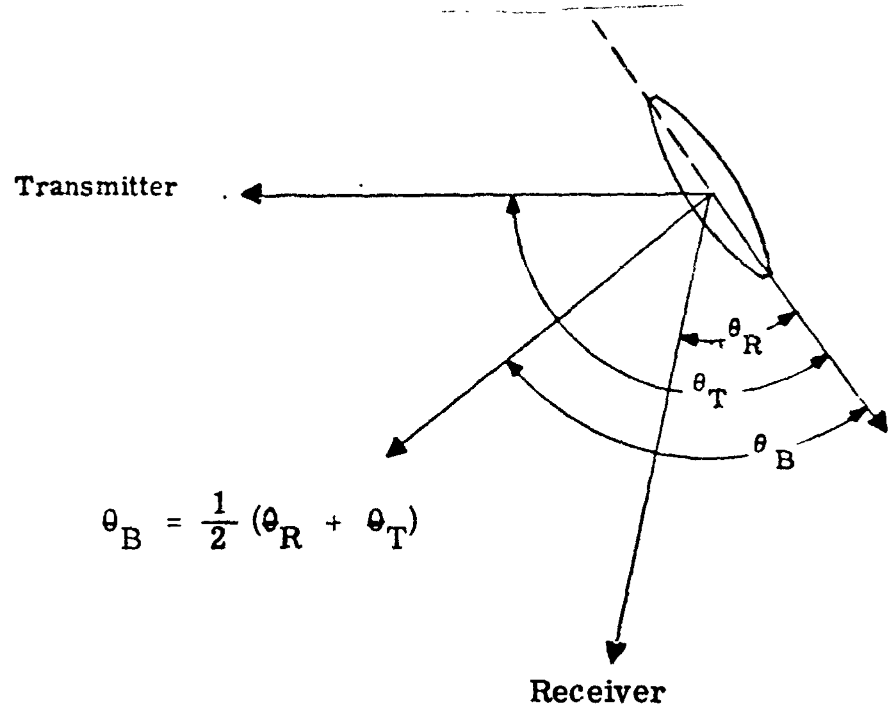

$$\theta_B = \frac{1}{2}(\theta_R + \theta_T)$$

(U) The output of the program consists of a summary of input data, a track history of vehicle locations, a summary of receiver locations, a chronological summary of detection probabilities and other pertinent data for each receiver at each time step, a mission effectiveness summary, and printer plots of the vehicle tracks also showing the sonobuoy locations. For purposes of efficiency, many of these outputs can be suppressed if desired.

(C) Certain assumptions must be made in any study of this type. These assumptions are of the following types: (1) all equipment is assumed to operate as designed; no system malfunctions have been included as program input; (2) human factors have been programmed based on ideal operator responses; no out-of-the-ordinary operator problems have been included; (3) the ocean is assumed to be describable by the mathematical model discussed below.

B. BISTATIC ACOUSTIC MODEL

(U) The bistatic acoustic model is used to calculate echo-to-background ratios in the presence of reverberation for fixed transmitter-receiver separation and a grid of target locations around the receiver. The work done up to the interim report used a model based on isovelocity ray-tracing with angular corrections made at the ray point ends to account for refraction. In the second phase of this study a detailed ray trace model was used. The outputs of these models have been shown to be consistent and do agree with data measured at sea.

(U) Tables of reverberation as a function of time of arrival at the receiver are also printed out for later use. The actual calculation of reverberation for a given time is carried out by summing the contributions from the surface, the bottom, and the deep scattering layer each of which is the result of an integration around an eliptical annulus representing equal time length paths from the transmitter to the scatterer to the receiver. These calculations can be carried out to include any number of specular bottom and surface contacts as well as the scattering contact.

(U) In the first part of the contract, for targets below the layer and transmitters and receivers in the layer, AMOS propagation losses were used. Later when it was desired to run cases involving either deep directional receivers or deep targets, it was felt that the AMOS data would not be applicable. For this reason, the pure ray-trace program was used. This, however, predicts no energy in the shadow zone for a receiver in the layer and a target below the layer at a range greater than 3-4 kyds.

(U) To solve this problem, a short study was undertaken to develop methods of calculating energy arriving in the shadow zone. (This study is described in detail in Appendix B.) This study was based on work performed for the Navy by Schweitzer[1], Medwin[2], and Nobel[3] and resulted in predictions of energy arriving into the shadow zone by means of surface scattering (including effects of bubble phenomena) and diffraction. This model applies to directional as well as omni arrays and is thus not reciprocal in cases such as a deep directional array and an in-layer target. The validity of the model is based on agreement with AMOS data in cases where AMOS holds.

---

1 B. J. Schweitzer, "Sound Scattering into the Shadow Zone below an Isothermal Layer," Journal of the Acoustical Society of America, Vol. 44, No. 2 (1968).

2 H. Medwin, "The Rough Surface and Bubble Effect on Sound Progagation in a Surface Duct," 28th Navy Symposium on Underwater Acoustics, Vol. 1, (Nov 17-18, 1970) (CONFIDENTIAL)

3 W. J. Noble, "Theory of the Shadow Zone Diffraction of Underwater Sound," Journal of the Acoustical Society of America, Vol. 28, No. 6 (1956).

Hazeltine
Corporation

SECTION III (C)

SYSTEMS DESCRIPTIONS

(U) In this study several different systems have been analyzed and therefore for the sake of conciseness and ease of reference, all of the systems and their parameters will be described in the four tables following.

SQS-26

(C)

Function:	Monostatic system and transmitter for bistatic buoys
No. of Elements:	
Horizontal: 20 Vertical: 8	(Cylindrical array simulated by planar configurations of equal beamwidth)
Element Spacing (ft):	
Horizontal: .611 Vertical: .695	
Element Shading:	Uniform
Operational Mode:	Bottom Bounce and Convergence Zone (120° Sector Insonification)
Source Level (dB).*	136 (BB/ODT); 142 (BB/TRACK)
Frequency (Hz):	3500
Pulse Length (ms):	500
Bandwidth (Hz):	100
Pulse Type:	LFM
FM Processing Gain (dB):	17

* measured relative to 1 μB at 1 yd.

Hazeltine
Corporation

41-X (Bistatic Sonobuoy)

(C)

Function: Bistatic and Passive Receiver

No. of Elements
  Horizontal: 1
  Vertical: 6

Element Spacing (ft)
  Horizontal: --
  Vertical: 1.05

Element Shading: Trizonal

Operational Mode: Direct Path

Signal Processing: (Bistatic processor is matched to transmitter waveform.)

CASS

(C)

Function: Monostatic Buoy

No. of Elements
  Horizontal: 1
  Vertical: 6

Element Spacing (ft)
  Horizontal: -
  Vertical: 0.256

Element Shading: Uniform

Operational Mode: Direct Path - Omnidirectional Transmission

Source Level (dB): 107

Frequency (Hz): 6500

Pulse Length (ms): 1000

Bandwidth (Hz): 400

Signal Processing Gain (dB): 26

Only FM performance was considered.

Hazeltine
Corporation

SQS-23

(C) Function: Monostatic System and Transmitter for Bistatic Buoys

No. of Elements

Horizontal: 20
Vertical: 8

Element Spacing (ft)

Horizontal: 0.428
Vertical: 0.487

Element Shading: Uniform

Operational Mode: Direct Path and Convergence Zone

Source Level (dB):* 133

Frequency (Hz): 5000

Pulse Length (ms): 30

Bandwidth (Hz): 320

Signal Processing Gain (dB): 9 (incoherent processing)

* measured relative to 1 μB at 1 yd.

SECTION IV (C)

NORTH ATLANTIC OPERATIONS ANALYSIS

A. ENVIRONMENT DESCRIPTION

(U) The environment studied is typical of early or late summer (night), and has the following parameters:

Water Depth	15,000 ft
Isothermal Layer Depth	150 ft
Deep Scattering Layer Depth	600 ft
Deep Scattering Layer Coefficient	-50 dB
Bottom Scattering Coefficient	-27 dB
Wind Speed	13 knots
Sea State	3
MGS Bottom Class	3

Velocity Profile

Depth (ft)	Velocity (ft/second)	Gradient (ft/second/ft)
0.0	5024.0	
		.0200
150.0	5027.0	
		-.1667
300.0	5002.0	
		-.0059
1310.0	4996.0	
		-.0533
3000.0	4906.0	
		-.0062
4600.0	4896.0	
		.0120
6600.0	4920.0	
		.0155
15000.0	5050.0	

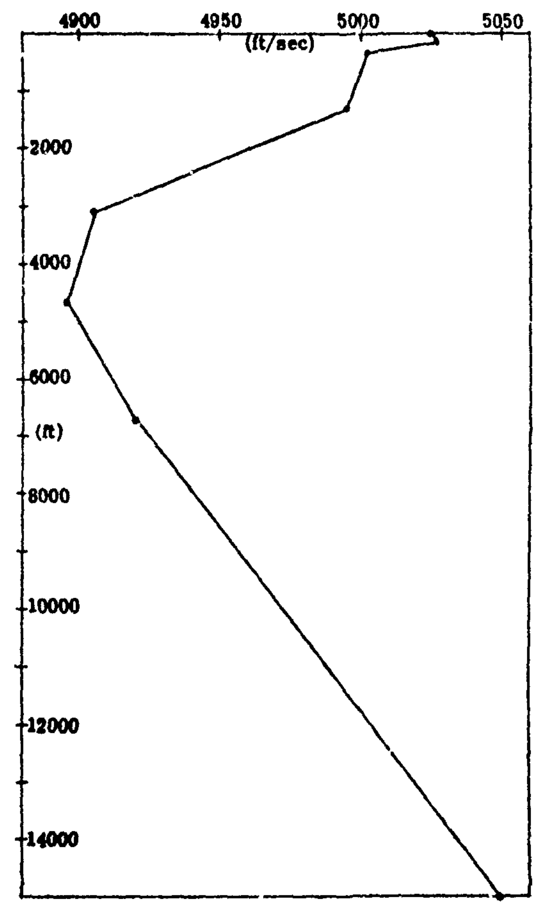

B. ACOUSTIC PERFORMANCE

(U) In order to make reasonably accurate estimates of optimum buoy locations for operations analysis exercises, it is useful to plot the coverage of these receivers under varying conditions. The following figures will illustrate some typical coverages although it should be borne in mind that these coverages will vary somewhat with bistatic separation and target strength.

(C) Figure 4-1 shows the coverage of a bistatic receiver as predicted by the earlier version of the bistatic acoustic model. In all of these figures, the shaded area represents the area of coverage occluded by the first bottom bounce specular arrival. This figure and all but the following figure represent coverage corresponding to a 120° sector insonification centered on the buoy. This represents a somewhat pessimistic coverage for contact investigation since the SQS-26 (BX) actually can operate with a 40° beam in the BB/TRACK mode. For comparison, figure 4-2 shows the same buoy using this narrower beam. In the BB/TRACK mode of the SQS-26 (CX) and (AX) a 10° transmit beam is used; this results in an area of coverage increased over the 40° and 120° beams due to increased source level and decreased off axis reverberation contributions.

(C) Figure 4-3 shows the coverage of the same buoy and conditions as figure 4-1, as predicted by the detailed ray tracing bistatic program including shadow zone propagation when it exists. Note that the coverage is quite similar except for a slight lateral broadening.

(C) During the first phase of this contract propagation losses were calculated using AMOS data. These data indicated a rapidly decreasing buoy coverage for a 60' receiver as the target went deeper. (A 50% decrease in coverage was found when the target went from 250' to 400'.) Coverages as predicted by the detailed ray tracing model with shadow zone propagation losses indicate that this is not true. Only slight differences in coverage were found as the target went to depths as deep as 1200'.

(C) Figure 4-4 shows the large increase in coverage observed if the target moves up into the layer.

(C) As a result of these coverages, it was found best to deploy the bistatic receivers at a depth of 60' in the North Atlantic when a layer is present. If there is no surface duct, then it is better to use these receivers at 1500' because of the extended ray path coverage.

(C) Figure 4-5 shows the coverage of a CASS buoy in the same environment showing the effects of varying target depth and target strength. The CASS buoy at 60' does not perform as well as at 1500' as will be seen later in the figures showing the results of the operations analysis computer runs.

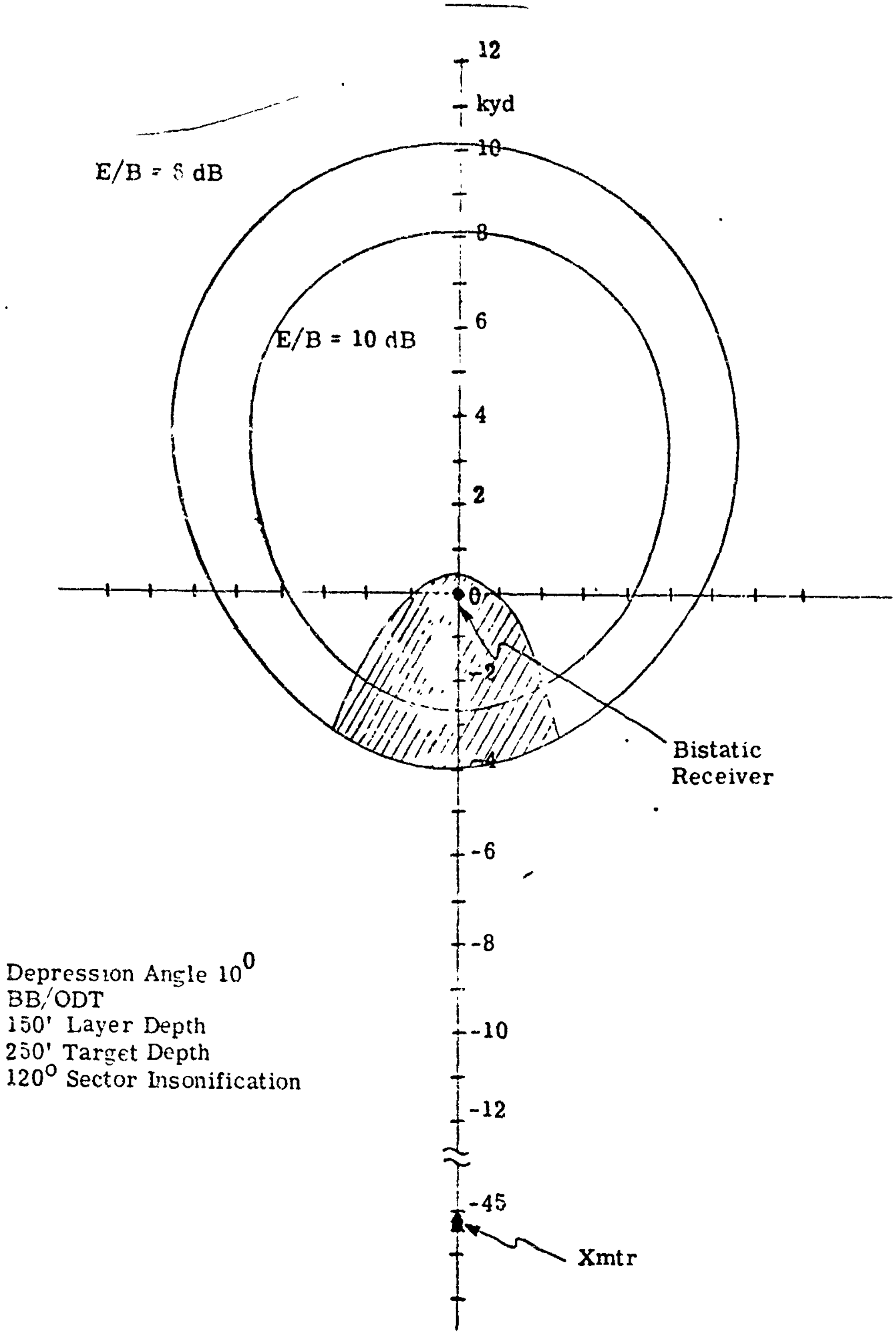

Figure 4-1 (C) Coverage of 41-X Sonobuoy Used with SQS-26 in BB/ODT Transmit Mode (Predicted with Isovelocity Ray Tracing)

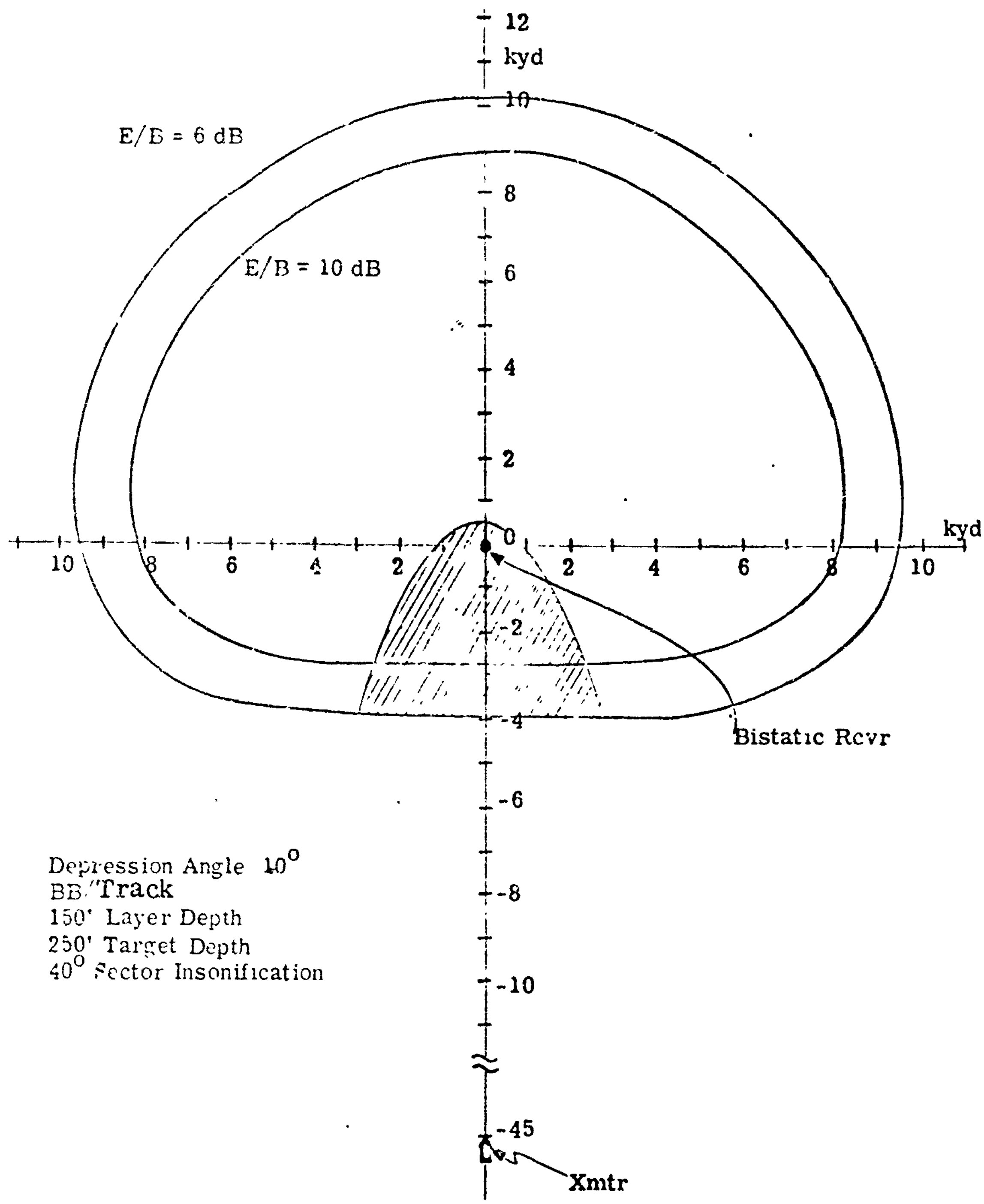

Figure 4-2 (C) Coverage of 41-X Sonobuoy Used with SQS-26 in BB/TRACK Transmit Mode (Predicted with Isovelocity Ray Tracing)

Hazeltine
Corporation

Figure 4-3

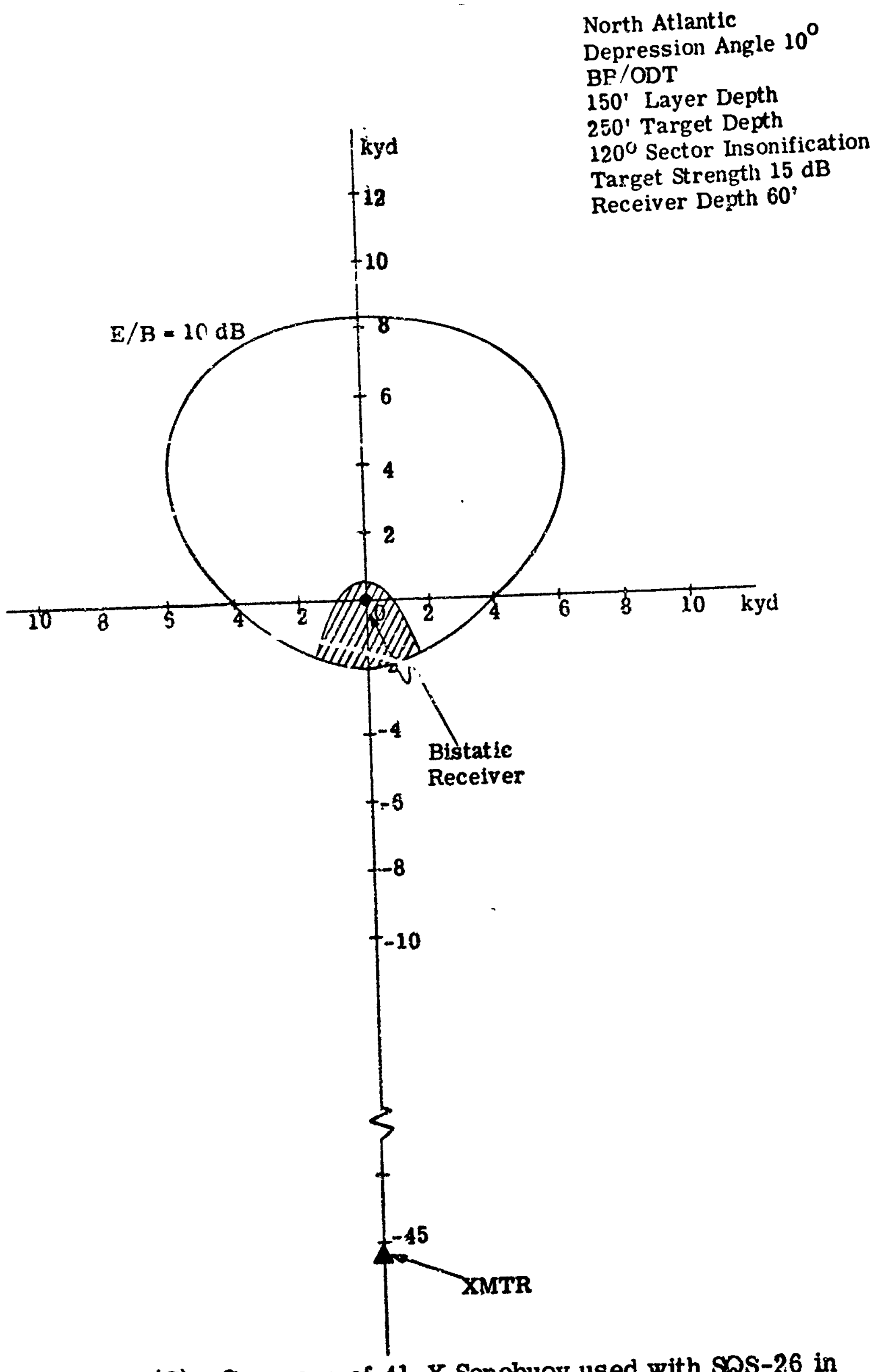

Figure 4-3 (C) Coverage of 41-X Sonobuoy used with SQS-26 in BB/ODT Transmit Mode

Hazeltine Corporation

Figure 4-4

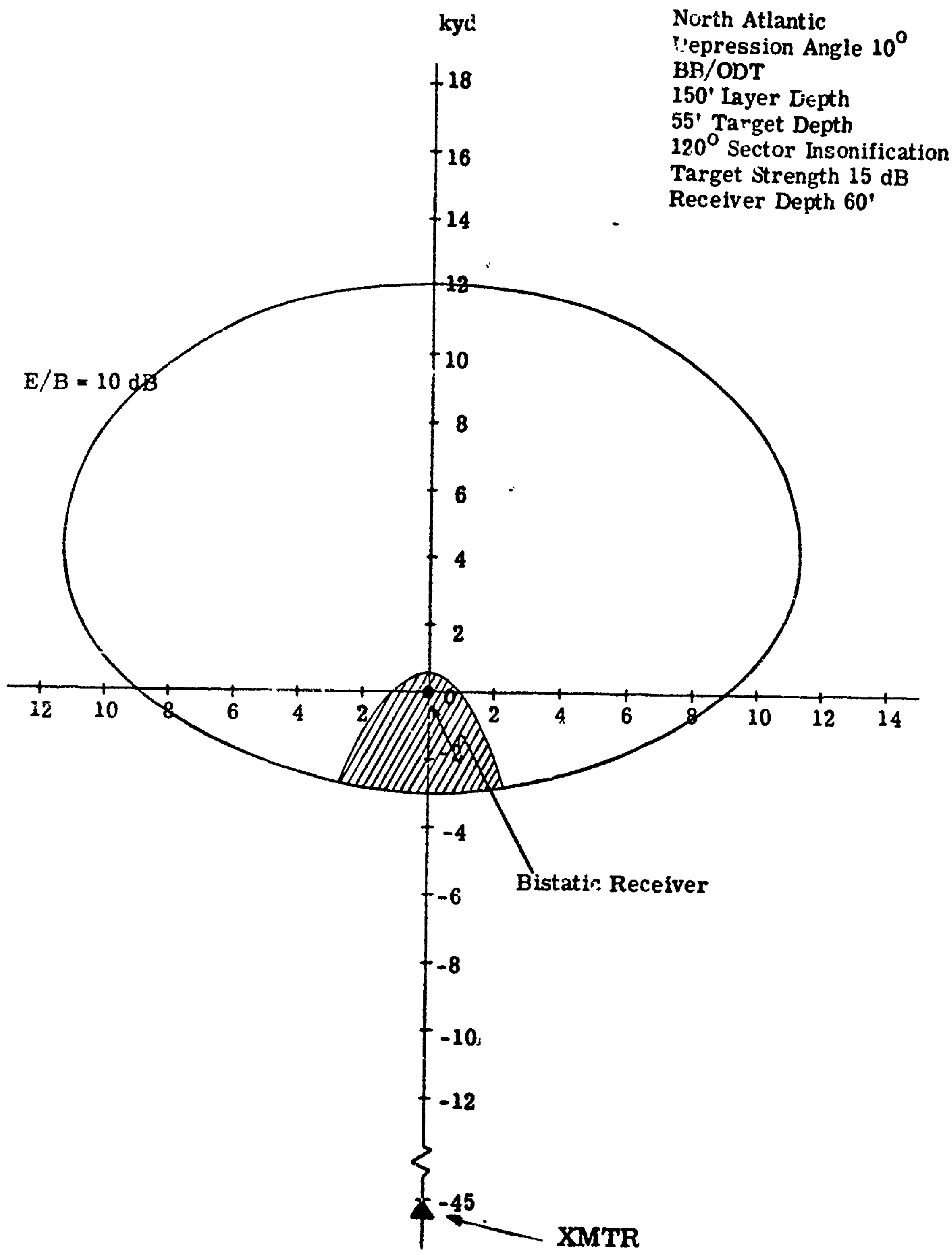

Figure 4-4 (C) Coverage of 41-X Sonobuoy; Target in Layer

North Atlantic
Depression Angle 0^{o}
Direct Path
150' Layer Depth
55'/300' Target Depths
Target Strengths 15/20 dB
Buoy Depth 1500'

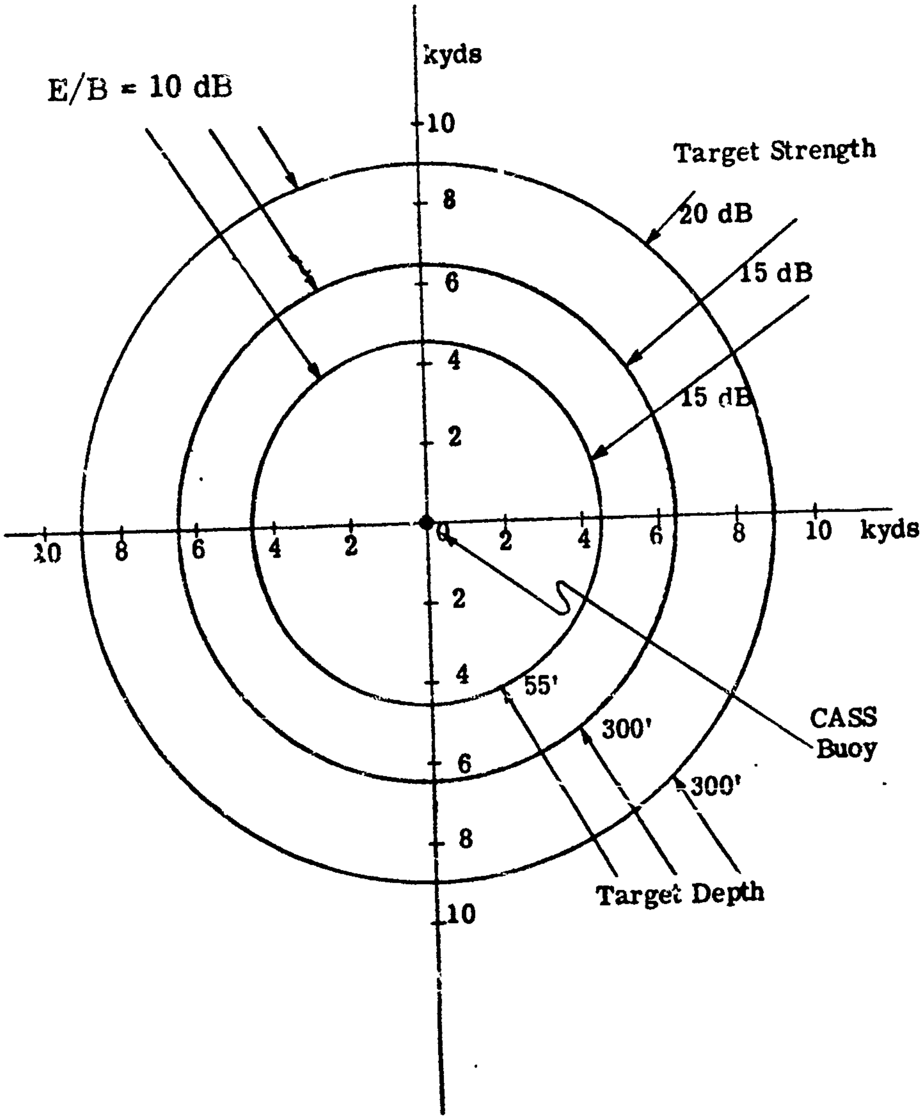

Figure 4-5 (C) Coverage of the CASS Buoy

(C) These buoy coverages will change as the bistatic separation changes. Optimum separations are about 45 kyds because for larger separations the coverage decreases due to propagation losses and for shorter separation the decrease is due to increased reverberation. Coverage is also good for large separations when the target is in the CZ. Thus, a good balance of BB and CZ insonification must be maintained by careful use of ship's doctrine and buoy placement.

(C) In the North Atlantic environment studied, the CZ starts at about 69 kyds and is 3-4 kyds wide. When calculating propagation loss tables which include the CZ, it was found important to bound the value of propagation loss at caustics predicted by the ray trace program. The method used was to bound these losses to a value which is no more than 10 dB less than those predicted by spherical spreading. In the light of corrections for caustics as calculated by the Navy[1] these bounded values are somewhat conservative and thus the CZ detections obtained should be valid.

C. CONVOY SCREENING SCENARIO

(U) This scenario is thoroughly described in the Interim Report and only the highlights are presented here. All of the computer run results will be found in Appendix A.

(C) All the cases studied in this scenario are related to the problem of redetecting a submarine attempting to penetrate a destroyer screen protecting a high value convoy. The initial detection is assumed to occur in the convergence zone at a range of about 70 kyd. The uncertainty in azimuthal target position is assumed to be $\pm 5^{\circ}$, and the uncertainty in range is considered negligible in comparison.

(C) The destroyer speed is in all cases kept at 15 knots and the submarine speed is assumed to be between 6 and 15 knots. (Higher submarine velocities would result in passive detection of the target by the remote sonobuoys due to greatly increased radiated noise levels with speed.)

(C) A below-layer target at 250 ft was chosen as being most likely. Two types of target tracks were considered: closest point of approach (CPA) and transit directly toward the picket line (180° from the N-S axis).

(C) As a result of analysis, it was found that two buoys would be sufficient to accomplish the task of redetection, and thus, in the analyses shown here only 1 or 2 buoys are used. Localization could be accomplished using MAD or additional buoys.

1 Private conversation with Mr. C. Spofford of the Office of Naval Research, (Maury Center)

(U) Each exercise illustrated will be discussed by reference to a figure showing the physical geometry and another figure showing graphically the effectiveness of each receiver used during that exercise. Using figures 4-6 and 4-9 as examples, their contents and meaning are described as follows:

(C) Figure 4-6 illustrates the geometry for a typical exercise showing the destroyer track, five submarine tracks spanning the $\pm 5^{\circ}$ in azimuthal uncertainty of the target datum, and the location of the remote sonobuoys with their nominal coverage indicated as described above. The large circles around the submarine tracks indicate the extreme possible locations of the target at the time the first sonobuoy is dropped. All exercises assume a launch delay of 10 minutes and a helo speed of 120 knots, with an average time late of 22 minutes.

(C) Also located on this figure is a table containing the mission cumulative probability of detections (CPD) for the three ship tracks used. The average is over the five submarine tracks run and the resulting value is the CPD for detection by at least 1 of the receivers (based on an expression of the form $1-(1-P_1)(1-P_2)(1-P_3)$ for three receivers, averaged over the five submarine tracks. The worst case value refers to the lowest of the individual submarine track CPDs described above. These figures then give a good indication of the mission effectiveness and its weakest point.

(C) Figure 4-9 illustrates the individual receiver data presentation for a typical set of exercises. This data gives the CPD at the end of the exercise for each of the receivers used and thus allows a direct comparison of the effectiveness of each receiver as well as a quick visual interpretation of the total mission effectiveness. For example, in this figure, the data for the exercise involving a target datum at 60° and a ship heading of 0° indicates that the total mission effectiveness was good mainly due to the monostatic performance while the bistatic receivers were not useful for these target tracks. The data for a target datum at 0° and a ship heading of 90° indicates just the opposite; the mission effectiveness is good due to the combined performance of the bistatic receivers while the monostatic performance is poor.

(C) Figures 4-6, 4-7, 4-8, and 4-9 show the results for a submarine in the transit mode at a speed of 10 knots, sub track of 180° and a depth of 250 ft. For the target datum at 0° the results are all quite good, the best being for a ship track of 90°. This is true because in general if the ship closes the target (as in the 0° and 45° ship tracks) the reverberation increases faster than the signal strength and so the E/B ratio

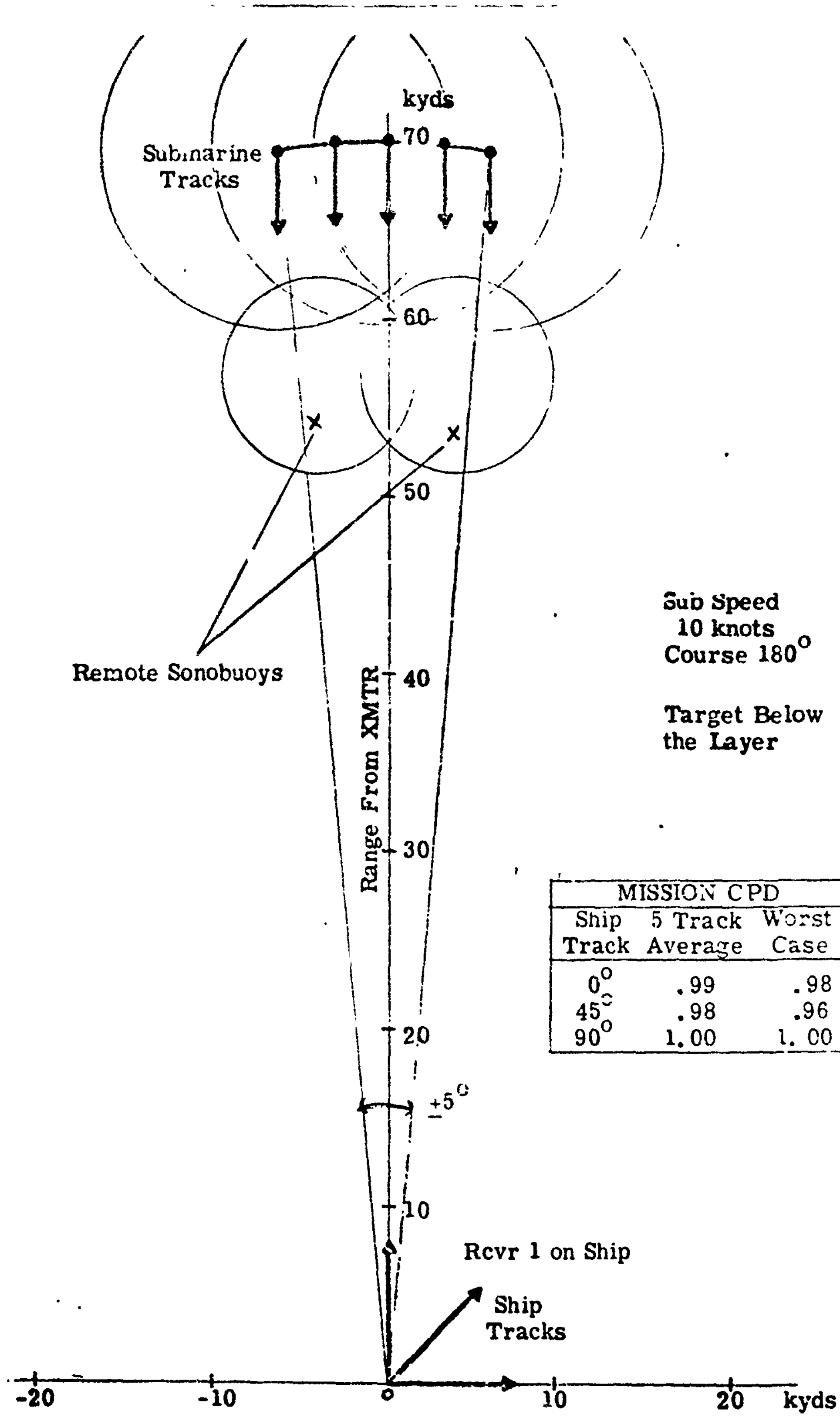

MISSION CPD		
Ship Track	5 Track Average	Worst Case
0°	.99	.98
45°	.98	.96
90°	1.00	1.00

Figure 4-6 (C) Convoy Screening Scenario - Target Heading 180° Datum at 0°

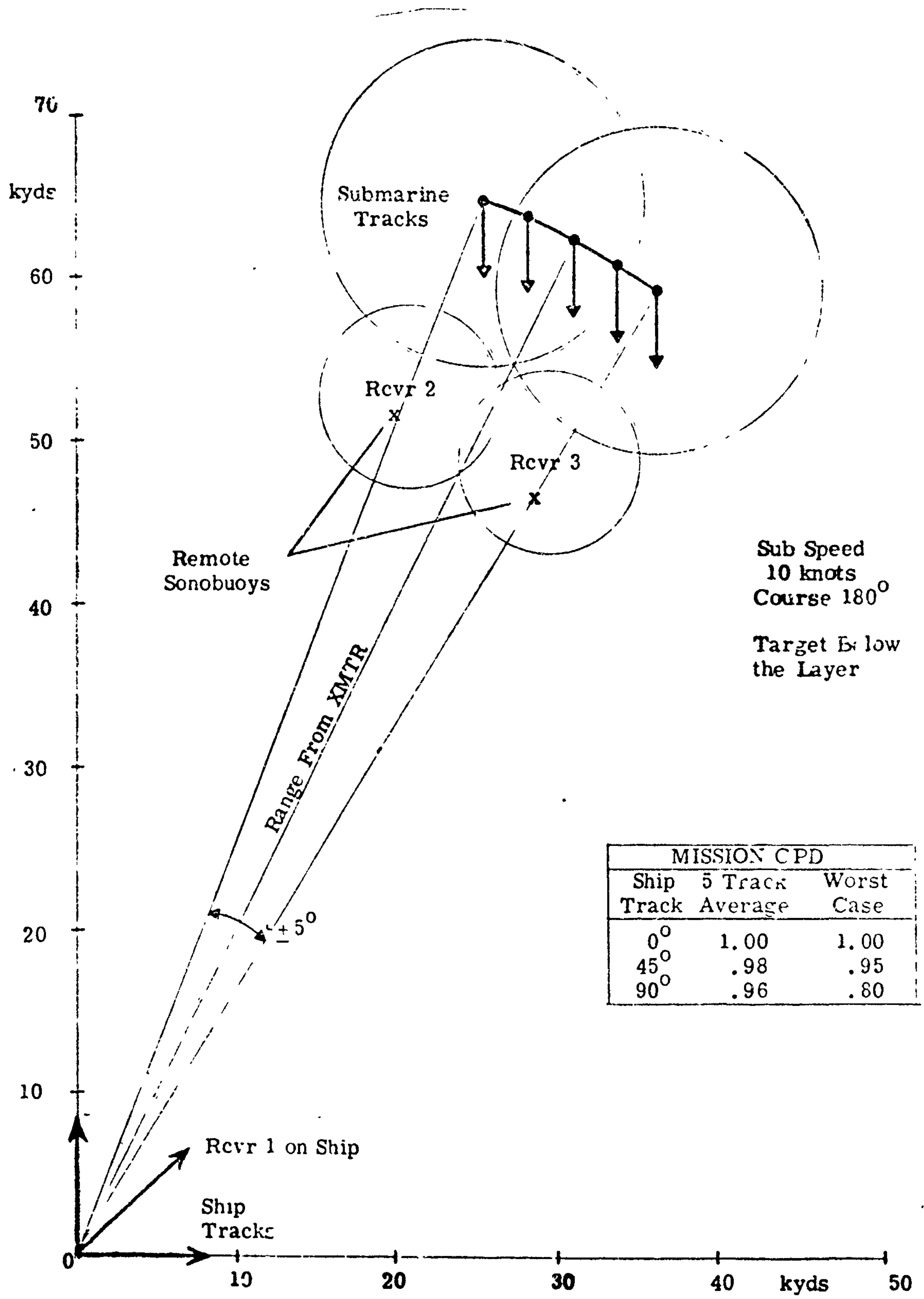

MISSION CPD		
Ship Track	5 Track Average	Worst Case
0°	1.00	1.00
45°	.98	.95
90°	.96	.80

Figure 4-7 (C) Convoy Screening Scenario - Target Heading 180°, Datum at 30°

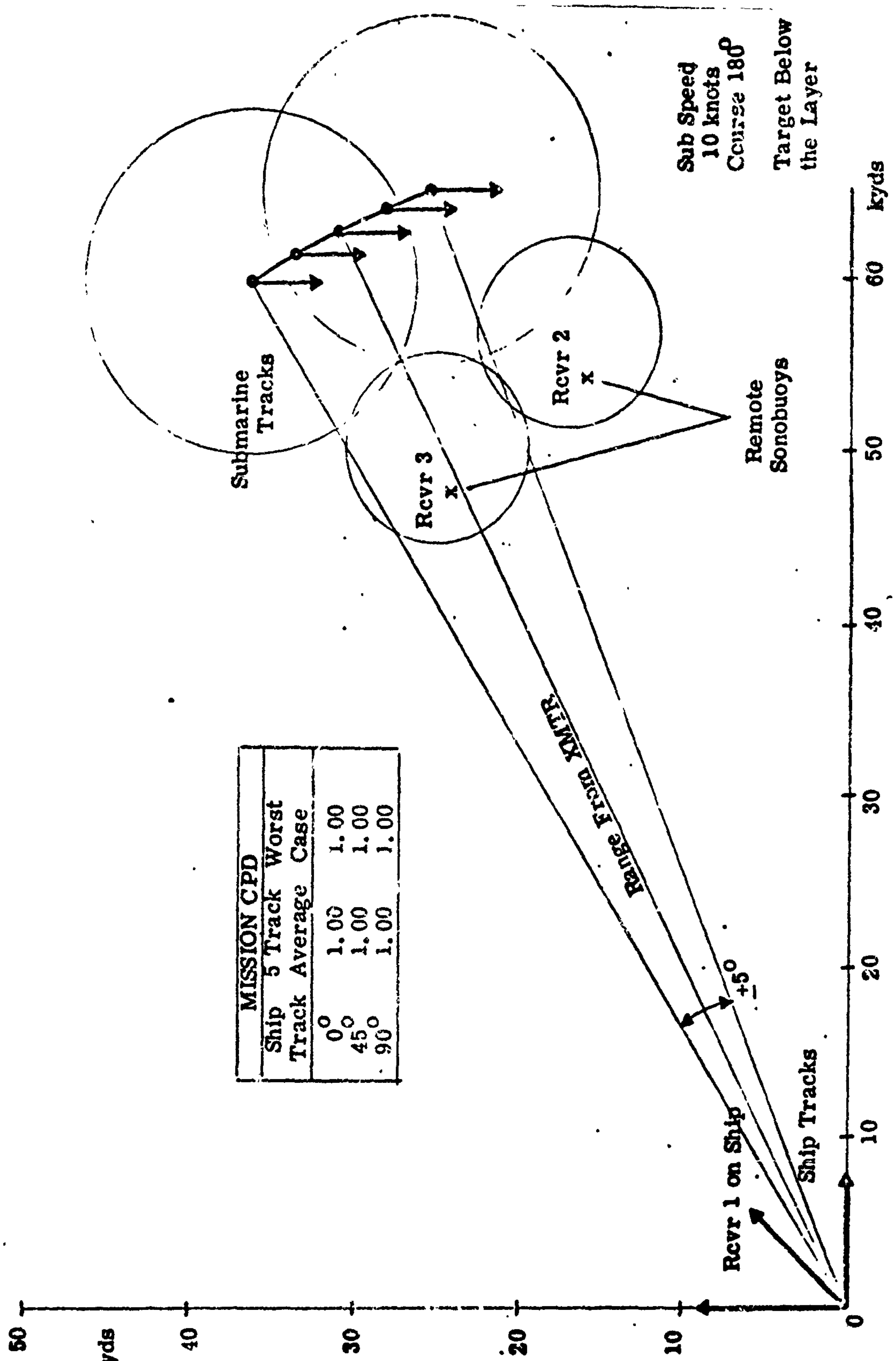

MISSION CPD		
Ship Track	5 Track Average	Worst Case
0°	1.00	1.00
45°	1.00	1.00
90°	1.00	1.00

Figure 4-8 (C) Convoy Screening Scenario - Target Heading 180°
Datum at 60°

Layer Depth 150 ft
Target Depth 250'
Sub Heading 180°
Sub Speed 10 knots

Δ Bistatic Performance (Rcvr 2)
X Bistatic Performance (Rcvr 3)
O Monostatic Performance

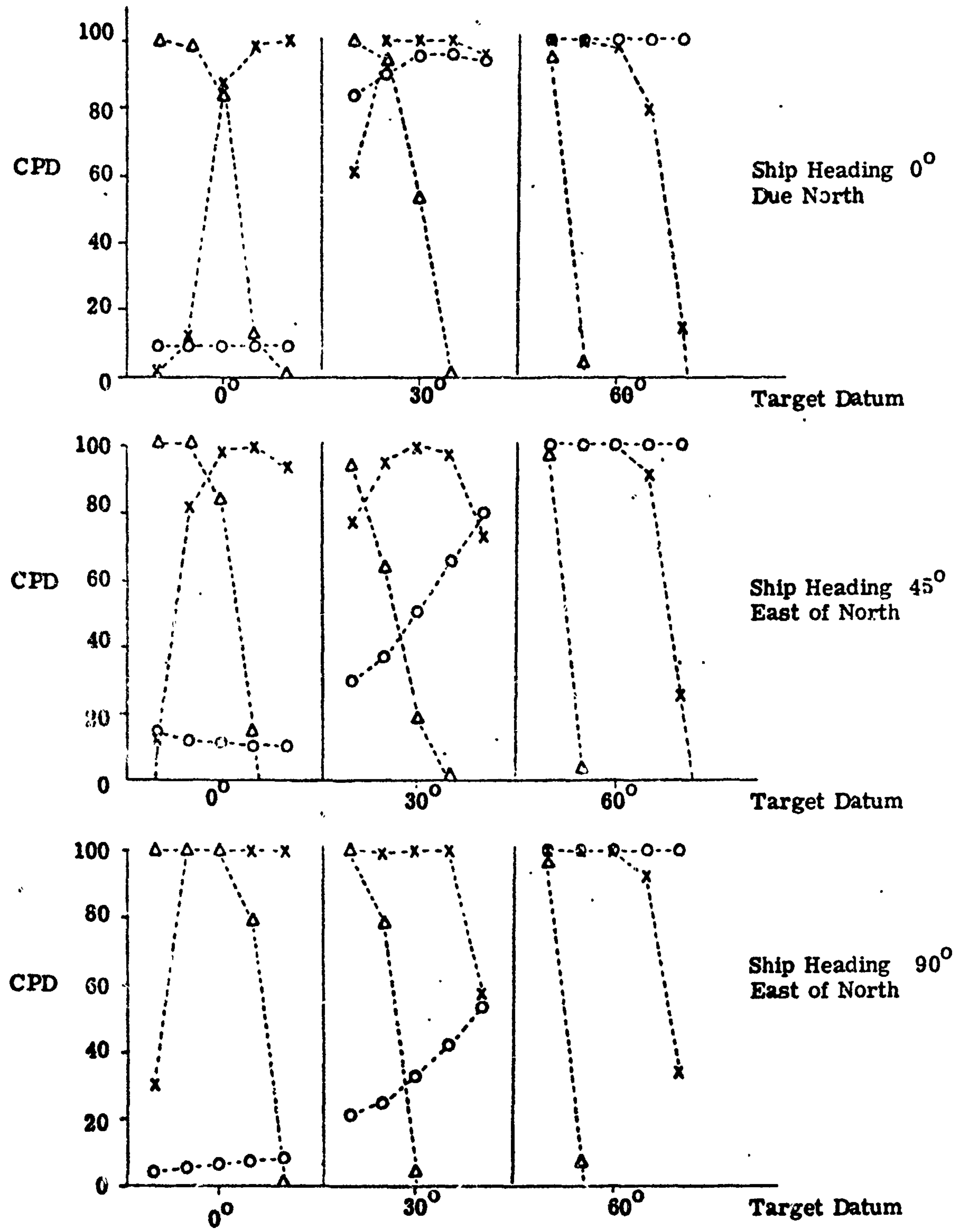

Figure 4-9 (C) Individual Receiver Performance in Convoy Screening Scenario

decreases. This result appears true in all cases and thus unless there are other reasons for doing so, it is not necessary or even wise for the ship to close the target.

(C) With a target datum at 30° the best results occur for a ship course of 0°. This is a demonstration of the effect of target aspect since this course causes the sub to present the best target aspect to the ship. The 90° course is clearly the worst because it tends to minimize the target aspect.

(C) For a datum at 60°, the mission CPD is quite good for all ship tracks primarily due to the high monostatic performance due to the target aspect. Bistatic performance is poor and it can be seen from the figures that this is due to a poor choice of locations for the buoys. The buoys in these and some other sets of exercises shown in the Appendix were placed so as to attempt to protect the full quadrant; however, it will be shown below that this can be accomplished more effectively using a somewhat different criterion for buoy placement. For targets on a a CPA course, it was found that the best results were obtained when the ship heading was determined in relation to the target datum. One buoy was planted with the sub and ship courses in mind. The data is shown in figures 4-10 through 4-13 and the results are very good except for the case of the ship heading straight at the target. Target datum beyond 25° are not analyzed since it has been shown earlier that these cases are easily covered due to improved target aspect in both the bistatic and monostatic modes.

(C) Figure 4-11, the geometry for ship tracks making an angle of 45° with respect to the datum illustrates a very effective concept. In a submarine CPA mode, if the ship's heading is chosen appropriately, the target can be made to travel along a path of minimum uncertainty. That is, the uncertainty of azimuth is $\pm 5^{\circ}$, but the tracks shown lie close to one another and thus the bistatic receiver is more effectively utilized.

(C) It is interesting to see the effect of a variation of target speed on the effectiveness of these same buoy plants for the ship heading of 45° relative to the datum. The performance was considerably reduced when the target had a speed of 15 knots. This is due to the change in target CPA heading which causes some tracks to run "inside" the buoy, causing it to be either outside the buoy coverage or in the area of specular interference.

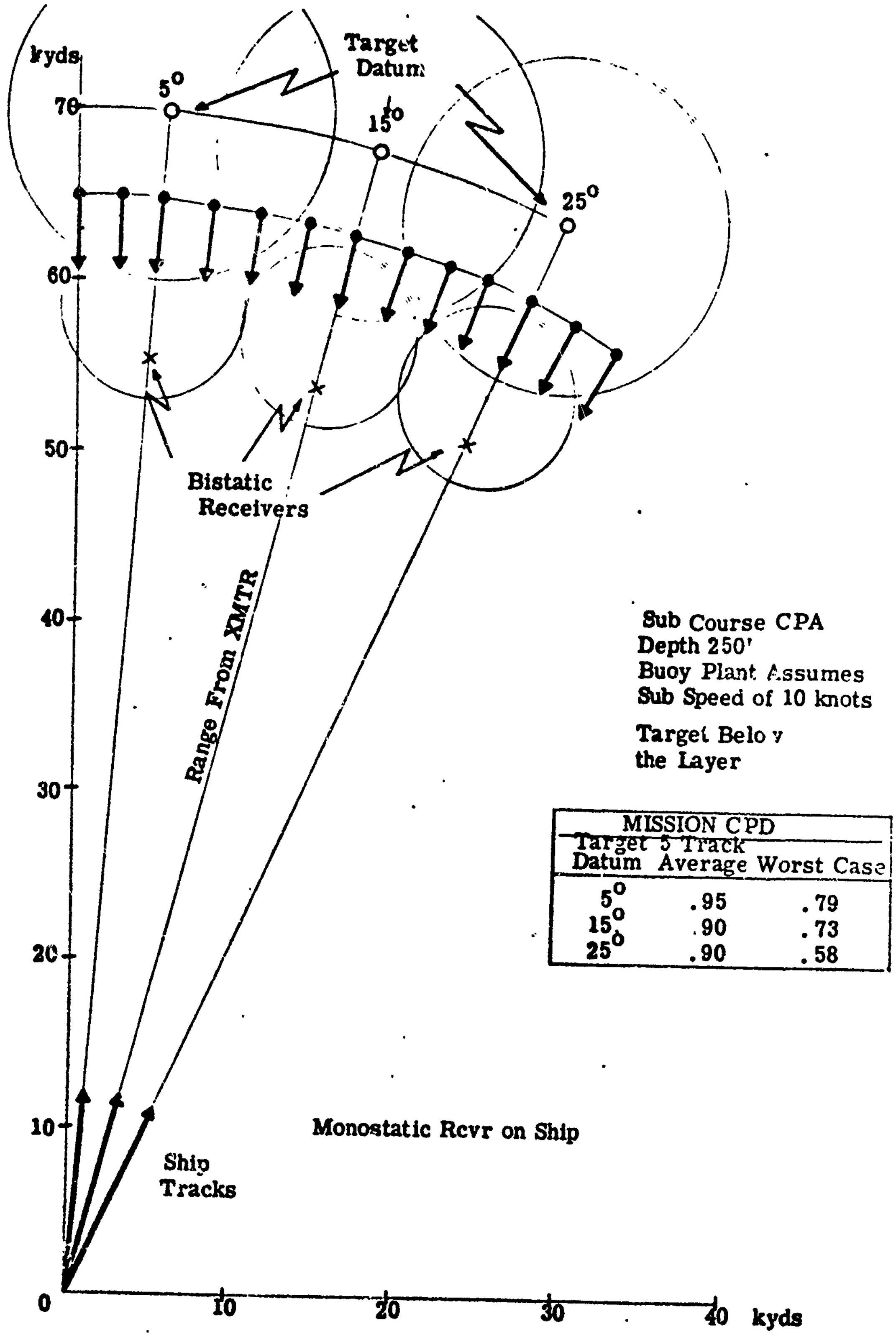

MISSION CPD

Target Datum	5 Track Average	Worst Case
5°	.95	.79
15°	.90	.73
25°	.90	.58

Figure 4-10 (C) Convoy Screening Scenario - Target Course CPA; Ship Course 0°

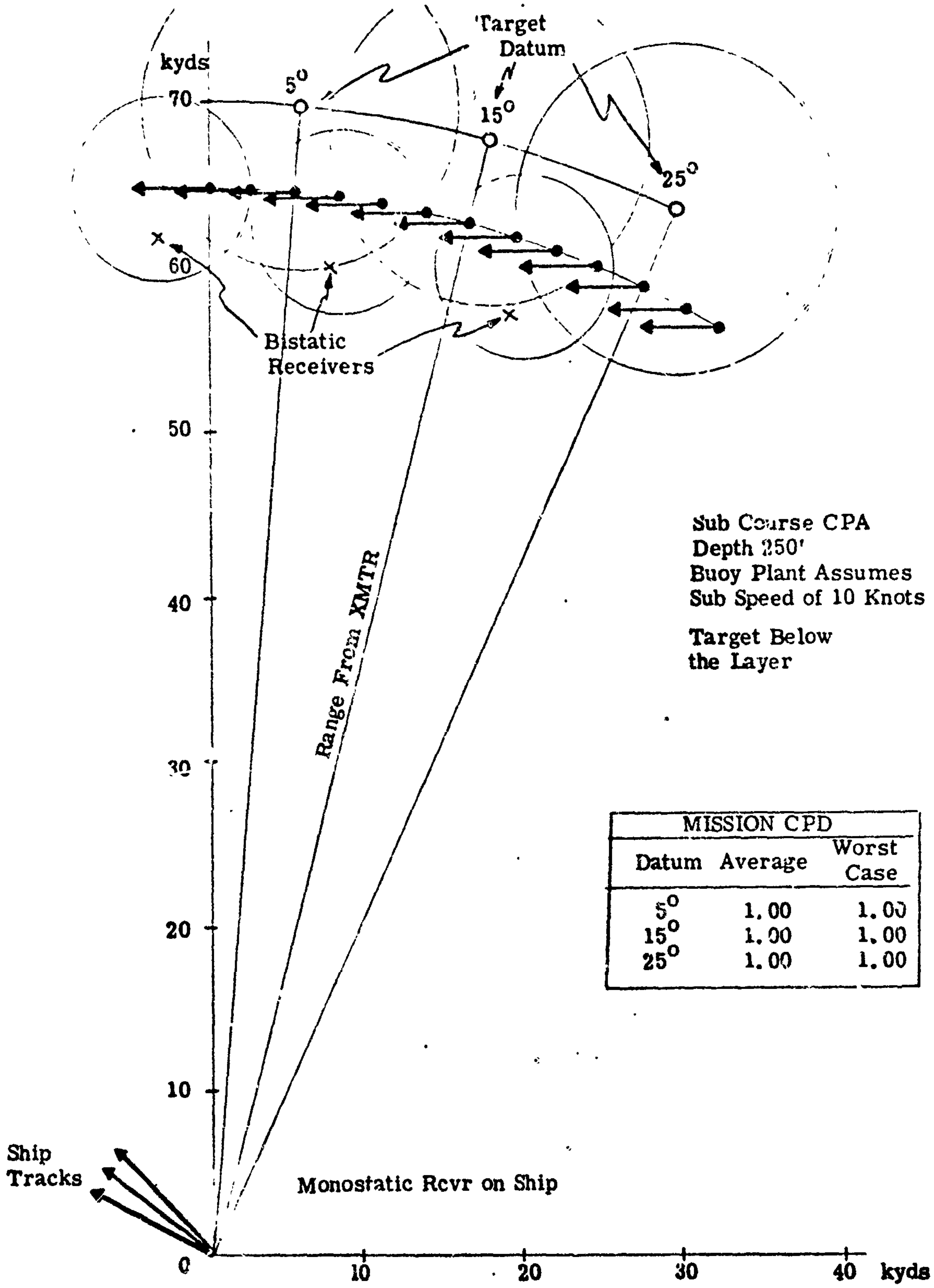

MISSION CPD		
Datum	Average	Worst Case
5°	1.00	1.00
15°	1.00	1.00
25°	1.00	1.00

Figure 4-11 (C) Convoy Screening Scenario - Target Course CPA; Ship Course 45°

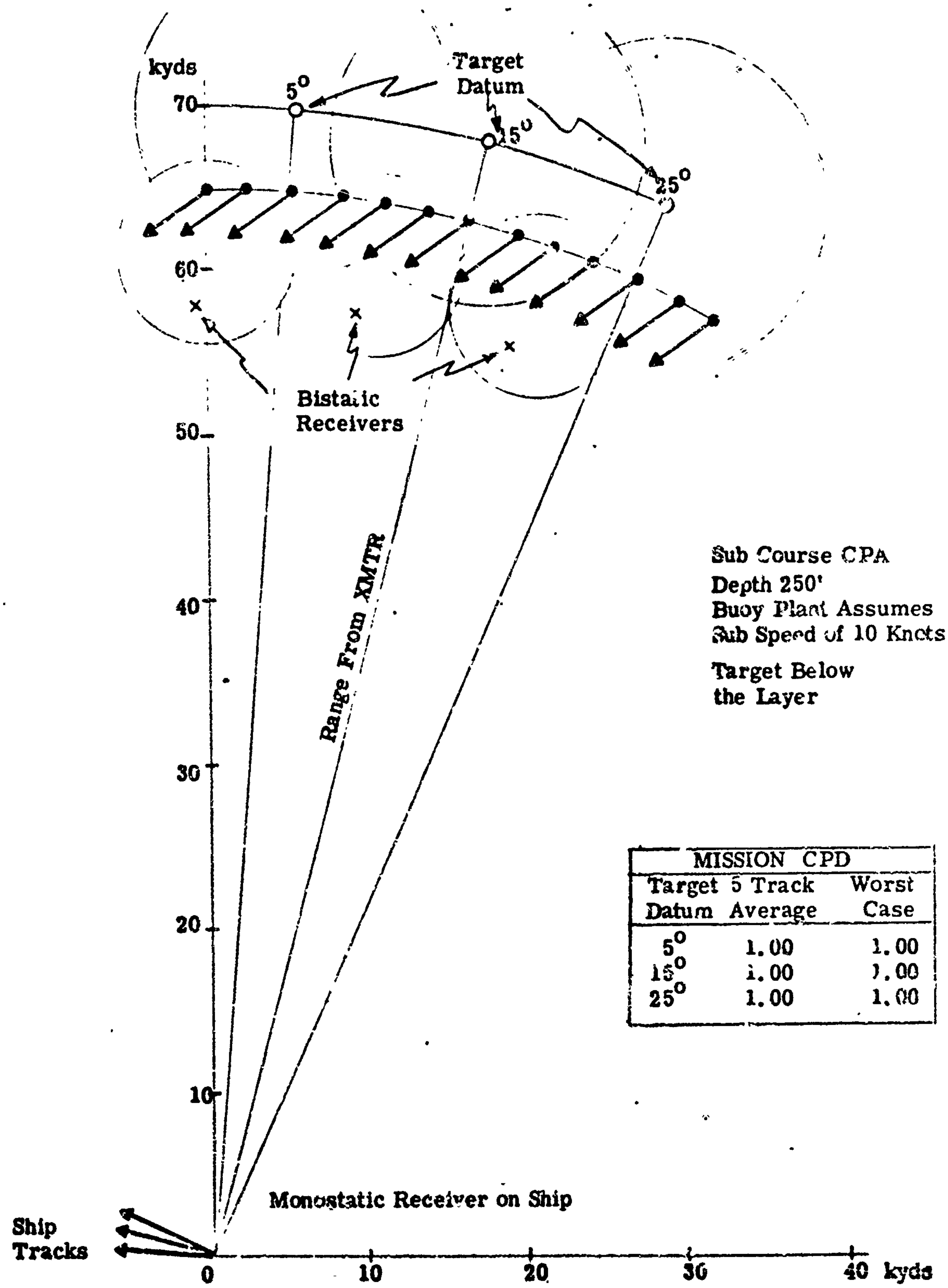

MISSION CPD		
Target Datum	5 Track Average	Worst Case
5°	1.00	1.00
15°	1.00	1.00
25°	1.00	1.00

Figure 4-12 (C) Convoy Screening Scenario - Target Course CPA; Ship Course 90°

Hazeltine Corporation

Figure 4-13

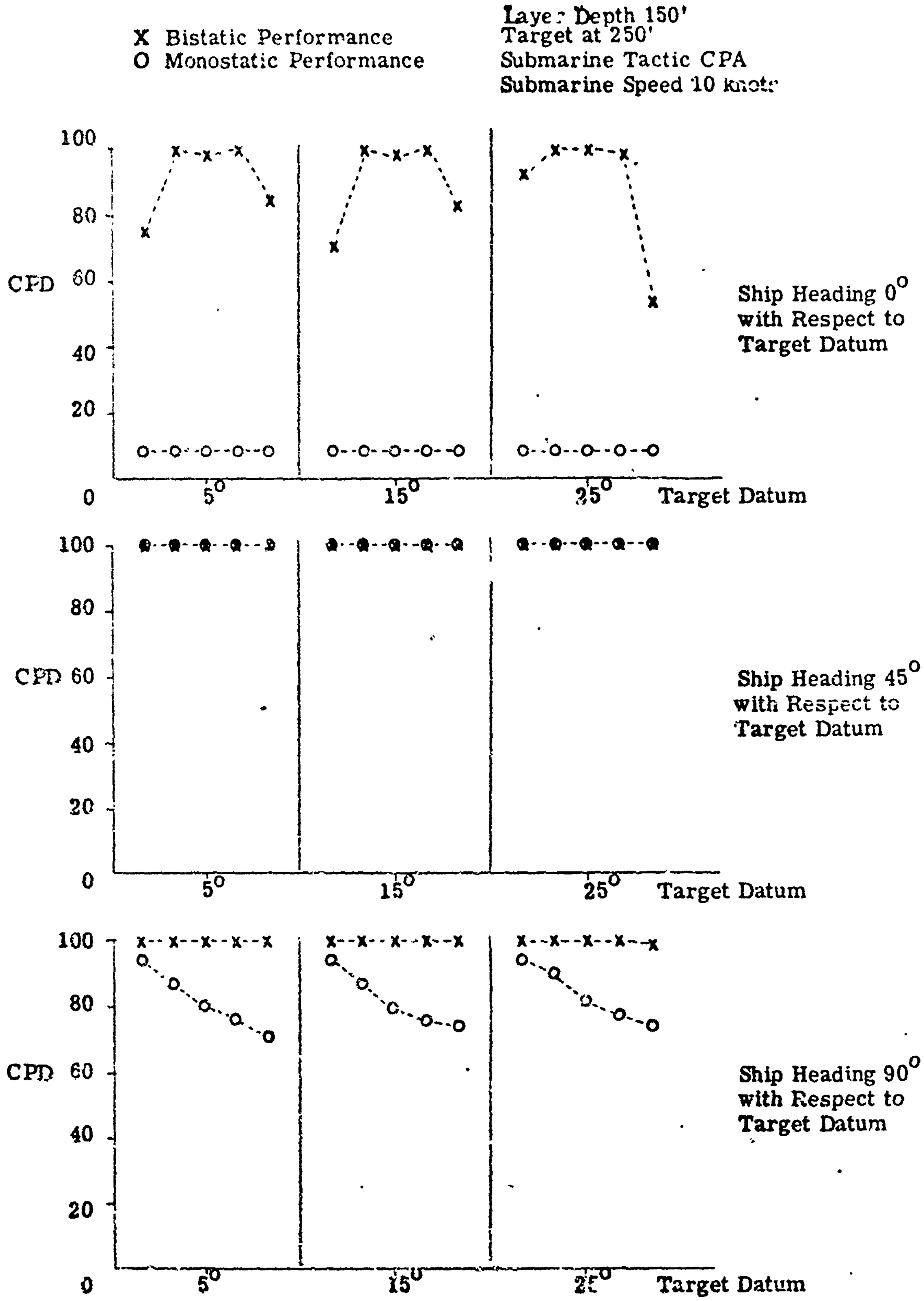

Figure 4-13 (C) Individual Receiver Performance in Convoy Screening Scenario

(C) A new buoy plant was tried to cover variations in target speed: near unity effectiveness was obtained for target velocities of 6, 10 and 15 knots. Thus, a signle buoy plant is extremely effective in detecting a target in the CPA mode regardless of the initial target datum.

(C) Earlier results have shown that two properly placed buoys can provide high effectiveness against a target traveling in a straight line toward the picket ship.

(C) In summary, for convoy screening, three buoys should be sufficient to prevent the penetration of a destroyer screen by any target once it has been detected in the convergence zone.

(C) An optimum strategy to accomplish the above is for the ship to follow a course which makes an angle of about 45° with respect to the target datum and to plant three sonobuoys, one which assumes a target track of CPA and two which assume a target track of 180°.

(C) For a submarine which chooses to follow a course other than CPA or 180° and which intends to attack the convoy further down range, an advancing screen can be used as illustrated in figure 4-14. This strategy forces the target to penetrate the buoy barrier in order to present a threat.

D. TARGET PROSECUTION SCENARIO

(C) Two scenarios are discussed here, one assumes an initial active CZ contact against a conventional submarine with an azimuthal undertainty of $\pm 5^{\circ}$. The second assumes a SOSUS detection against an SLBN target. Many computer runs were made to determine optimum buoy configuration and ship tactics and only the highlights will be presented in this section. A full summary of computer runs is contained in Appendix A.

(C) The goal of this analysis is to redetect a target which may attempt to evade the ship. This is accomplished for each scenario by calculating the cumulative probability of detection for each submarine track as the submarine runs in a different straight line track from the datum. For each target datum, 12 sub tracks are run with courses from 0° to 330° in steps of 30°. In order to verify that this was a fine enough sampling, one scenario was analyzed with 15° target track increments with little change in total mission effectiveness.

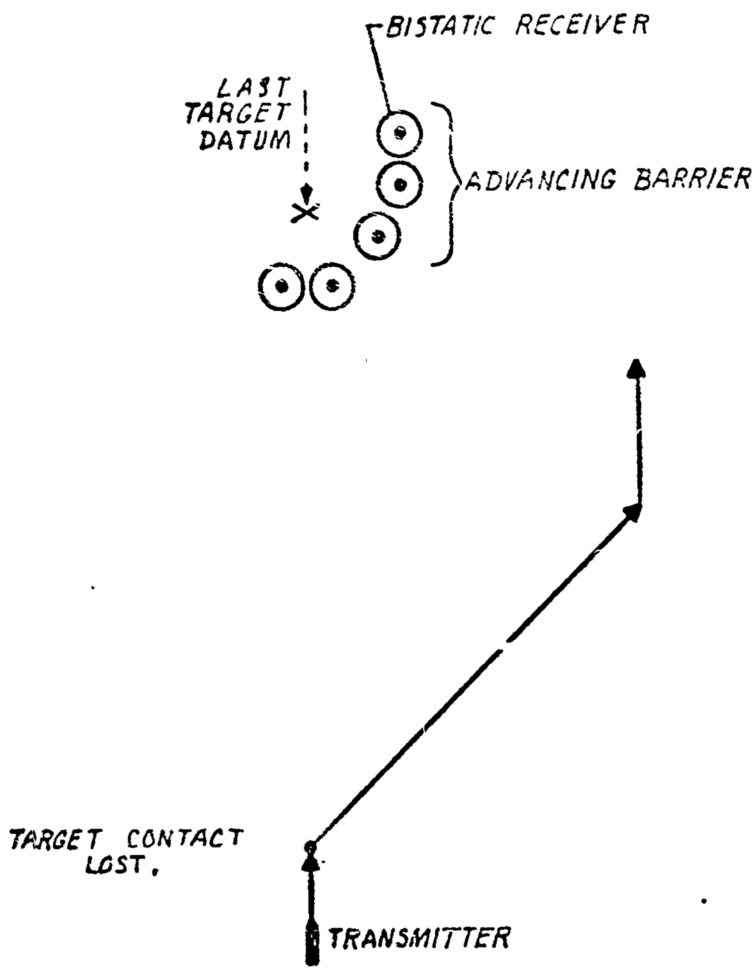

Figure 4-14 (C) Advancing Barrier for Convoy Screening

(C) Buoy plants were determined from 10^{o} target datum uncertainty plus time late considerations. Runs were made for target datum spanning 10^{o} uncertainty. There was little performance variation with actual target position across this uncertainty. Therefore, for subsequent analysis only one datum was considered.

(C) Each figure is self-contained in that the scenario and results are all contained on the illustration. The data in the upper right gives the scenario, system data and initial conditions. The sketch in the upper left shows the ship's track, the target datum and the buoys numbered in the order in which they are dropped by the helicopter. This is followed by one or more sets of radial lines which represent the various target tracks followed by the submarine from the indicated datum. The numbers located on the center of these lines represent the total mission effectiveness against a target following that track. (For an explanation of total mission effectiveness, see Section IV-C.) The numbers at the end of each line represent the cumulative probability of detection for each useful receiver for that track and the receiver number. (Thus, .95-6 means receiver 6 had a CPD of .95 for that target track.) The number M is the average of the total mission effectiveness over all the tracks and is thus most indicative of the success of the strategy used. P_{MULT} is the average multistatic effectiveness over all the tracks using only the highest individual CPD for each track. P_{BIST} is the same as P_{MULT} using only the highest bistatic receiver CPD. P_{MONO} is as above using only the monostatic system performance. P_{BIST} and P_{MONO} thus give a relative weight to the importance played by the monostatic receiver and the bistatic receiver in obtaining the total mission effectiveness. It will be observed in the following two sections that the SQS-26 monostatic system plays an important role in mission effectiveness when the target elects either to run toward the ship at an angle which results in a good target aspect or when the target moves away from the ship in such a manner as to keep it in the ship's CZ for some reasonable period of time. An intelligent target would probably avoid these courses but then the bistatic buoys will come into play more often.

(C) Several 6-buoy plants were tried and the best of these is shown in figure 4-15. While the performance is fairly good, there are several weak spots in the coverage and therefore 8-buoy plants were tried with several different ship tactics. The best of these is shown in figure 4-16. Here the total mission effectiveness is over 90 percent and this holds for target datum spanning the entire 10^{o} azimuthal uncertainty. The ship's strategy here is to run a dog-leg course towards the datum in order to maintain

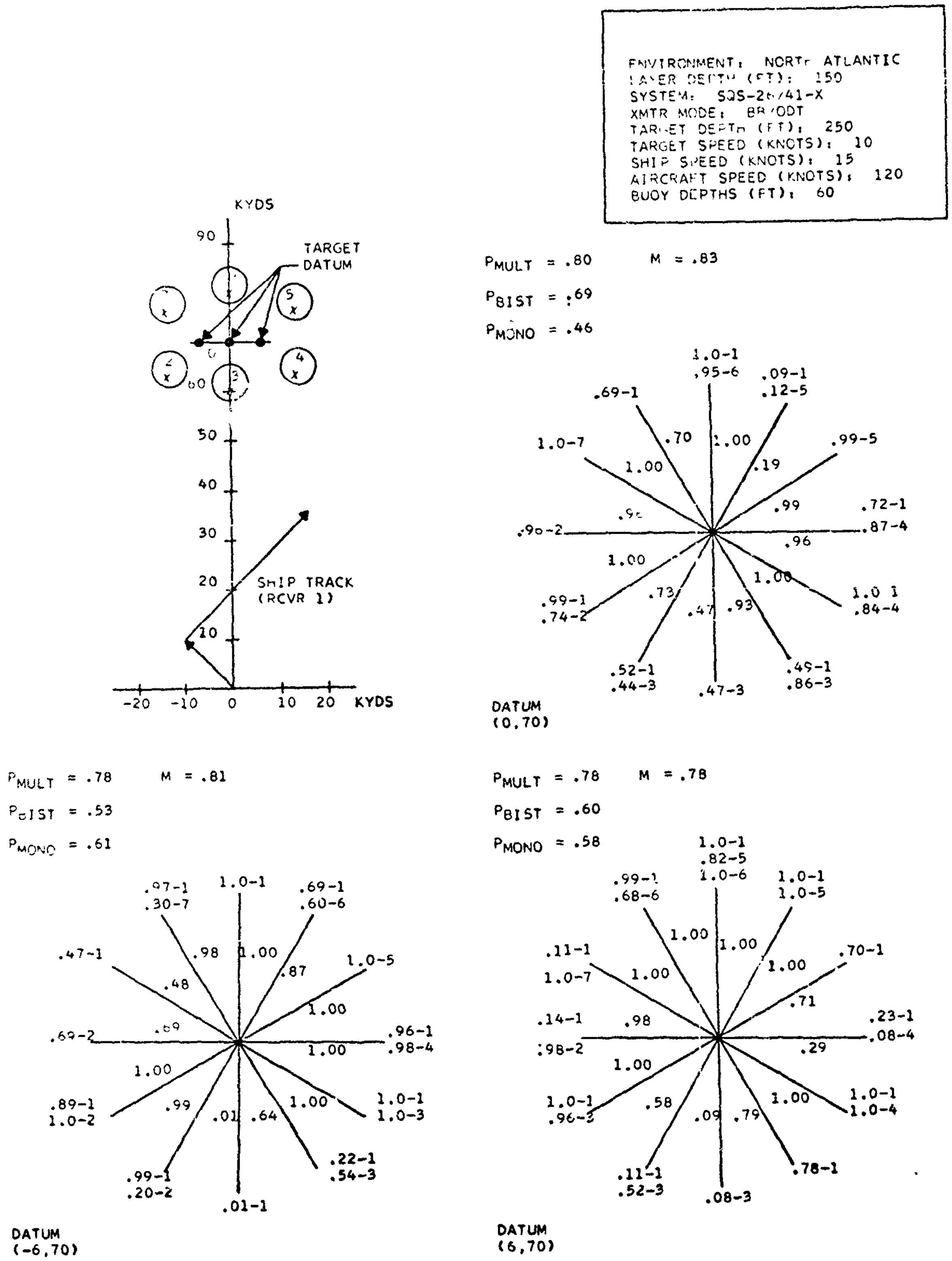

Figure 4-15 (C) Target Prosecution in North Atlantic; 6 Buoy Plant

ENVIRONMENT: NORTH ATLANTIC
LAYER DEPTH (FT.): 150
SYSTEM: S.S-26/41-X
XMTR MODE: RB/ODT
TARGET DEPTH (FT): 250
TARGET SPEED (KNOTS): 10
SHIP SPEED (KNOTS): 15
AIRCRAFT SPEED (KNOTS): 120
BUOY DEPTHS (FT): 60

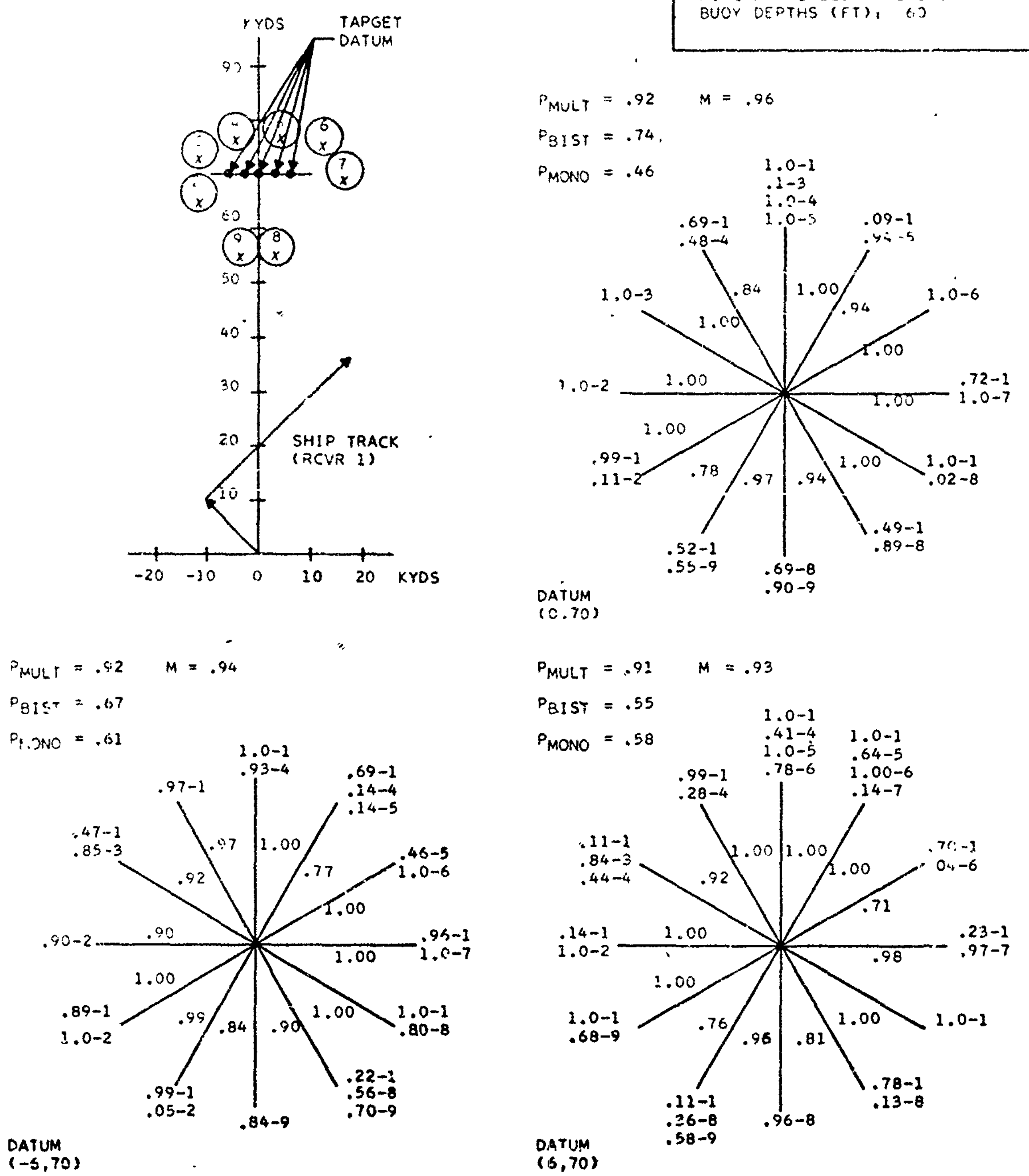

Figure 4-16 (C) Target Prosecution in North Atlantic; 8 Buoy Plant

CZ coverage for targets running away from the ship while not closing too rapidly on targets headed towards the ship. The buoys are planted on a spiral determined by the time late of the 120 knot helicopter at each location. Gaps in buoy coverage are left where monostatic detection is virtually assured due to a closing target with good aspect. This particular plant was analyzed in detail and the remainder of the runs are shown in Appendix A.

(C) An important result found here is that in about 50 percent of the cases the target is detected simultaneously by two or more receivers and thus localization is possible. Such a localization could be followed up either by a weapons drop or by a MAD sweep followed by a weapons drop.

(C) In order to investigate the effects of time late, several scenarios were run assuming rocket launched sonobuoys where the delivery speed was about 1400 knots. This significantly reduces the time late spiral and thus reduces the number of buoys required for detection.

(C) In this case, it was found that 3 buoys were sufficient to give performance equal to that of 8 helo-dropped buoys. This run is shown in figure 4-17 where it was found best to run the ship straight at the datum at a reduced speed of 6 knots, which maximizes the time the target remains in the CZ.

(C) Because of the much smaller uncertainty area when using rocket launched sonobuoys, it is possible to operate the SQS-26 in the BB/TRACK mode where it has a source level of 142 dB and reduced reverberation interference. This will result in increased buoy coverage and now two buoys will give the coverage of the 3 used previously.

(C) In this BB/TRACK mode of the SQS-26 (AX) or (CX) the monostatic performance is considerably increased. However, the bistatic receivers are still required in order to hold the target for localization.

(C) Target prosecution studies were also carried out against an SLBN type submarine. The SLBN is considerably larger than a conventional submarine and is assumed to average 5 dB more target strength. CZ contact prosecution of such a target was considered trivial, based on results for a conventional submarine. Instead, a brief study was made to determine the uncertainty area which could be covered by 8 buoys against an SLBN.

Hazeltine Corporation

Figure 4-17

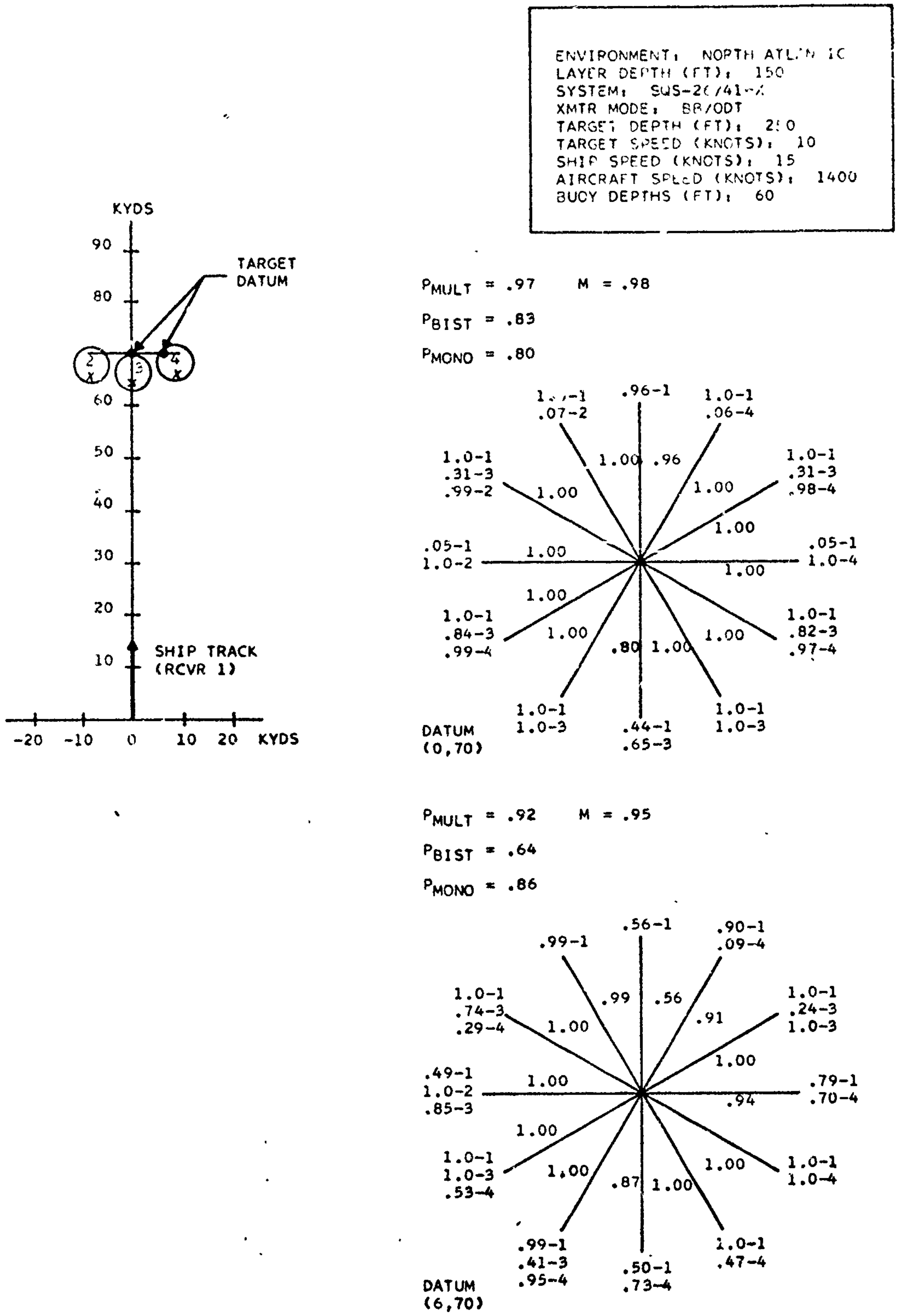

Figure 4-17 (C) Target Prosecution in North Atlantic; 3 Rocket-Launched Buoys

(C) The buoy plant is shown in figure 4-18 along with some of the target tracks run. The ship is assumed to be about 90 kyd from the center of the uncertainty area and thus its tactic is to first make a high speed sprint towards the datum and then slow down to a speed of 15 knots. This avoids the possibility of the sub running outside the range of the SQS-26 transmitter.

(C) Thirteen target tracks were run for each target direction; one at the center of the uncertainty area, and four each on circles of radii 10, 20, and 30 kyds.

(C) The results for these runs are shown in figure 4-19. With the exception of a few weak spots, the effectiveness of the multistatic system against this type of target is quite good. These results could probably be improved even more if the buoy plant were slightly modified.

(C) Thus, it appears that a multistatic system comprised of the SQS-26 and 8 remote sonobuoys can be effective against an SLBN in an uncertainty area of about 700 nm^2 (a radius of 15 nm). This area could be increased even more by utilizing two ships and increasing the spacing of the buoys.

(C) For purposes of comparison, an analysis of the CASS system was made in the same scenario as that of the SQS-26/41-X system shown in figure 4-16. The performance of the system against a 300' target is illustrated in figure 4-20. Additional target depths of 55' and 600' were analyzed; these results appear in the appendix.

(C) The operations analysis model cannot presently be used to analyze CW systems and therefore the CASS system was analyzed in the FM mode even for high (10 knot) doppler targets. Use of an acoustic program developed to analyze CW systems shows that the range coverage of the CASS buoy in the CW mode is almost identical to the coverage in the FM mode as shown in figure 4-5. The variation of coverage with target aspect in the FM system does not correspond to variations of coverage due to target doppler. The difference is that the CW system would contact the target somewhat sooner (as the target was approaching the buoy). then lose it temporarily (target at beam aspect) and then again contact the target as it started moving away from the buoy. The net area coverage however predicts almost identical system performance. Thus, the analysis of the CASS system can be accomplished using FM predictions.

Environment: North Atlantic
Layer Depth (ft): 150
System: SQS-26/41-X
Xmtr Mode: BB/ODT
Target Depth (ft): 250
Target Speed (knots): 10
Ship Speed (knots): 30/15
Aircraft Speed (knots): 120

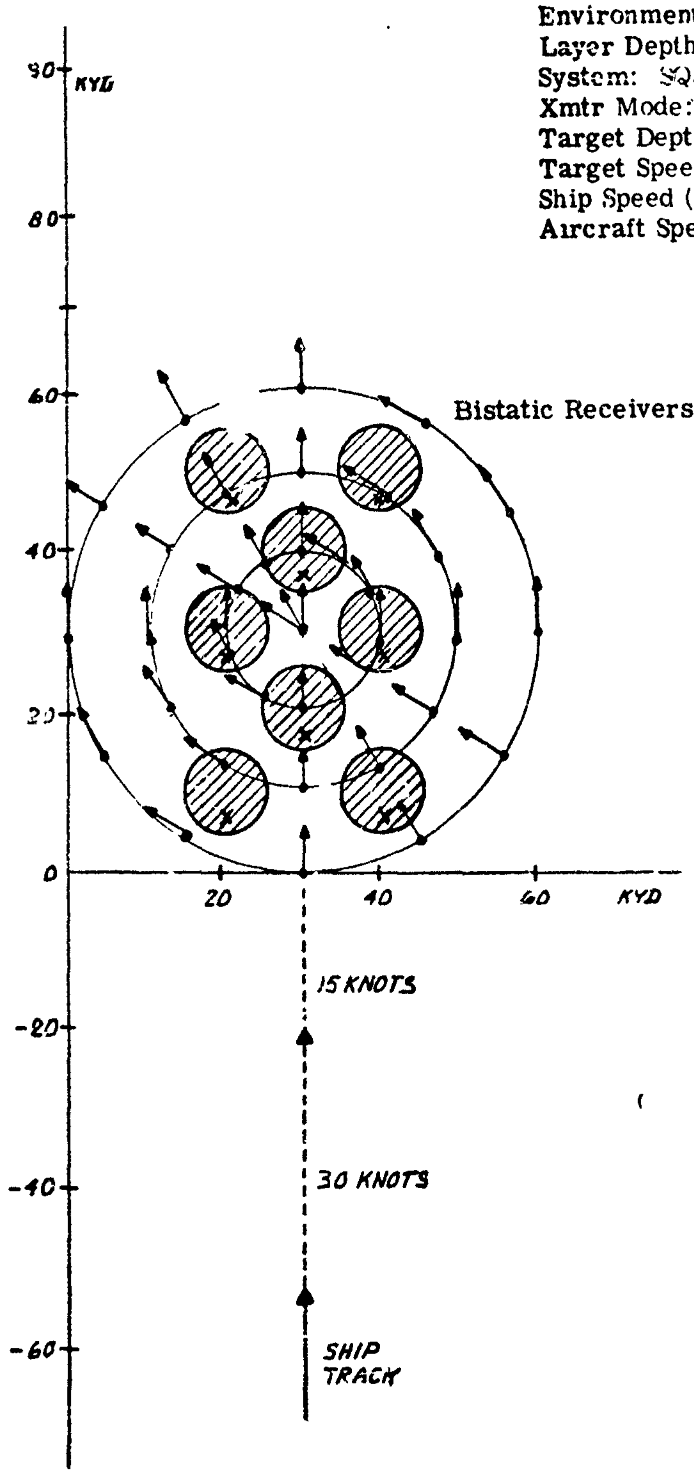

Figure 4-18 (C) Scenario for Anti-SLBN Analysis in North Atlantic

Hazeltine Corporation

First Run Is in Center, Then 4 Runs Each on Circles of Radii 10, 20, 30 kyds. Runs on Each Circle Go Clockwise Starting with Datum in Direction of Target Track

	180°		210°		240°		270°		300°		330°		360°	
Run	MONO	MULTI	MONO	MULTI	MONO	MULTI	MONO	MULTI	MONO	MULTI	MONO	MULTI	MONO	MULTI
1	.65	1.00	1.00	1.00	1.00	1.00	1.00	1.00	1.00	1.00	.97	1.00	.74	1.00
2	.44	.70	1.00	1.00	1.00	1.00	1.00	1.00	1.00	1.00	.75	1.00	.41	.86
3	.81	1.00	1.00	1.00	1.00	1.00	1.00	1.00	1.00	1.00	.99	1.00	.81	.97
4	.71	.99	1.00	1.00	1.00	1.00	1.00	1.00	1.00	1.00	1.00	1.00	.82	96
5	.81	1.00	.93	1.00	1.00	1.00	1.00	1.00	1.00	1.00	.87	1.00	.81	.97
6	.03	.15	1.00	1.00	1.00	1.00	1.00	1.00	.97	.97	.49	.53	.24	.24
7	1.00	1.00	1.00	1.00	1.00	1.00	1.00	1.00	1.00	1.00	1.00	1.00	.93	1.00
8	.73	1.00	.99	1.00	1.00	1.00	.90	1.00	1.00	1.00	.99	1.00	.42	1.00
9	1.00	1.00	.63	1.00	1.00	1.00	1.00	1.00	.97	1.00	.85	.86	.93	1.00
10	.00	.00	1.00	1.00	1.00	1.00	1.00	1.00	.86	.86	.18	.18	.06	.06
11	1.00	1.00	1.00	1.00	1.00	1.00	1.00	1.00	1.00	1.00	1.00	1.00	.98	.98
12	.53	.99	.88	1.00	1.00	1.00	1.00	1.00	1.00	1.00	.89	1.00	.00	.96
13	1.00	1.00	.55	.99	.39	.39	1.00	1.00	.64	.66	.94	.94	.98	.98
Avg.	.67	.83	.92	1.00	.95	.95	.92	.92	.96	.96	.84	.88	.62	.84

Data for SLBN Analysis

Figure 4-19 (C) Mission Effectiveness for Anti-SLBN Analysis

ENVIRONMENT: NORTH ATLANTIC
LAYER DEPTH (FT): 150
SYSTEM: SQS-26/CASS
XTR MODE: BB/ODT, DP
TARGET DEPTH (FT): 300
TARGET SPEED (KNOTS): 10
SHIP SPEED (KNOTS): 15
AIRCRAFT SPEED (KNOTS): 120
BUOY DEPTHS (FT): 1500

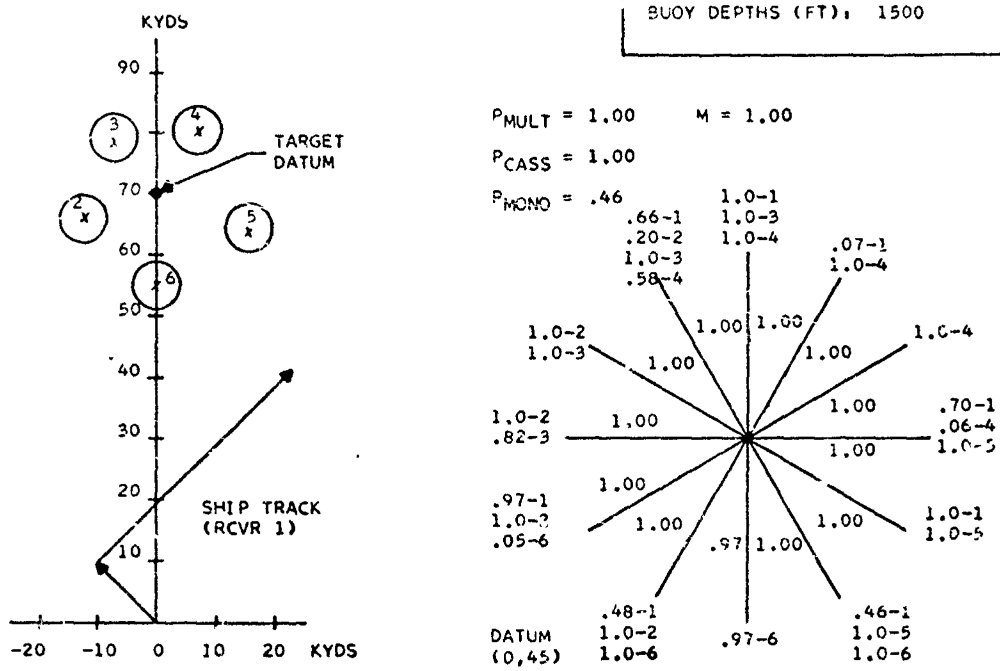

Figure 4-20 (C) CASS System for Target Prosecution in North Atlantic

(C) In the North Atlantic, it is found that the SQS-26/41-X system operates best with the receivers at 60' because the deep (1500') bistatic receivers have more reverberation. Reverberation is not a major problem for the CASS system; the deep system performs better against below layer targets than the shallow (60') CASS system because of improved propagation conditions.

(C) Five CASS buoys were deployed around the same time late spiral as that used for the bistatic case. The system effectiveness is shown in figure 4-20. Comparing these results with those of figure 4-16, it is clear that equivalent performance could probably be achieved with only 4 CASS buoys.

(C) The CASS system was also analyzed for targets at 55' and 600'. For the deeper target, there is little difference in system performance. For a target at 55', however, the CASS system at 1500' performs somewhat poorly due to the target being in the layer and the non-reciprococity of shadow zone propagation to a directional buoy with a depression angle of 0^{o}. In contrast, the bistatic system with a shallow receiver will perform well against an in-layer target. This situation could, of course, be remedied by deploying CASS at 60' but then the performance for below layer targets would suffer.

(C) To compare the bistatic receivers with CASS is not straightforward. CASS alerts the target to the fact that the localization process has begun. In addition, detection of high speed targets (greater than 15 knots) would require the delivery of passive buoys (e.g., SSQ-41). Different target depths also affect the comparison as shown above.

(C) Ignoring these differences, we may compare the systems on the basis of four CASS buoys to eight 41-X buoys.

(C) The cost of a CASS buoy is around $800 while that of the 41-X is about $100. Thus, the bistatic system has a cost effectiveness advantage of four-to-one over CASS. From a tactical point of view, the bistatic system is superior in that a target hearing an active source pinging at close range will alter its course to present a reduced aspect to that buoy thus reducing buoy performance, while in the bistatic system the transmitter is at a large distance and the target has no way of knowing whether it has been detected. If the ship cannot get within CZ distance of the target in time, then CASS would be the better system for target prosecution because it is a self-contained system needing only an aircraft to deliver it. Except for this case, however, it appears that the bistatic system is superior to CASS for target prosecution.

SECTION V (C)

MEDITERRANEAN OPERATIONS ANALYSIS

A. ENVIRONMENT DESCRIPTION

(U) Two Mediterranean environments were studied; one where a 100' layer was present typical of the months from October to March, and another where no layer was present which is usual for the months from April to September. The parameters describing the environments studied are shown below:

WINTER

Water Depth (ft)	12000.0	
DSL Depth (ft)	150.0	1000 (day)
Layer Depth (ft)	100.0	
Bottom Scat. Coef. (dB)	-28.0	
DSL Scat. Coef. (dB)	-50.0	-60.0 (day)
Wind Speed (knots)	13.0	
Sea State	3.0	
MGS Bottom Class	3	

Hazeltine Corporation

VELOCITY PROFILE

Depth (ft)	Velocity (ft/sec)	Gradient (ft/sec/ft)
0.0	5024.6	
		.0250
100.0	5027.1	
		-.8140
150.0	4986.4	
		-.1340
200.0	4979.7	
		-.0200
350.0	4976.7	
		.1967
380.0	4982.6	
		.0075
500.0	4983.5	
		-.0140
700.0	4980.7	
		.0168
12000.0	5170.3	

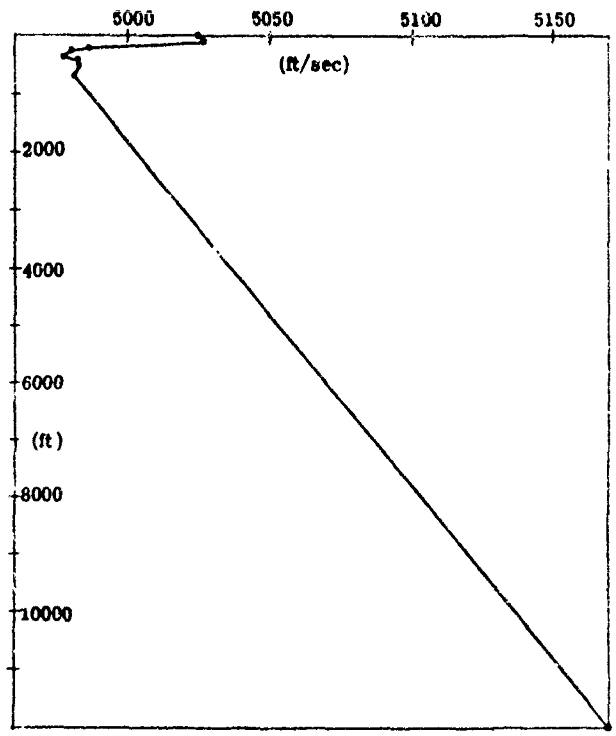

SUMMER

Water Depth (ft)	12000.0
DSL Depth (ft)	500.0
Layer Depth (ft)	0.0
Bottom Scat. Coef. (dB)	-28.0
DSL Scat. Coef. (dB)	-50.0
Wind Speed (knots)	13.0
Sea State	3.0
MGS Bottom Class	3

VELOCITY PROFILE

Depth (ft)	Velocity (ft/sec)	Gradient (ft/sec/ft)
0.0	5024.1	
		-.0125
80.0	5023.1	
		-.0467
140.0	5020.3	
		-.6767
200.0	4979.7	
		-.0450
500.0	4966.2	
		.0118
1000.0	4972.1	
		.0136
3000.0	4999.3	
		.0165
6000.0	5048.7	
		.0170
12000.0	5150.5	

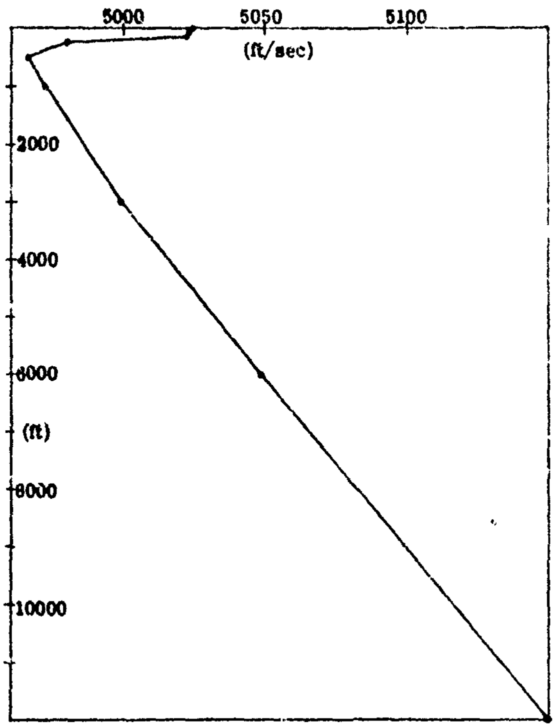

B. ACOUSTIC PERFORMANCE

(C) The coverage of a bistatic receiver at a depth of 60' and separated from the SQS-26 transmitter by 25 kyds in an environment with a layer is shown in figure 5-1. The very broad coverage is a good indicator that the system will perform very well in this environment. The odd shape of the contour is due to the start of the CZ at a range of 32 kyds from the transmitter. As the bistatic separation increases to 45 kyds, the coverage becomes more circular with the width reduced by about 30 percent. For deep receivers (1500') the coverage for below layer targets is better than for shallow receivers; however, for in-layer targets the coverage area is only about 6 kyds in diameter..

(C) For a velocity profile with no layer, the coverage for a 60' buoy is shown in figure 5-2. This poor coverage is due to the fact that there is a shadow zone caused by the receiver being near the surface but there is no surface duct to propagate energy for scattering into this shadow zone.

Hazeltine
Corporation

Figure 5-1

Mediterranean
Depression Angle 5°
BB/ODT
100' layer Depth
55'/300' Target Depths
120° Sector Insonification
Target Strength 15 dB
Receiver Depth 60'

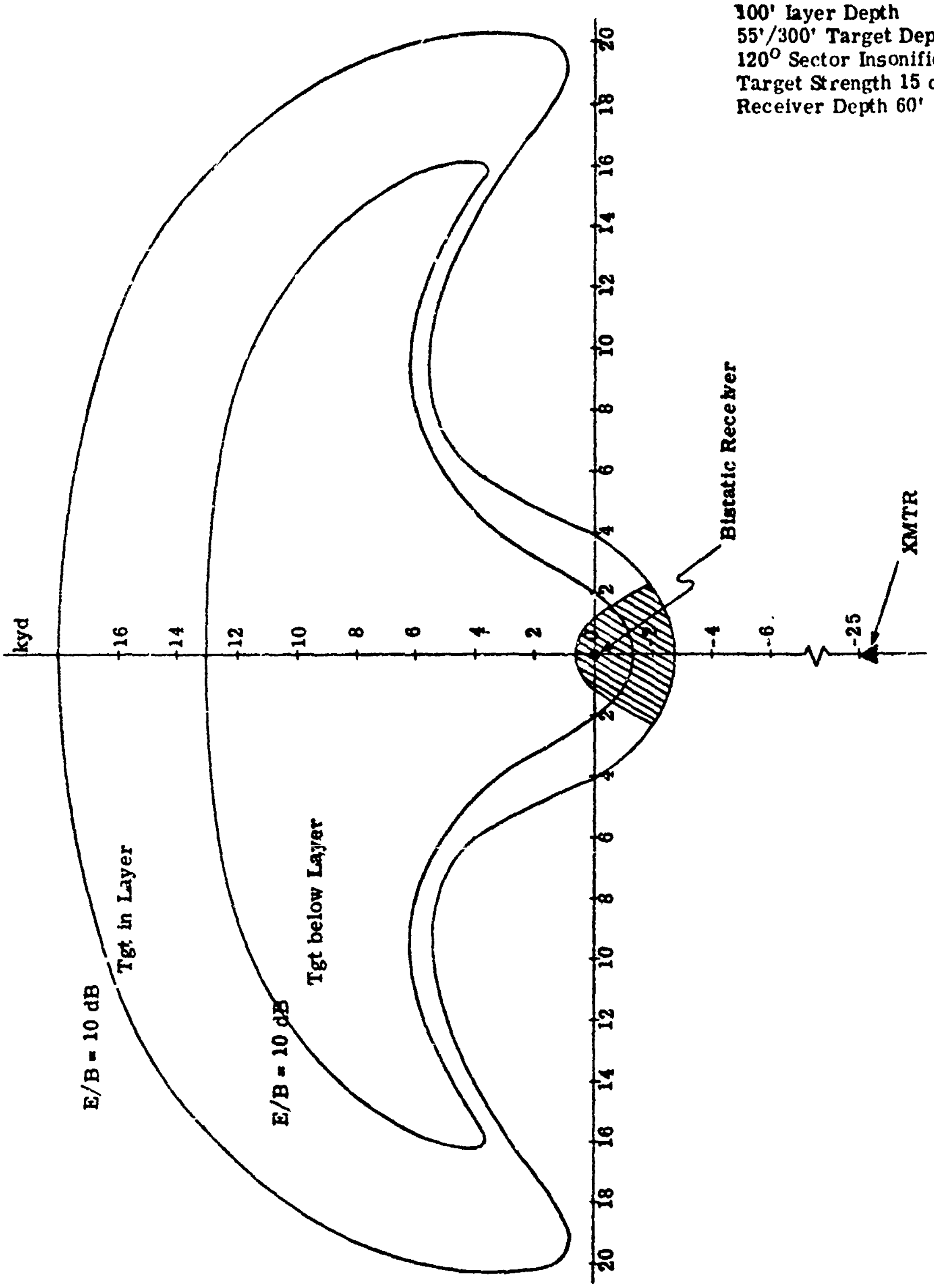

Figure 5-1 (C) Coverage of 41-X Sonobuoy; Mediterranean with Surface Duct; Receiver at 60'

Hazeltine
Corporation

Figure 5-2

Mediterranean
Depression Angle 5°
BB/ODT
No Layer
55'/300' Target Depths
120° Sector Insonification
Target Strength 15 dB
Receiver Depth 60'

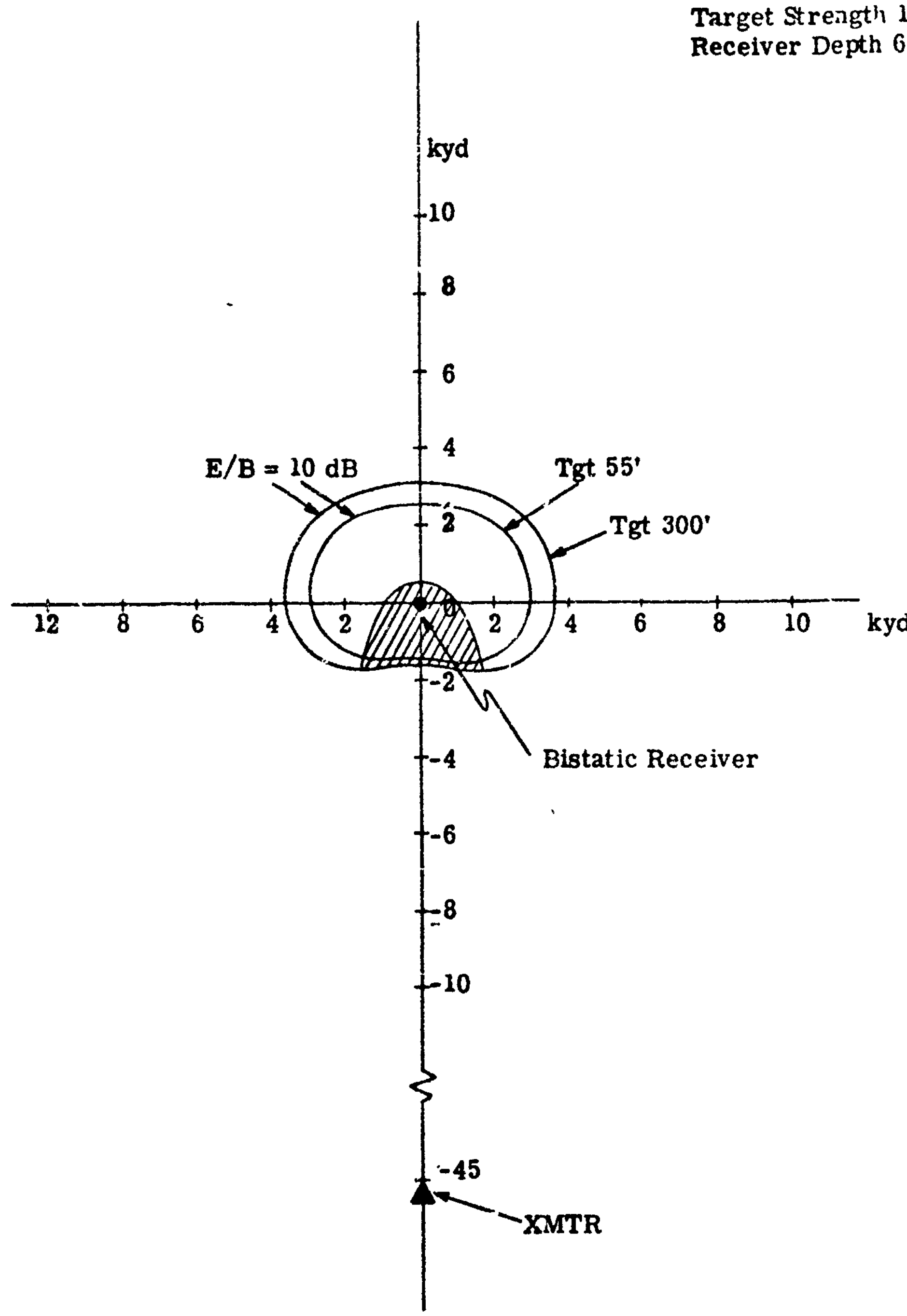

Figure 5-2 (C) Coverage of 41-X Sonobuoy; Mediterranean with No Surface Duct; Receiver at 60'

(C) For a deep receiver in this environment, the coverage is much improved as shown in figure 5-3.

(C) Another interesting fact about these environments is that a receiver at 1500' is in a depressed sound channel and therefore propagation losses from a target to the receiver are quite low over very long ranges so performance is limited in this case mainly by the losses in the transmitter/ target path.

(C) Because the critical depths in the Mediterranean environments are only about half that of the North Atlantic, the CZ appears at about half the range of that in the Atlantic. The CZ's begin at about 32 and 36 knots respectively for profiles with and without a layer and reach out to about 57 kyds. This very broad CZ allows virtually all detections to be made in the CZ area and the resulting system performance can be expected to be quite good. Because of the appearance of the first CZ at 32 kyds, it was considered feasible to investigate the possibility of target contact and prosecution in the second CZ which starts at 64 kyds and extends out beyond 80 kyds. As will be seen below, this performance turns out to be fairly good.

(C) It is interesting to compare the performance of the multistatic system when the SQS-26 is replaced by the SQS-23. Figure 5-4 shows the relative monostatic performance of the 26 and 23 in the Mediterranean. It is clear from the figures that the monostatic performance of the 26 will be very good resulting in near unity cumulative detection probabilities for targets which pass through the zone. SQS-23 coverage is considerably smaller and this performance will be correspondingly lower.

(C) Figure 5-5 shows the coverage of a bistatic receiver using the SQS-23 as transmitter. Comparing this with figure 5-1, the performance using the SQS-26, gives a good indication of the decreased performance to be expected in exercises using the SQS-23/41-X multistatic system.

C. SCREENING SCENARIO IN THE MEDITERRANEAN

(C) Very little need be said about the effectiveness of convoy screening in this environment. If a comparison is made of the buoy coverages in the North Atlantic and Mediterranean and it is recalled that convoy screening is very successful in the North Atlantic, then it must be concluded that screening operations in the Mediterranean will be highly successful and the same doctrine could be used here.

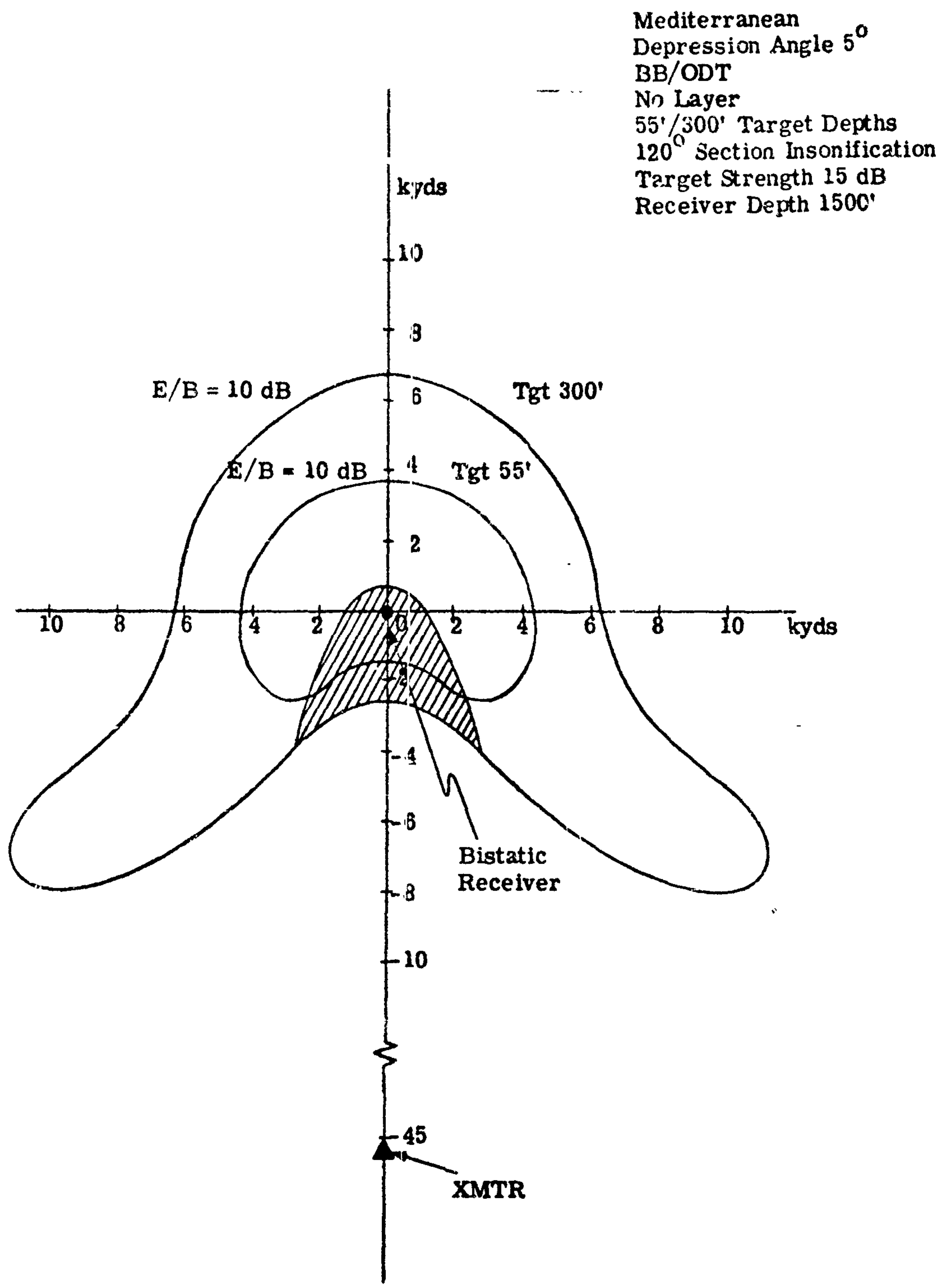

Figure 5-3 (C) Coverage of 41-X Sonobuoy; Mediterranean with no Surface Duct; Receiver at 1500'

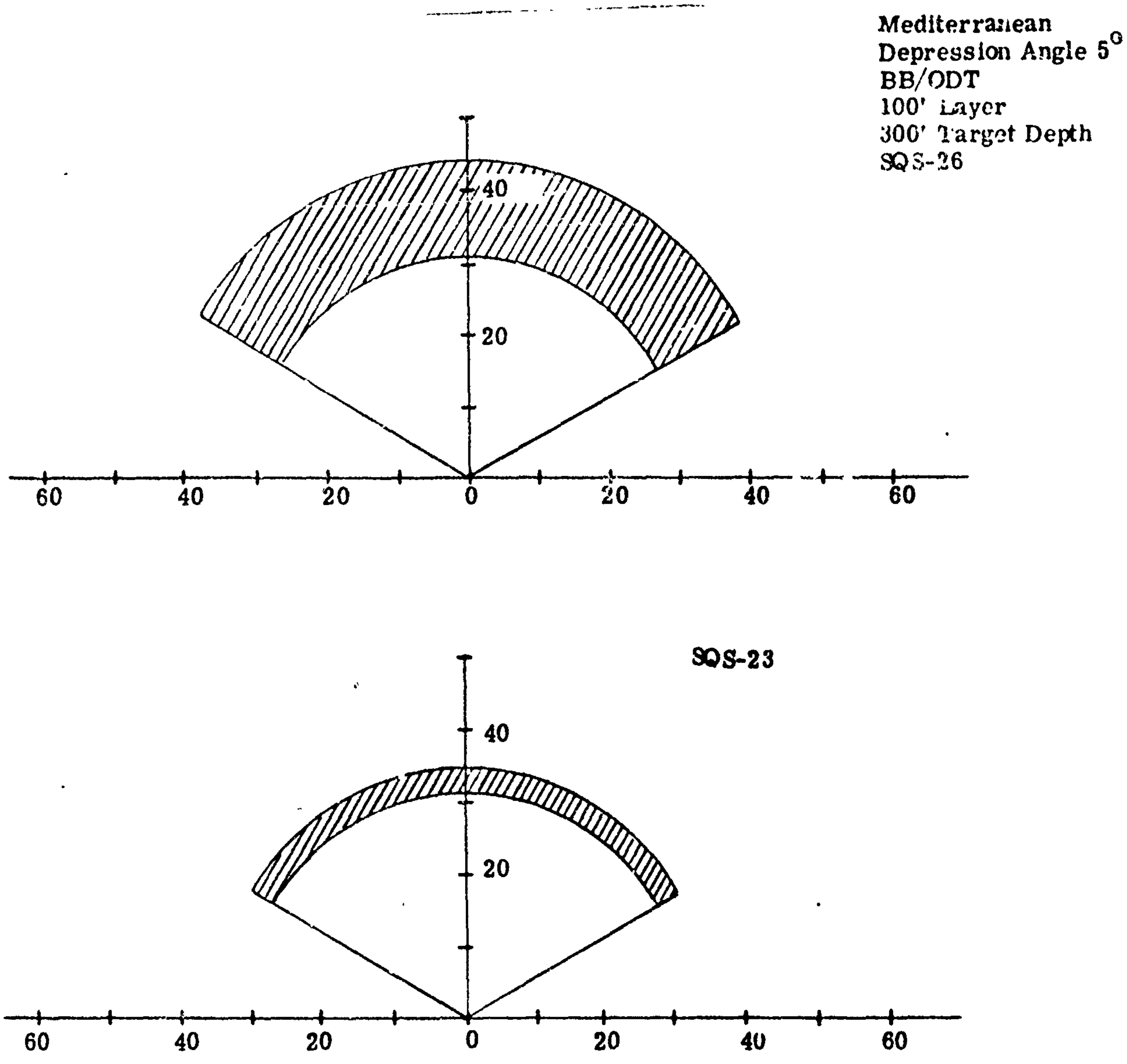

E/B > 10 dB in Shaded Areas

Figure 5-4 (C) Comparison of SQS-26 and SQS-23 Monostatic Coverage

Hazeltine
Corporation

Figure 5-5

Mediterranean
Depression Angle 0^{o}
DP/CZ
100' Layer
55' Target Depth
Target Strength 15 dB
Receiver Depth 60'

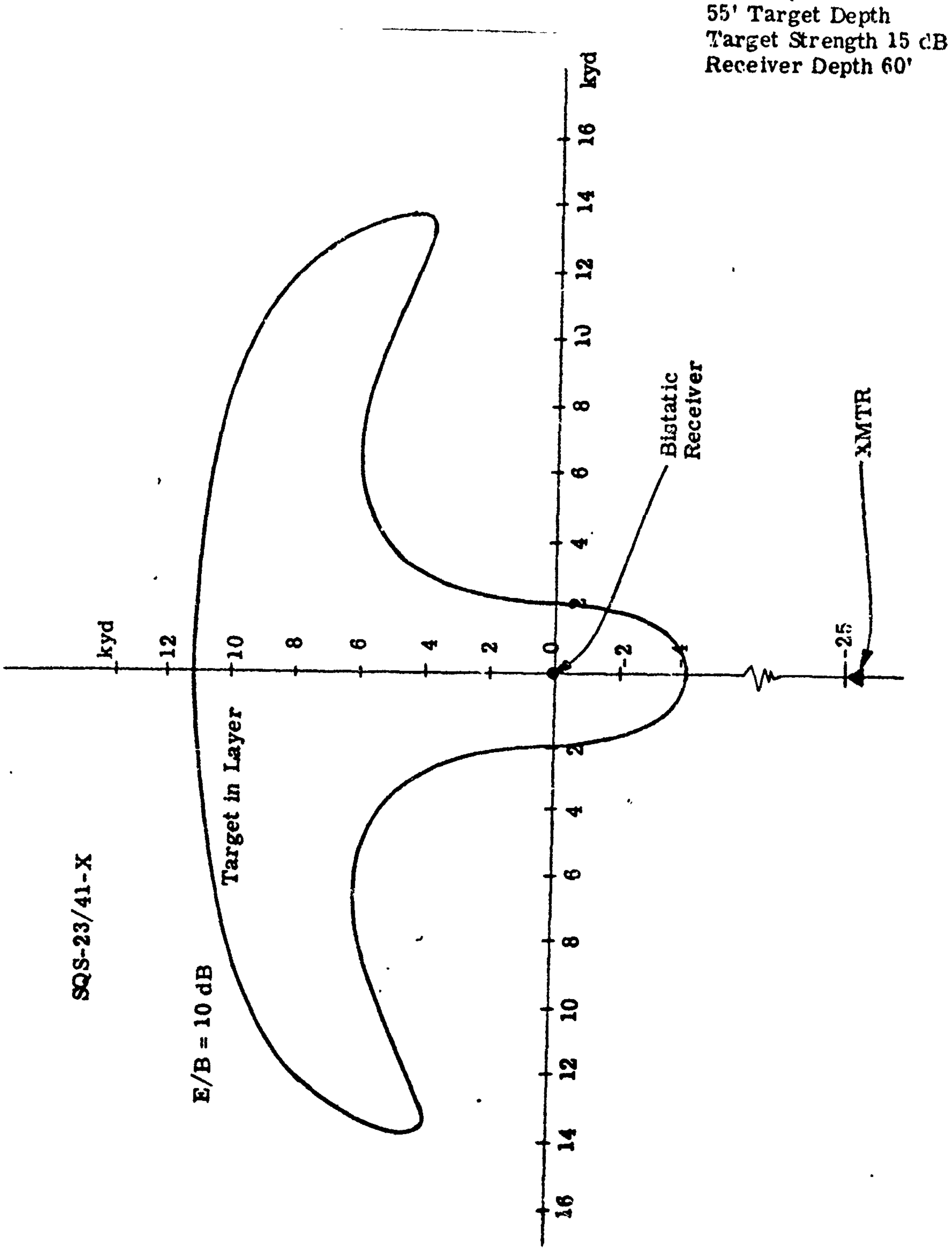

Figure 5-5 (C) Coverage of 41-X Sonobuoy in Mediterranean Using SQS-23 Transmitter

D. TARGET PROSECUTION IN THE MEDITERRANEAN

(C) This scenario assumes a target datum near the middle of the CZ, (40 kyds with layer, 45 kyds without layer). An azimuthal uncertainty of $\pm 5^{\circ}$ is assumed and buoys are deployed on a time late spiral determined by the track of a 120 knot helicopter.

(C) Figure 5-6 shows the best of a series of 6 buoy plants for a target at 300' using 1500' receivers. As can be seen the mission effectiveness is very high and because of the overlap of buoy coverages, the probability of simultaneous detection and thus of localization is quite high.

(U) A series of 4 buoy plants were run and some of the results are shown here.

(C) Figure 5-7 and figure 5-8 show that, for below-layer targets, a set of deep receivers performs somewhat better than shallow ones. Figure 5-9 and figure 5-10, however, show that for a target in the layer, the shallow receivers perform considerably better. Therefore, unless the target depth is known, it is better to deploy shallow receivers in a Mediterranean environment with a layer. A test was also run for a daytime scenario where the DSL moves down to about 1000'; there was little change in system performance.

(C) Figures 5-11 and 5-12 show that for an environment with no layer and a shallow target, bistatic performance is relatively poor for receivers at both depths. One would expect the deep receivers to be slightly more effective based on the buoy coverage shown in figures 5-2 and 5-3; the shallow receivers have slightly better performance. This is due to the difference in arrival times of specular interference which reduced the coverage of the deep receiver.

(C) Figures 5-13 and 5-14 show that, as predicted, the deep receivers do significantly better against 300' targets. This performance has been found to hold true for targets as deep as 1200'.

(C) A few runs were made to see if target prosecution could be carried out in the second CZ if a contact was made there. Figure 5-15 shows the best results which were obtained. One of the problems which is encountered in operating in the second CZ is the fact that the sonar is normally pinging with a 60 sec period for first CZ detections and, therefore, reverberation from a later pulse may interfere with the monostatic performance of the echo from the previous pulse. Nevertheless, it does look feasible to operate bistatically in the second CZ if sufficient sonobuoys are available.

ENVIRONMENT: MEDITERRANEAN
LAYER DEPTH (FT): 100
SYSTEM: SQS-26/41-X
XMTR MODE: BB/ODT
TARGET DEPTH (FT): 300
TARGET SPEED (KNOTS): 10
SHIP SPEED (KNOTS): 15
AIRCRAFT SPEED (KNOTS): 120
BUOY DEPTHS (FT): 1500

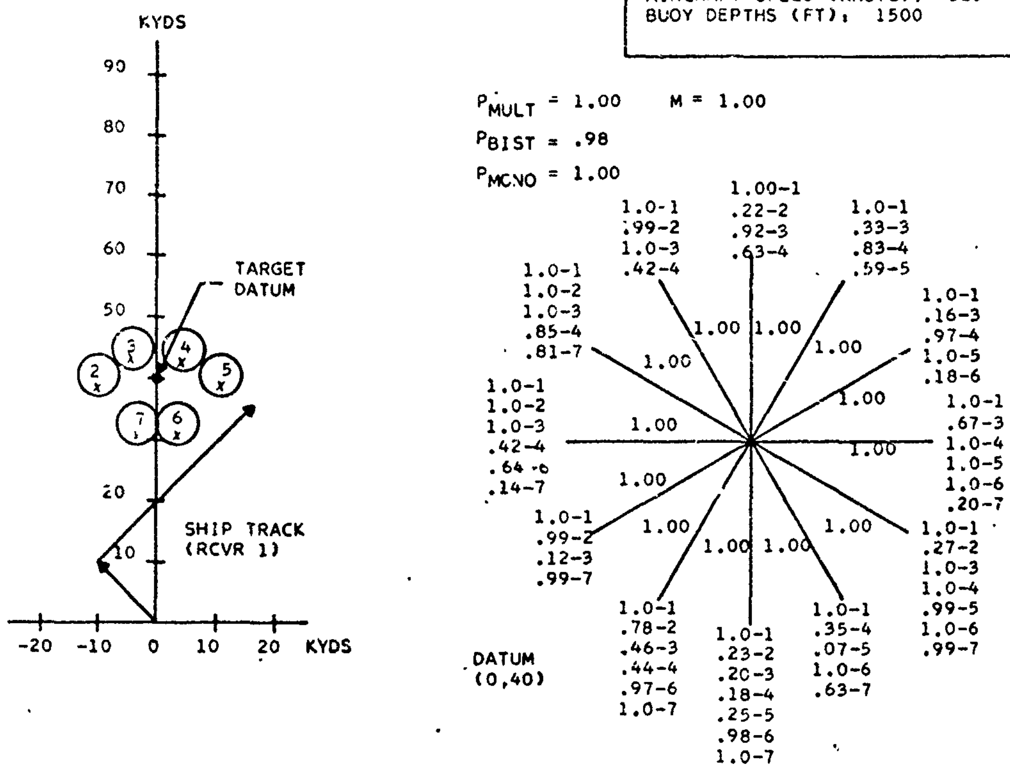

Figure 5-6 (C) Target Prosecution in Mediterranean; 6 Buoy Plant; Target Below Layer; Receivers at 1500'

Hazeltine Corporation

Figure 5-7

ENVIRONMENT: MEDITERRANEAN
LAYER DEPTH (FT): 100
SYSTEM: SQS-26/41-X
XMTR MODE: BB/ODT
TARGET DEPTH (FT): 300
TARGET SPEED (KNOTS): 10
SHIP SPEED (KNOTS): 15
AIRCRAFT SPEED (KNOTS): 120
BUOY DEPTHS (FT): 60

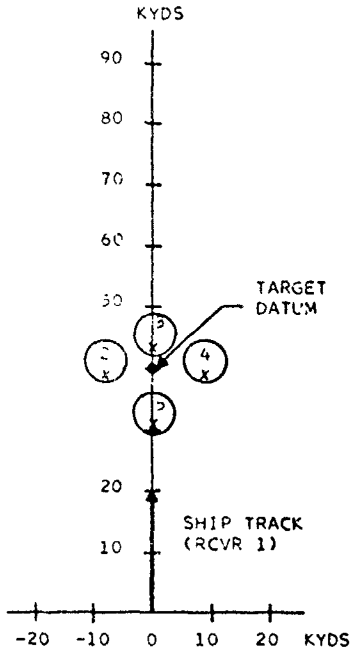

P_{MULT} = 1.00 M = 1.00

P_{BIST} = .78

P_{MONO} = 1.00

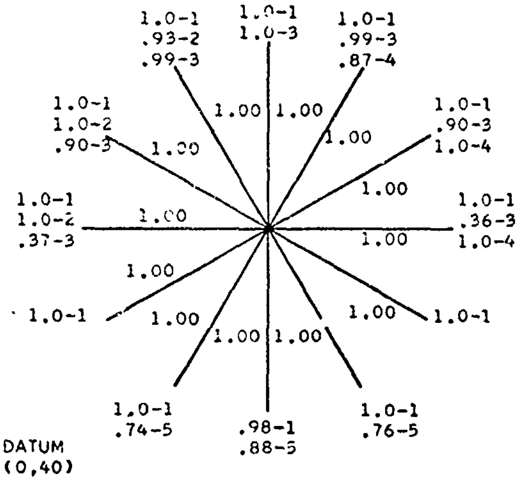

P_{MULT} = 1.00 M = 1.00

P_{BI} = .72

P_{MONO} = 1.00

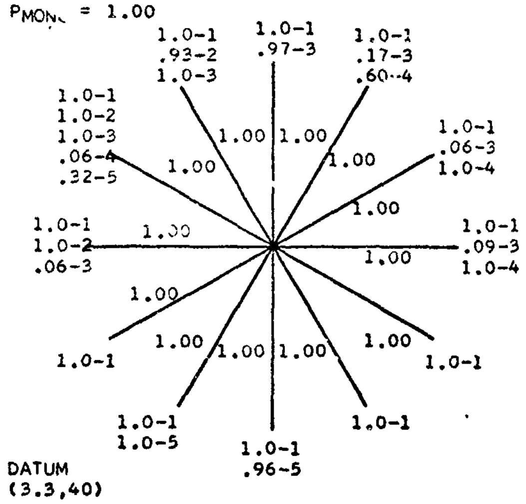

Figure 5-7 (C) Target Prosecution in Mediterranean; 4 Buoy Plant; Target Below Layer; Receivers at 60'

Hazeltine Corporation

Figure 5-8

ENVIRONMENT: MEDITERRANEAN
LAYER DEPTH (FT): 100
SYSTEM: SQS-26/41-X
XMTR MODE: BB/CDT
TARGET DEPTH (FT): 300
TARGET SPEED (KNOTS): 10
SHIP SPEED (KNOTS): 15
AIRCRAFT SPEED (KNOTS): 120
BUOY DEPTHS (FT): 1500

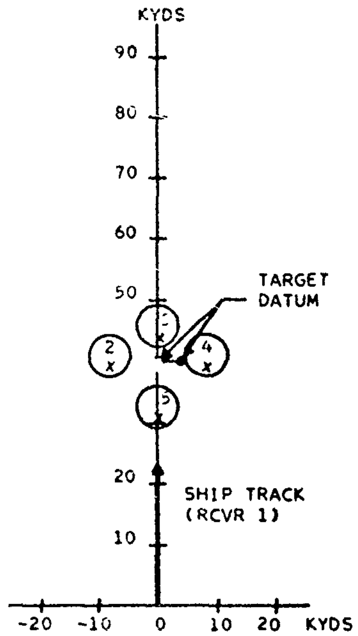

P_{MULT} = 1.00 M = 1.00

P_{BIST} = .91

P_{MONO} = 1.00

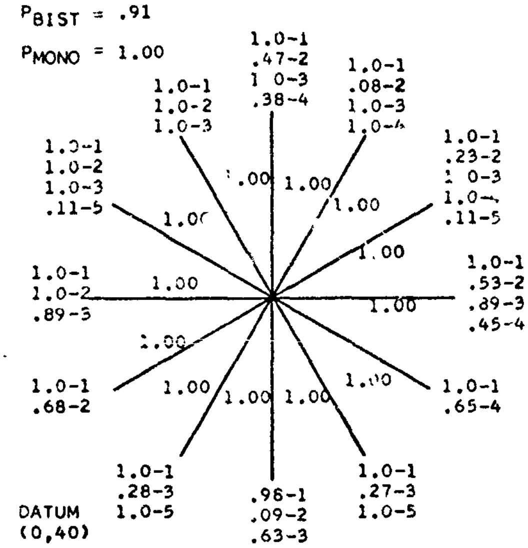

P_{MULT} = 1.00 M = 1.00

P_{BIST} = .92

P_{MONO} = 1.00

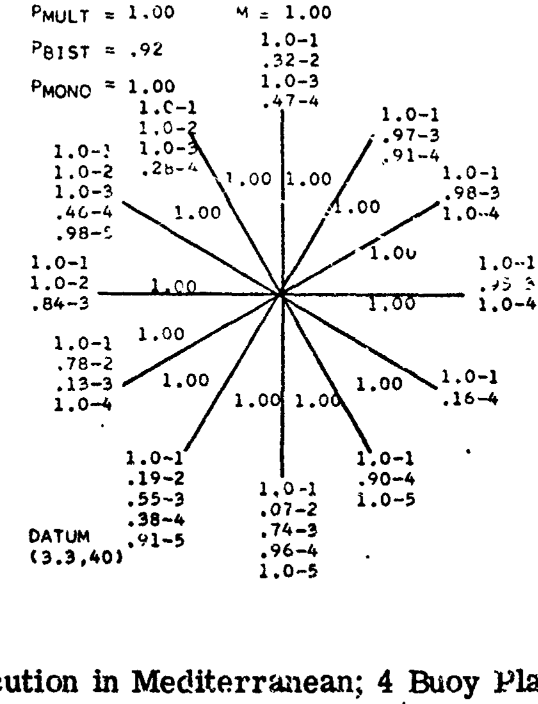

Figure 5-8 (C) Target Prosecution in Mediterranean; 4 Buoy Plant; Target Below Layer; Receivers at 1500′

ENVIRONMENT: MEDITERRANEAN
LAYER DEPTH (FT): 100
SYSTEM: SQS-26/41-X
XMTR MODE: BB/ODT
TARGET DEPTH (FT): 55
TARGET SPEED (KNOTS): 10
SHIP SPEED (KNOTS): 15
AIRCRAFT SPEED (KNOTS): 120
BUOY DEPTHS (FT): 60

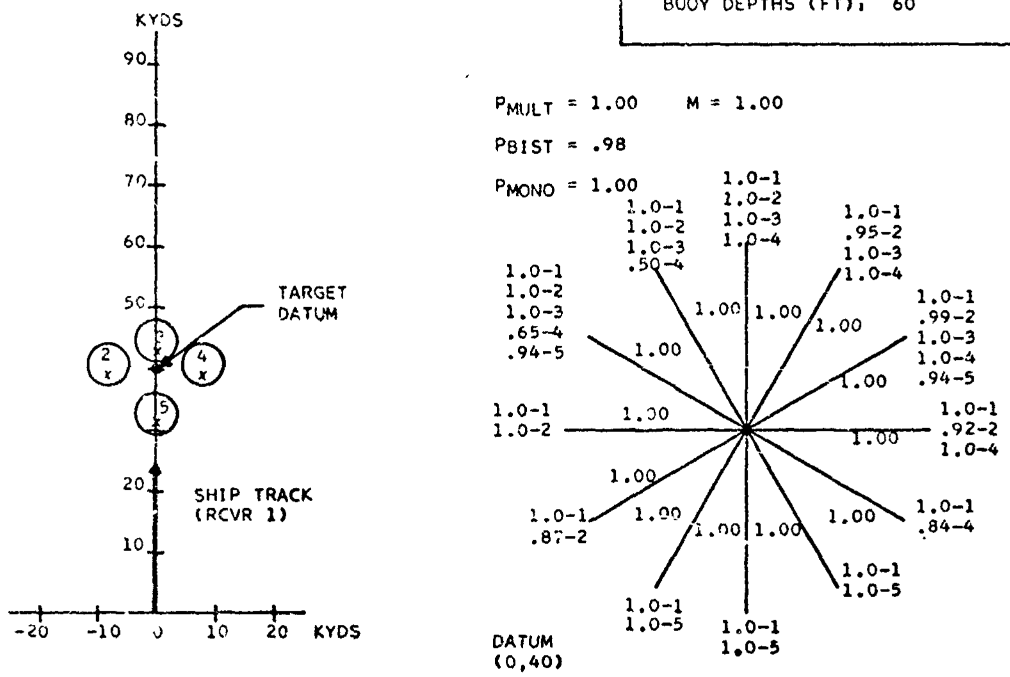

Figure 5-9 (C) Target Prosecution in Mediterranean; 4 Buoy Plant; Target in Layer; Receivers at 60'

Hazeltine
Corporation

Figure 5-10

ENVIRONMENT: MEDITERRANEAN
LAYER DEPTH (FT): 100
SYSTEM: SQS-26/41-X
XMTR MODE: BB/ODT
TARGET DEPTH (FT): 55
TARGET SPEED (KNOTS): 10
SHIP SPEED (KNOTS): 15
AIRCRAFT SPEED (KNOTS): 120
BUOY DEPTHS (FT): 1500

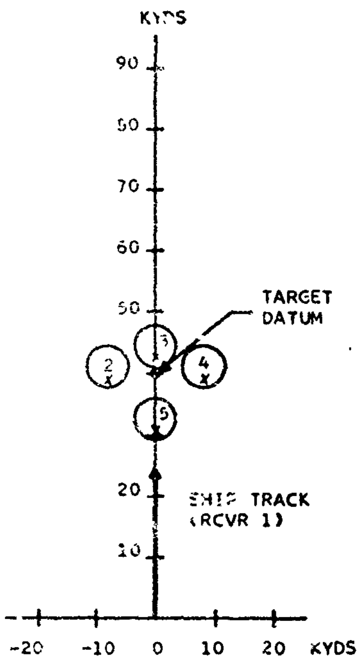

P_{MULT} = 1.00 M = 1.00

P_{BIST} = .65

P_{MONO} = 1.00

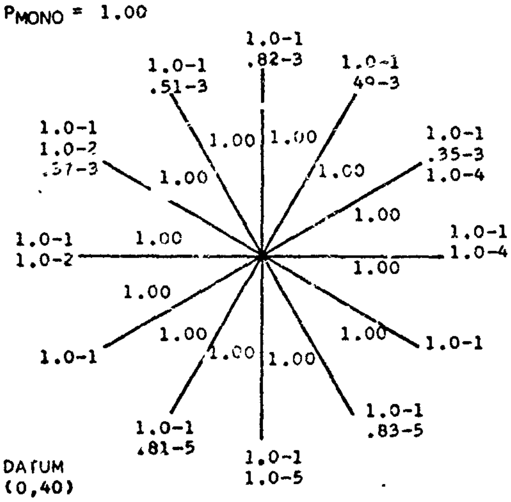

Figure 5-10 (C) **Target Prosecution in Mediterranean; 4 Buoy Plant; Target in Layer; Receivers at 1500'**

ENVIRONMENT: MEDITERRANEAN
LAYER DEPTH (FT): (NO SURFACE DUCT)
SYSTEM: SQS-26/41-X
XMTR MODE: BB/ODT
TARGET DEPTH (FT): 55
TARGET SPEED (KNOTS): 10
SHIP SPEED (KNOTS): 15
AIRCRAFT SPEED (KNOTS): 120
BUOY DEPTHS (FT): 60

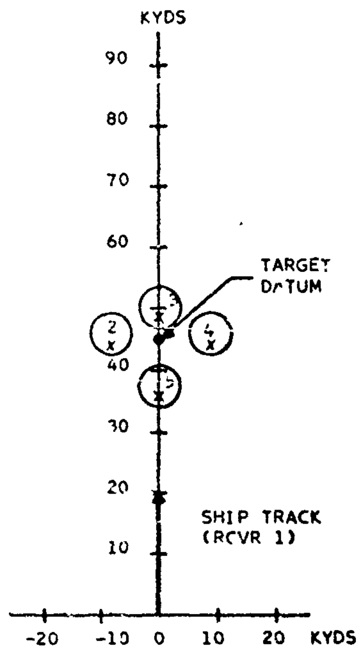

P_{MULT} = 1.00 M = 1.00

P_{BIST} = .58

P_{MONO} = 1.00

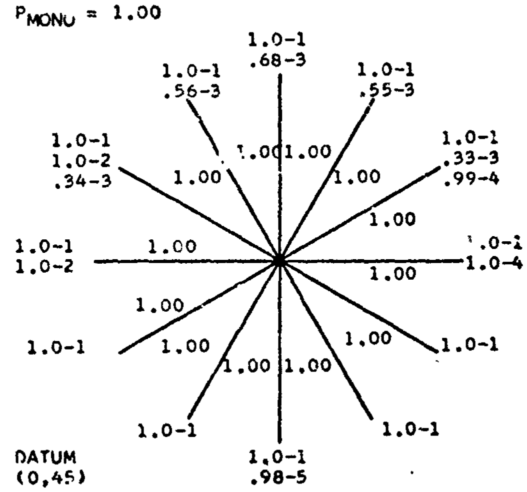

Figure 5-11 (C) Target Prosecution in Mediterranean; 4 Buoy Plant; No Layer Present; Target at 55'; Receivers at 60'

Hazeltine Corporation

Figure 5-12

ENVIRONMENT: MEDITERRANEAN
LAYER DEPTH (FT): (NO SURFACE DUCT)
SYSTEM: SQS-26/41-X
XMTR MODE: BB/ODT
TARGET DEPTH (FT): 55
TARGET SPEED (KNOTS): 10
SHIP SPEED (KNOTS): 15
AIRCRAFT SPEED (KNOTS): 120
BUOY DEPTHS (FT): 1500

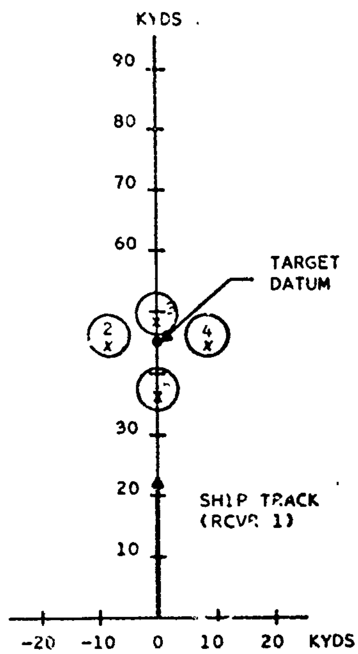

P_{MULT} = 1.00 M = 1.00
P_{BIST} = .46
P_{MONO} = 1.00

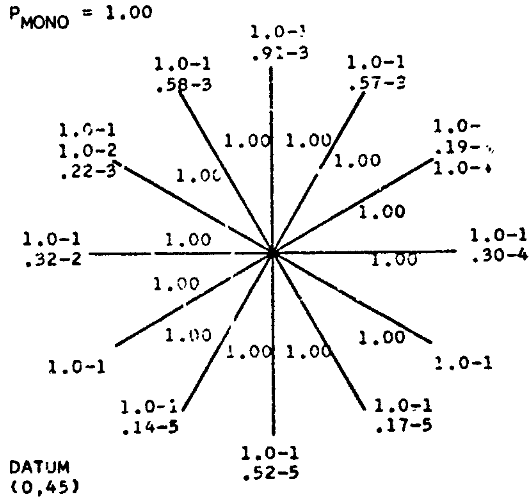

Figure 5-12 (C) Target Prosecution in Mediterranean; 4 Buoy Plant; No Layer Present; Target at 55'; Receivers at 1500'

Hazeltine
Corporation

Figure 5-13

ENVIRONMENT: MEDITERRANEAN
LAYER DEPTH (FT): (NO SURFACE DUCT)
SYSTEM: SQS-26/41-X
XMTR MODE: BB/OD
TARGET DEPTH (FT): 300
TARGET SPEED (KNOTS): 10
SHIP SPEED (KNOTS): 15
AIRCRAFT SPEED (KNOTS): 120
BUOY DEPTHS (FT): 60

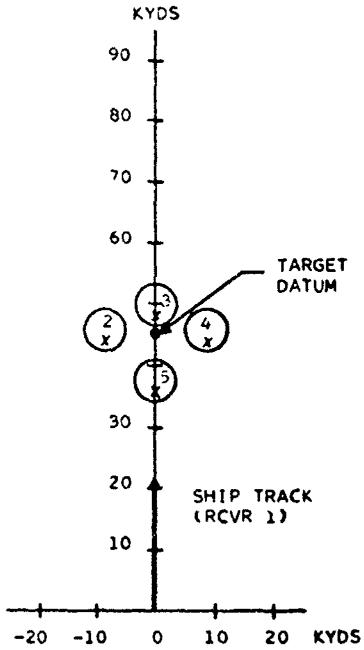

P_{MULT} = 1.00 M = 1.00

P_{BIST} = .39

P_{MONO} = 1.00

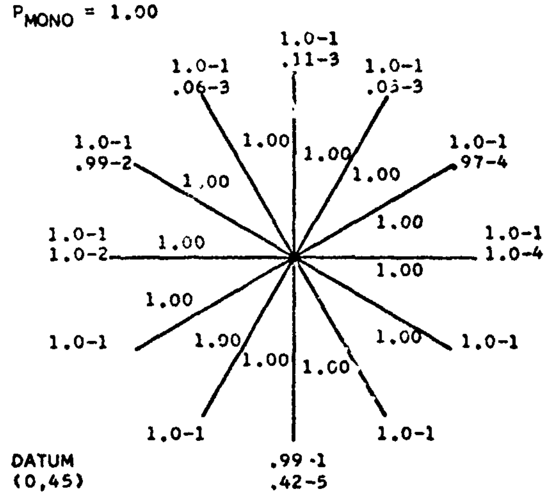

Figure 5-13 (C) Target Prosecution in Mediterranean; 4 Buoy Plant; No Layer Present; Target at 300'; Receivers at 60'

Hazeltine
Corporation

Figure 5-14

ENVIRONMENT: MEDITERRANEAN
LAYER DEPTH (FT): (NO SURFACE DUCT)
SYSTEM: SQS-26/41-X
XMTR MODE: PP/ODT
TARGET DEPTH (FT): 300
TARGET SPEED (KNOTS): 10
SHIP SPEED (KNOTS): 15
AIRCRAFT SPEED (KNOTS): 120
BUOY DEPTHS (FT): 1500

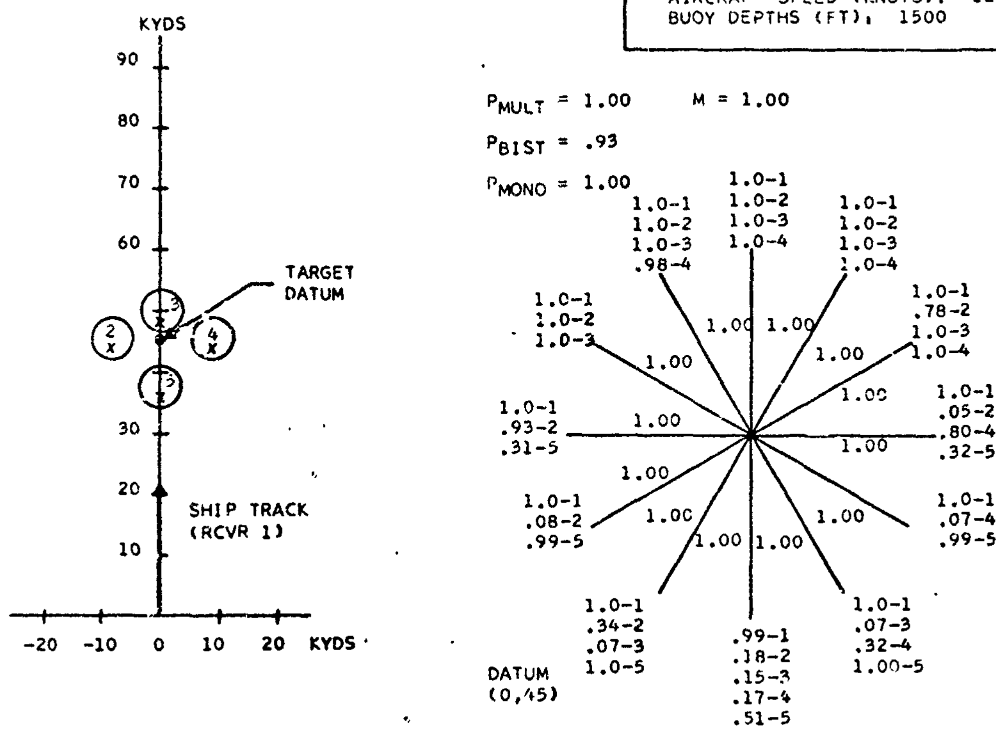

Figure 5-14 (C) Target Prosecution in Mediterranean; 4 Buoy Plant; No Layer Present; Target at 300'; Receivers at 1500'

Hazeltine
Corporation

Figure 5-15

ENVIRONMENT: MEDITERRANEAN
LAYER DEPTH (FT): 100
SYSTEM: SQS-26/41-X
XMTR MODE: BB/ODT (2ND CZ)
TARGET DEPTH (FT): 300
TARGET SPEED (KNOTS): 10
SHIP SPEED (KNOTS): 15
AIRCRAFT SPEED (KNOTS): 120
BUOY DEPTHS (FT): 1500

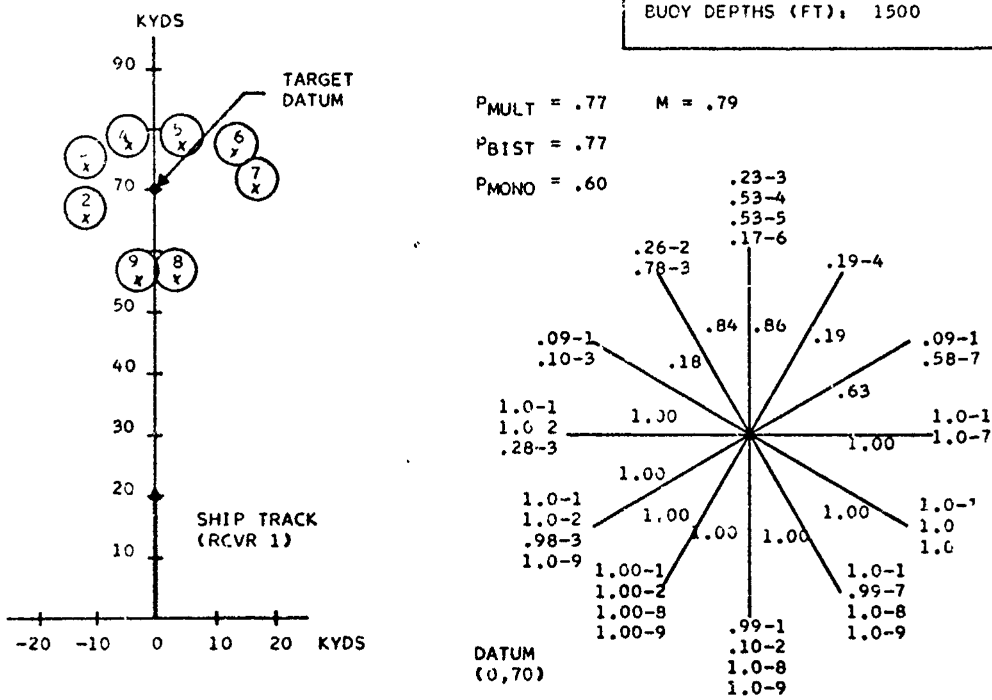

Figure 5-15 (C) Target Prosecution in Mediterranean Using Second CZ

(C) Predictions of the results for operations analysis utilizing an SQS-23/41-X system in the Mediterranean have already been described in Section V-2. The system will perform well bistatically, but because of the limited performance of the 23 monostatically there is less likelihood of obtaining localization using this system.

(C) Although operations analysis was not run for this system, it is clear from a comparison of typical buoy coverages that the SQS-23/41-X system in the Mediterranean will have performance equivalent to the SQS-26/41-X system in the North Atlantic.

SECTION VI (C)

CONCLUSIONS AND RECOMMENDATIONS

(C) Operations analysis conducted during this study, combined with the results of at-sea bistatic exercises lead to the conclusion that the addition of a bistatic capability to the present monostatic systems can provide significant advantages over existing sonar systems. Because of the passive capability of the bistatic receiver, these advantages can be obtained with little extra cost in most exercises since at present, passive buoys are often used in these scenarios.

(C) The multistatic approach offers several tactical advantages over present systems, the main one being the fact that a target hearing an active ship transmitter cannot easily find an escape route since it is unaware of the location of the remote sonobuoys. In contrast, the CASS system has the ability to operate in locations further from the ship since it contains its own transmitter.

(C) An important result of the addition of a bistatic capability is the target localization and depth estimate which can be obtained. This subject should be pursued further in future studies.

(U) Although only a few environments have been studied in detail, it is apparent that the multistatic system concept will be useful in most of the major oceans and seas.

(U) The results of studies of multistatic systems over the last four years indicate that bistatics offer a highly useful adjunct to the Navy's existing sonar capabilities and that these systems merit further investigations both analytical and experimental.

Hazeltine
Corporation

APPENDIX A (C)

PART 1

CONVOY SCREENING IN THE NORTH ATLANTIC

Figure	Environment	Mission	Datum	Buoys	Ship Course	Sub Course	XMTR	A/C
A-1	N.A.	Screen	0°	2-60'	Straight	180°	26 BB/ODT	Helo
A-2	"	"	30°	"	at 15	10 knots	"	"
A-3	"	"	60°	"	knots	250'	"	"
A-4	"	"	(Individual Receiver Performance Summary)					
A-5	"	"	0°	2-60'	Straight	CPA	26 BB/ODT	Helo
A-6	"	"	30°	"	at 15	10 knots	"	"
A-7	"	"	60°	"	knots	250'	"	"
A-8	"	"	(Individual Receiver Performance Summary)					
A-9	"	"	0°	2-60'	Straight	180°	26 BB/ODT	Helo
A-10	"	"	30°	"	at 15	6 knots	"	"
A-11	"	"	60°	"	knots	250'	"	"
A-12	"	"	(Individual Receiver Performance Summary)					
A-13	"	"	0°	2-60'	Straight	CPA	26 BB/ODT	Helo
A-14	"	"	30°	"	at 15	6 knots	"	"
A-15	"	"	60°	"	knots	250'	"	"
A-16	"	"	(Individual Receiver Performance Summary)					
A-17	"	"	0°	1-60'	Straight	180°	BB/ODT	Helo
A-18	"	"	30°	"	at 15	10 knots	"	"
A-19	"	"	60°	"	knots	250'	"	"
A-20	"	"	(Individual Receiver Performance Summary)					
A-21	"	"	0°	1-60'	Straight	CPA	26 BB/ODT	Helo
A-22	"	"	30°	"	at 15	10 knots	"	"
A-23	"	"	60°	"	knots	250'	"	"
A-24	"	"	(Individual Receiver Performance Summary)					
A-25	"	"	5, 15, 25°	1-60'	0° Rel.	CPA	26 BB/ODT	Helo
A-26	"	"	"	"	45° Rel.	10 knots	"	"
A-27	"	"	"	"	90° Rel.	250'	"	"
A-28	"	"	(Individual Receiver Performance Summary)					
A-29	"	"	5, 15, 25°	1-60'	0° Rel.	CPA	26 BB/ODT	Helo
A-30	"	"	"	"	45° Rel.	10 knots	"	"
A-31	"	"	"	"	90° Rel.	400'	"	"
A-32	"	"	(Individual Receiver Performance Summary)					
A-33	"	"	(Individual Receiver Performance Summary)					
A-34	"	"	5, 15, 25°	1-60'	45° Rel.	CPA	26 BB/ODT	Helo
A-35	"	"	(Individual Receiver Performance Summary)					

Figure A-1

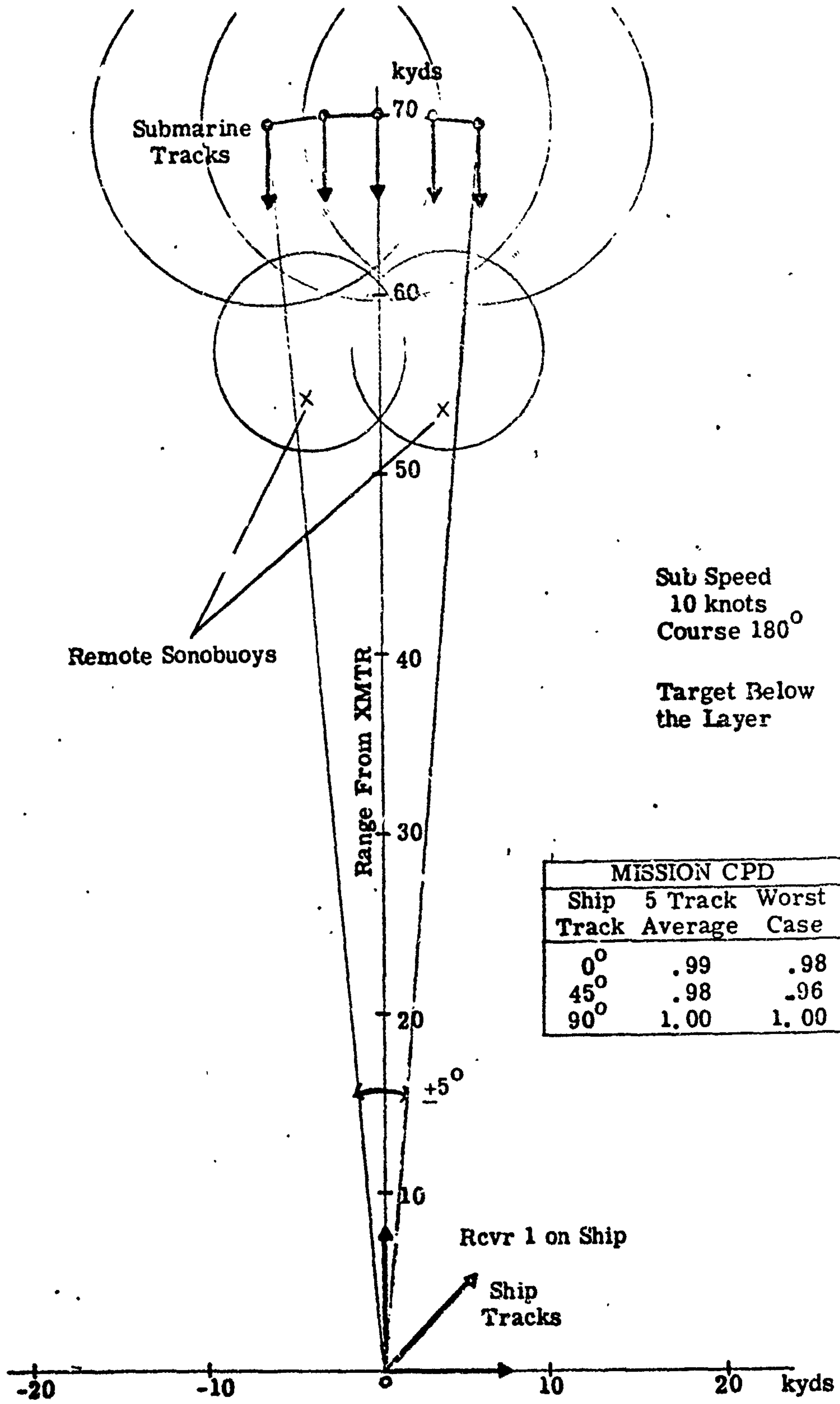

Sub Speed
10 knots
Course 180°

Target Below the Layer

MISSION CPD

Ship Track	5 Track Average	Worst Case
0°	.99	.98
45°	.98	.96
90°	1.00	1.00

Hazeltine
Corporation

Figure A-2

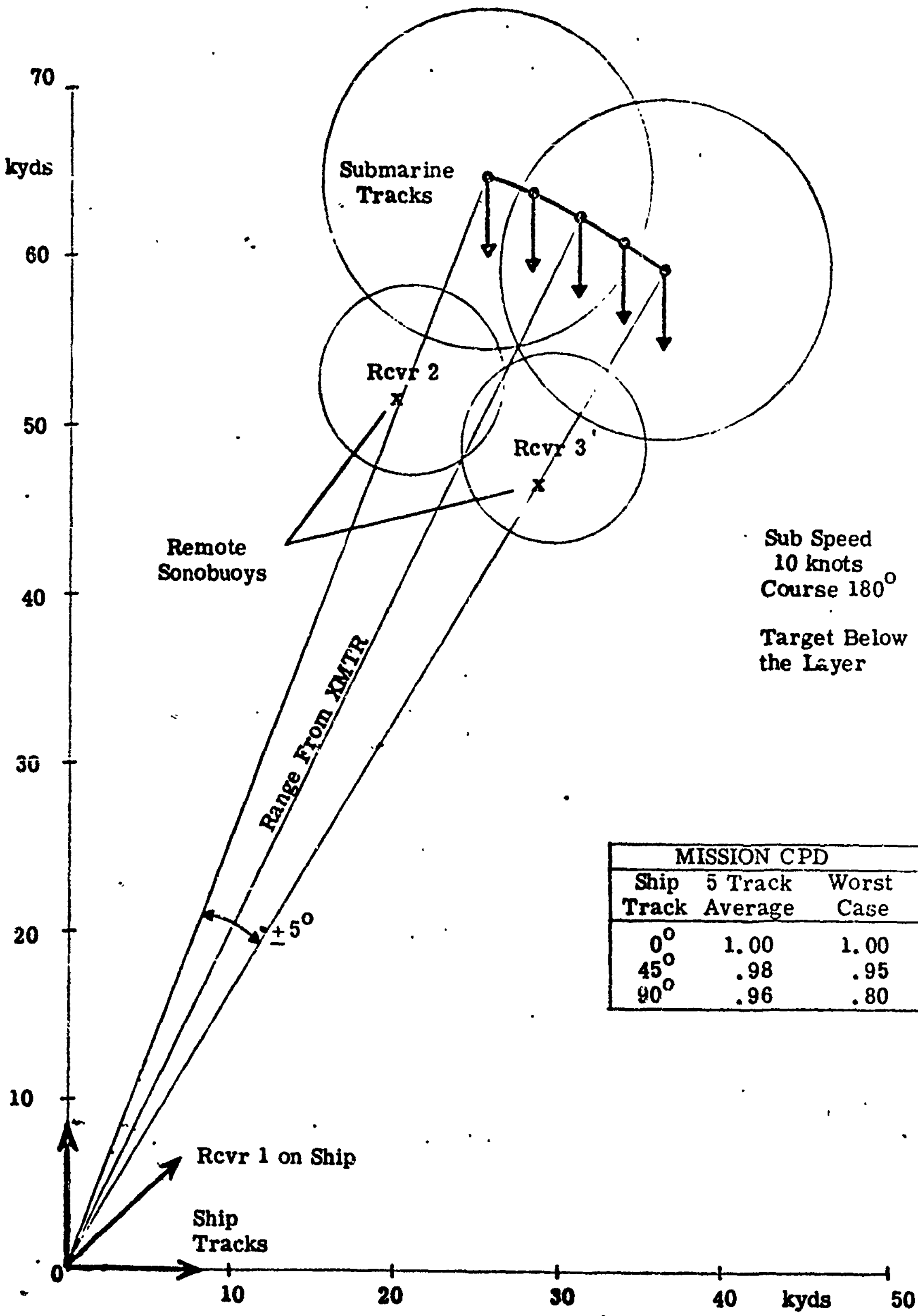

MISSION CPD		
Ship Track	5 Track Average	Worst Case
0°	1.00	1.00
45°	.98	.95
90°	.96	.80

Hazeltine
Corporation

Figure A-3

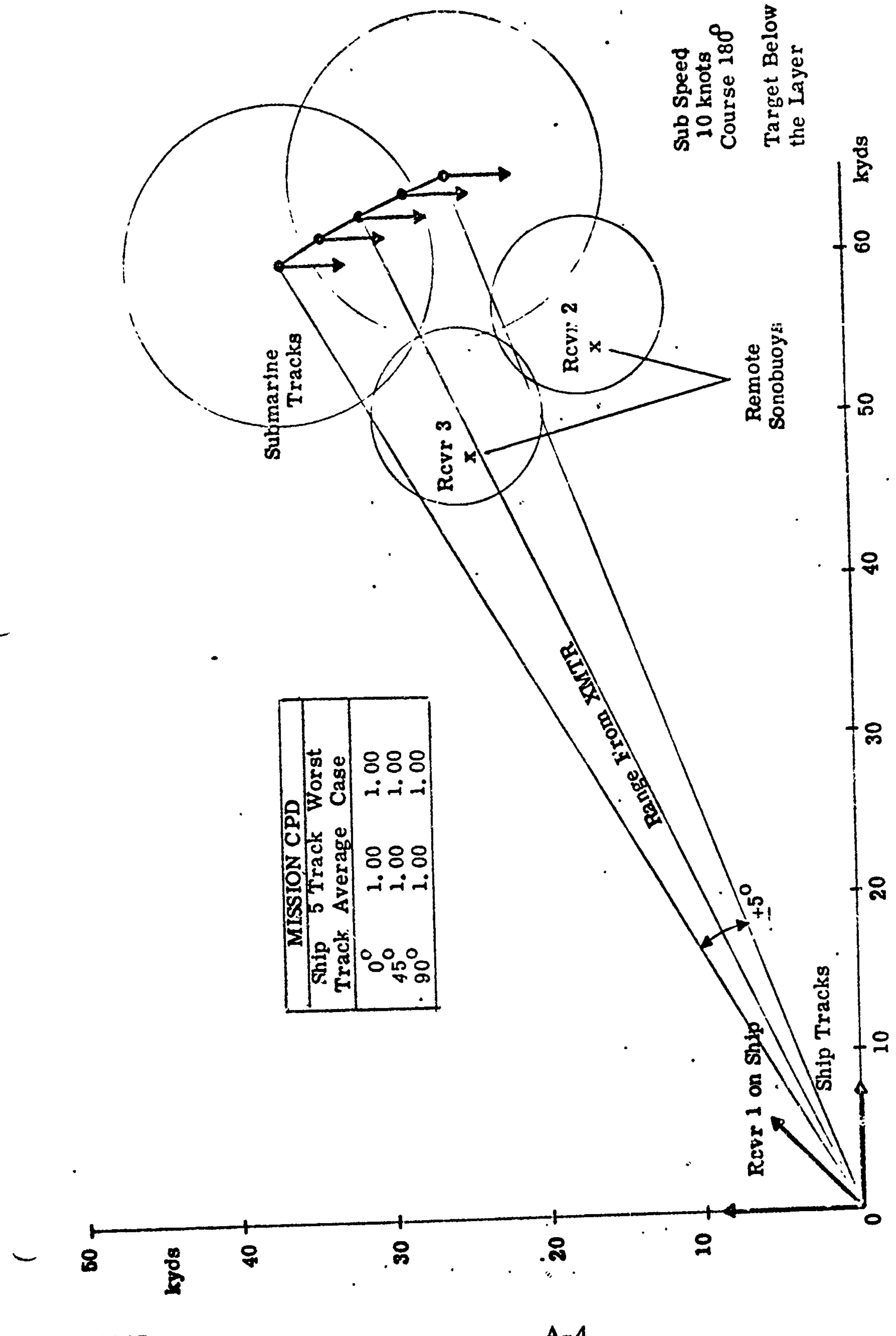

MISSION CPD		
Ship Track	5 Track Average	Worst Case
0°	1.00	1.00
45°	1.00	1.00
90°	1.00	1.00

Hazeltine Corporation

Figure A-4

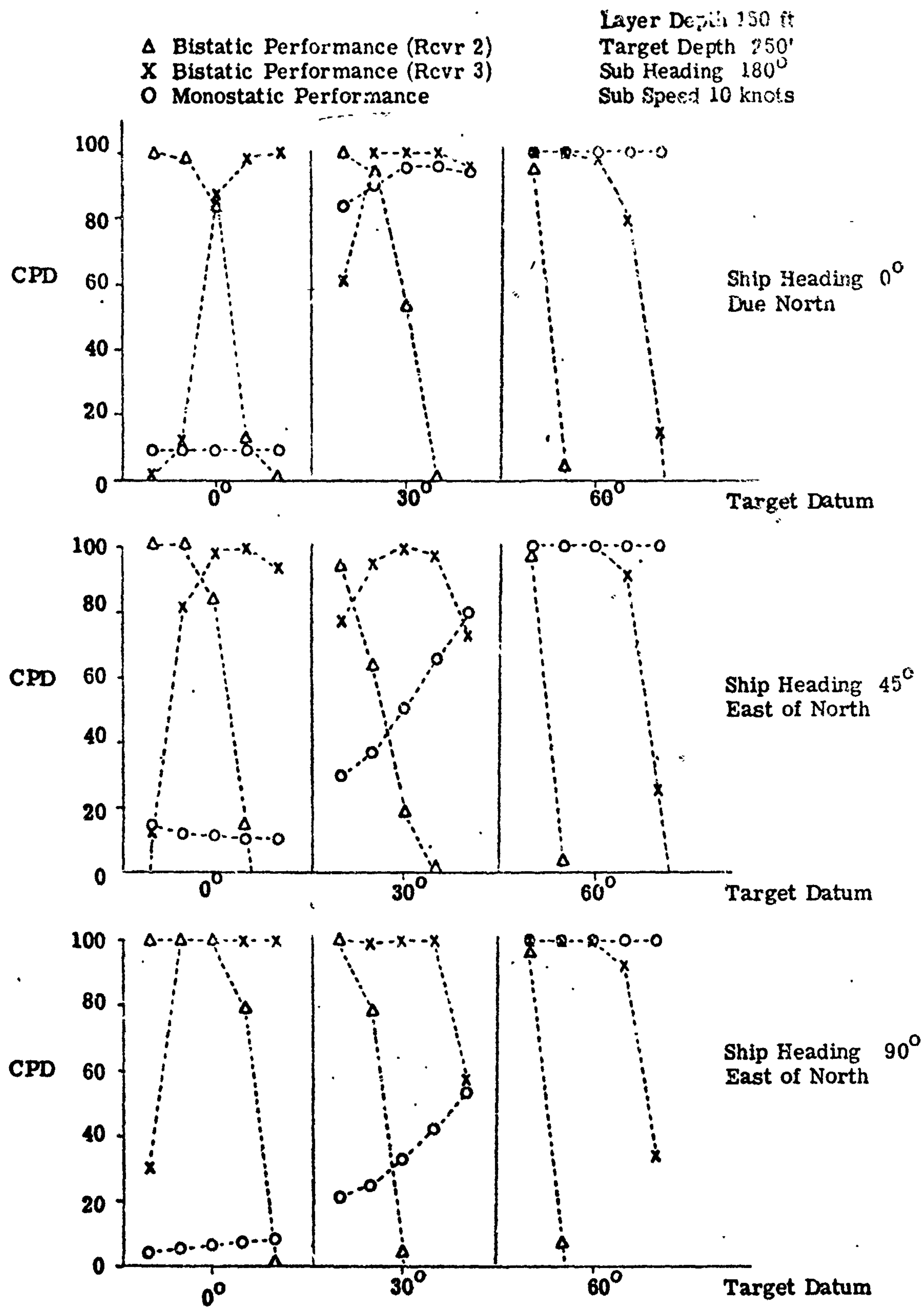

Hazeltine Corporation

Figure A-5

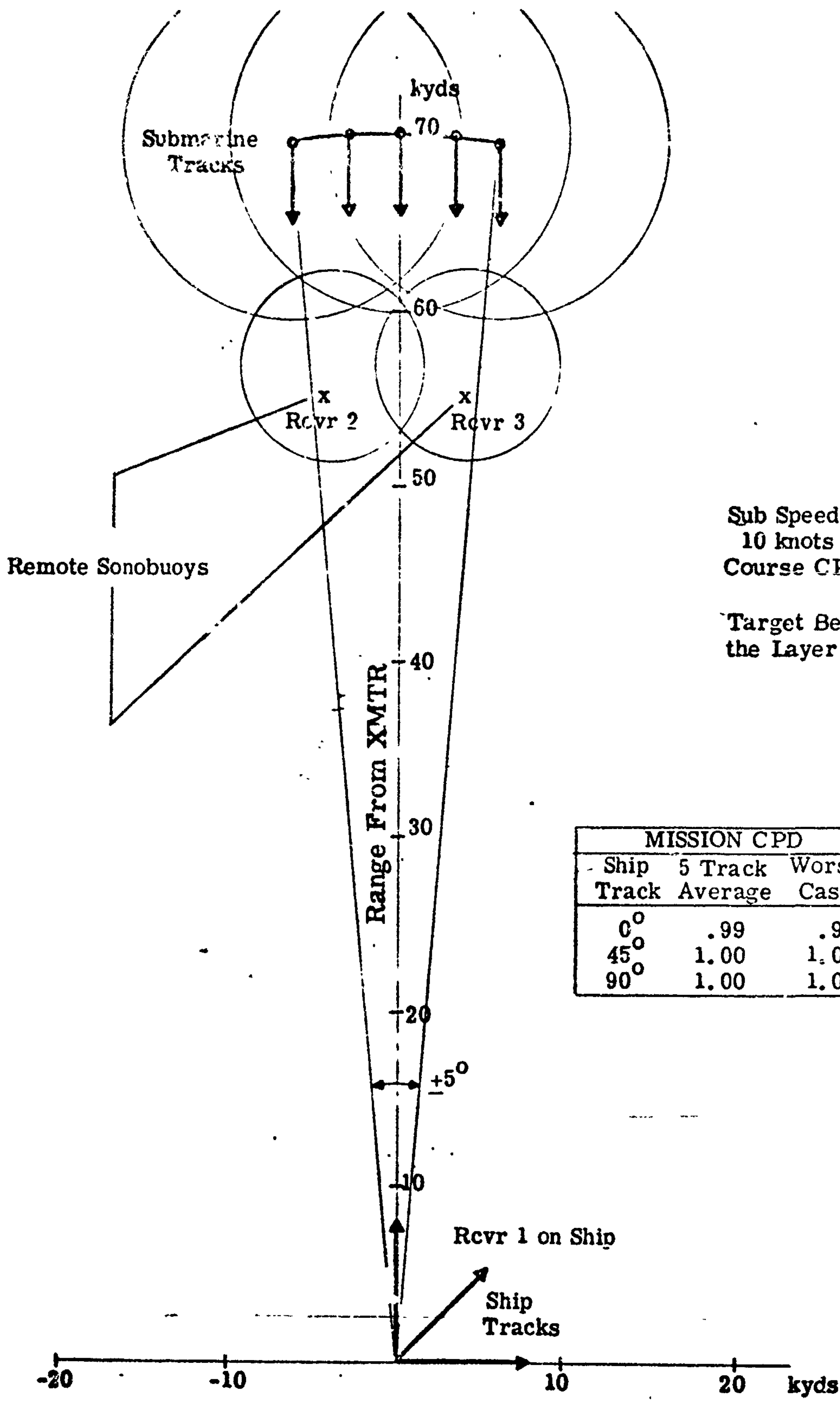

Sub Speed
10 knots
Course CPA

Target Below the Layer

MISSION CPD		
Ship Track	5 Track Average	Worst Case
0°	.99	.98
45°	1.00	1.00
90°	1.00	1.00

Hazeltine Corporation

Figure A-6

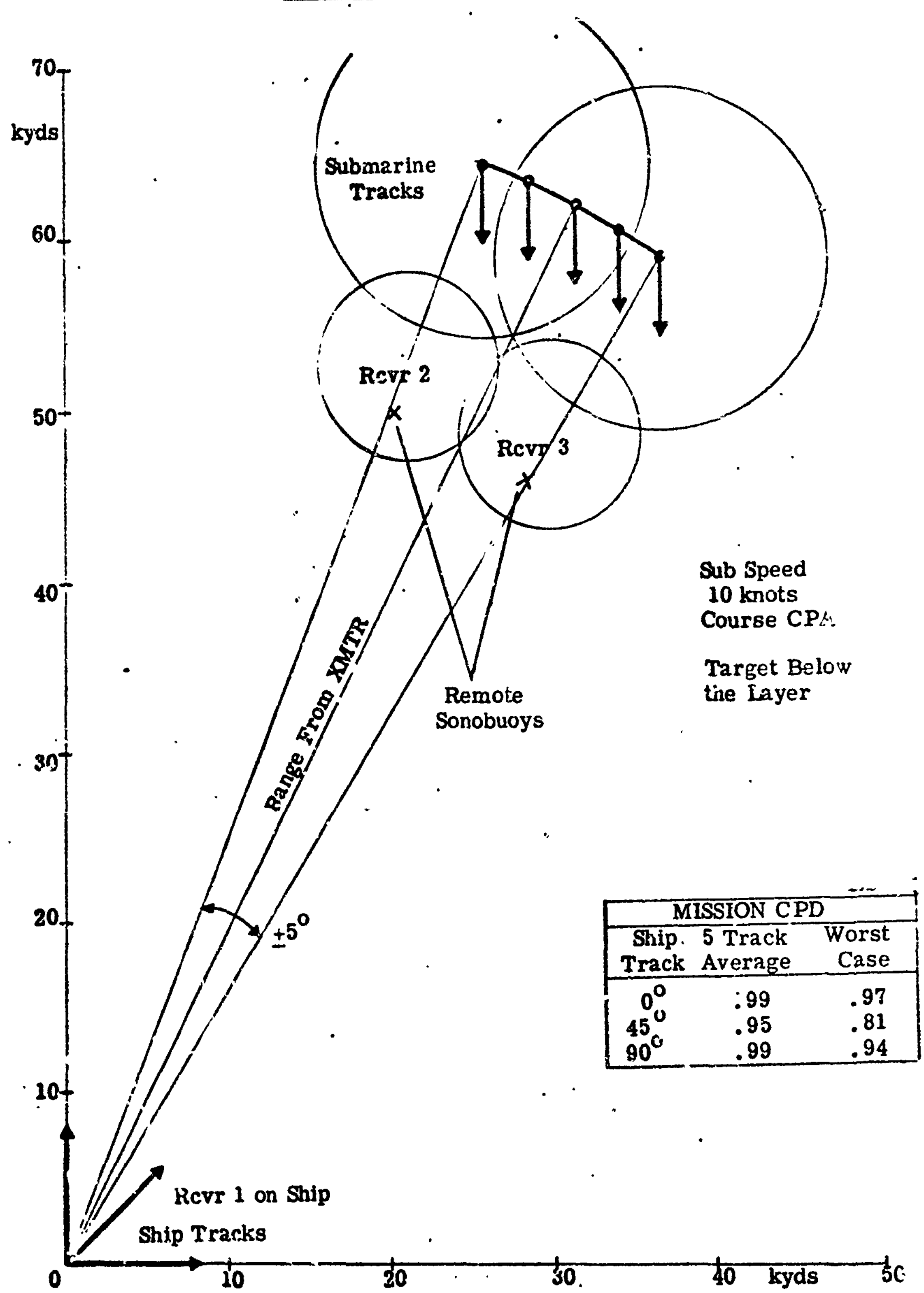

MISSION CPD		
Ship Track	5 Track Average	Worst Case
0°	.99	.97
45°	.95	.81
90°	.99	.94

Figure A-7

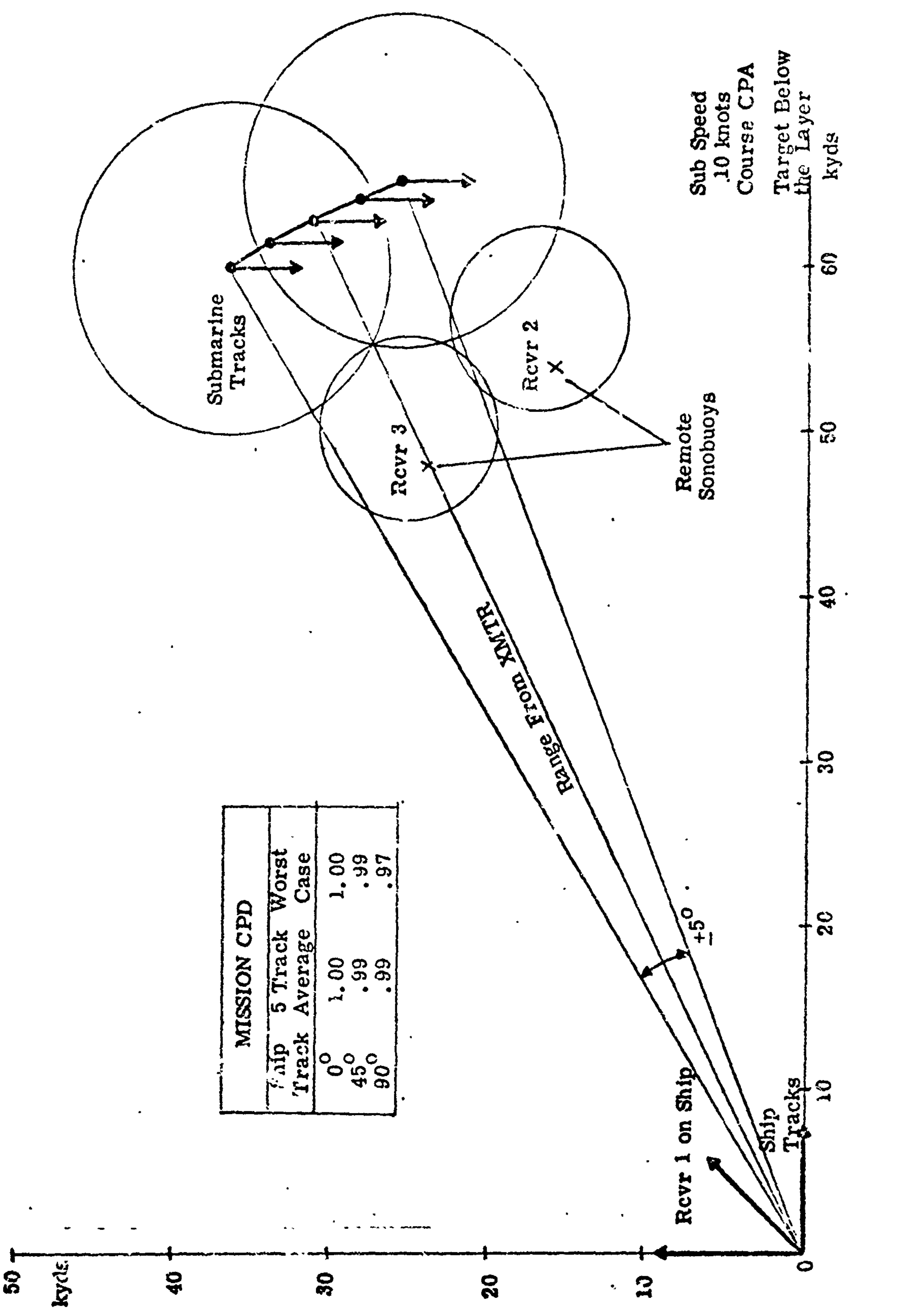

Ship Track	5 Track Average	Worst Case
0°	1.00	1.00
45°	.99	.99
90°	.99	.97

Hazeltine
Corporation

Figure A-8

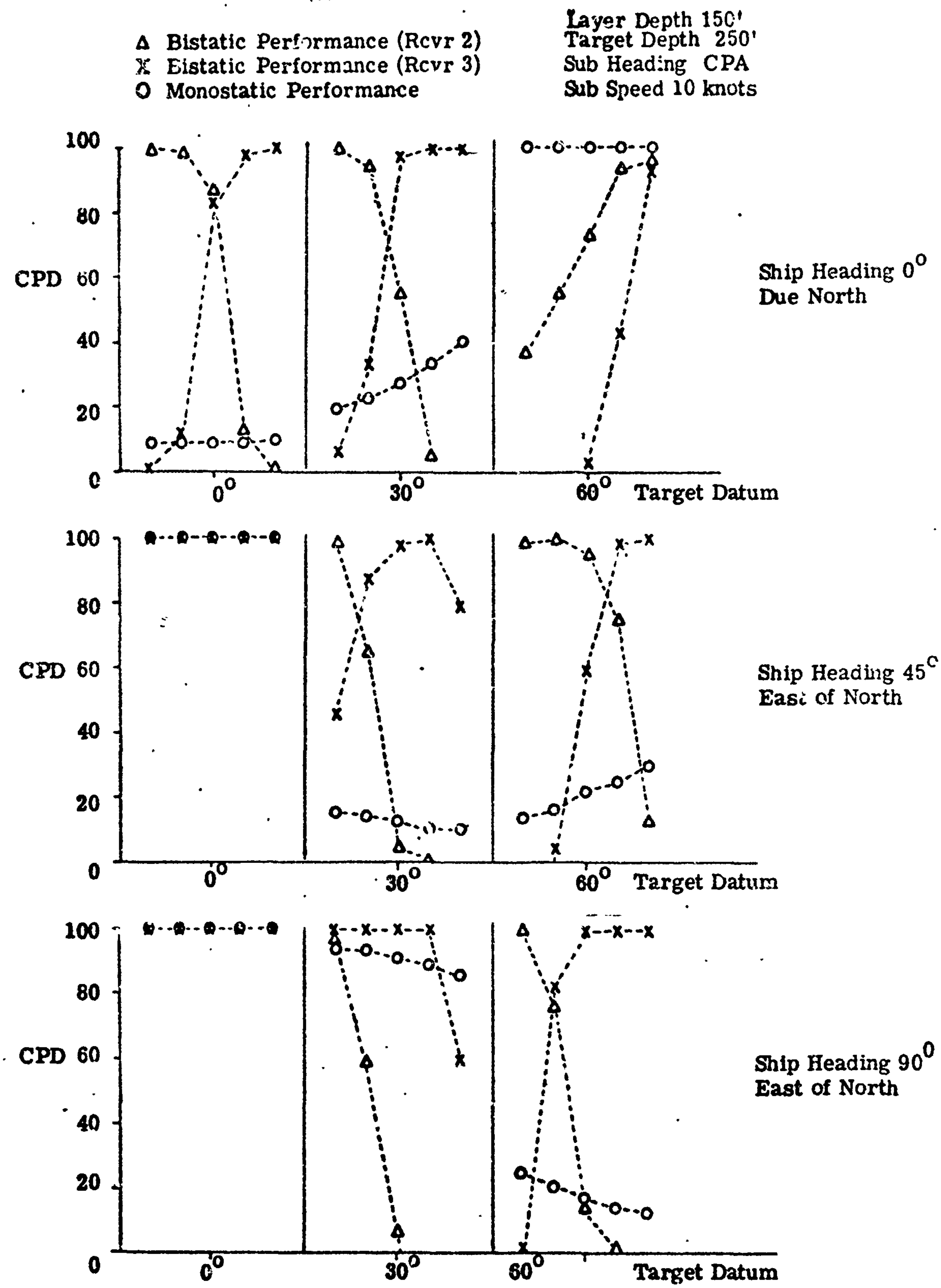

Figure A-9

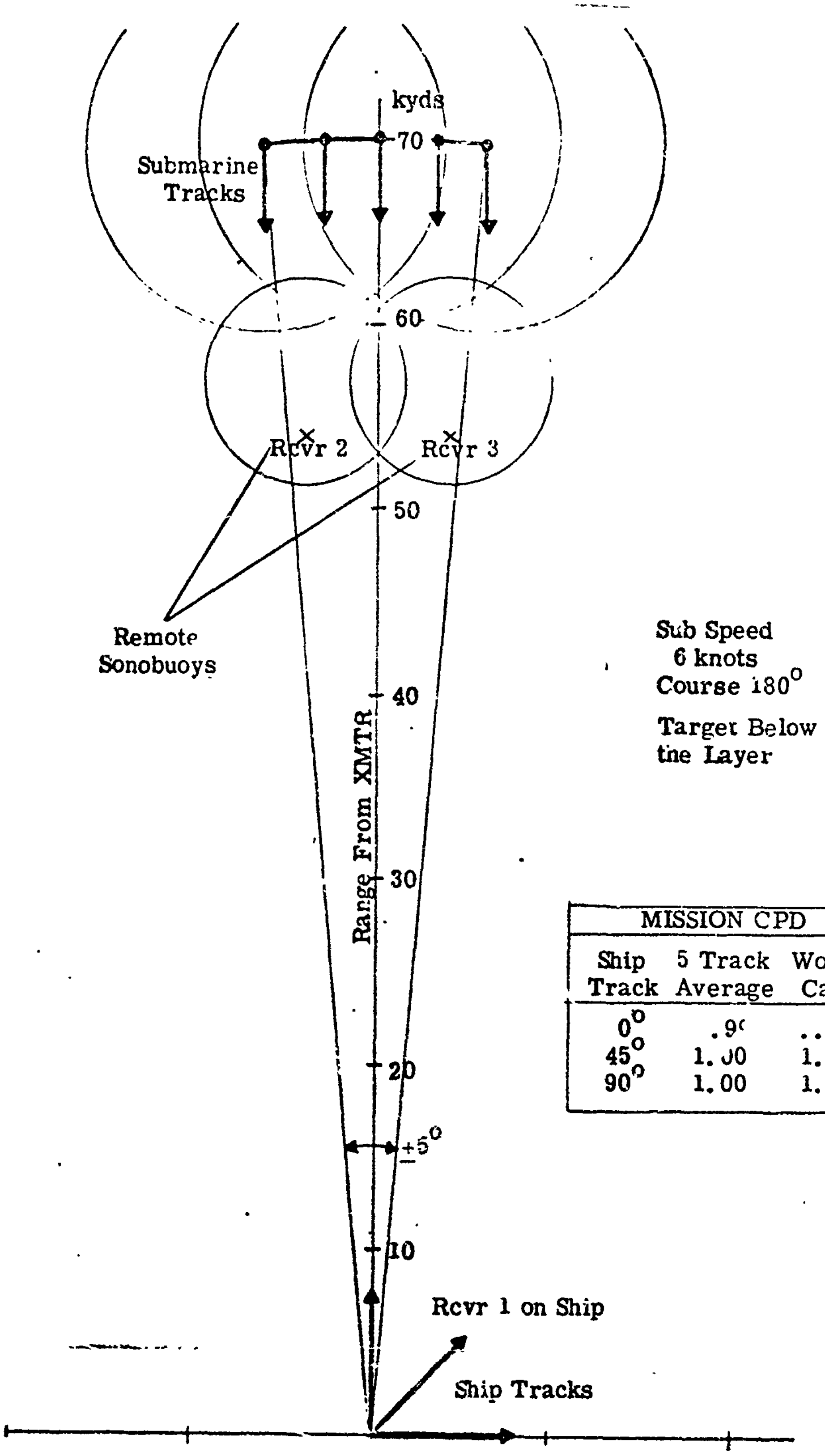

MISSION CPD		
Ship Track	5 Track Average	Worst Case
0°	.9[illegible]	..96
45°	1.00	1.00
90°	1.00	1.00

Hazeltine Corporation

Figure A-10

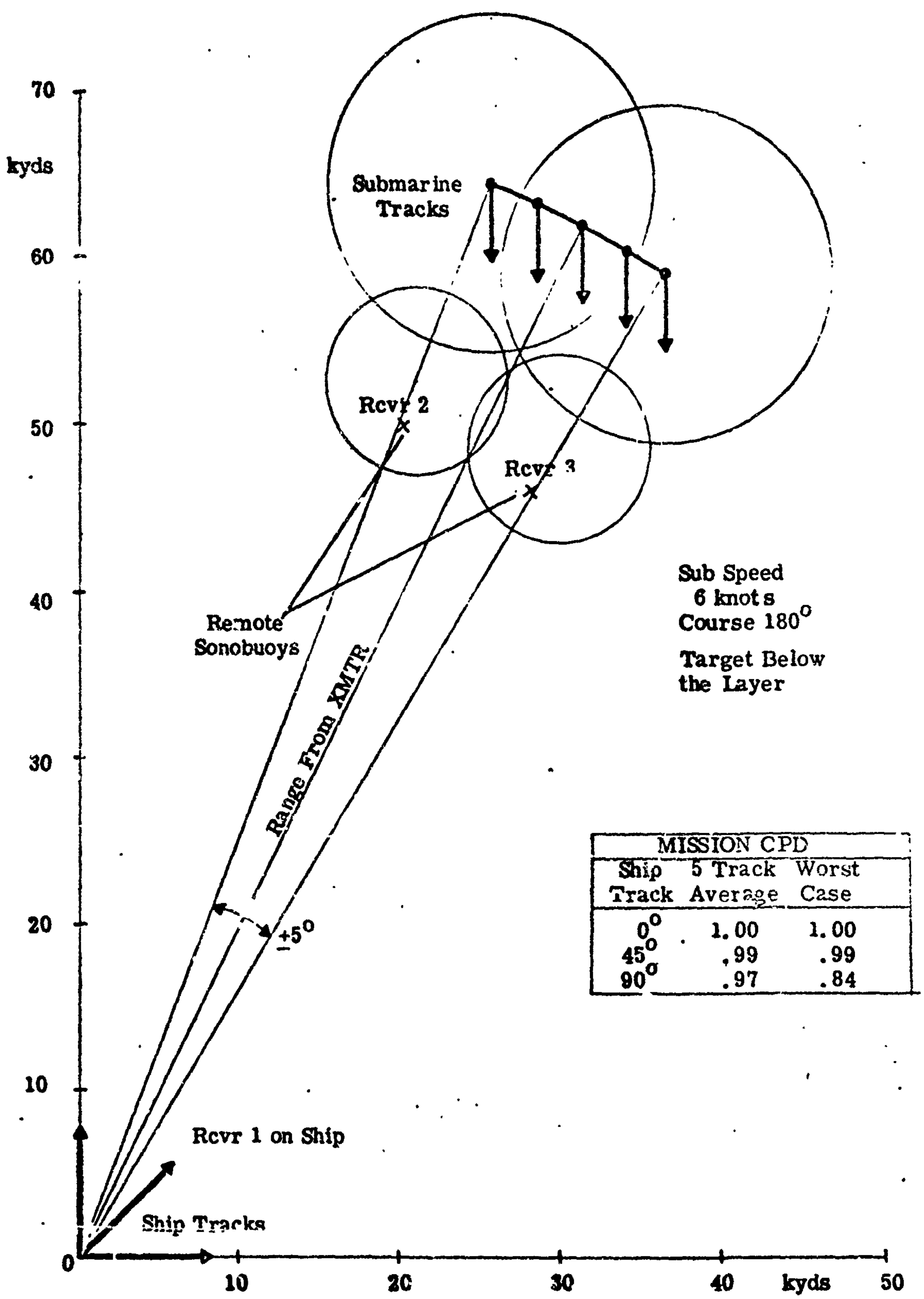

MISSION CPD		
Ship Track	5 Track Average	Worst Case
0°	1.00	1.00
45°	.99	.99
90°	.97	.84

Hazeltine
Corporation

Figure A-11

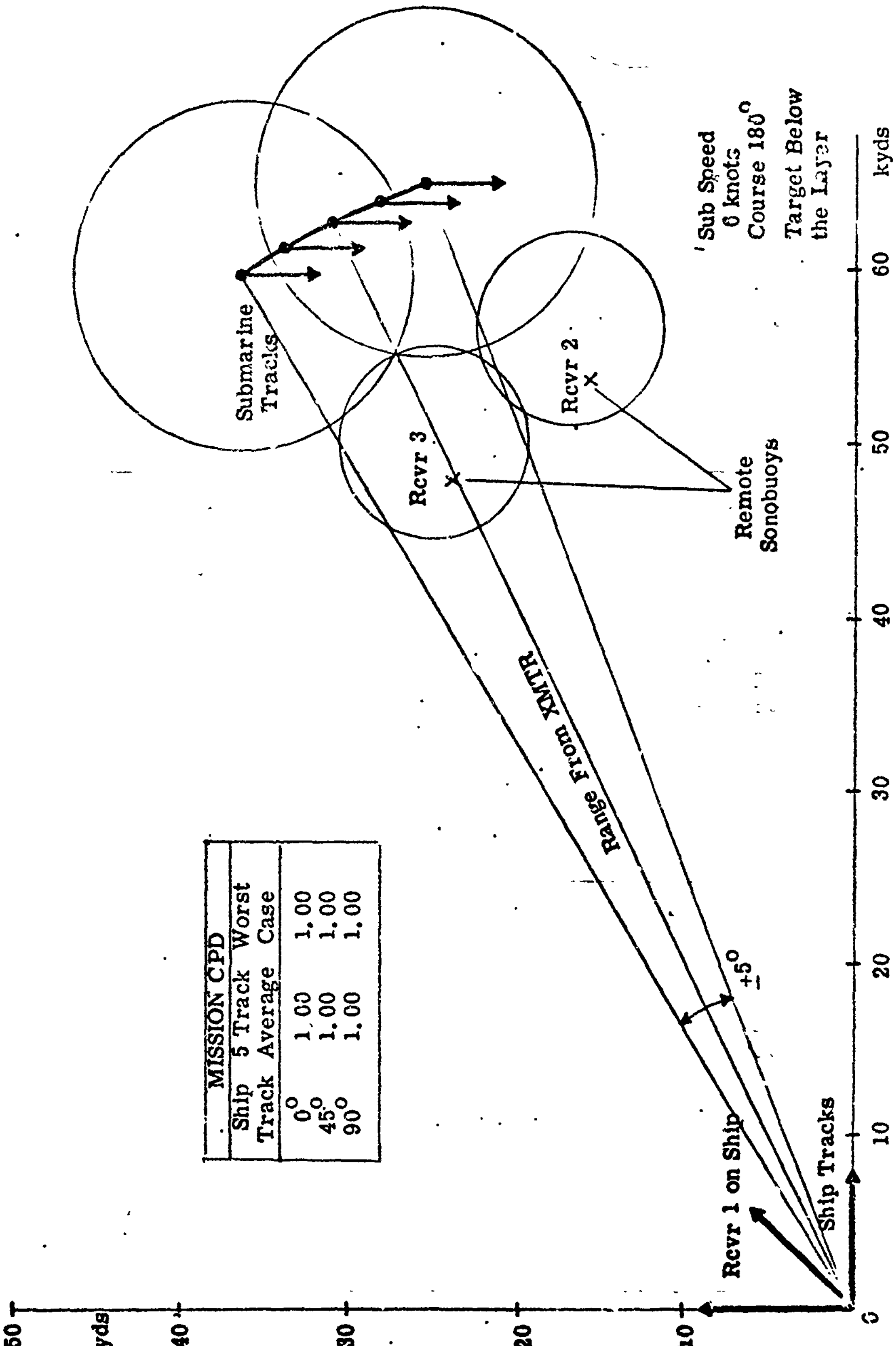

MISSION CPD

Ship Track	5 Track Average	Worst Case
0°	1.00	1.00
45°	1.00	1.00
90°	1.00	1.00

Figure A-12

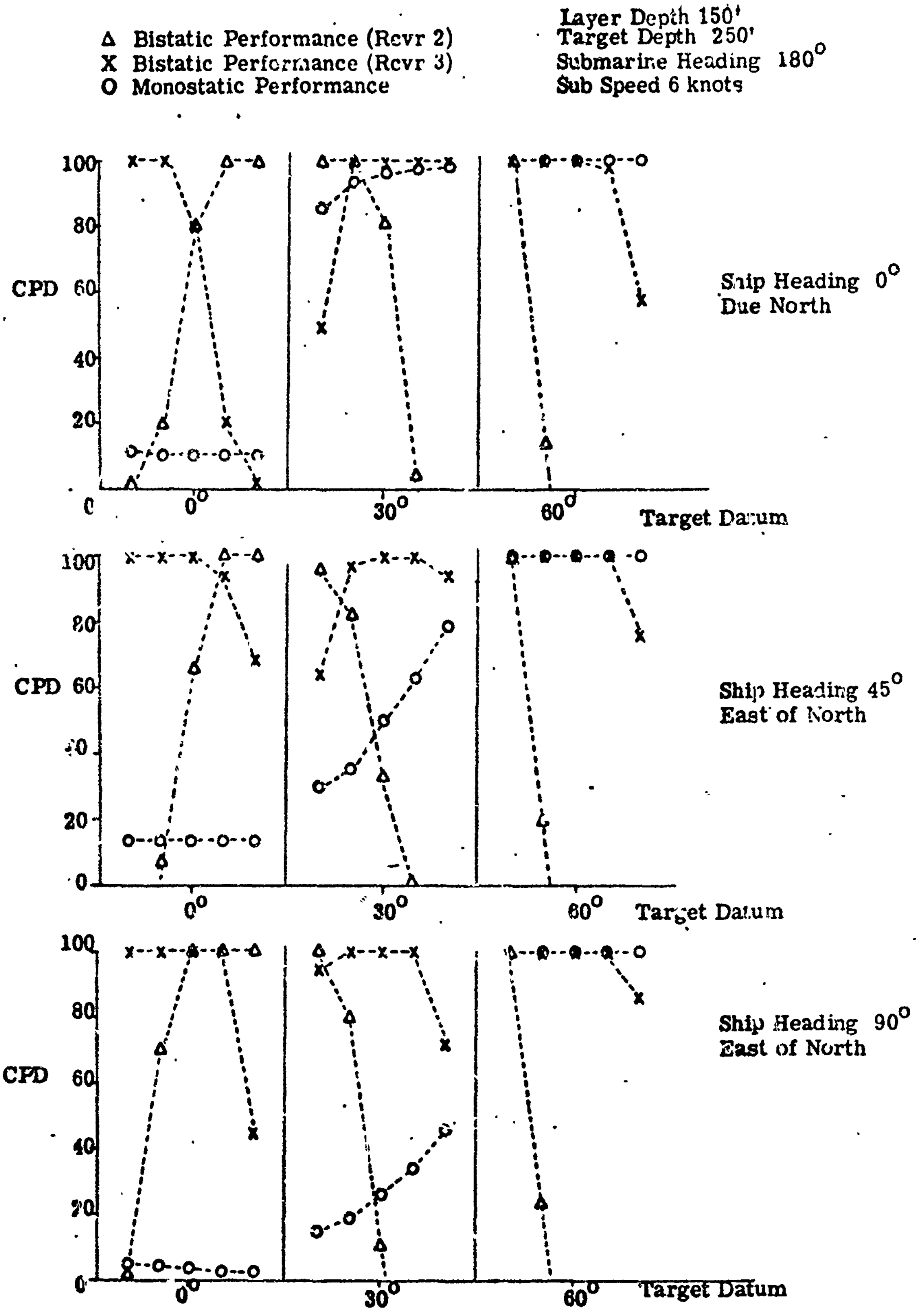
Δ Bistatic Performance (Rcvr 2)
X Bistatic Performance (Rcvr 3)
O Monostatic Performance
Layer Depth 150'
Target Depth 250'
Submarine Heading 180°
Sub Speed 6 knots
CPD
0
20
40
60
80
100
0°
30°
60°
Target Datum
Ship Heading 0° Due North
Ship Heading 45° East of North
Ship Heading 90° East of North

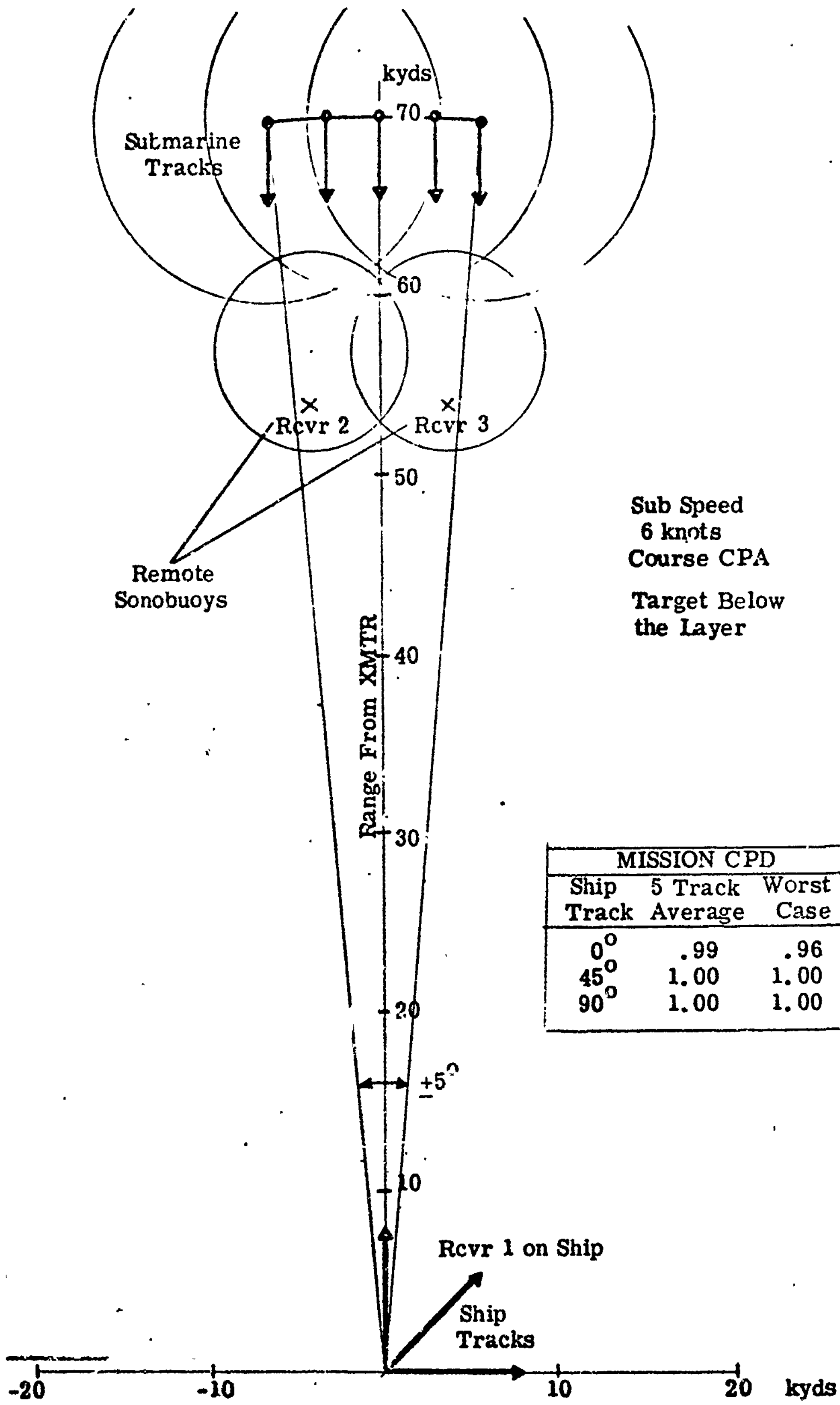

MISSION CPD		
Ship Track	5 Track Average	Worst Case
0°	.99	.96
45°	1.00	1.00
90°	1.00	1.00

Figure A-14

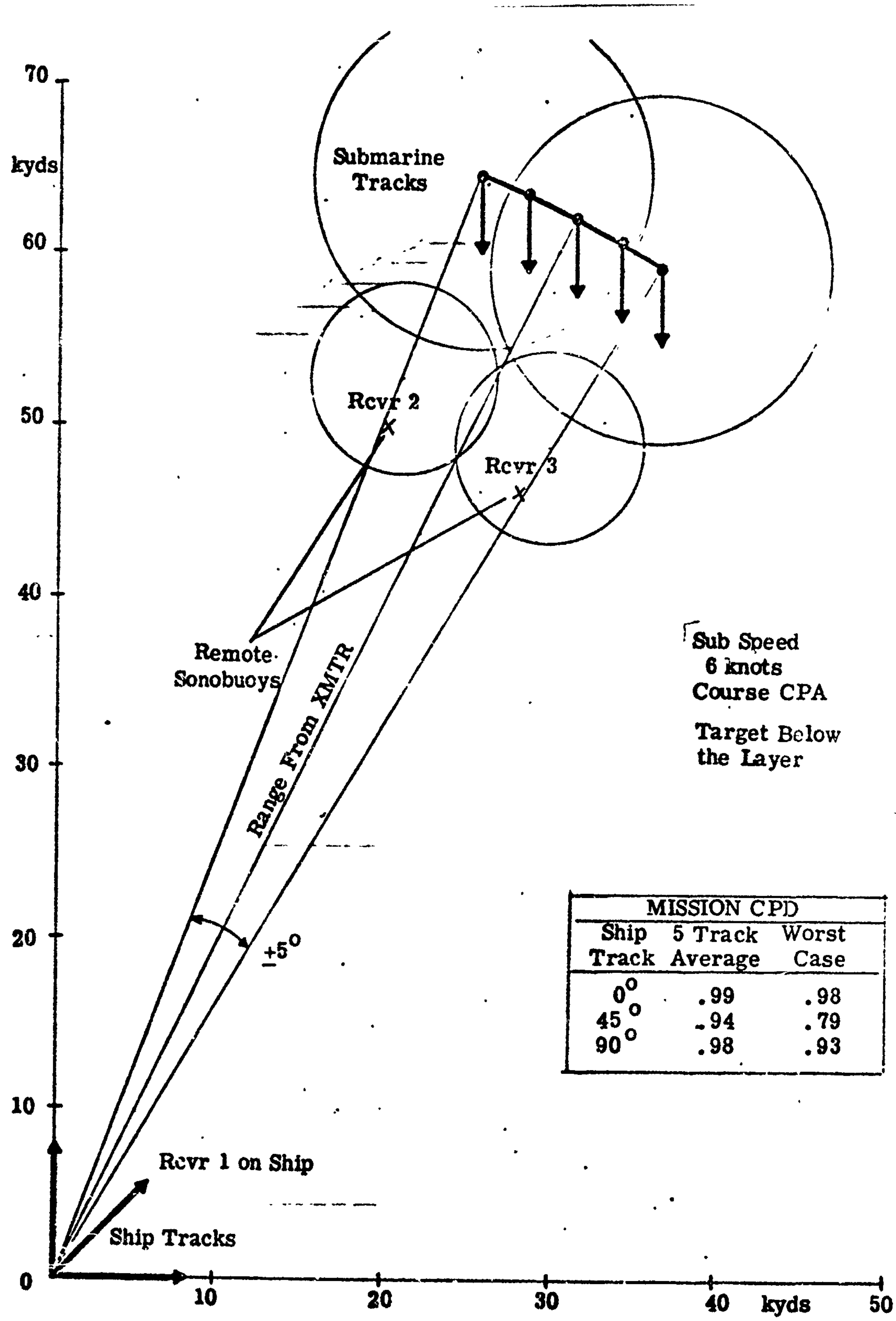

MISSION CPD

Ship Track	5 Track Average	Worst Case
0°	.99	.98
45°	.94	.79
90°	.98	.93

Hazeltine
Corporation

Figure A-15

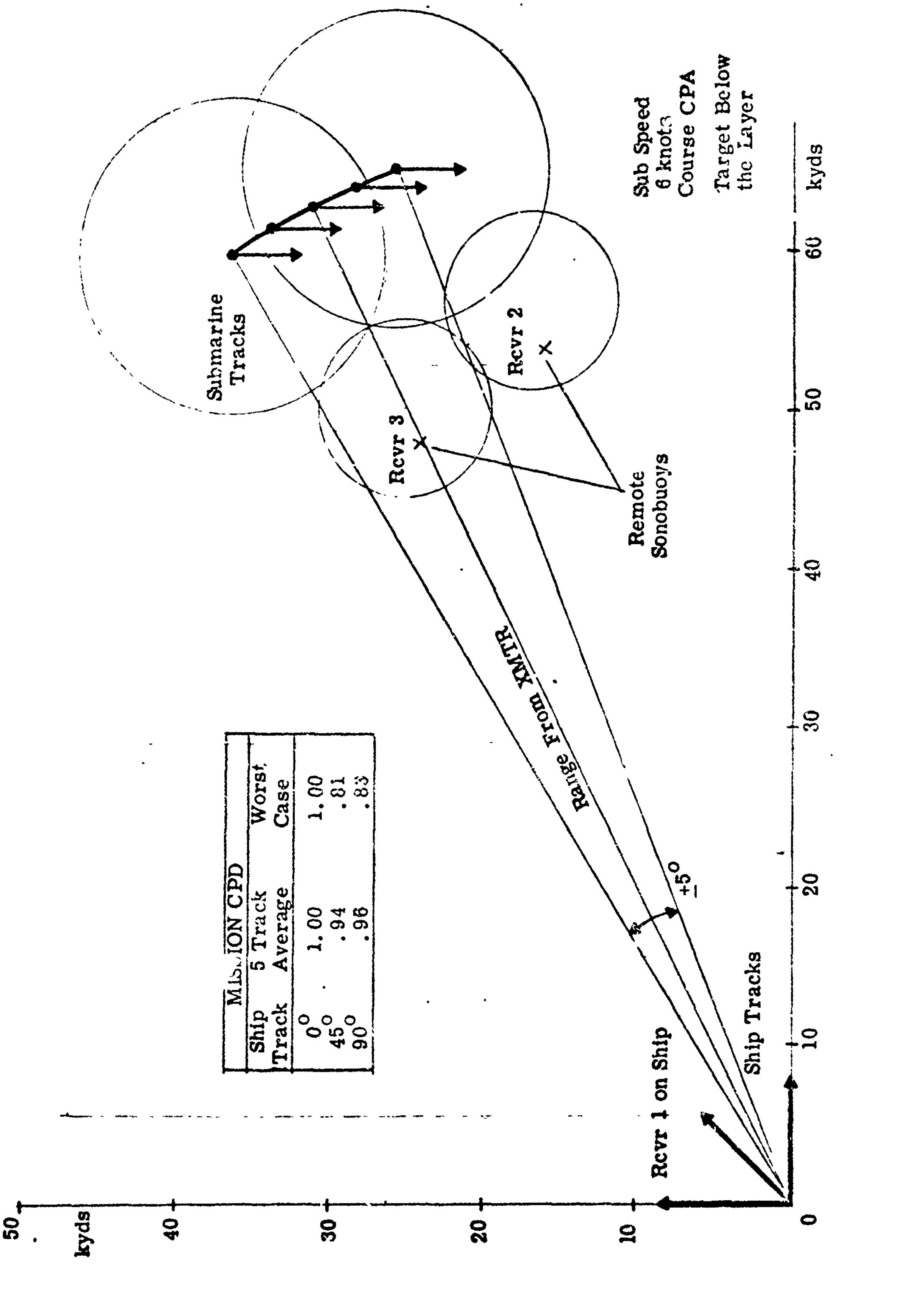

MISSION CPD		
Ship Track	5 Track Average	Worst Case
0^{o}	1.00	1.00
45^{o}	.94	.81
90^{o}	.96	.83

Hazeltine Corporation

Figure A-16

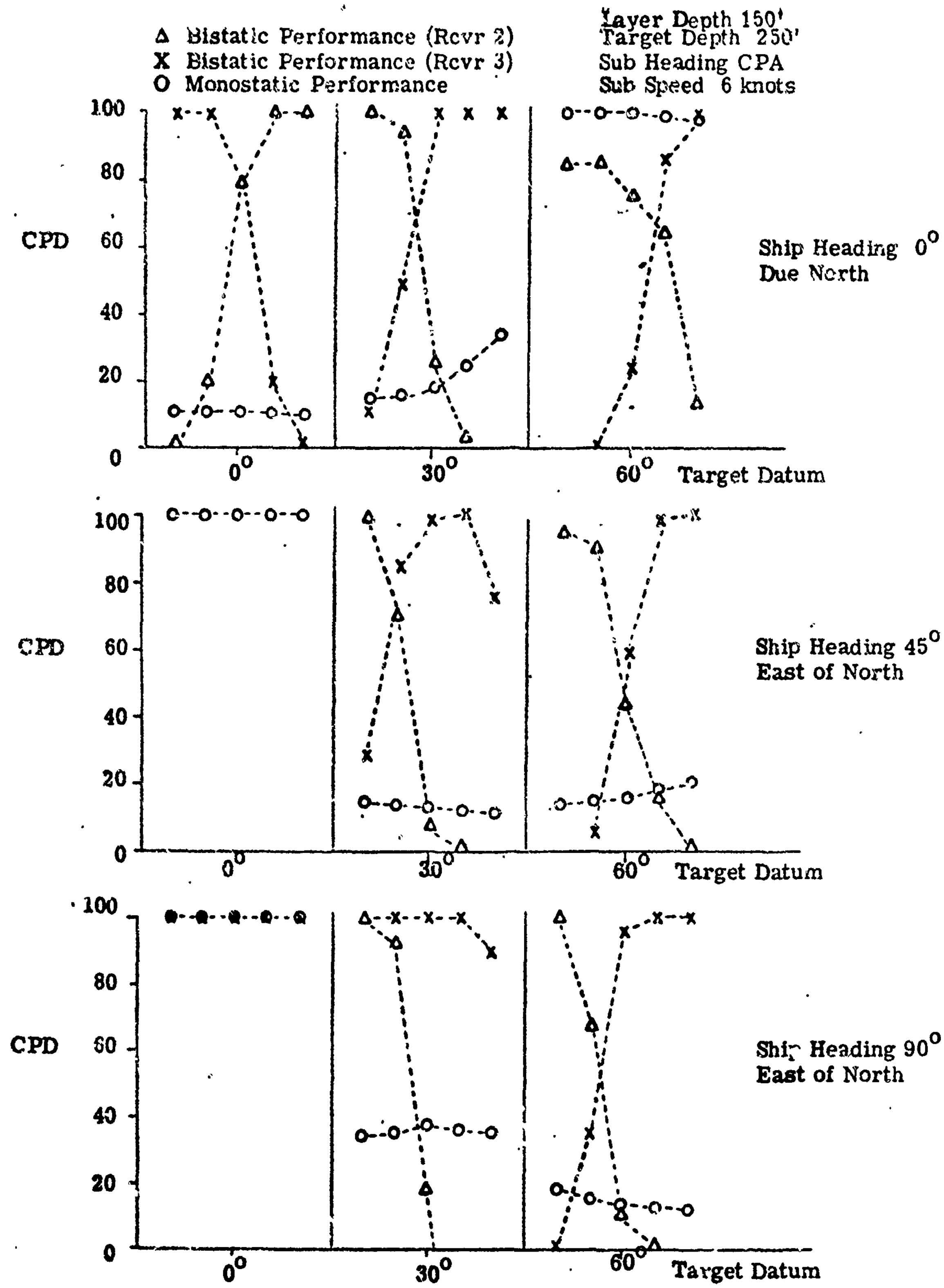

Hazeltine Corporation

Figure A-17

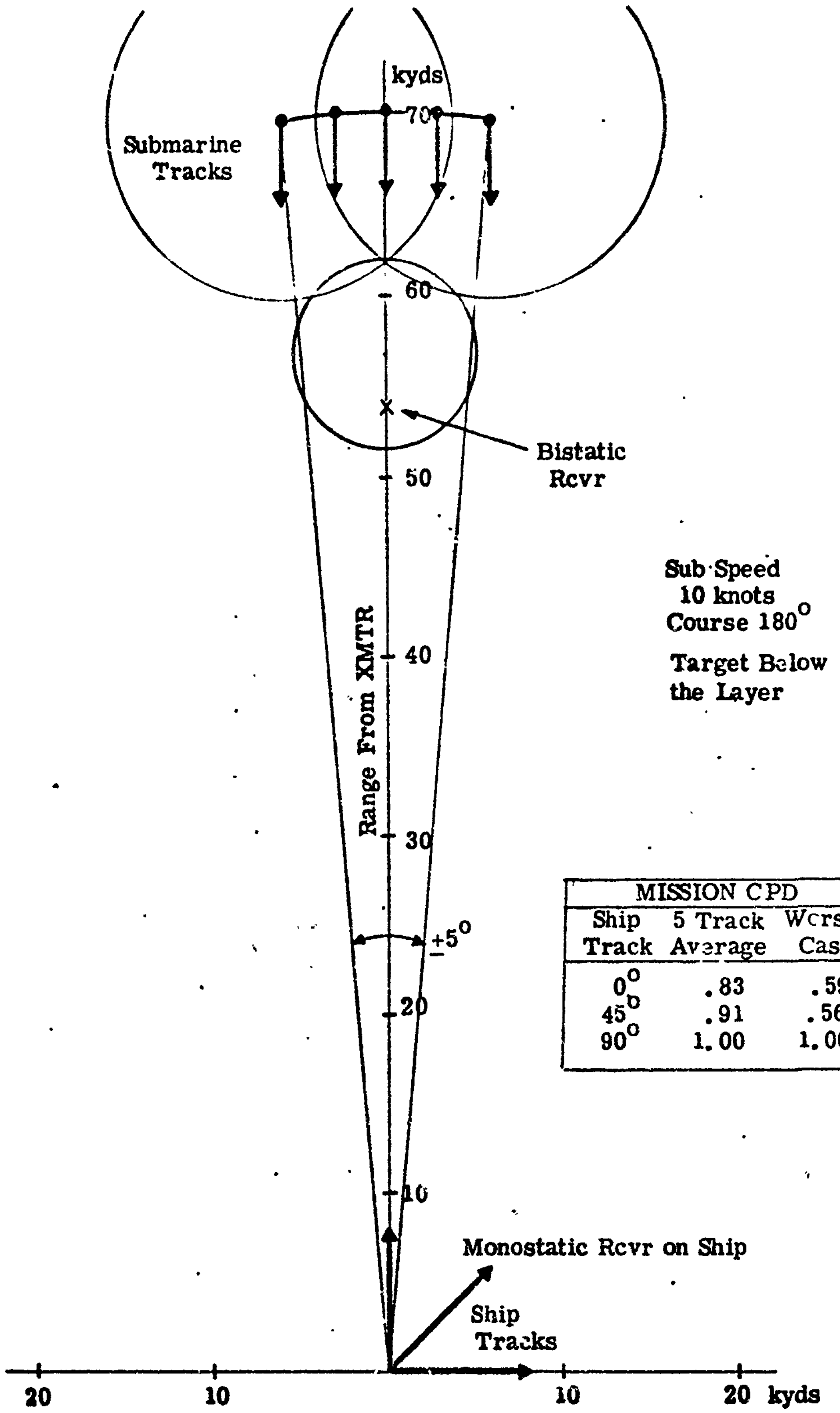

MISSION CPD		
Ship Track	5 Track Average	Worst Case
0°	.83	.59
45°	.91	.56
90°	1.00	1.00

Hazeltine
Corporation

Figure A-18

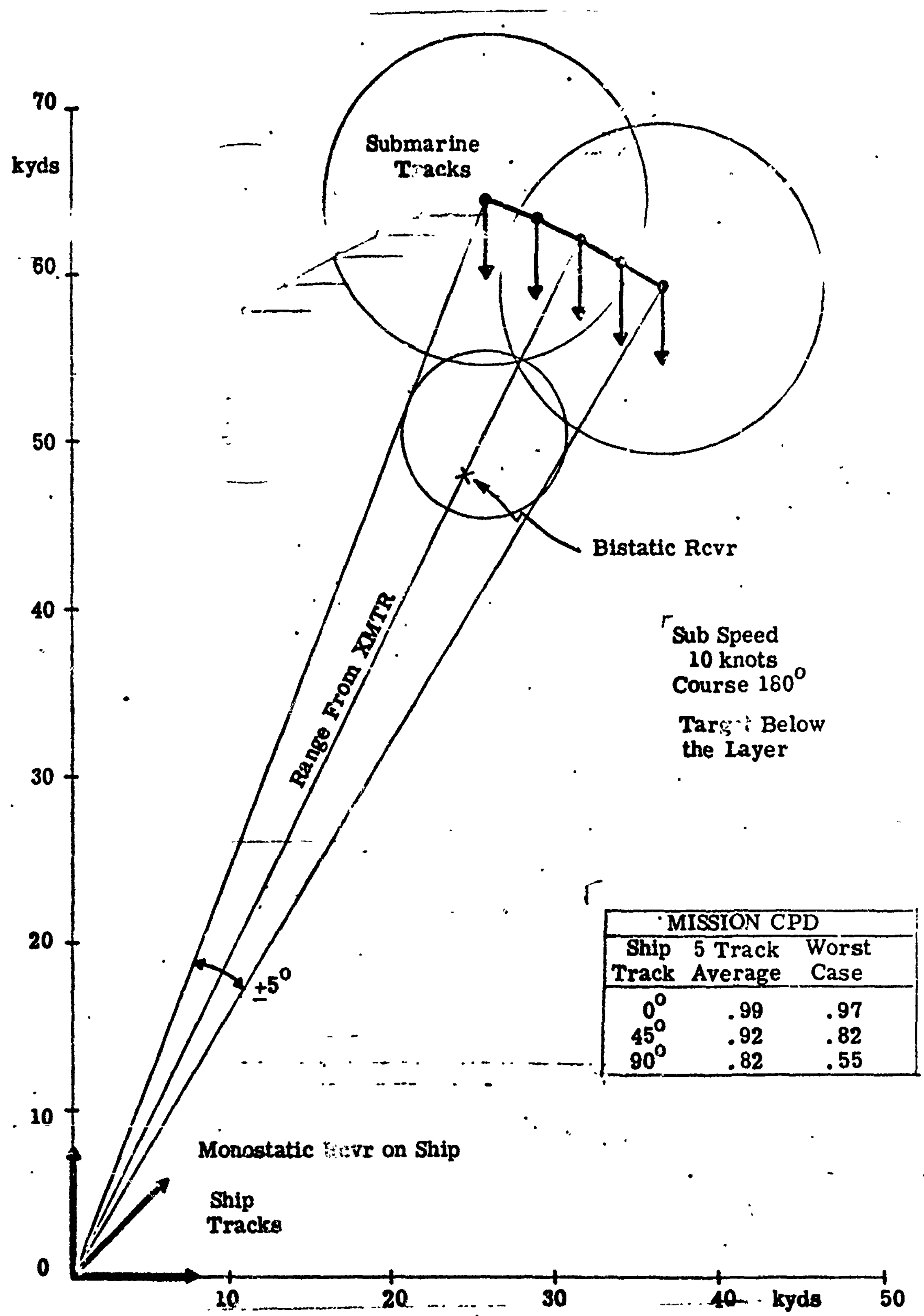

MISSION CPD		
Ship Track	5 Track Average	Worst Case
0°	.99	.97
45°	.92	.82
90°	.82	.55

Figure A-19

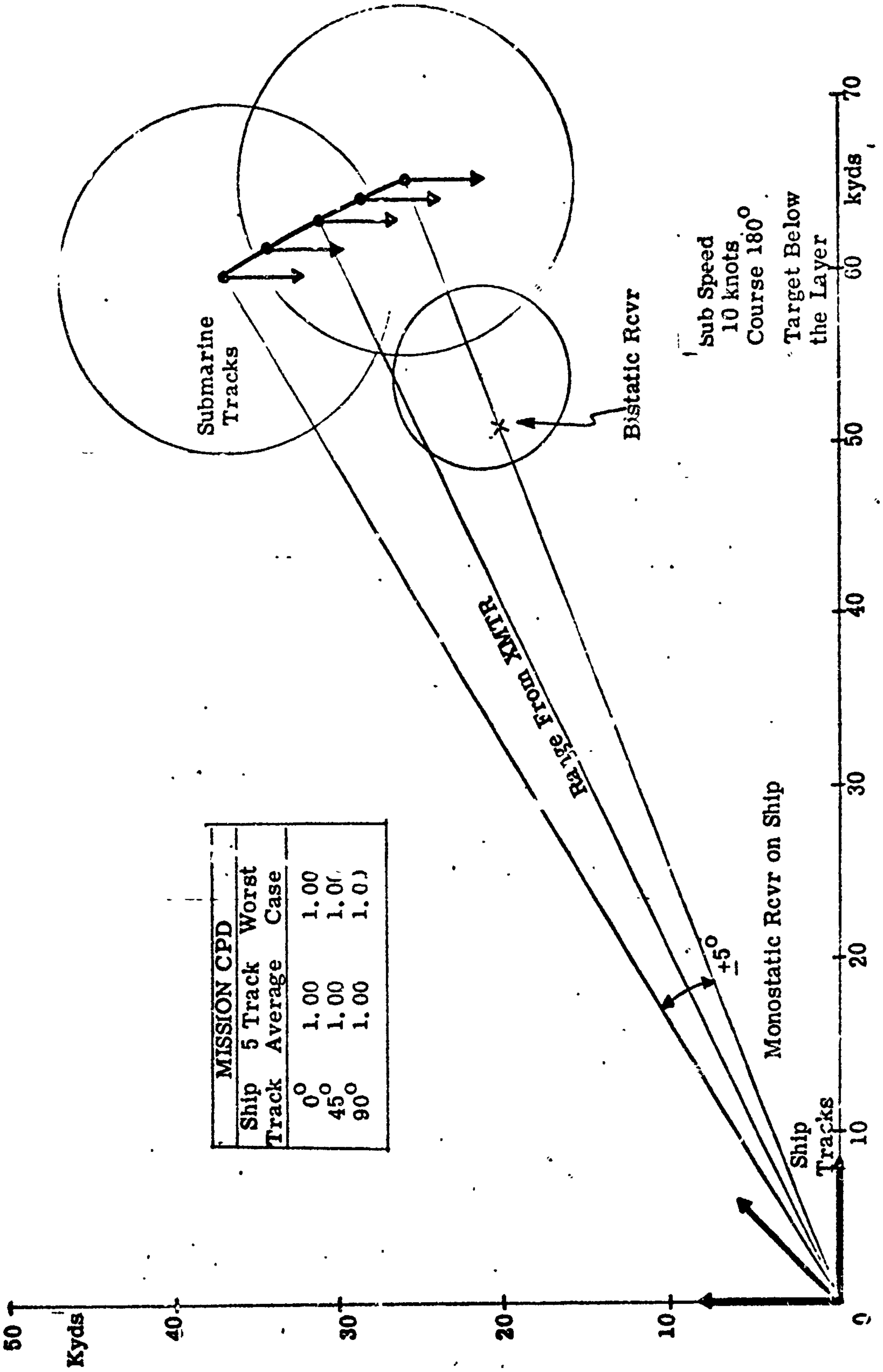

MISSION CPD		
Ship Track	5 Track Average	Worst Case
0°	1.00	1.00
45°	1.00	1.00
90°	1.00	1.00

Figure A-20

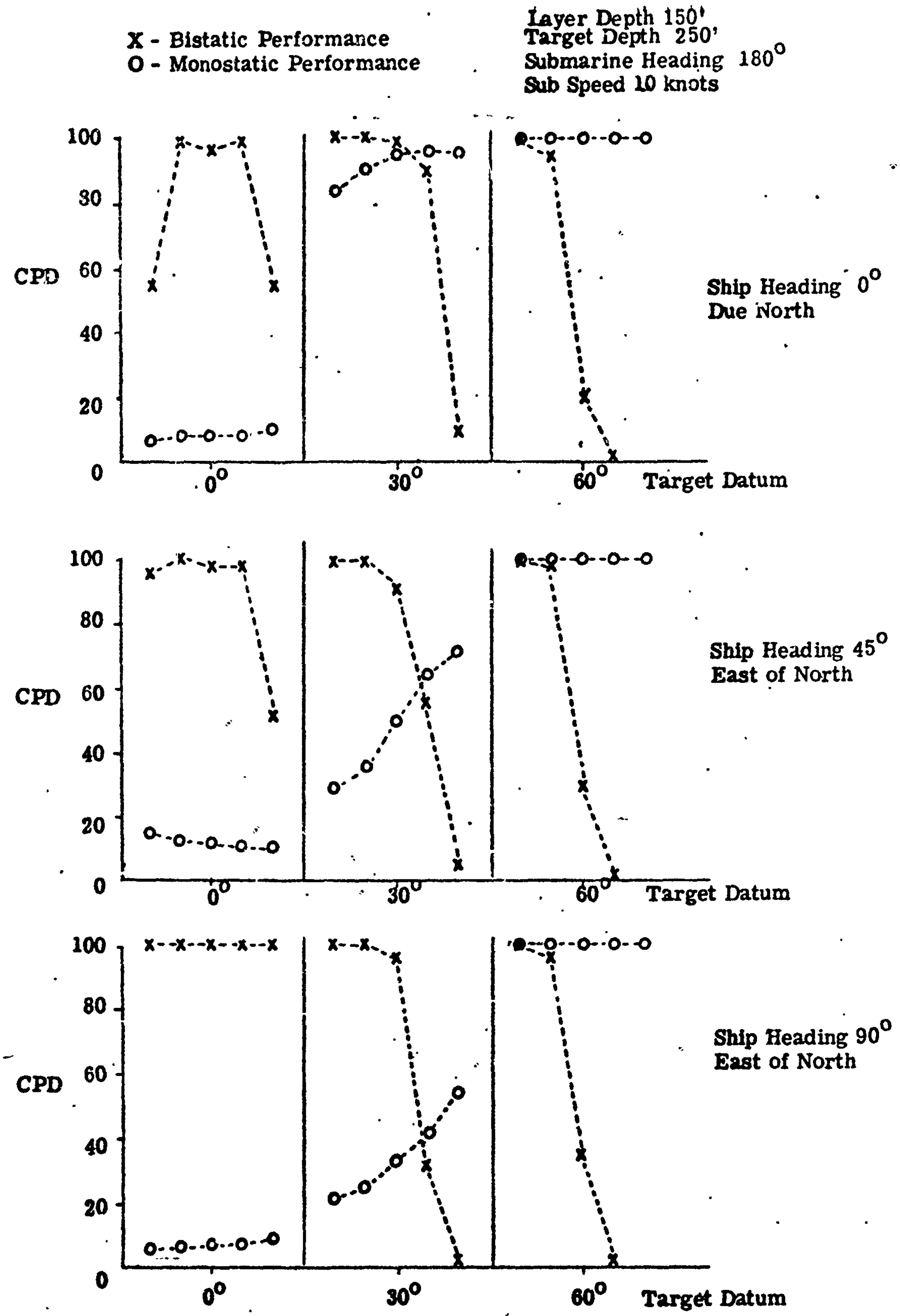
X - Bistatic Performance
O - Monostatic Performance
Layer Depth 150'
Target Depth 250'
Submarine Heading 180°
Sub Speed 10 knots
CPD
100
80
60
40
20
0
0°
30°
60°
Target Datum
Ship Heading 0°
Due North
Ship Heading 45°
East of North
Ship Heading 90°
East of North

Hazeltine Corporation

Figure A-20

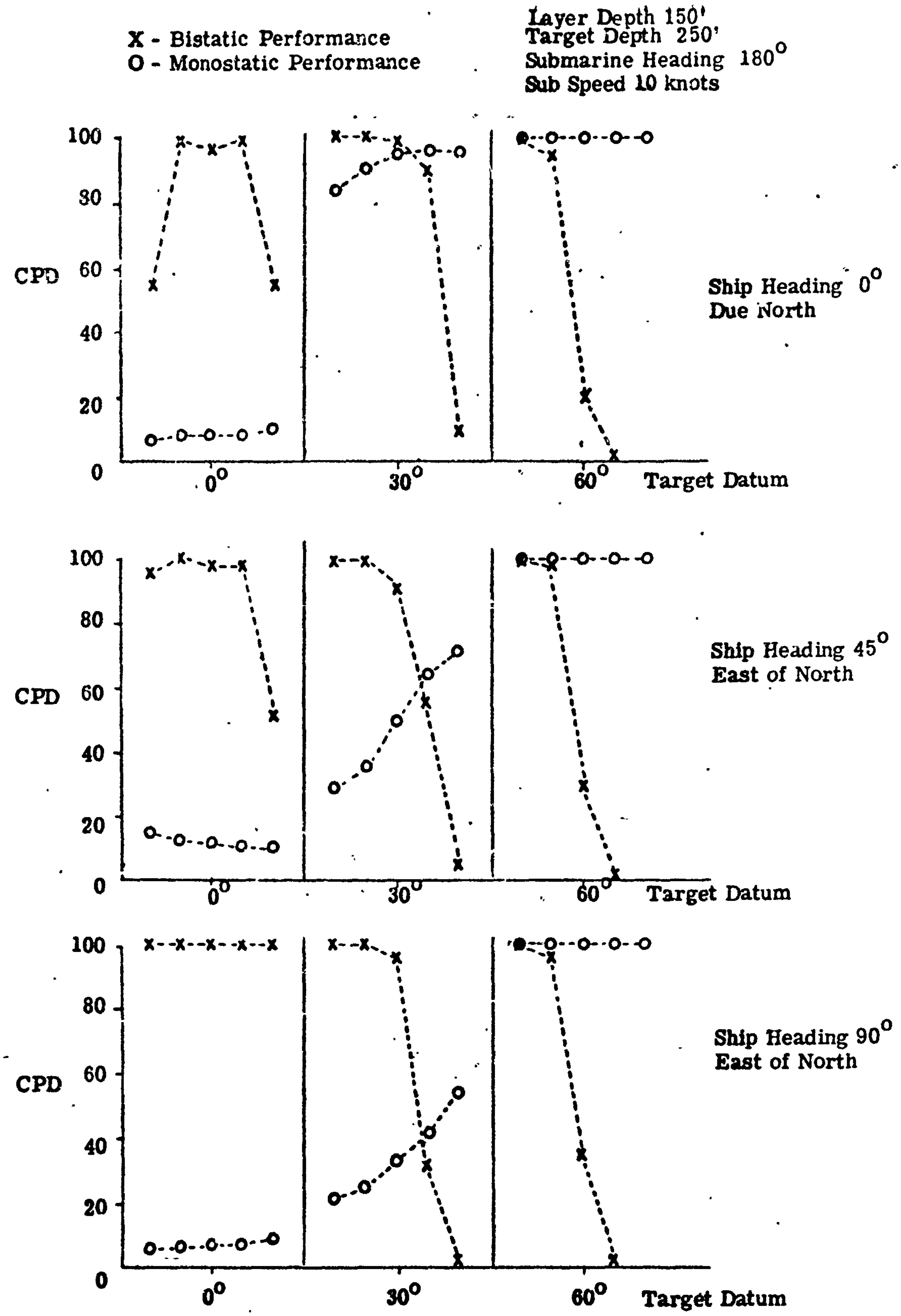

Figure A-21

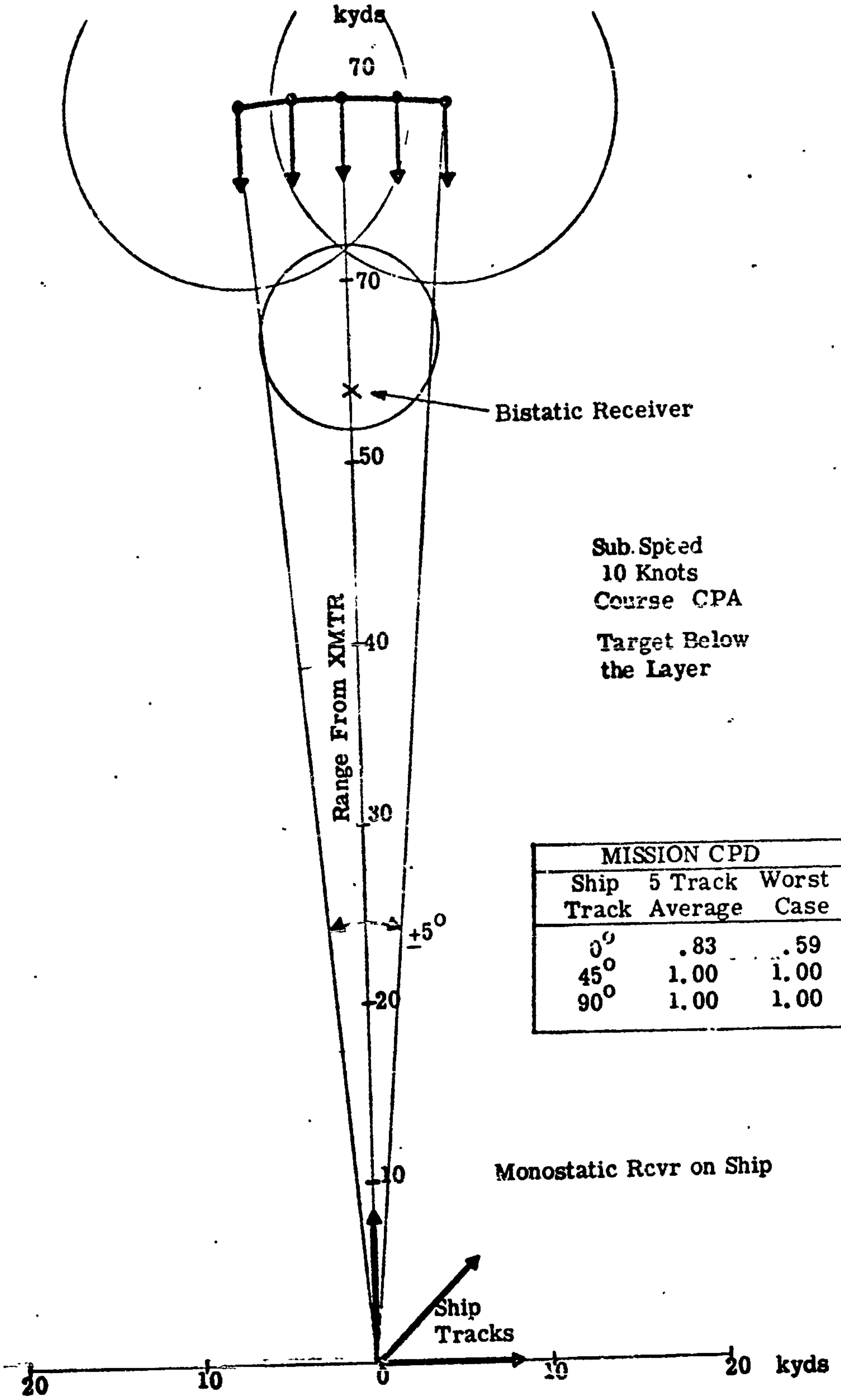

Sub. Speed
10 Knots
Course CPA

Target Below
the Layer

MISSION CPD		
Ship Track	5 Track Average	Worst Case
0°	.83	.59
45°	1.00	1.00
90°	1.00	1.00

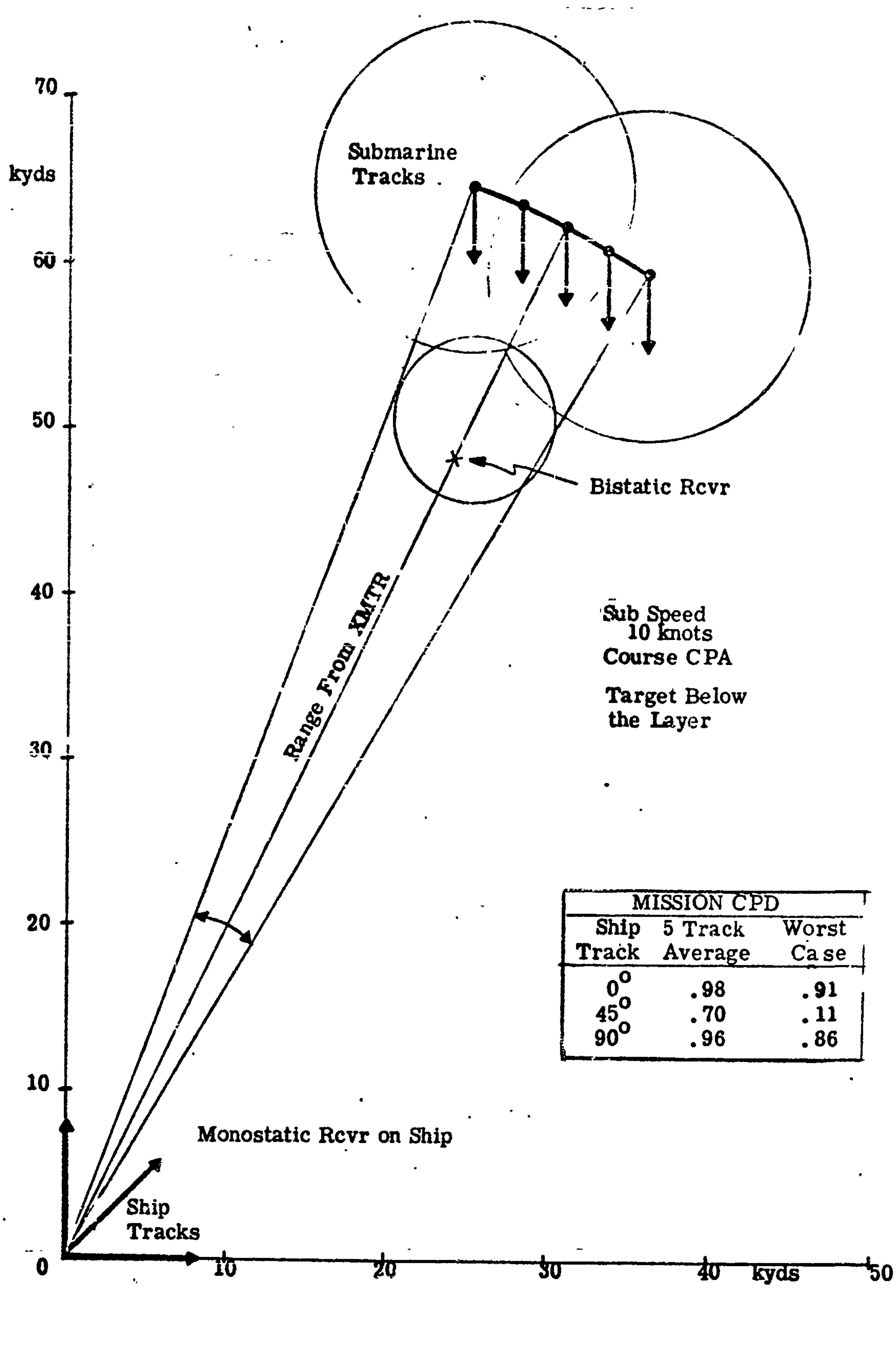

MISSION CPD		
Ship Track	5 Track Average	Worst Case
0^o	.98	.91
45^o	.70	.11
90^o	.96	.86

Hazeltine
Corporation

Figure A-23

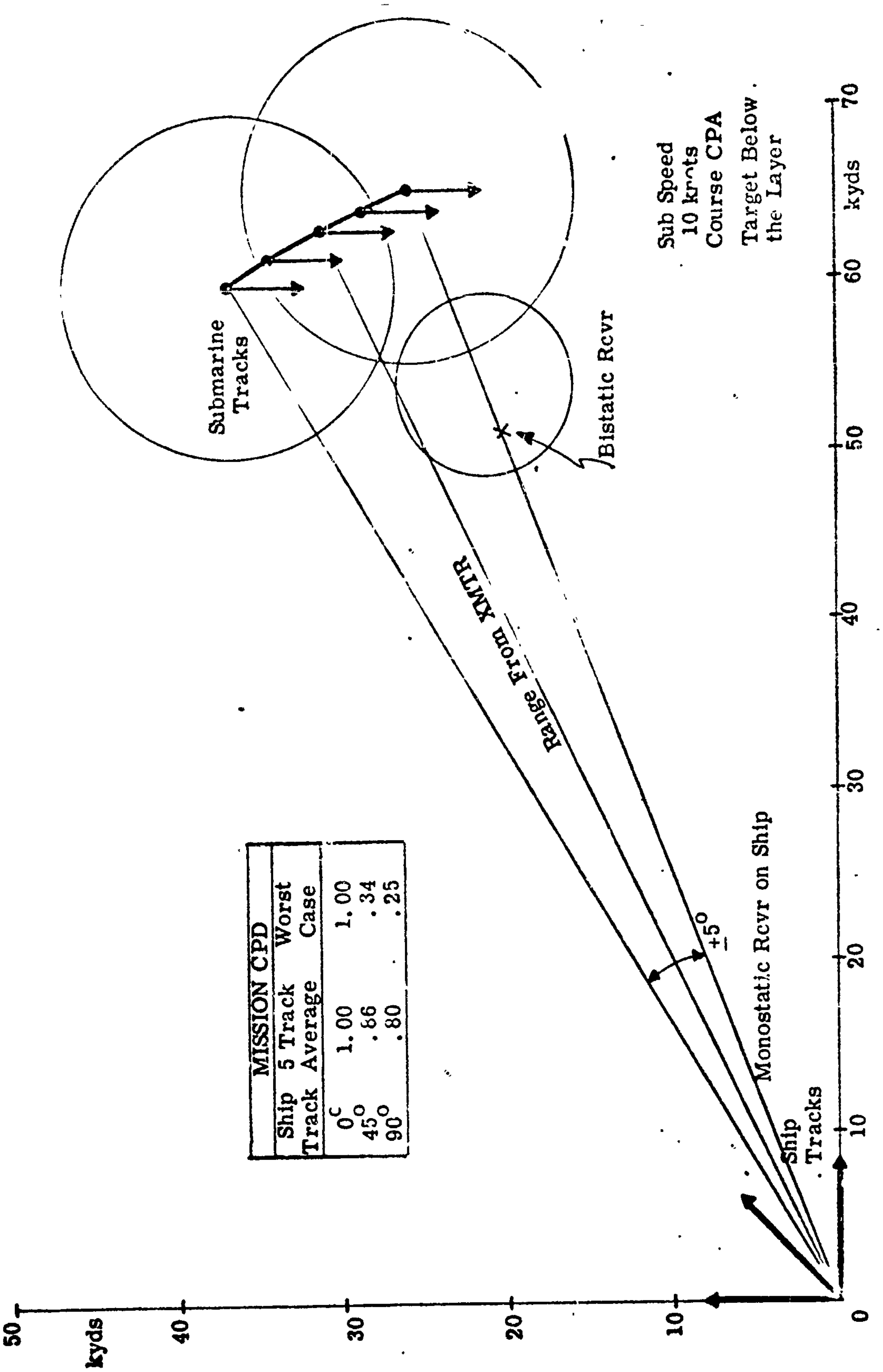

MISSION CPD

Ship Track	5 Track Average	Worst Case
0^o	1.00	1.00
45^o	.86	.34
90^o	.80	.25

Hazeltine
Corporation

Figure A-24

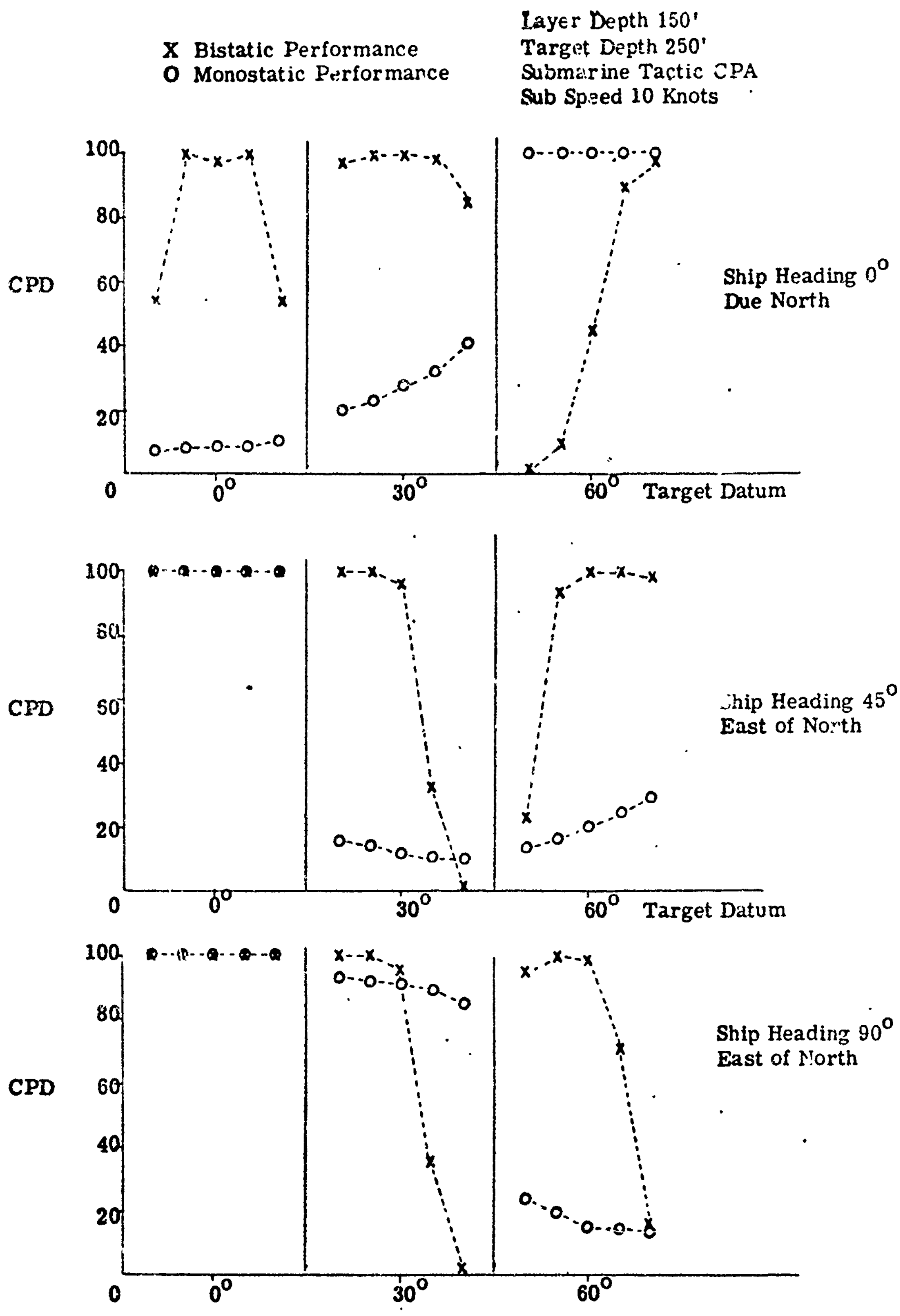

Figure A-25

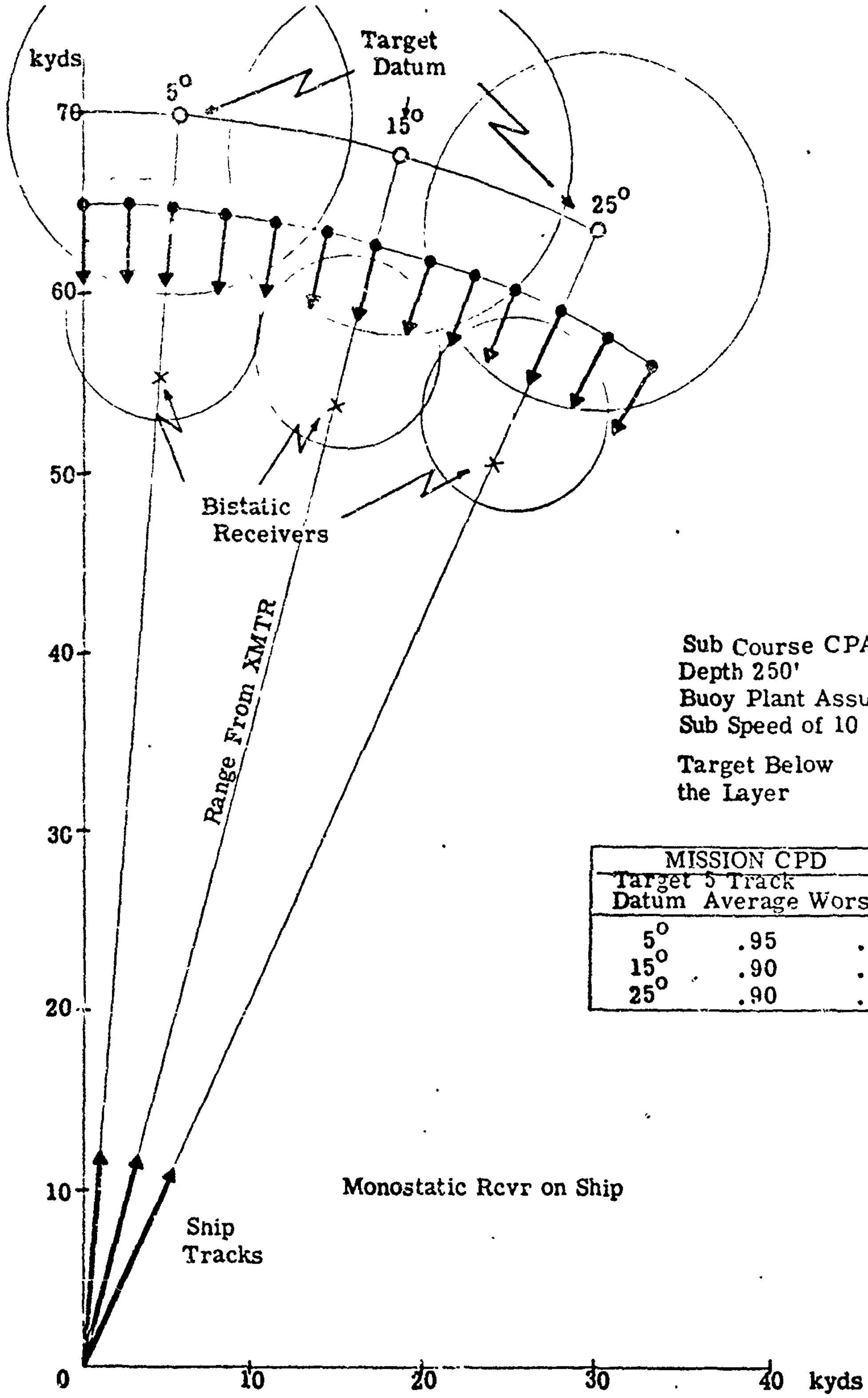

Sub Course CPA
Depth 250'
Buoy Plant Assumes
Sub Speed of 10 knots

Target Below
the Layer

MISSION CPD		
Target Datum	5 Track Average	Worst Case
5°	.95	.79
15°	.90	.73
25°	.90	.58

Hazeltine Corporation

Figure A-26

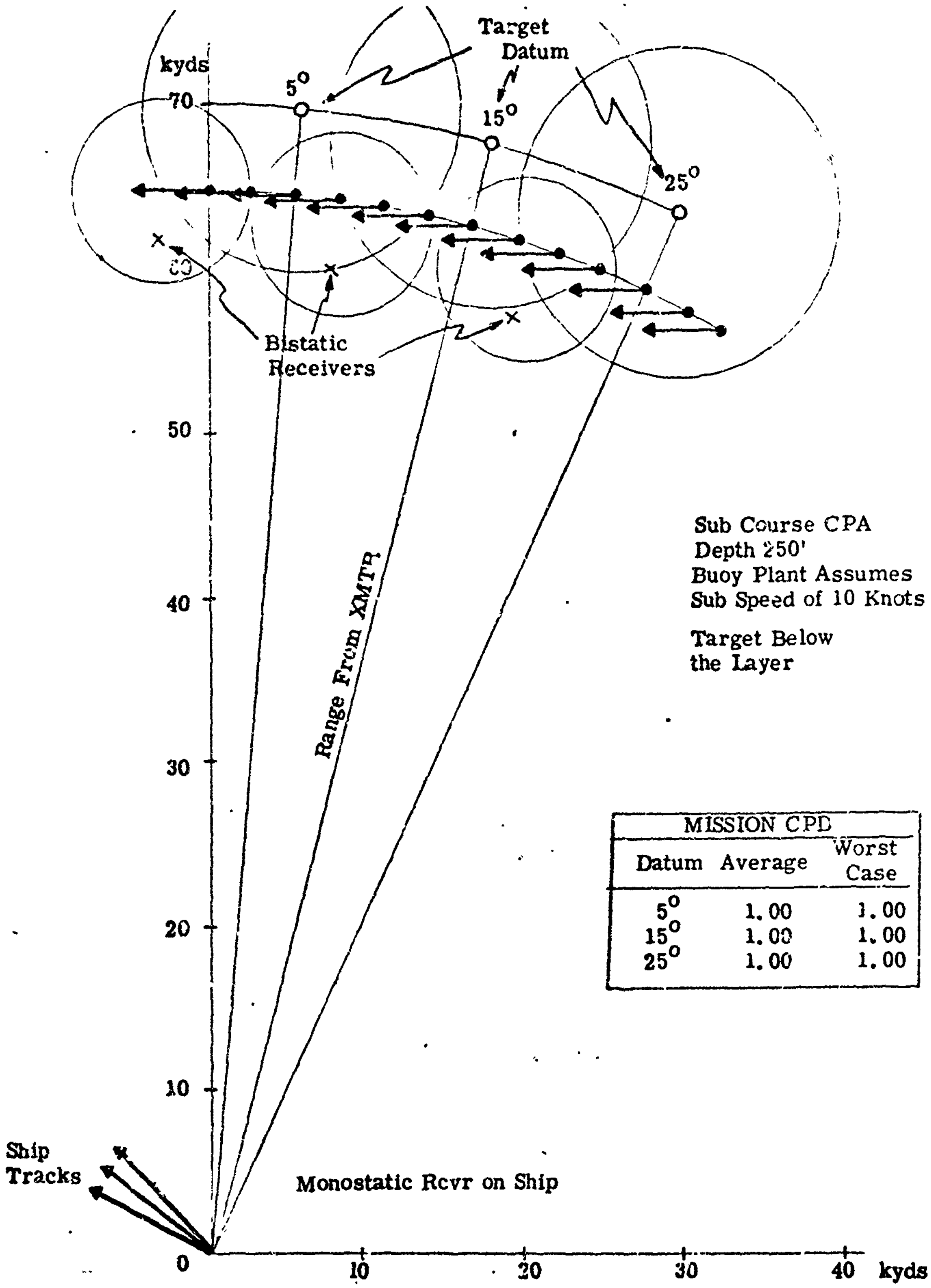

MISSION CPD		
Datum	Average	Worst Case
5°	1.00	1.00
15°	1.00	1.00
25°	1.00	1.00

Figure A-27

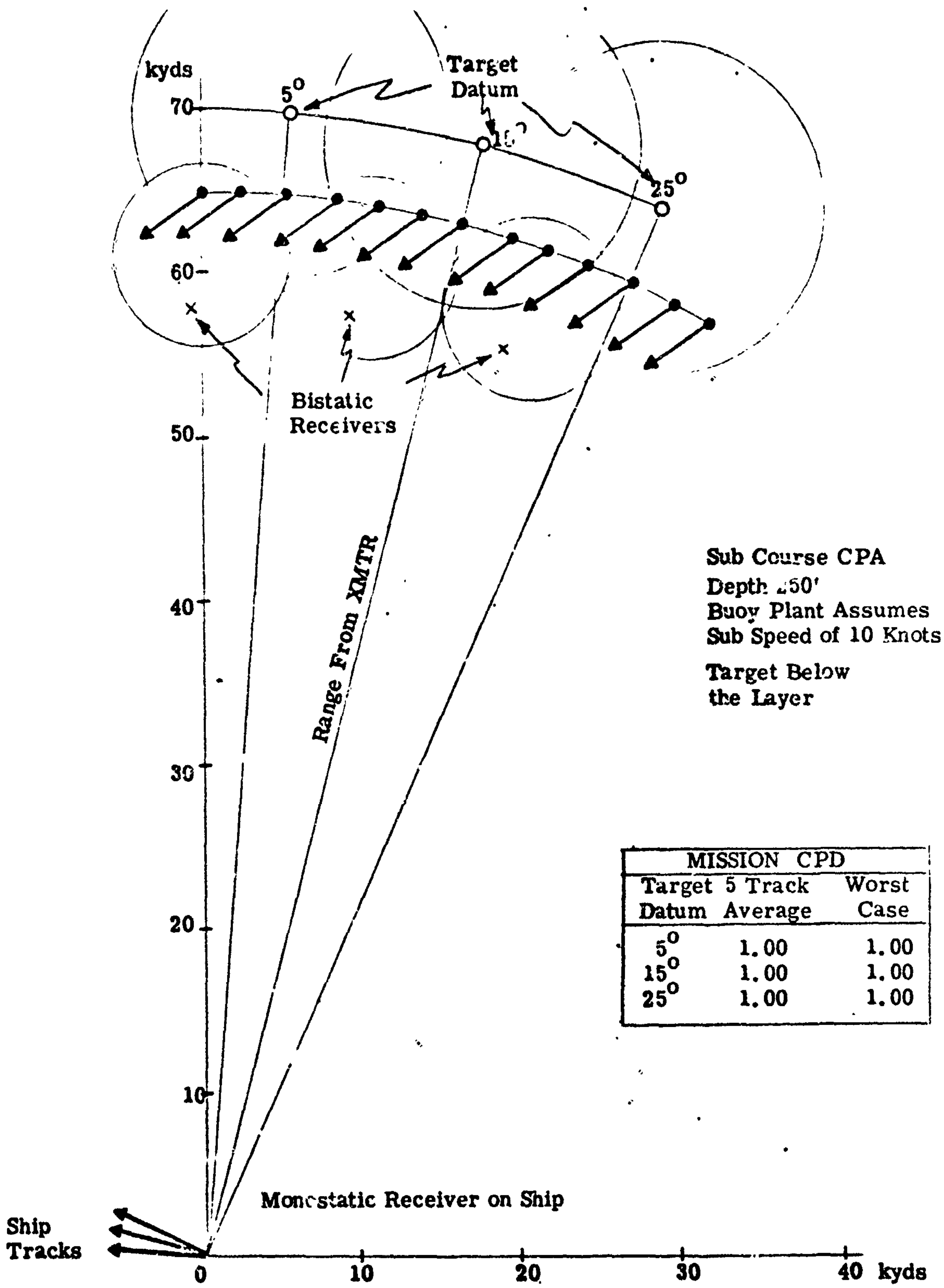

MISSION CPD		
Target Datum	5 Track Average	Worst Case
5°	1.00	1.00
15°	1.00	1.00
25°	1.00	1.00

Hazeltine Corporation

Figure A-28

X Bistatic Performance
O Monostatic Performance

Layer Depth 150'
Target at 250'
Submarine Tactic CPA
Submarine Speed 10 knots

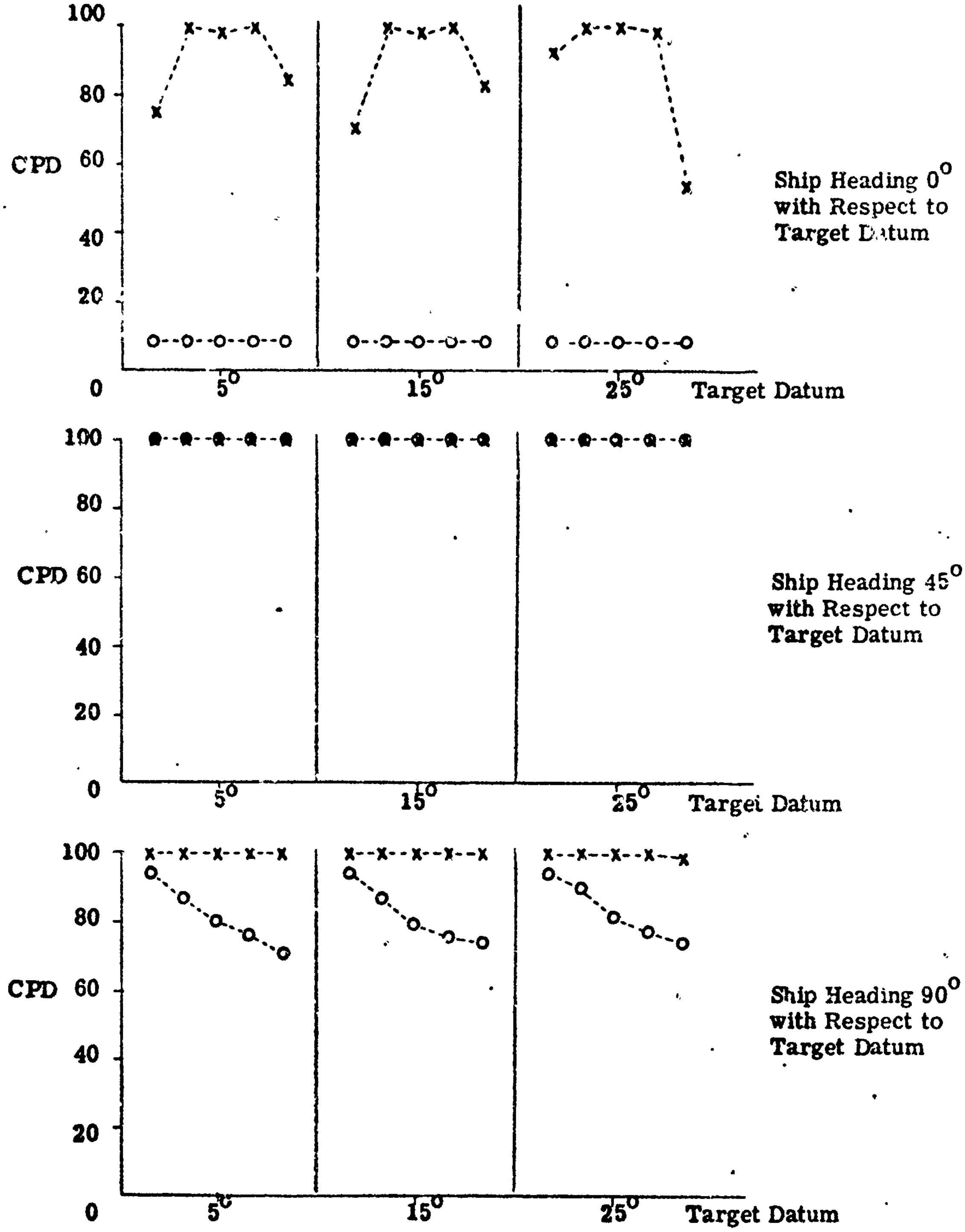

Hazeltine
Corporation

Figure A-29

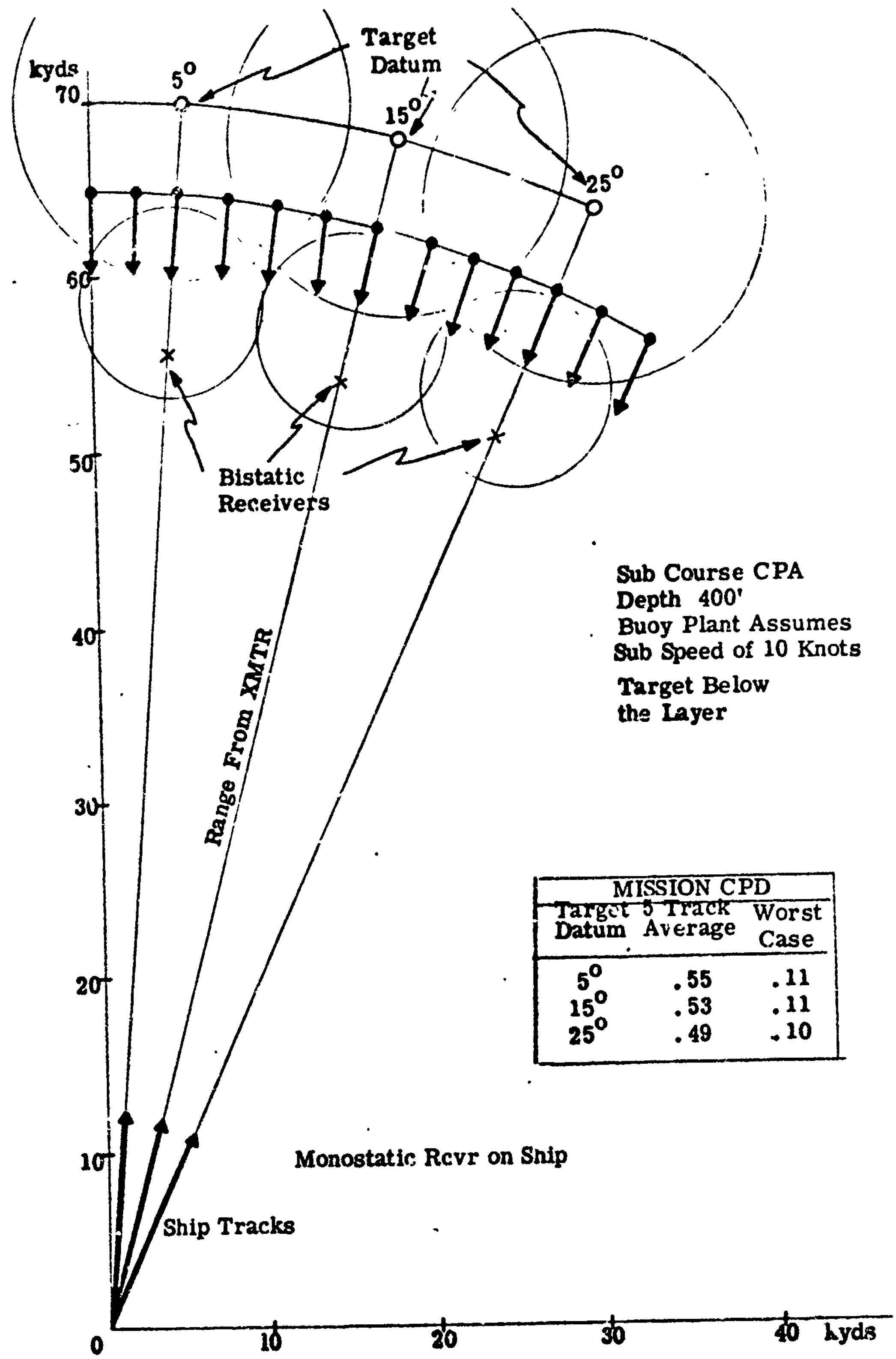

MISSION CPD		
Target Datum	5 Track Average	Worst Case
5°	.55	.11
15°	.53	.11
25°	.49	.10

Figure A-30

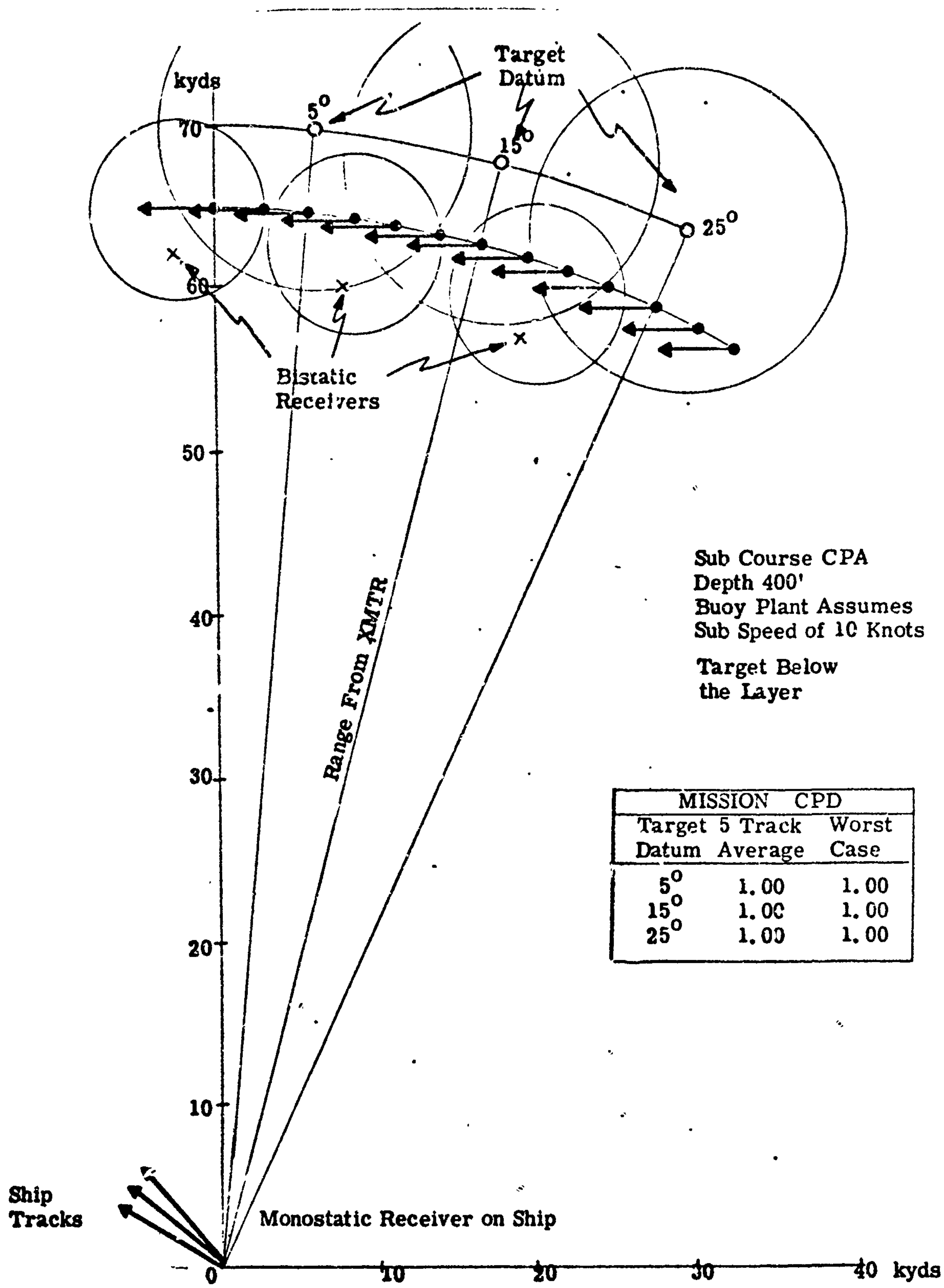

Sub Course CPA
Depth 400'
Buoy Plant Assumes
Sub Speed of 10 Knots

Target Below
the Layer

MISSION CPD		
Target Datum	5 Track Average	Worst Case
5°	1.00	1.00
15°	1.00	1.00
25°	1.00	1.00

Hazeltine Corporation

Figure A-31

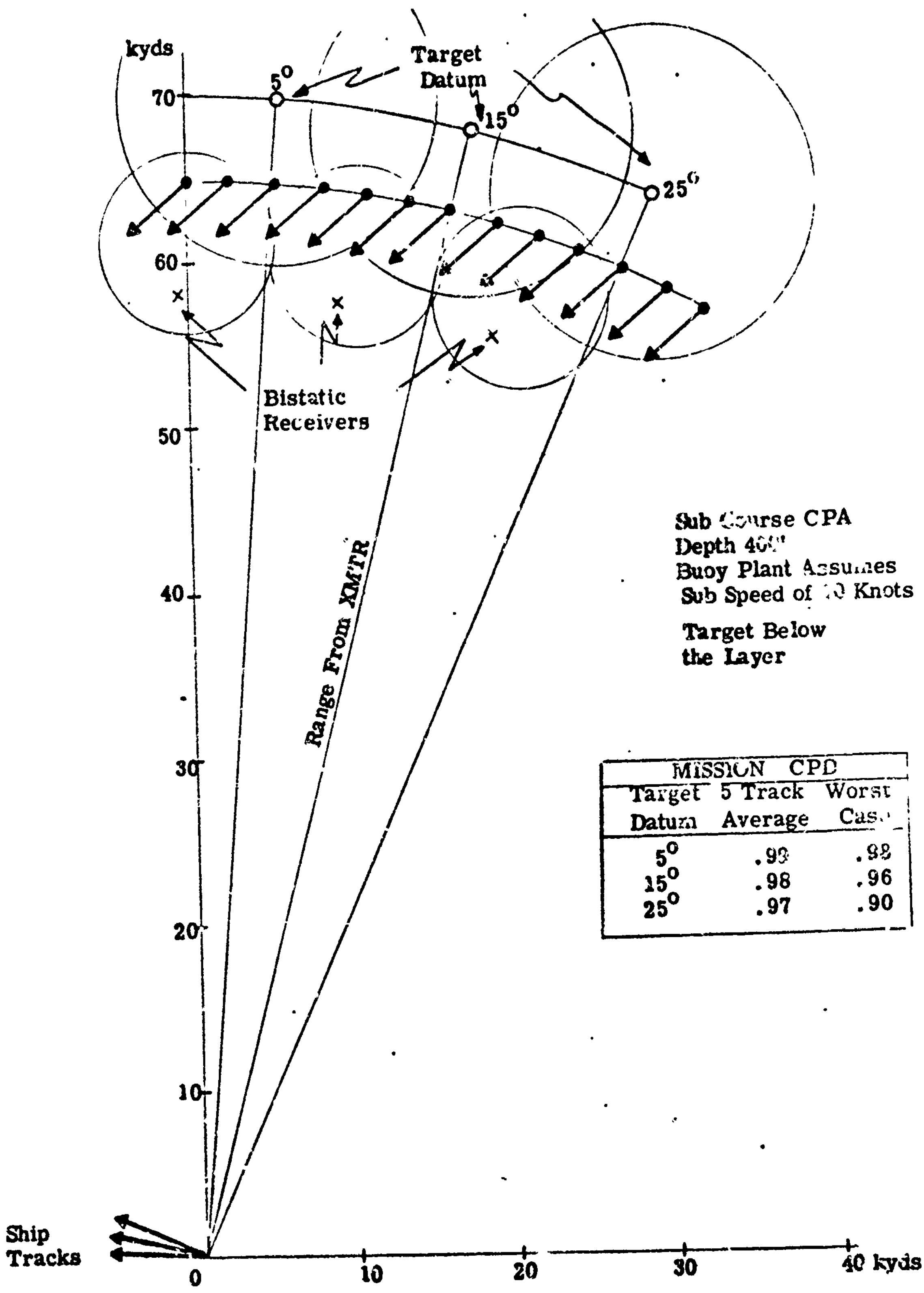

MISSION CPD		
Target Datum	5 Track Average	Worst Case
5°	.99	.98
15°	.98	.96
25°	.97	.90

Hazeltine
Corporation

Figure A-32

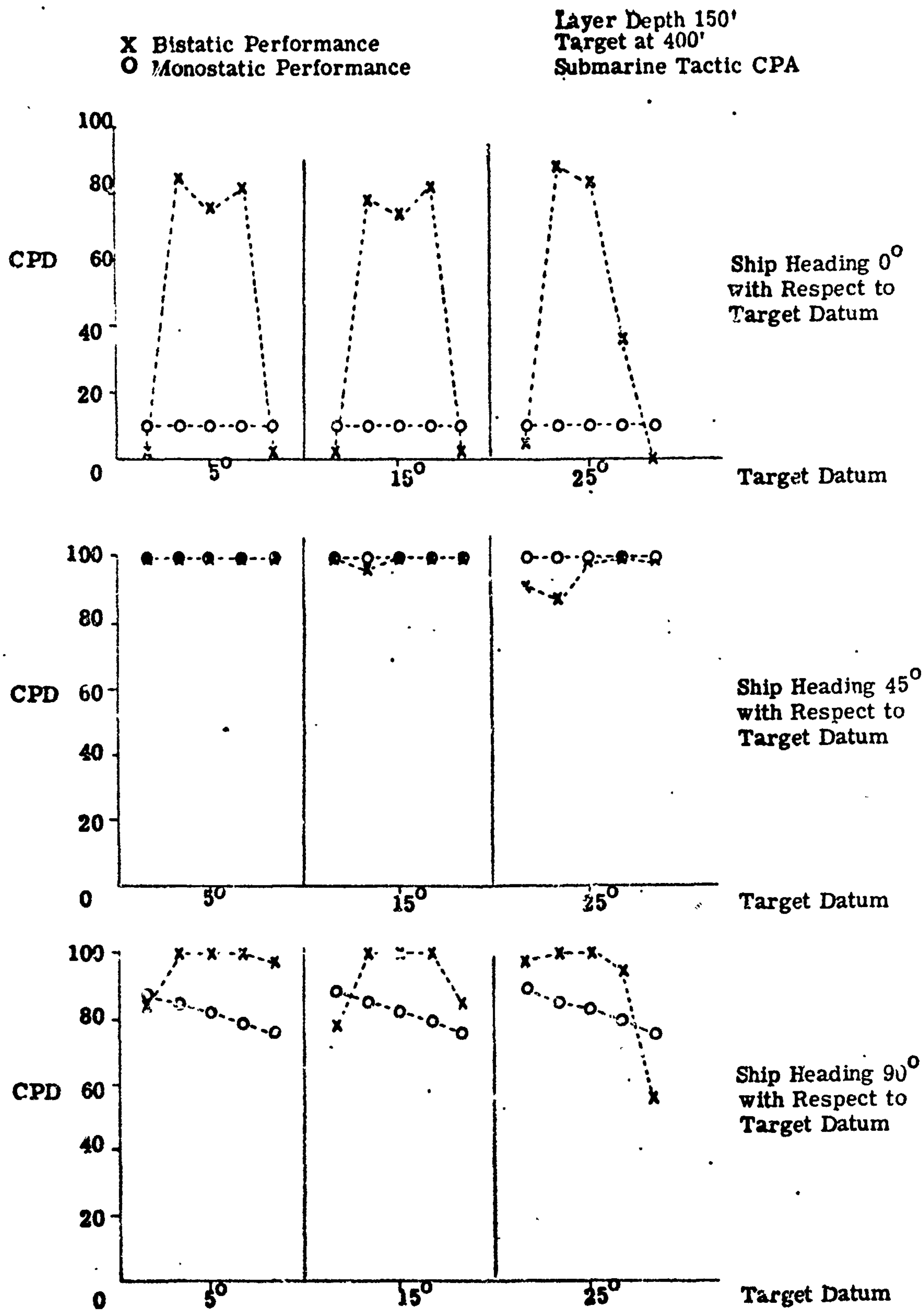

Hazeltine
Corporation

Figure A-33

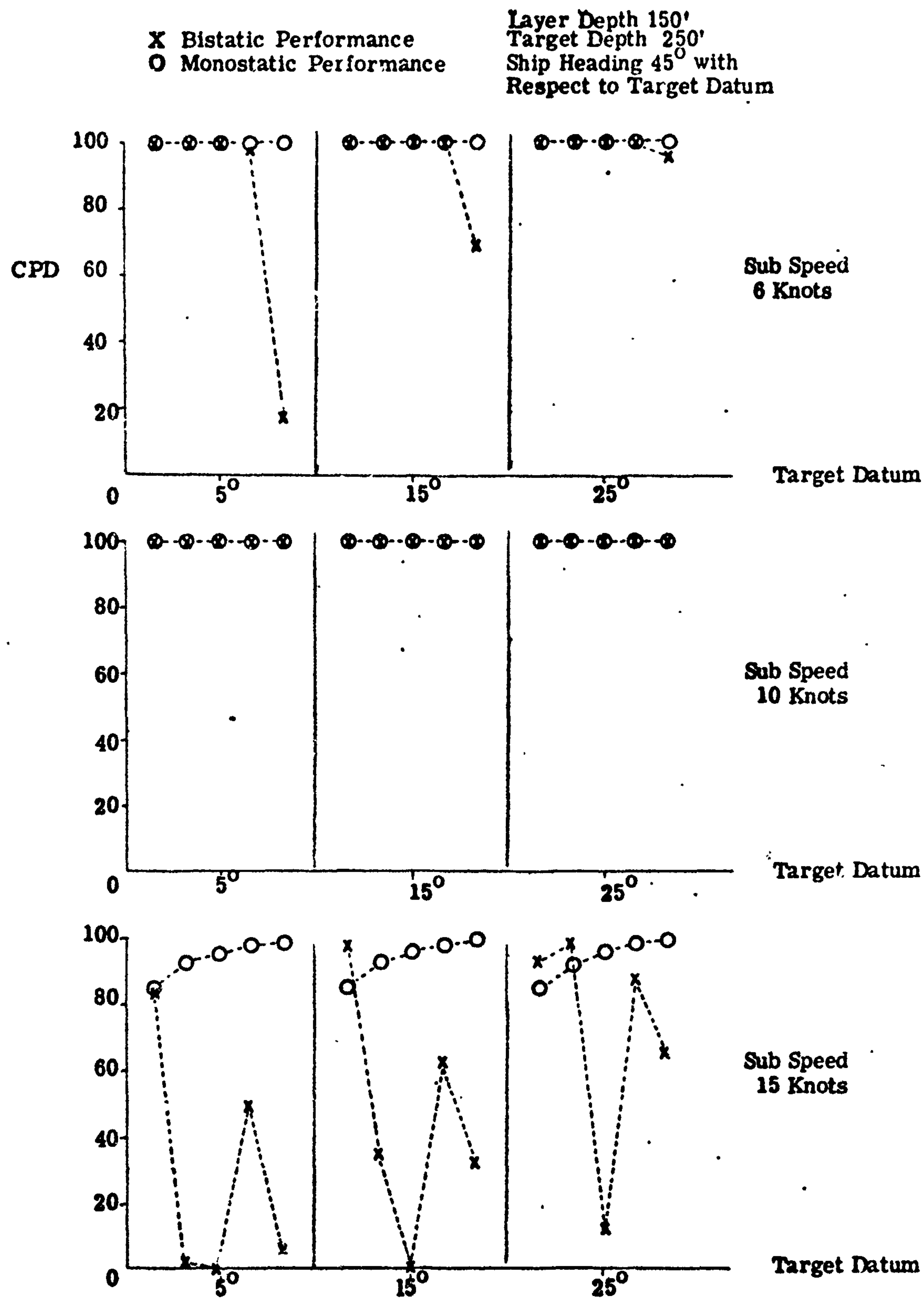

Figure A-34

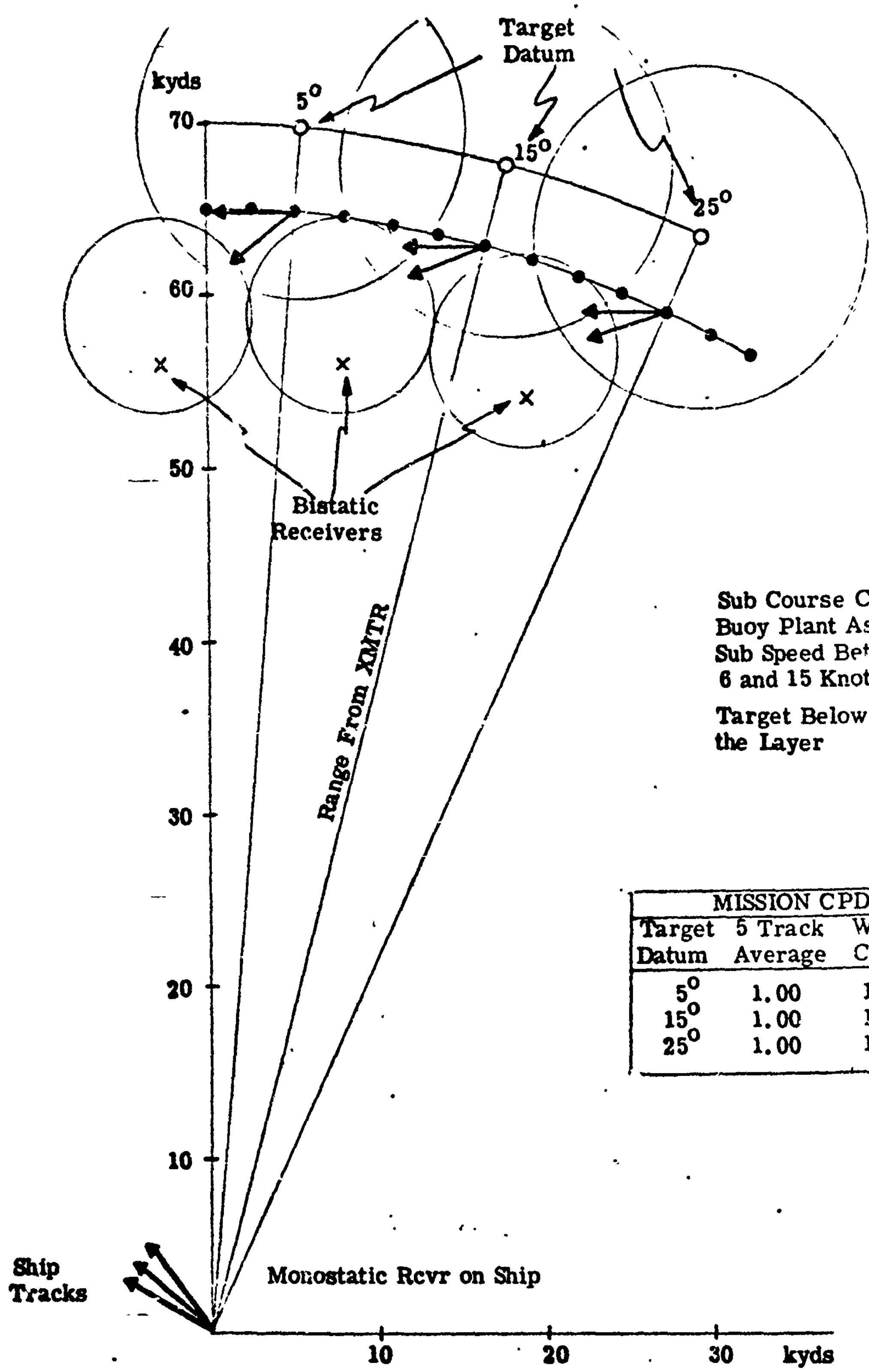

Sub Course CPA
Buoy Plant Assumes
Sub Speed Between
6 and 15 Knots

Target Below
the Layer

MISSION CPD		
Target Datum	5 Track Average	Worst Case
5°	1.00	1.00
15°	1.00	1.00
25°	1.00	1.00

Hazeltine
Corporation

Figure A-35

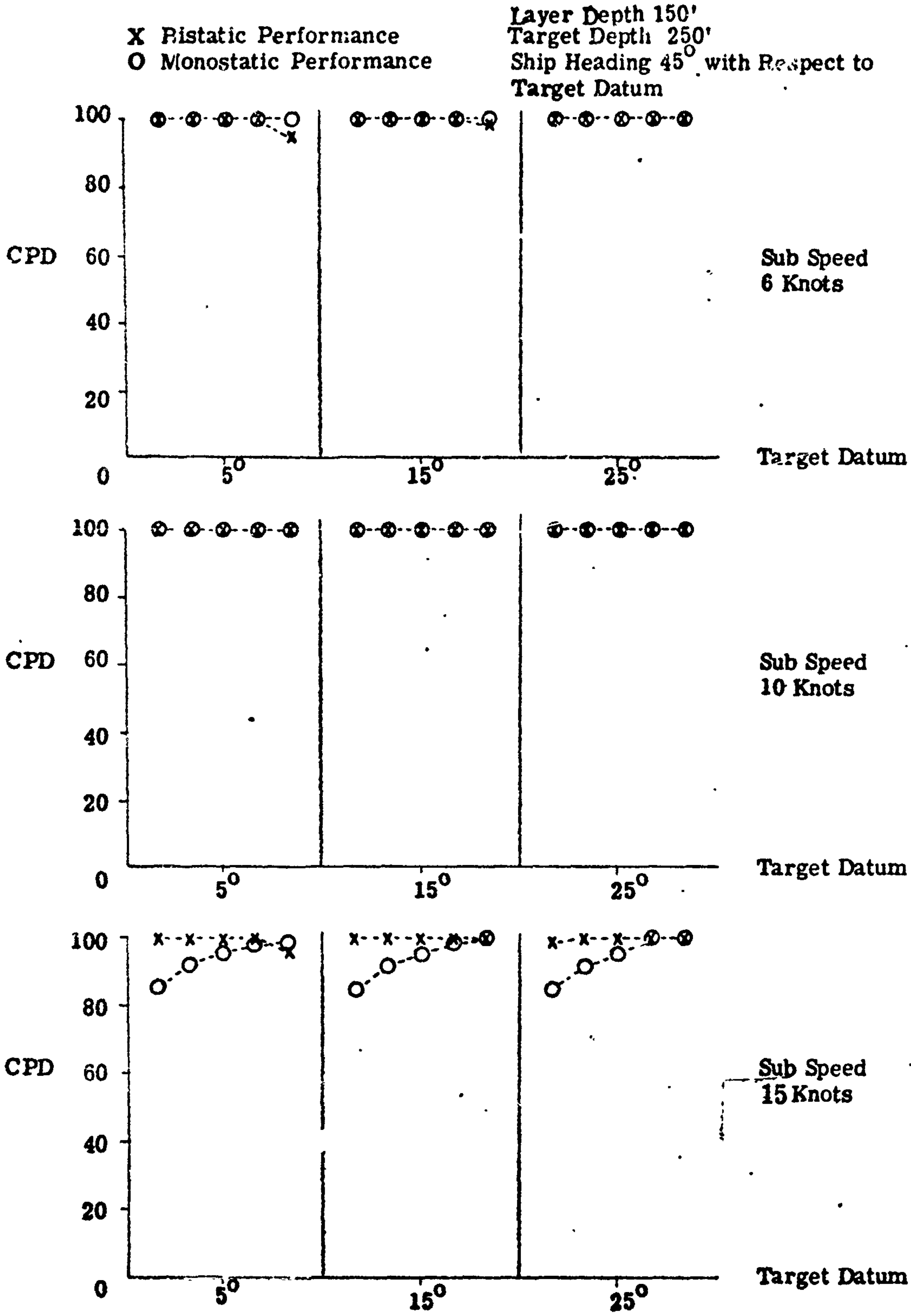

APPENDIX A (C)

PART 2

TARGET PROSECUTION

Figure	Environment	Mission	Datum	Buoys	Ship Course	Sub Course	XMTR	A/C
A-36	"	Detect	0°-250'	6-60'	Zig-Zag	0-360°	26 BB/ODT	Helo
A-37	"	"	"	"	"	"	"	"
A-38	"	"	"	"	45° Rel.	"	"	"
A-39	"	"	"	"	0° Rel.	"	"	"
A-40	"	"	"	8-60'	0° Rel.	"	"	"
A-41	"	"	"	"	Zig-Zag	"	"	"
A-42	"	"	"	"	"	"	"	"
A-43	"	"	"	3-60'	"	"	"	Rocket
A-44	"	"	"	"	0° Rel.	"	"	"
A-45	"	"	"	"	"	"	26 BB/TRACK	"
A-46	"	"	"	2-60'	"	"	"	"
A-47	"	"	"	8-60'	Zig-Zag	"	26 BB/ODT	Helo
A-48	"	"	"	"	0° Rel.	"	"	"
A-49	"	"	"	"	"	"	"	"
A-50	"	"	"	"	Dog-Leg	"	"	"
A-51	"	"	"	3-60'	0° Rel.	"	26 BB/TRACK	Rocket
A-52	"	"	"	2-60'	"	"	"	"
A-53	Med.	"	"	6-60'	"	"	26 BB/ODT	Helo
A-54	"	"	"	"	Dog-Leg	"	"	"
A-55	"	"	0°-300'	"	0° Rel.	"	"	"
A-56	"	"	"	6-1500'	"	"	"	"
A-57	"	"	"	6-60'	Zig-Zag	"	"	"
A-58	"	"	"	6-1500'	"	"	"	"
A-59	"	"	"	4-60'	0° Rel.	"	"	"
A-60	"	"	"	4-1500'	"	"	"	"
A-61	"	"	0°-55'	4-60'	"	"	"	"
A-62	"	"	"	4-1500'	"	"	"	"
A-63	"	"	0°-600'	4-60'	"	"	"	"
A-64	"	"	"	4-1500'	"	"	"	"
A-65	"	"	0°-300'	8-60'	"	"	(26 BB/ODT	"
A-66	"	"	"	8-1500'	"	"	2nd CZ)	"
A-67	"	"	"	4-60'	"	"	26 BB/ODT	"
A-68	"*	"	0°-55'	"	"	"	"	"
A-69	"*	"	"	4-1500'	"	"	"	"
A-70	"*	"	0°-300'	4-60'	"	"	"	"
A-71	"*	"	"	4-1500'	"	"	"	"
A-72	"*	"	0°-600'	4-60'	"	"	"	"
A-73	"*	"	"	4-1500'	"	"	"	"
A-74	N.A.	"	0°-55'	5-1500'	"	"	CASS	"
A-75	"	"	0°-300'	"	Zig-Zag	"	"	"
A-76	"	"	0°-600'	"	"	"	"	"

* No Surface Duct Present

Hazeltine Corporation

Figure A-36

ENVIRONMENT: NORTH ATLANTIC
LAYER DEPTH (FT): 150
SYSTEM: SQS-26/41-X
XMTR MODE: BB/ODT
TARGET DEPTH (FT): 250
TARGET SPEED (KNOTS): 10
SHIP SPEED (KNOTS): 15
AIRCRAFT SPEED (KNOTS): 120
BUOY DEPTHS (FT): 60

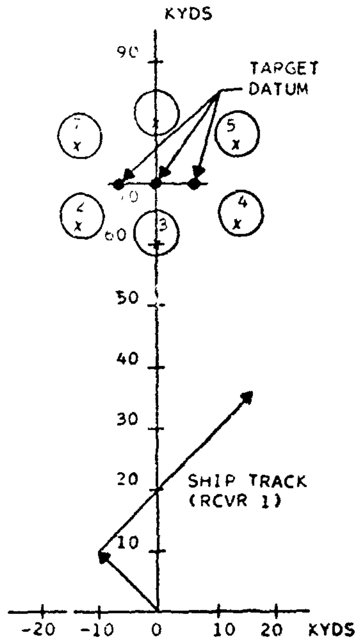

P_{MULT} = .80 M = .83
P_{BIST} = .69
P_{MONO} = .46

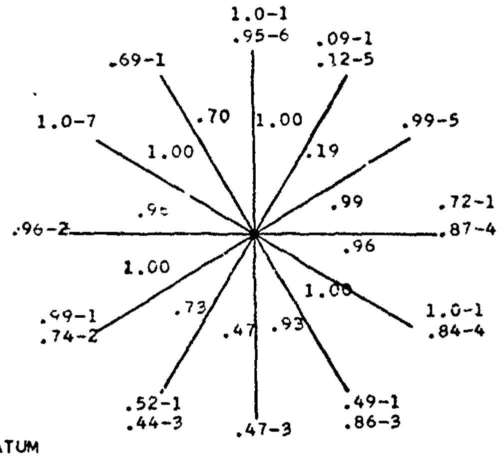

DATUM
(0,70)

P_{MULT} = .78 M = .81
P_{BIST} = .53
P_{MONO} = .61

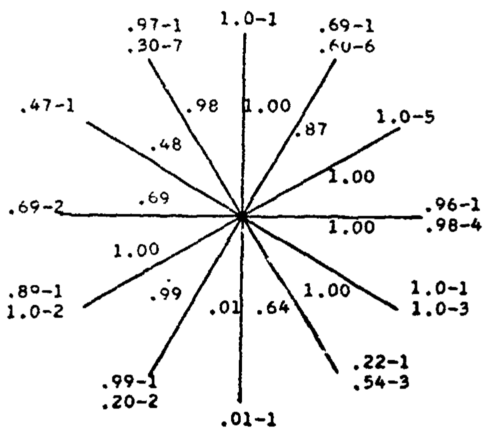

DATUM
(-6,70)

P_{MULT} = .78 M = .78
P_{BIST} = .80
P_{MONO} = .58

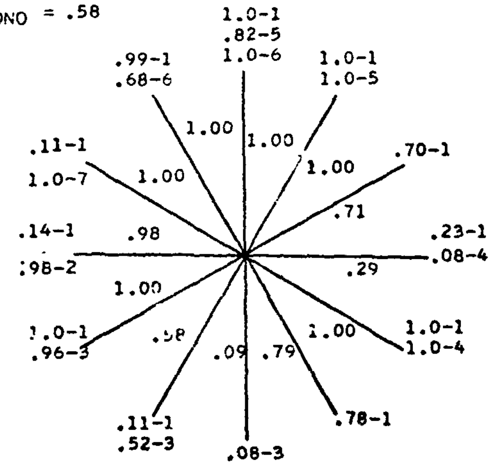

DATUM
(6,70)

Hazeltine Corporation

Figure A-37(1)

ENVIRONMENT: NORTH ATLANTIC
LAYER DEPTH (FT): 150
SYSTEM: SQS-26/41-X
XMTR MODE: BM/ODT
TARGET DEPTH (FT): 250
TARGET SPEED (KNOTS): 10
SHIP SPEED (KNOTS): 15
AIRCRAFT SPEED (KNOTS): 120
BUOY DEPTHS (FT): 60

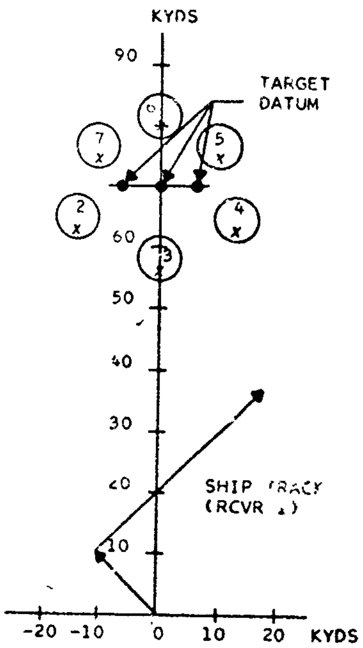

P_{MULT} = .81 M = .83

P_{BIST} = .68

P_{MONO} = .46

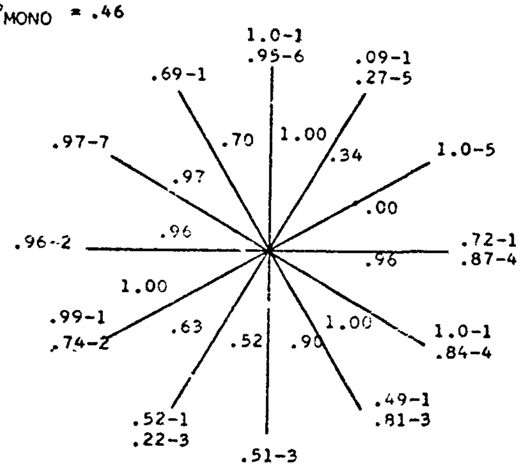

DATUM
(0,70)

P_{MULT} = .83 M = .83

P_{BIST} = .53

P_{MONO} = .61

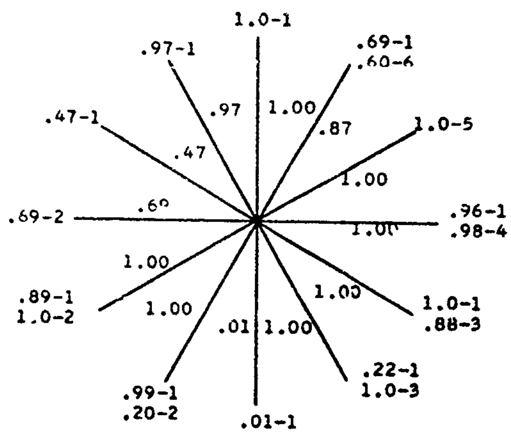

DATUM
(-6,70)

P_{MULT} = .82 M = .82

P_{BIST} = .63

P_{MONO} = .58

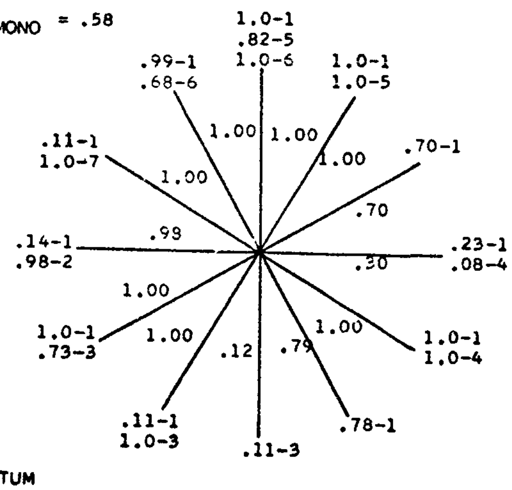

DATUM
(6,70)

P_{MULT} = .78 M = .76
P_{BIST} = .61
P_{MONO} = .47

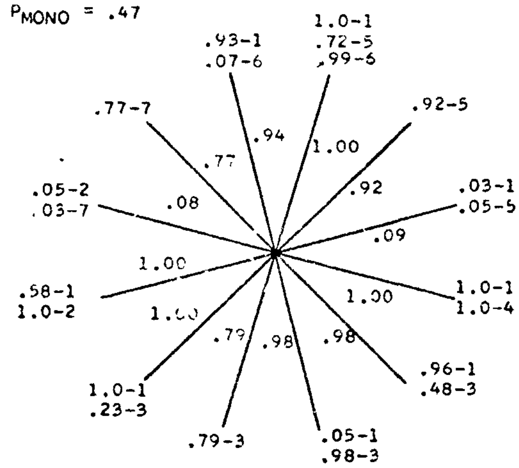

DATUM
(0,70)

P_{MULT} = .66 M = .68
P_{BIST} = .48
P_{MONO} = .51

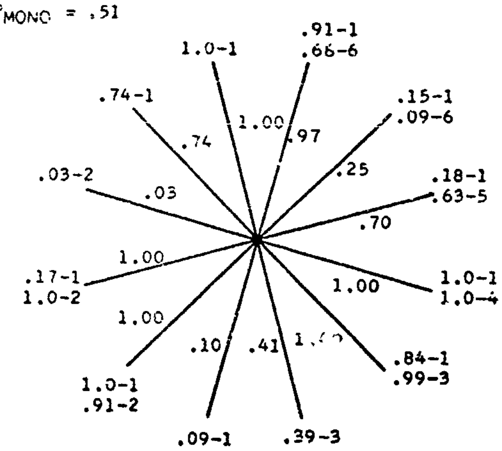

DATUM
(-6,70)

P_{MULT} = .81 M = .81
P_{BIST} = .64
P_{MONO} = .66

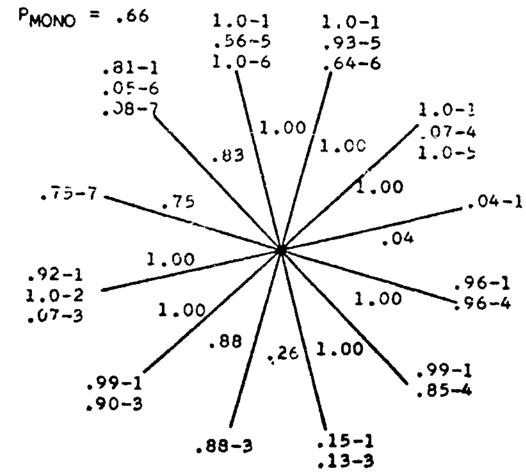

DATUM
(6,70)

Hazeltine Corporation

Figure A-38

ENVIRONMENT: NORTH ATLANTIC
LAYER DEPTH (FT): 1.0
SYSTEM: SQS-26/41-X
XMTR MODE: BB/ODT
TARGET DEPTH (FT): 250
TARGET SPEED (KNOTS): 10
SHIP SPEED (KNOTS): 15
AIRCRAFT SPEED (KNOTS): 120
BUOY DEPTHS (FT): 60

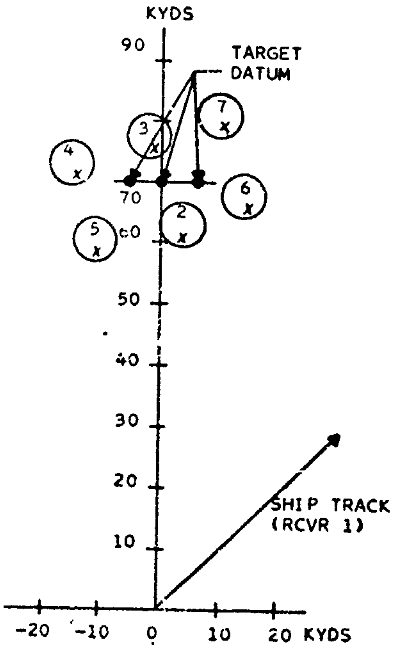

P_{MULT} = .81 M = .83
P_{BIST} = .75
P_{MONO} = .52

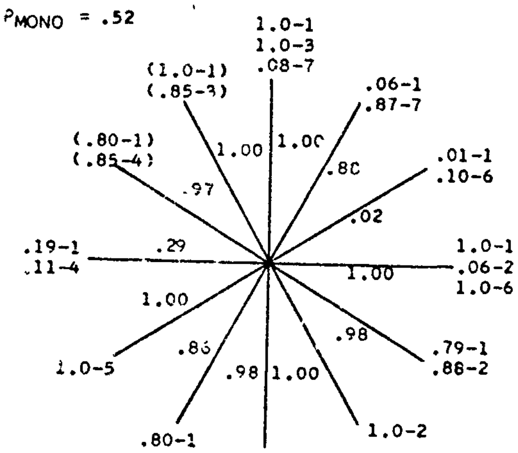

DATUM
(0,70)

P_{MULT} = .83 M = .84
P_{BIST} = .59
P_{MONO} = .61

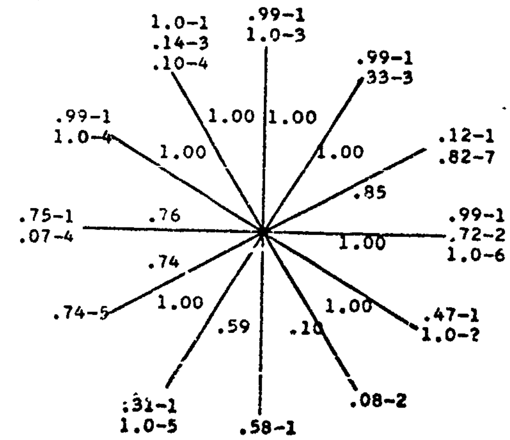

DATUM
(-6,70)

P_{MULT} = .70 M = .72
P_{BIST} = .49
P_{MONO} = .56

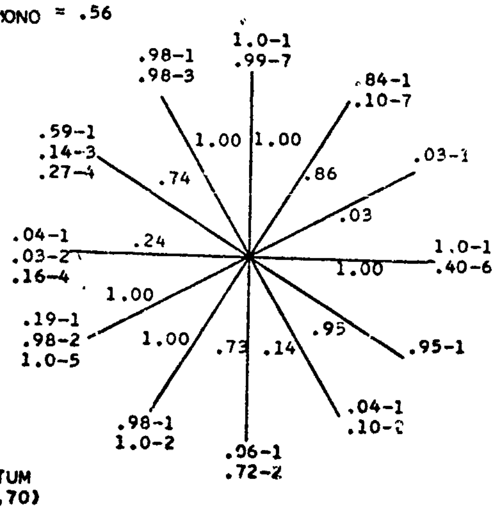

DATUM
(6,70)

6165

Hazeltine
Corporation

Figure A-39

ENVIRONMENT: NORTH ATLANTIC
LAYER DEPTH (FT): 150
SYSTEM: SQS-26/41-X
XMTR MODE: E. /OUT
TARGET DEPTH (FT): 250
TARGET SPEED (KNOTS): 10
SHIP SPEED (KNOTS): 15
AIRCRAFT SPEED (KNOTS): 120
BUOY DEPTHS (FT): 60

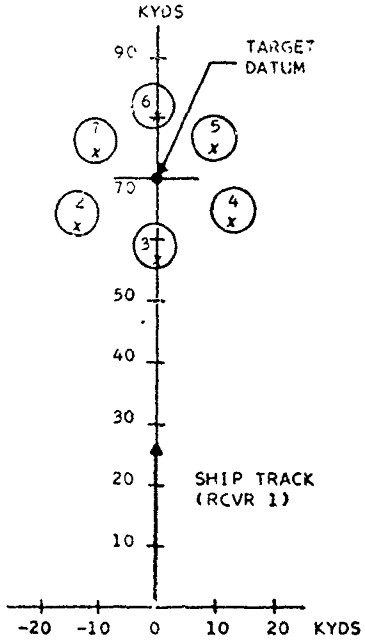

P_{MULT} = .69   M = .71

P_{BIST} = .57

P_{MONO} = .33

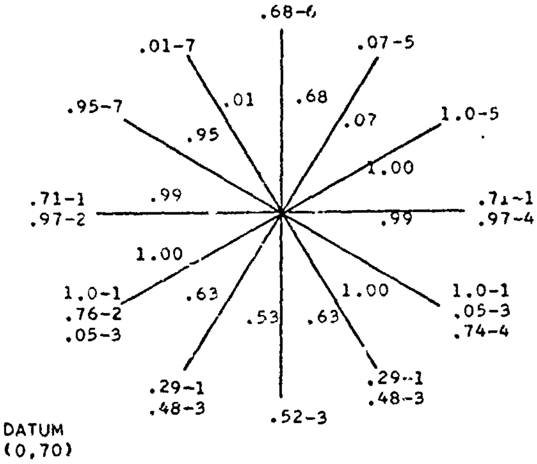

Hazeltine
Corporation

Figure A-40

ENVIRONMENT: NORTH ATLANTIC
LAYER DEPTH (FT): 150
SYSTEM: SQS-26/41-X
XMTR MODE: BB/ODT
TARGET DEPTH (FT): 250
TARGET SPEED (KNOTS): 10
SHIP SPEED (KNOTS): 15
AIRCRAFT SPEED (KNOTS): 120
BUOY DEPTHS (FT): 60

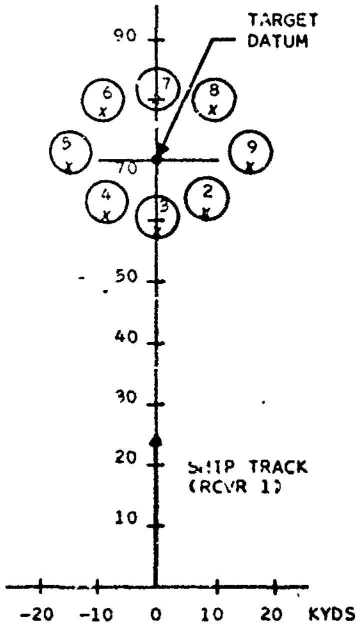

P_{MULT} = .72 M = .74

P_{BIST} = .72

P_{MONO} = .33

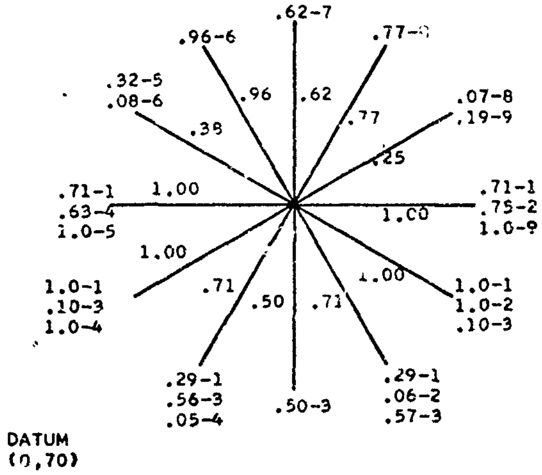

Hazeltine Corporation

Figure A-41

ENVIRONMENT: NORTH ATLANTIC
LAYER DEPTH (FT): 150
SYSTEM: SS-26/41-X
XMTR MODE: PP/ODT
TARGET DEPTH (FT): 250
TARGET SPEED (KNOTS): 10
SHIP SPEED (KNOTS): 15
AIRCRAFT SPEED (KNOTS): 120
BUOY DEPTHS (FT): 60

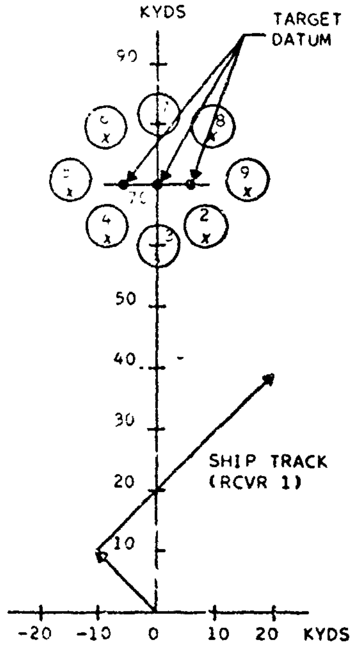

P_{MULT} = .70 M = .74

P_{BIST} = .66

P_{MONO} = .46

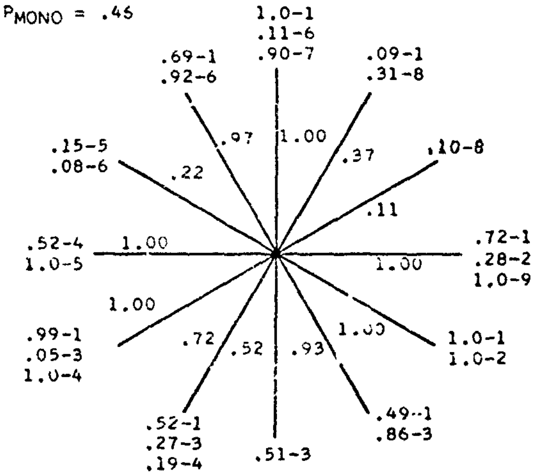

DATUM
(0,70)

P_{MULT} = .91 M = .94

P_{BIST} = .71

P_{MONO} = .61

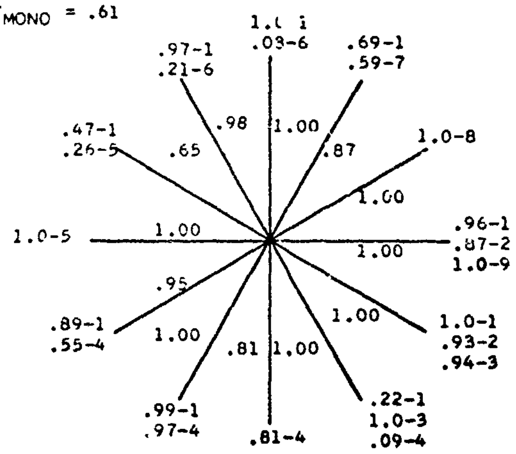

DATUM
(-6,70)

P_{MULT} = .88 M = .89

P_{BIST} = .78

P_{MONO} = .58

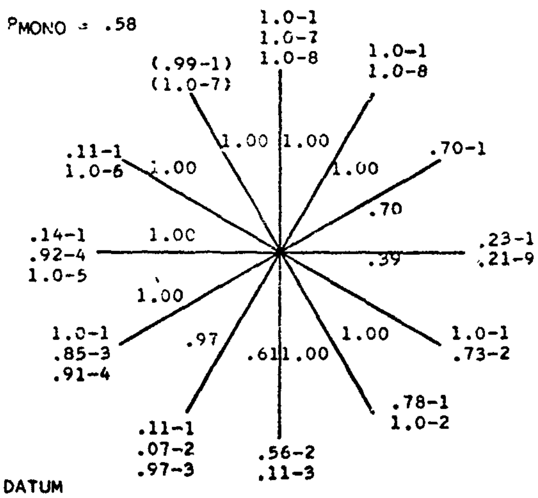

DATUM
(6,70)

Hazeltine
Corporation

Figure A-42(1)

ENVIRONMENT: NORTH ATLANTIC
LAYER DEPTH (FT) 150
SYSTEM: SJS-26/4-X
XMTR MODE: BB/ODT
TARGET DEPTH (FT): 250
TARGET SPEED (KNOTS): 10
SHIP SPEED (KNOTS): 15
AIRCRAFT SPEED (KNOTS): 120
BUOY DEPTHS (FT): 60

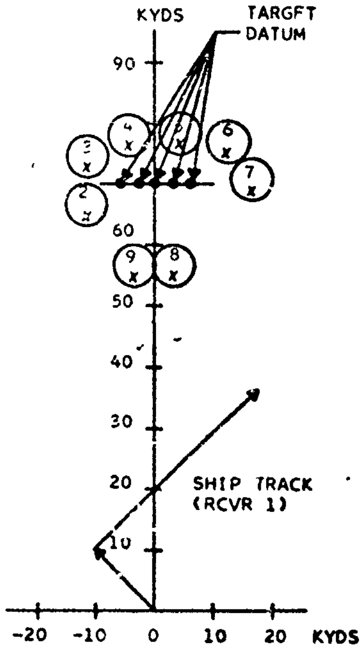

P_{MULT} = .92 M = .96
P_{BIST} = .74
P_{MONO} = .46

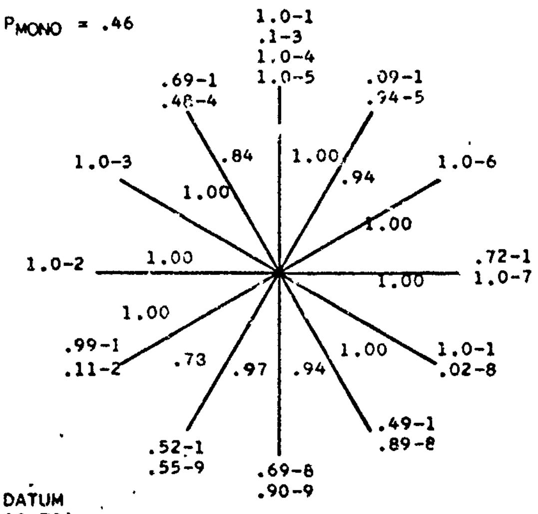

DATUM
(0,70)

P_{MULT} = .92 M = .94
P_{BIST} = .67
P_{MONO} = .61

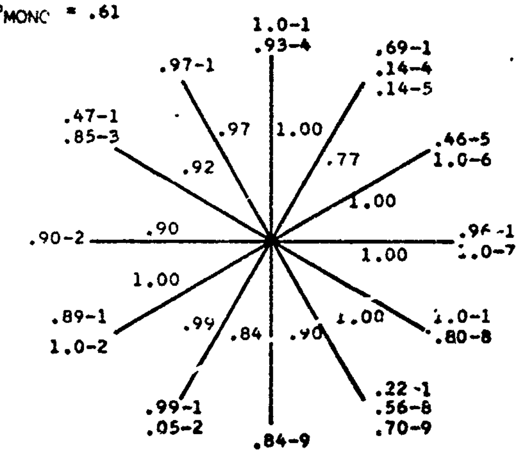

DATUM
(-6,70)

P_{MULT} = .91 M = .93
P_{BIST} = .55
P_{MONO} = .58

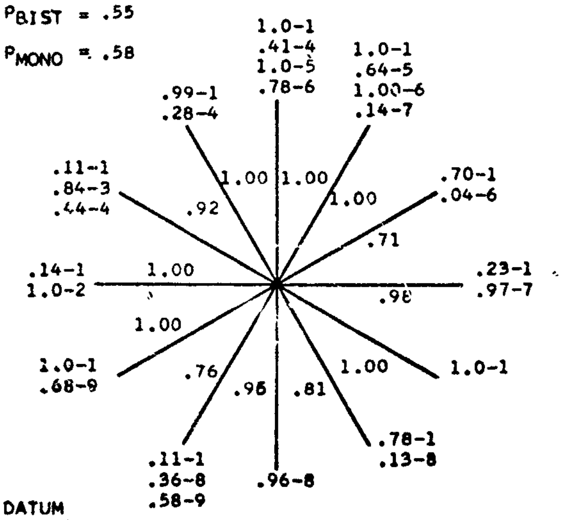

DATUM
(6,70)

Figure A-42(2)

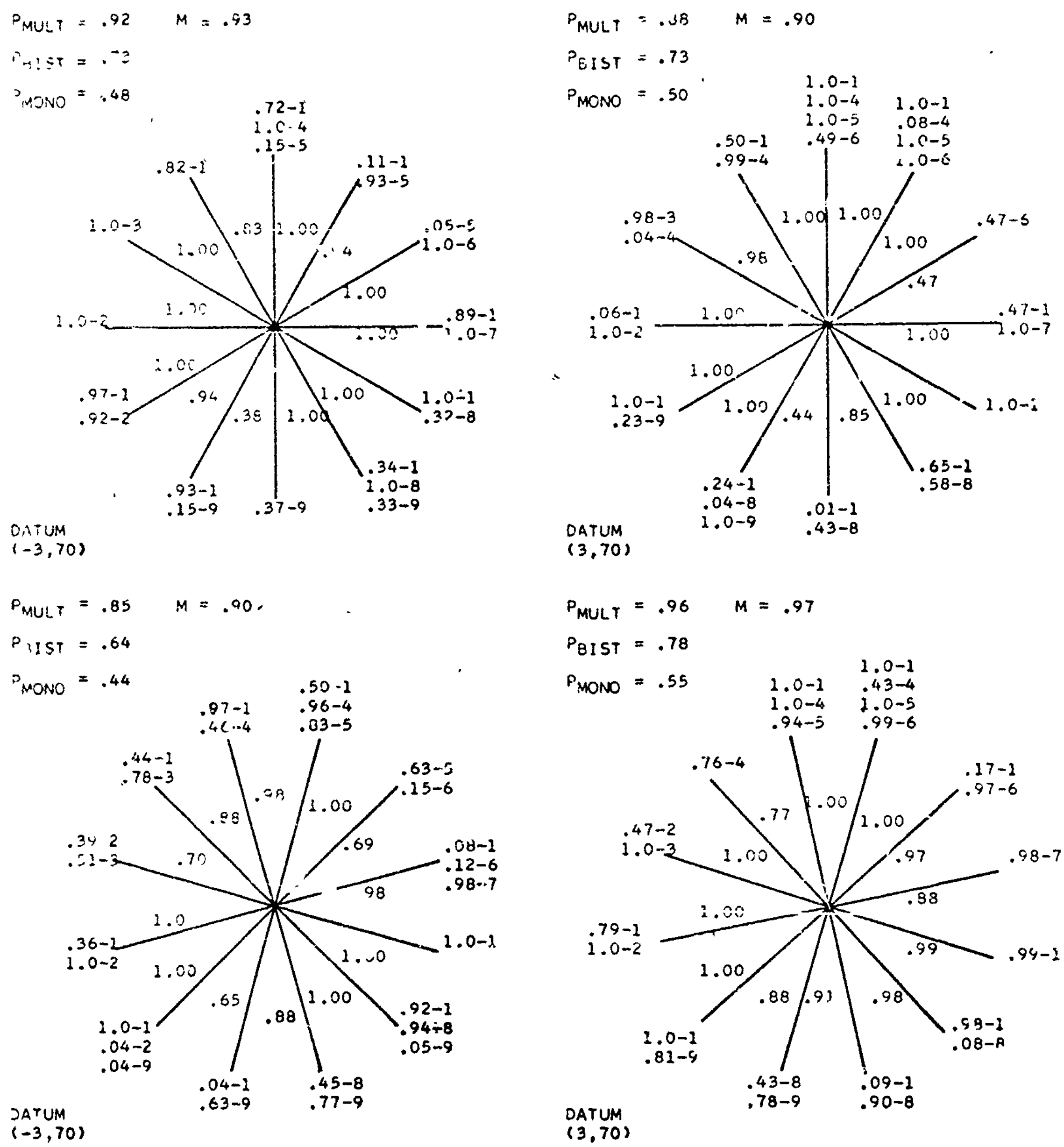
P_{MULT} = .92 M = .93
P_{BIST} = .73
P_{MONO} = .48
DATUM
(-3,70)
P_{MULT} = .88 M = .90
P_{BIST} = .73
P_{MONO} = .50
DATUM
(3,70)
P_{MULT} = .85 M = .90
P_{BIST} = .64
P_{MONO} = .44
DATUM
(-3,70)
P_{MULT} = .96 M = .97
P_{BIST} = .78
P_{MONO} = .55
DATUM
(3,70)

Hazeltine
Corporation

Figure A-42(3)

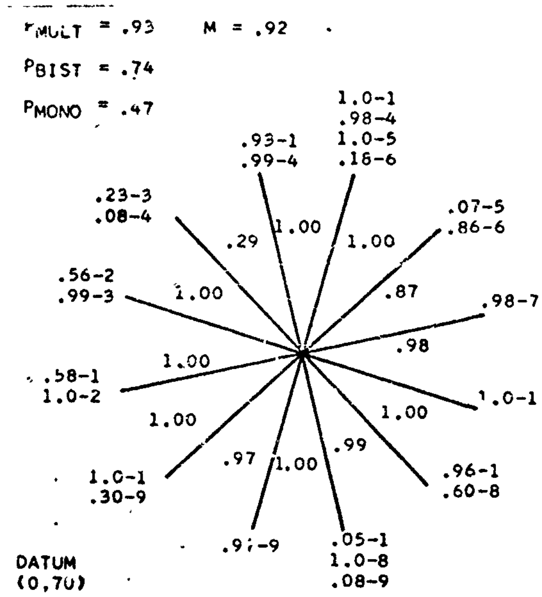

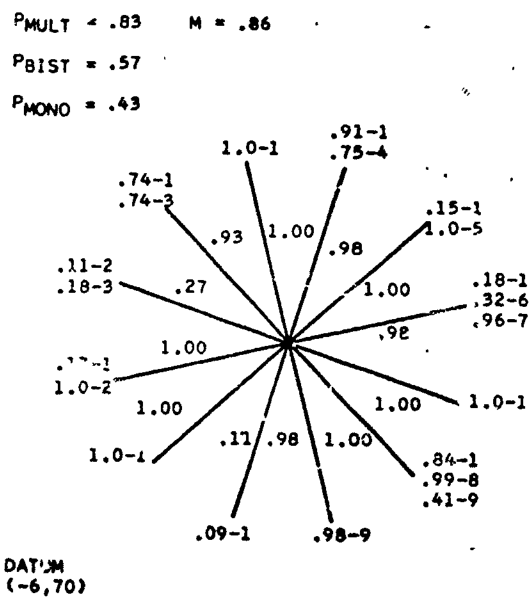

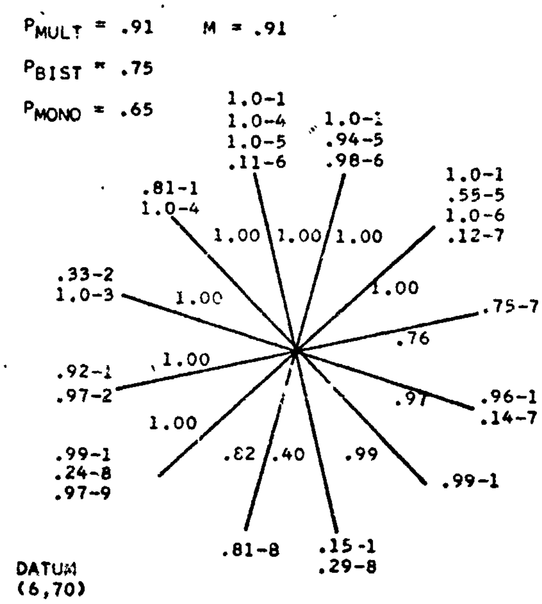

6165

Figure A-43

ENVIRONMENT: NORTH ATLANTIC
LAYER DEPTH (FT): 150
SYSTEM: SQS-26/41-X
XMTR MODE: BB/ODT
TARGET DEPTH (FT): 250
TARGET SPEED (KNOTS): 10
SHIP SPEED (KNOTS): 15
AIRCRAFT SPEED (KNOTS): 1400
BUOY DEPTHS (FT): 60

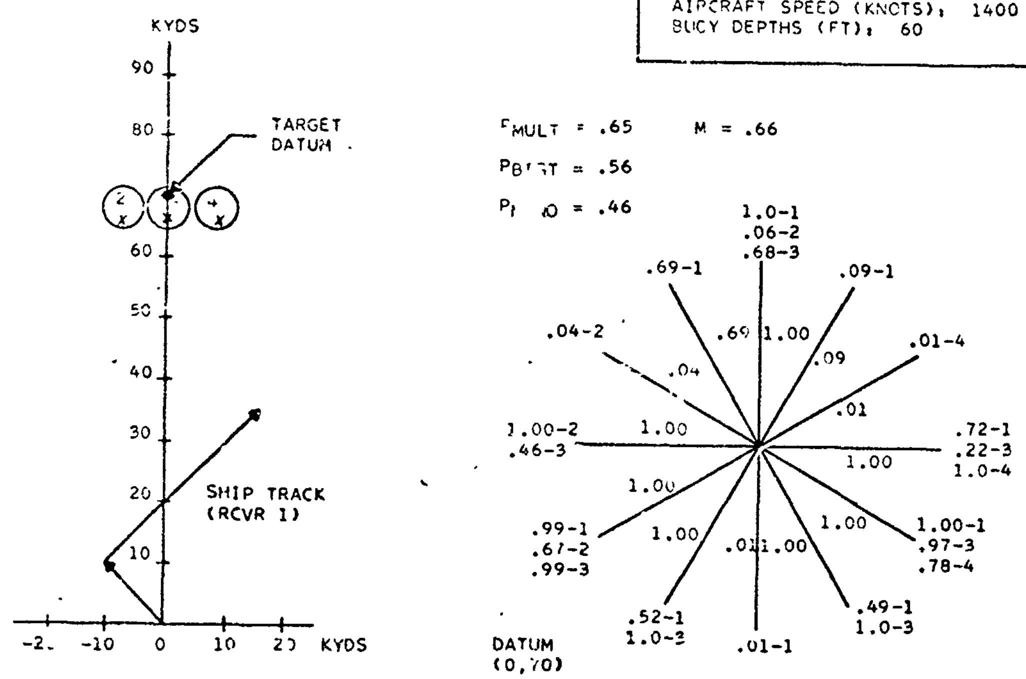

Hazeltine Corporation

Figure A-44

ENVIRONMENT: NORTH ATLANTIC
LAYER DEPTH (FT): 150
SYSTEM: SQS-26/41-X
XMTR MODE: BB/ODT
TARGET DEPTH (FT): 250
TARGET SPEED (KNOTS): 10
SHIP SPEED (KNOTS): 15
AIRCRAFT SPEED (KNOTS): 1400
BUOY DEPTHS (FT): 60

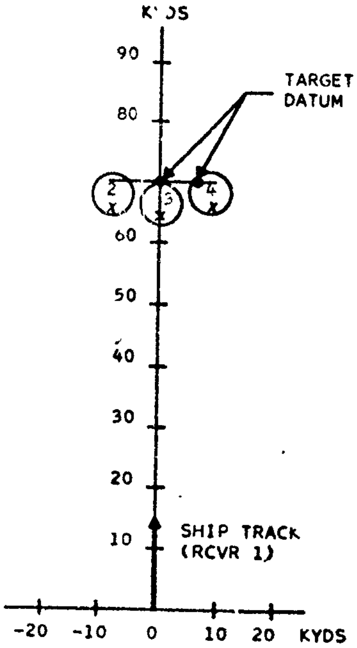

P_{MULT} = .97 M = .98

P_{BIST} = .83

P_{MONO} = .80

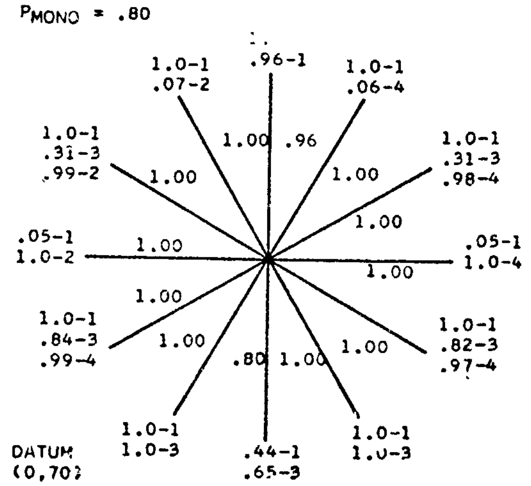

P_{MULT} = .92 M = .95

P_{BIST} = .64

P_{MONO} = .86

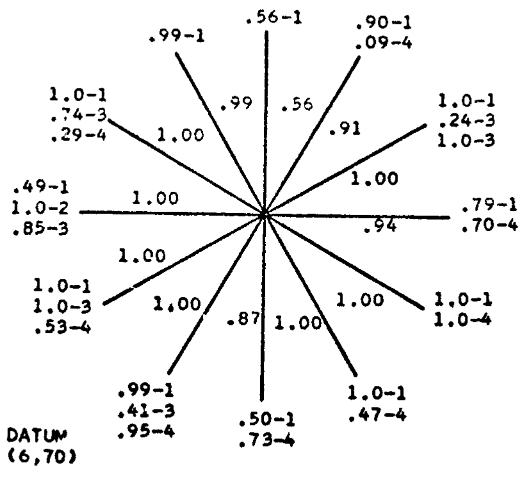

Hazeltine
Corporation

Figure A-45

ENVIRONMENT: NORTH ATLANTIC
LAYER DEPTH (FT): 150
SYSTEM: SQS-26/41-X
XMTR MODE: BB/TRACK
TARGET DEPTH (FT): 250
TARGET SPEED (KNOTS): 10
SHIP SPEED (KNOTS): 15
AIRCRAFT SPEED (KNOTS): 1400
BUOY DEPTHS (FT): 60

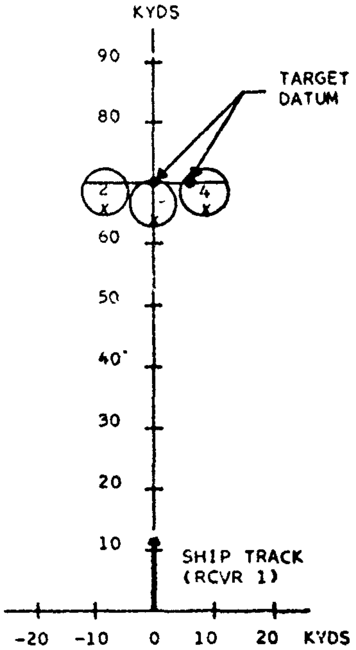

P_{MULT} = .99 M = 1.00

P_{BIST} = .90

P_{MONO} = .99

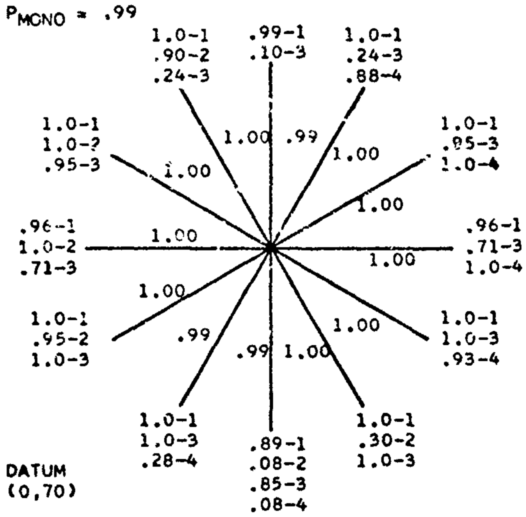

DATUM
(0,70)

P_{MULT} = .99 M = .99

P_{BIST} = .89

P_{MONO} = .99

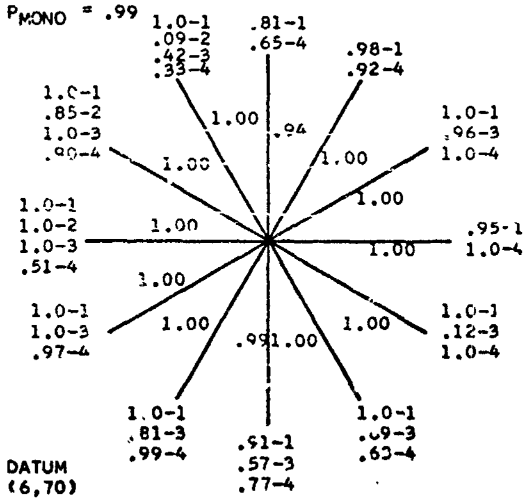

DATUM
(6,70)

Hazeltine
Corporation

Figure A-46

ENVIRONMENT: NORTH ATLANTIC
LAYER DEPTH (FT): 150
SYSTEM: SQS-26/41-X
XMTR MODE: BB/TRACK
TARGET DEPTH (FT): 250
TARGET SPEED (KNOTS): 10
SHIP SPEED (KNOTS): 15
AIRCRAFT SPEED (KNOTS): 1400
BUOY DEPTHS (FT): 60

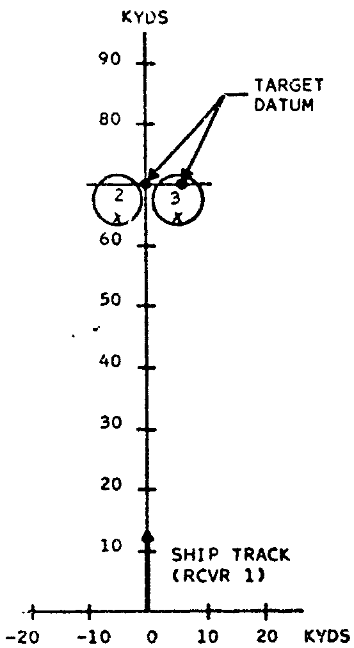

P_{MULT} = .99 M = 1.00

P_{BIST} = .84

P_{MONO} = .99

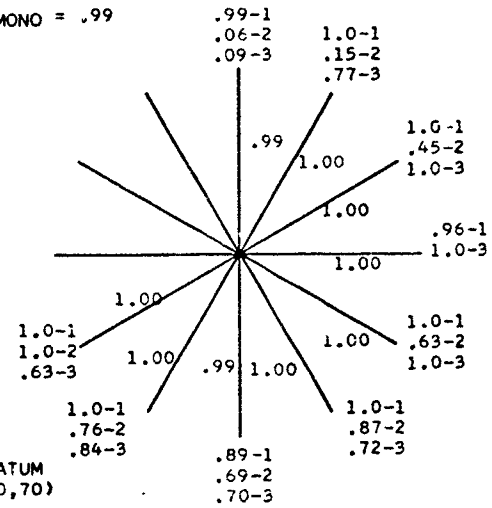

DATUM
(0,70)

P_{MULT} = .98 M = .98

P_{BIST} = .80

P_{MONO} = .98

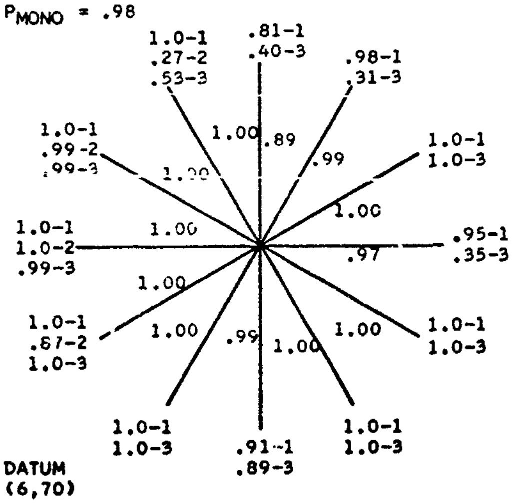

DATUM
(6,70)

Hazeltine
Corporation

Figure A-47

ENVIRONMENT: NORTH ATLANTIC
LAYER DEPTH (FT): 150
SYSTEM: SQS-26/41-X
XMTR MODE: 6B/ODT
TARGET DEPTH (FT): 250
TARGET SPEED (KNOTS): 10
SHIP SPEED (KNOTS): 15
AIRCRAFT SPEED (KNOTS): 120
BUOY DEPTHS (FT): 60

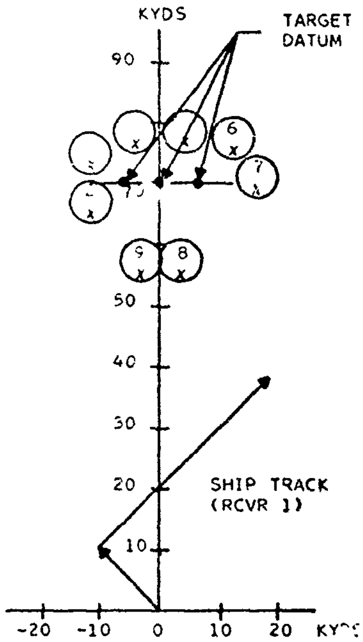

P_{MULT} = .88 M = .91
P_{BIST} = .72
P_{MONO} = .31

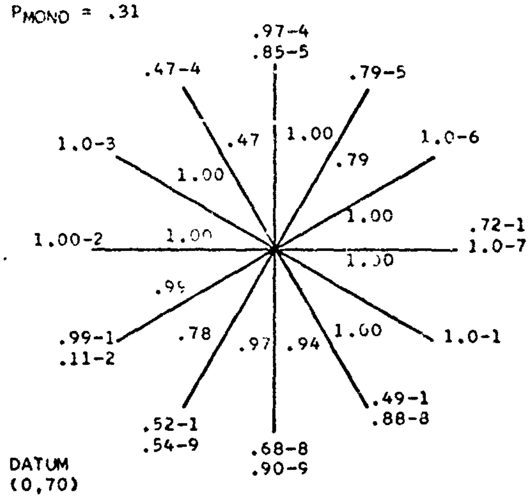

P_{MULT} = .78 M = .79
P_{BIST} = .67
P_{MONO} = .34

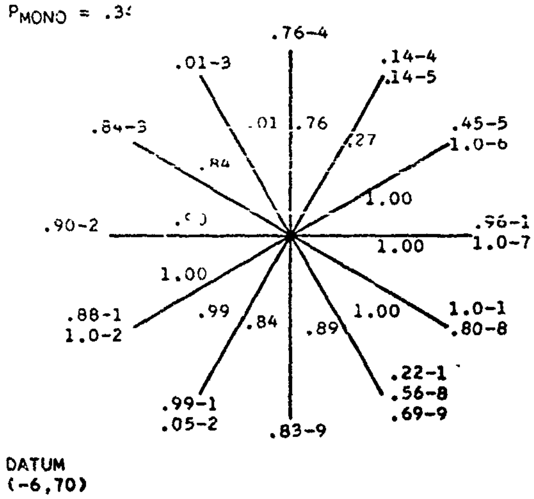

P_{MULT} = .79 M = .81
P_{BIST} = .63
P_{MONO} = .27

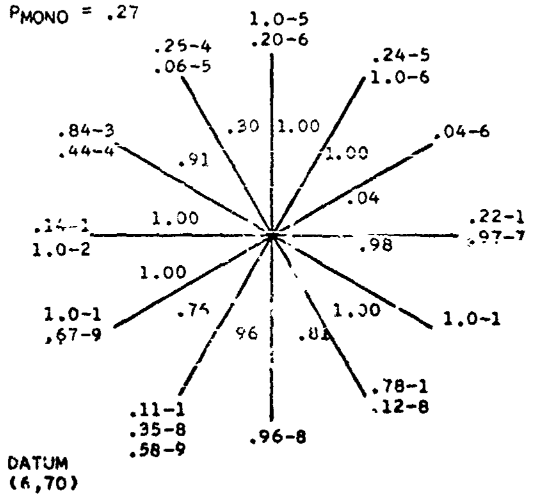

Hazeltine Corporation

Figure A-48

ENVIRONMENT: NORTH ATLANTIC
LAYER DEPTH (FT): 150
SYSTEM: SUS-26/41-X
XMTR MODE: 5B/ODT
TARGET DEPTH (FT): 250
TARGET SPEED (KNOTS): 10
SHIP SPEED (KNOTS): 10
AIRCRAFT SPEED (KNOTS): 120
BUOY DEPTHS (FT): 60

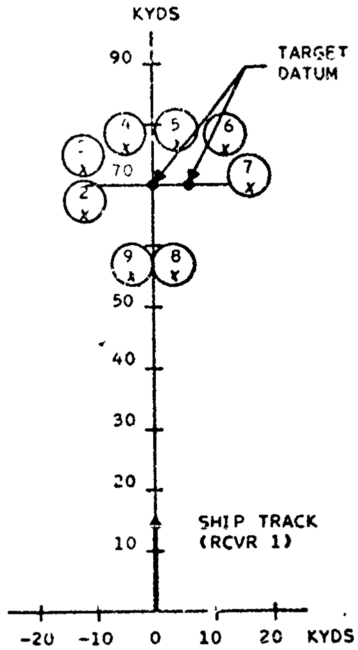

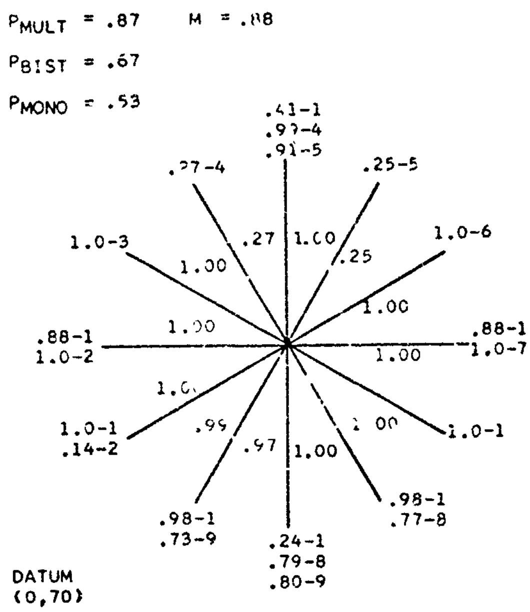

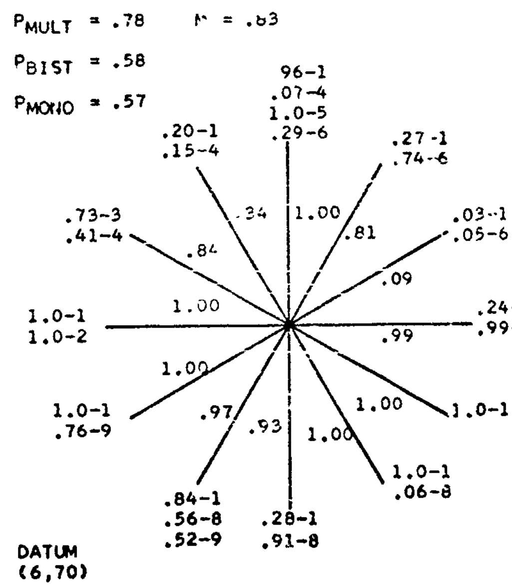

Hazeltine Corporation

Figure A-49

ENVIRONMENT: NORTH ATLANTIC
LAYER DEPTH (FT): 150
SYSTEM: SQS-26/41-X
XMTR MODE: B3/ODT
TARGET DEPTH (FT): 250
TARGET SPEED (KNOTS): 10
SHIP SPEED (KNOTS): 6
AIRCRAFT SPEED (KNOTS): 120
BUOY DEPTHS (FT): 60

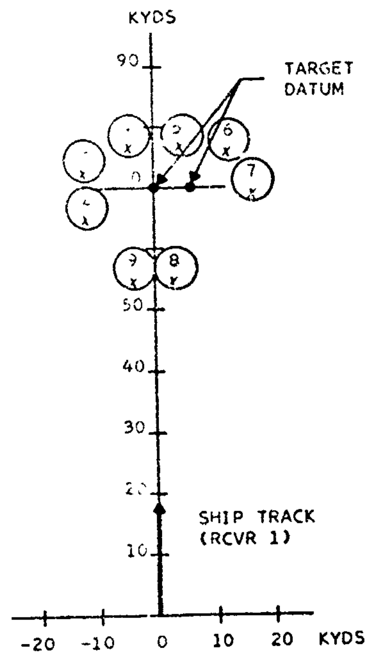

P_{MULT} = 93 M = .96

P_{BIST} = .74

P_{MONO} = .67

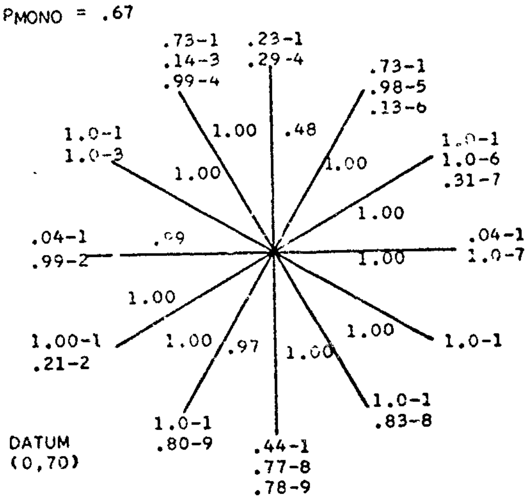

P_{MULT} = .92 M = .93

P_{BIST} = .64

P_{MONO} = .69

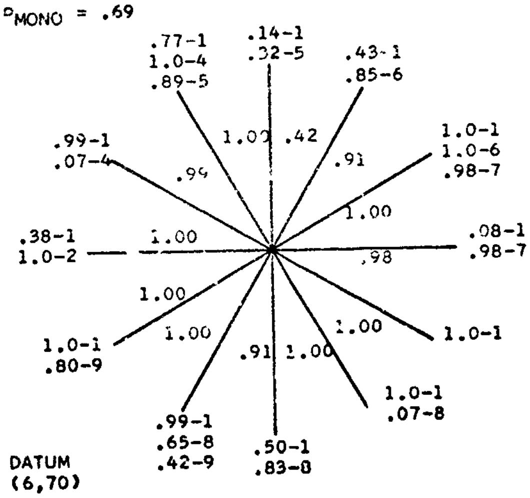

6165

Hazeltine
Corporation

Figure A-50

ENVIRONMENT: NORTH ATLANTIC
LAYER DEPTH (FT): 150
SYSTEM: SQS-26/41-X
XMTR MODE: BB/ODT
TARGET DEPTH (FT): 250
TARGET SPEED (KNOTS): 10
SHIP SPEED (KNOTS): 30/10
AIRCRAFT SPEED (KNOTS): 120
BUOY DEPTHS (FT): 60

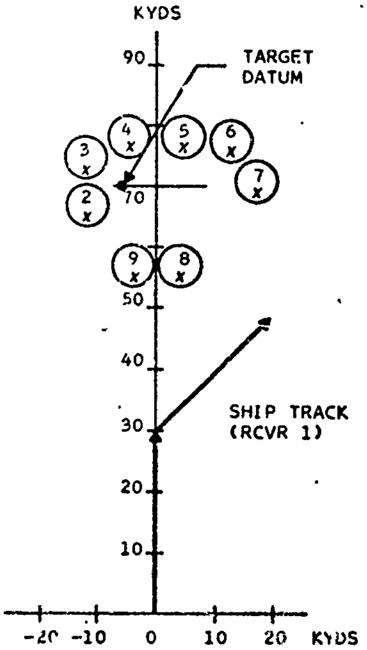

P_{MULT} = .75 M = .74

P_{BIST} = .68

P_{MONO} = .38

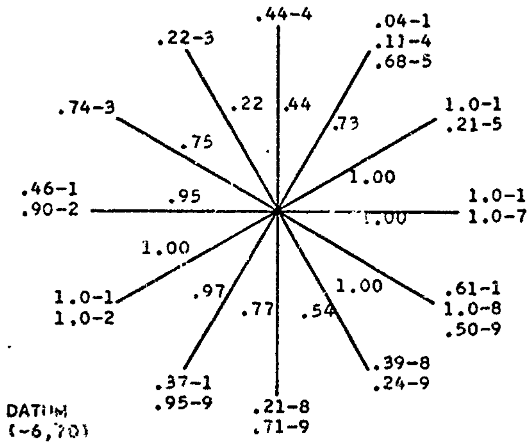

Hazeltine Corporation

Figure A-51

ENVIRONMENT: NORTH ATLANTIC
LAYER DEPTH (FT): 150
SYSTEM: SQS-26/41-X
XMTR MODE: BB/TRACK
TARGET DEPTH (FT): 250
TARGET SPEED (KNOTS): 10
SHIP SPEED (KNOTS): 15
AIRCRAFT SPEED (KNOTS): 1400
BUOY DEPTHS (FT): 60

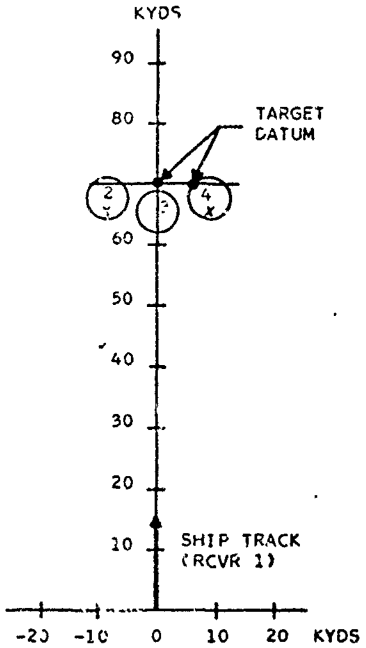

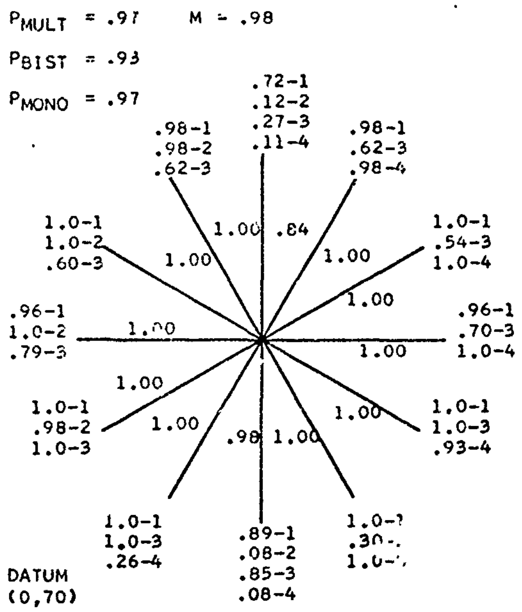

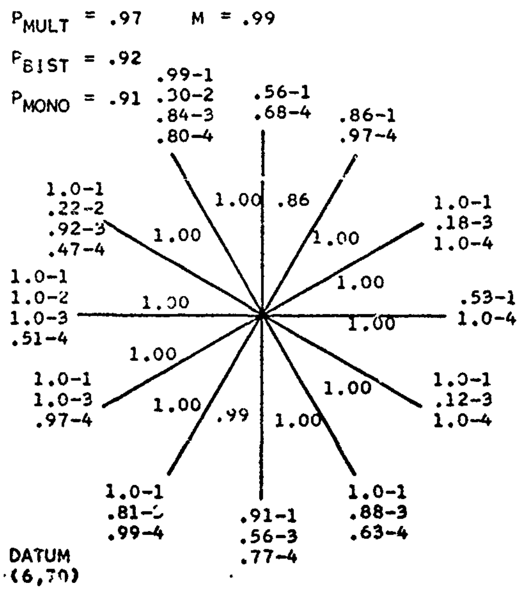

Hazeltine
Corporation

Figure A-52

ENVIRONMENT: NORTH ATLANTIC
LAYER DEPTH (FT): 150
SYSTEM: SQS-26/41-X
XMTR MODE: BB/TRACK
TARGET DEPTH (FT): 250
TARGET SPEED (KNOTS): 10
SHIP SPEED (KNOTS): 15
AIRCRAFT SPEED (KNOTS): 1400
BUOY DEPTHS (FT): 60

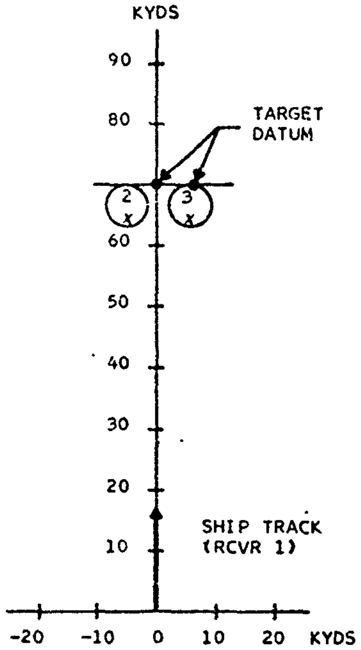

P_{MULT} = .97 M = .99

P_{BIST} = .89

P_{MONO} = .97

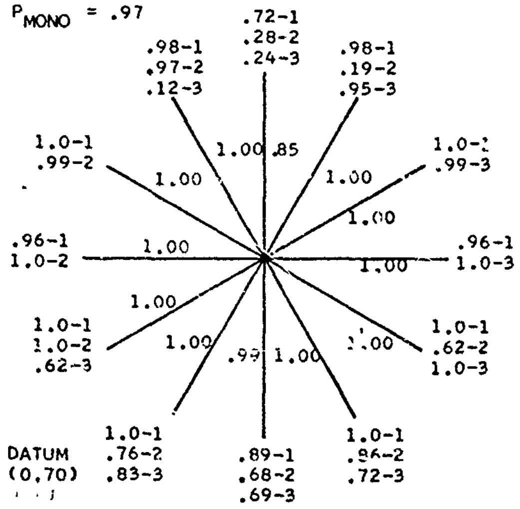

P_{MULT} = .92 M = .95

P_{BIST} = .84

P_{MONO} = .91

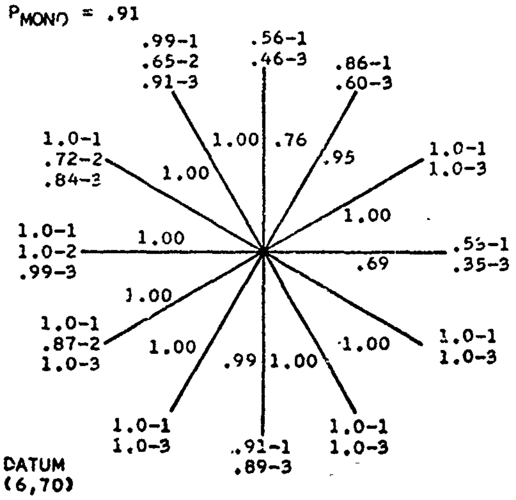

Hazeltine Corporation

Figure A-53

ENVIRONMENT: MEDITERRANEAN
LAYER DEPTH (FT): 100
SYSTEM: SQS-26/41-X
XMTR MODE: BB/ODT
TARGET DEPTH (FT): 250
TARGET SPEED (KNOTS): 10
SHIP SPEED (KNOTS): 15
AIRCRAFT SPEED (KNOTS): 120
BUOY DEPTHS (FT): 60

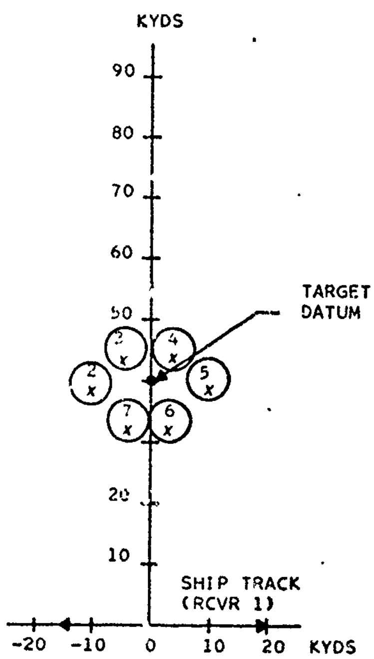

P_{MULT} = .96 M = .96

P_{BIST} = .77

P_{MONO} = .96

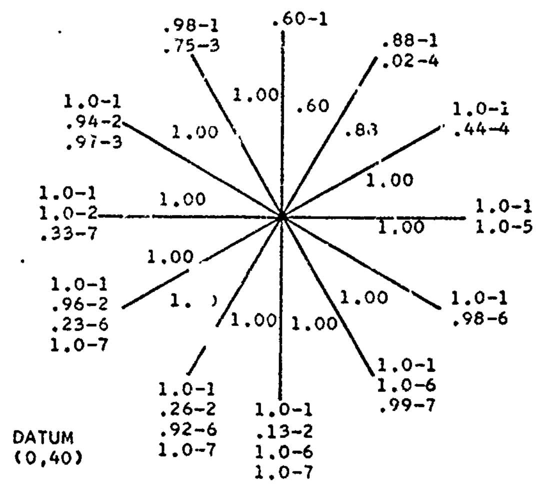

Hazeltine
Corporation

Figure A-54

ENVIRONMENT: MEDITERRANEAN
LAYER DEPTH (FT): 100
SYSTEM: SQS-26/41-X
XMTR MODE: BB/ODT
TARGET DEPTH (FT): 250
TARGET SPEED (KNOTS): 10
SHIP SPEED (KNOTS): 15
AIRCRAFT SPEED (KNOTS): 120
BUOY DEPTHS (FT): 60

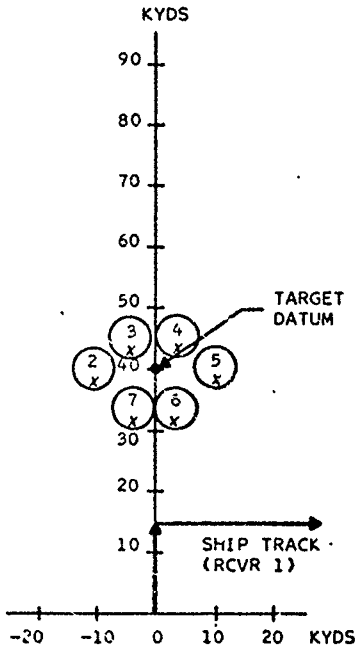

P_{MULT} = 1.0 M = 1.00

P_{BIST} = .98

P_{MONO} = .98

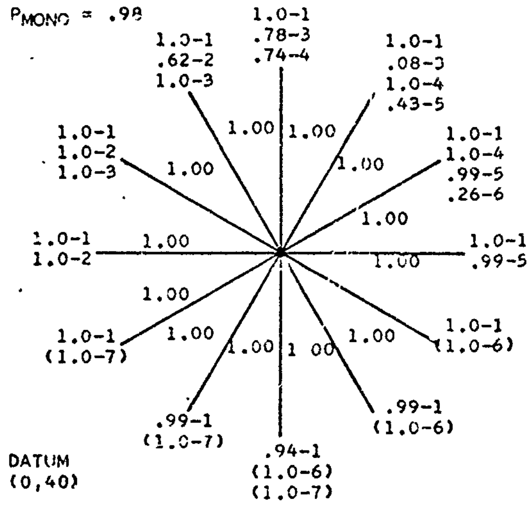

Hazeltine Corporation

Figure A-55

ENVIRONMENT: MEDITERRANEAN
LAYER DEPTH (FT): 100
SYSTEM: SQS-26/41-X
XMTR MODE: BB/ODT
TARGET DEPTH (FT): 300
TARGET SPEED (KNOTS): 10
SHIP SPEED (KNOTS): 15
AIRCRAFT SPEED (KNOTS): 120
BUOY DEPTHS (FT): 60

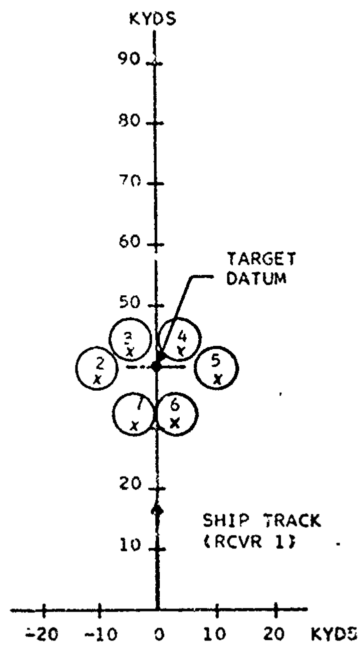

P_{MULT} = 1.00 M = 1.00

P_{BIST} = .83

P_{MONO} = 1.00

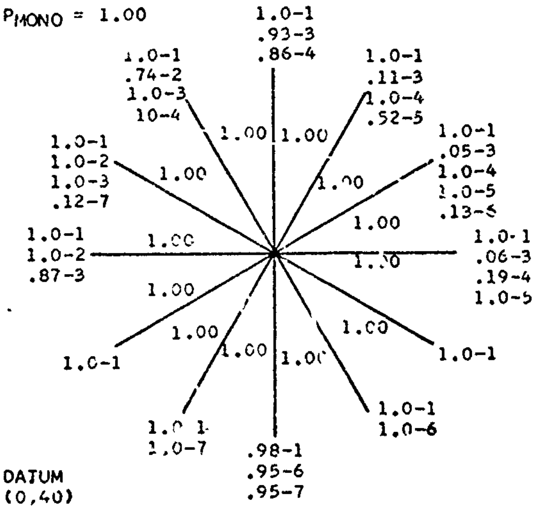

DATUM (0,40)

Hazeltine
Corporation

Figure A-56

ENVIRONMENT: MEDITERRANEAN
LAYER DEPTH (FT): 100
SYSTEM: SQS-26/41-X
XMTR MODE: BB/ODT
TARGET DEPTH (FT): 300
TARGET SPEED (KNOTS): 10
SHIP SPEED (KNOTS): 15
AIRCRAFT SPEED (KNOTS): 120
BUOY DEPTHS (FT): 1500

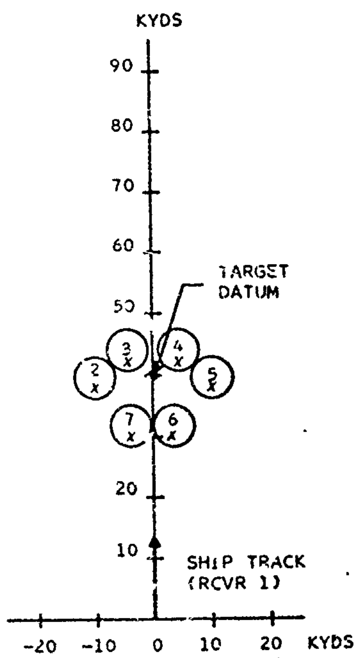

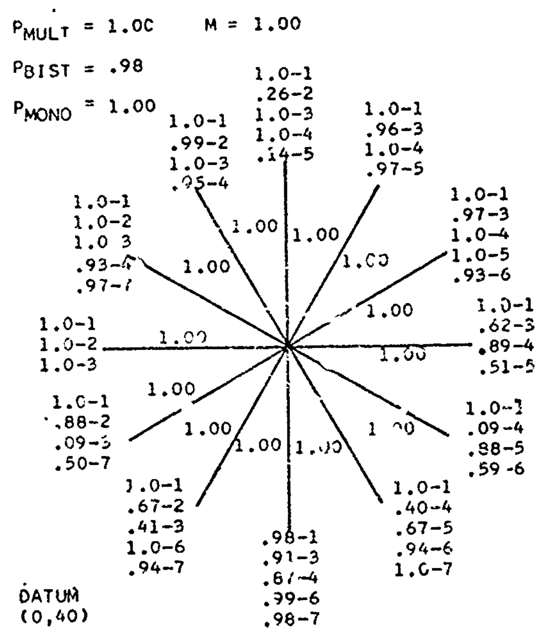

Hazeltine
Corporation

Figure A-57

ENVIRONMENT: MEDITERRANEAN
LAYER DEPTH (FT): 100
SYSTEM: SQS-26/41-X
XMTR MODE: BB/ODT
TARGET DEPTH (FT): 300
TARGET SPEED (KNOTS): 10
SHIP SPEED (KNOTS): 15
AIRCRAFT SPEED (KNOTS): 120
BUOY DEPTHS (FT): 60

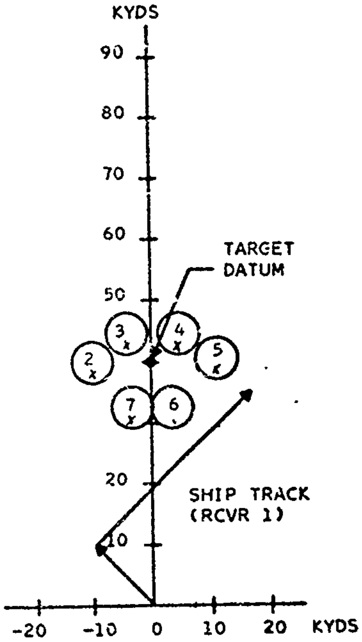

P_{MULT} = 1.00 M = 1.00

P_{BIST} = .93

P_{MONO} = 1.00

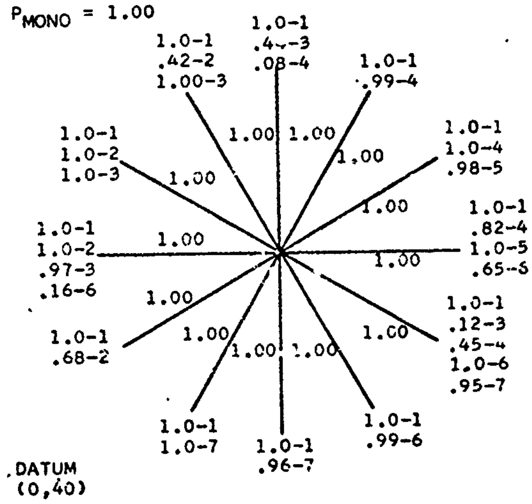

Hazeltine
Corporation

Figure A-58

ENVIRONMENT: MEDITERRANEAN
LAYER DEPTH (FT): 100
SYSTEM: SQS-26/41-X
XMTR MODE: BB/ODT
TARGET DEPTH (FT): 300
TARGET SPEED (KNOTS): 10
SHIP SPEED (KNOTS): 15
AIRCRAFT SPEED (KNOTS): 120
BUOY DEPTHS (FT): 1500

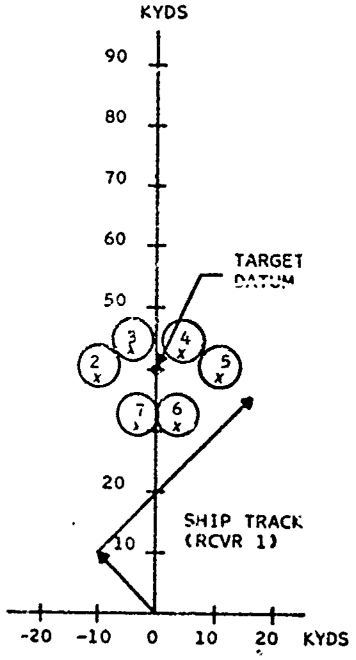

P_{MULT} = 1.00 M = 1.00

P_{BIST} = .98

P_{MONO} = 1.00

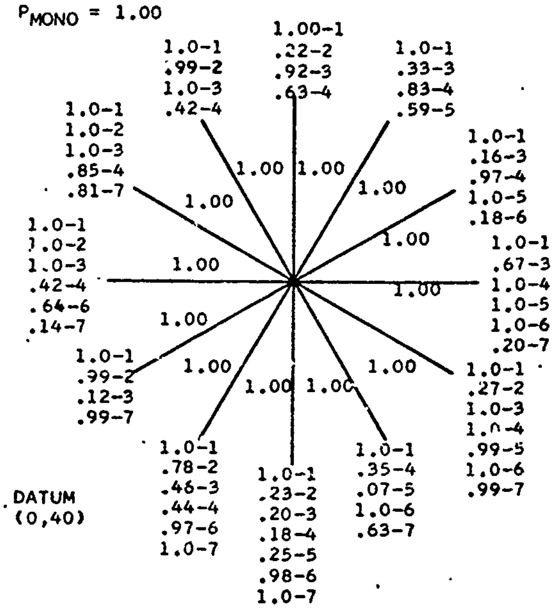

6165

Hazeltine
Corporation

Figure A-59

ENVIRONMENT: MEDITERRANEAN
LAYER DEPTH (FT): 100
SYSTEM: SQS-26/41-X
XMTR MODE: BB/ODT
TARGET DEPTH (FT): 300
TARGET SPEED (KNOTS): 10
SHIP SPEED (KNOTS): 15
AIRCRAFT SPEED (KNOTS): 120
BUOY DEPTHS (FT): 60

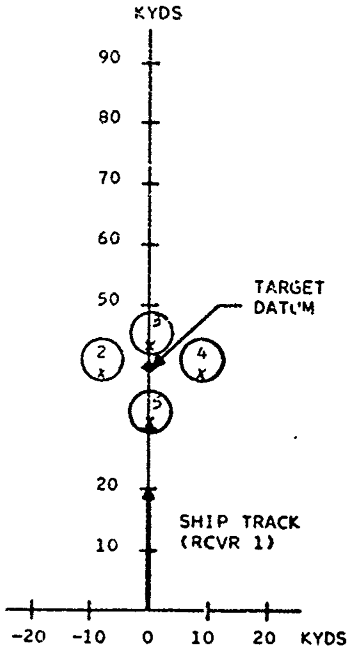

P_{MULT} = 1.00 M = 1.00

P_{BIST} = .78

P_{MONO} = 1.00

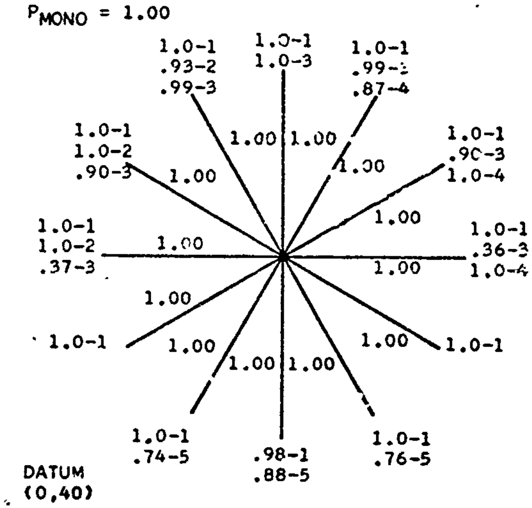

P_{MULT} = 1.00 M = 1.00

P_{BIST} = .72

P_{MONO} = 1.00

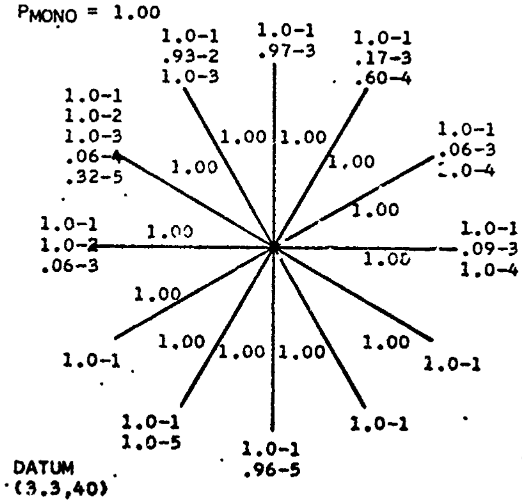

Hazeltine
Corporation

Figure A-60

ENVIRONMENT: MEDITERRANEAN
LAYER DEPTH (FT): 100
SYSTEM: SQS-26/41-X
XMTR MODE: BB/ODT
TARGET DEPTH (FT): 300
TARGET SPEED (KNOTS): 10
SHIP SPEED (KNOTS): 15
AIRCRAFT SPEED (KNOTS): 120
BUOY DEPTHS (FT): 1500

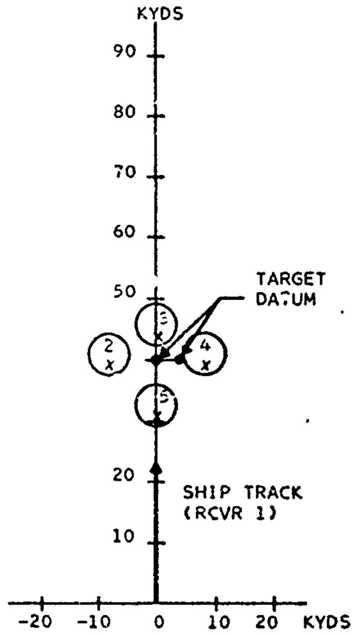

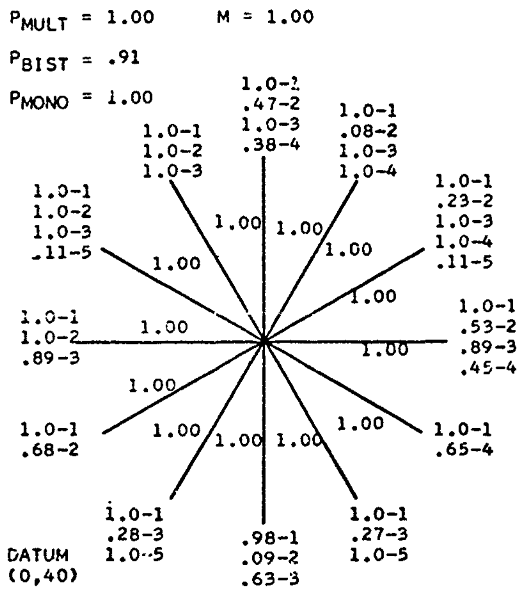

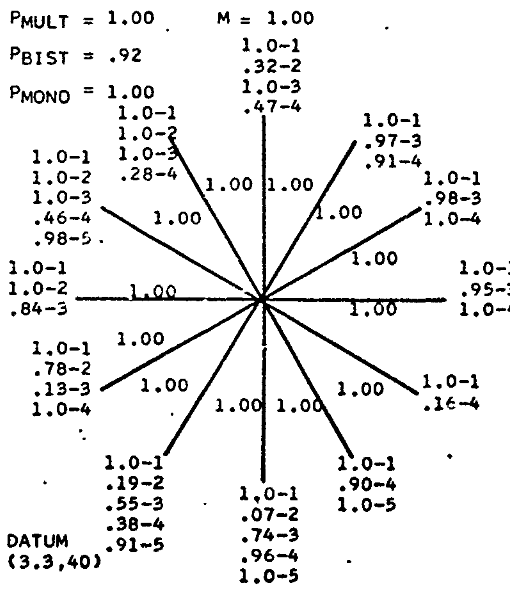

Hazeltine
Corporation

Figure A-61

ENVIRONMENT: MEDITERRANEAN
LAYER DEPTH (FT): 100
SYSTEM: SQS-26/41-X
XMTR MODE: BB/ODT
TARGET DEPTH (FT): 55
TARGET SPEED (KNOTS): 10
SHIP SPEED (KNOTS): 15
AIRCRAFT SPEED (KNOTS): 120
BUOY DEPTHS (FT): 60

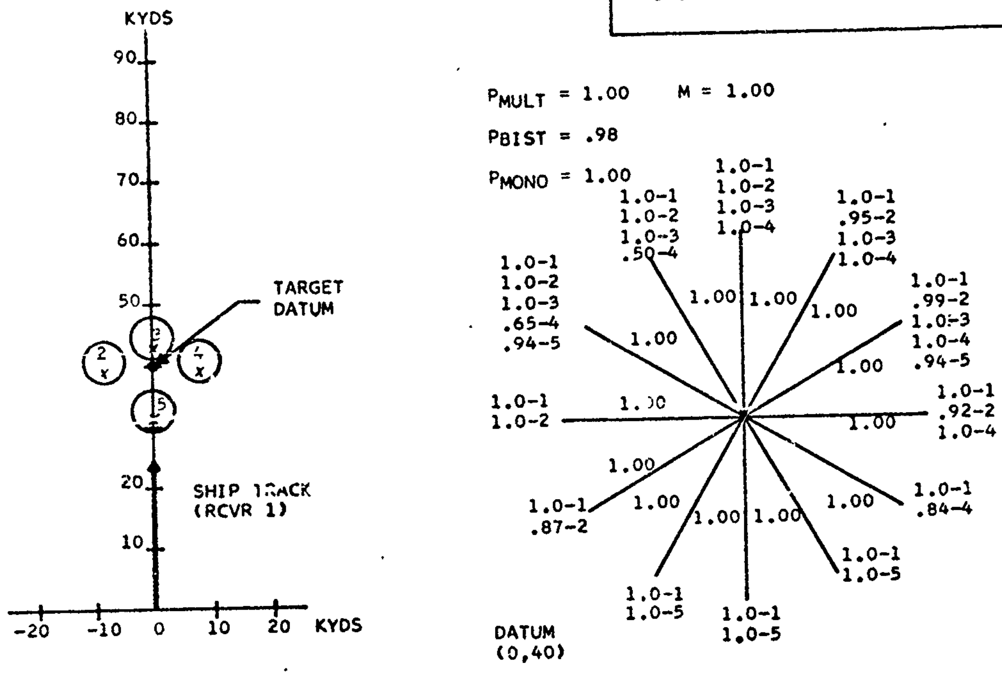

6165

Hazeltine Corporation

Figure A-62

ENVIRONMENT: MEDITERRANEAN
LAYER DEPTH (FT): 100
SYSTEM: SQS-26/41-X
XMTR MODE: BB/ODT
TARGET DEPTH (FT): 55
TARGET SPEED (KNOTS): 10
SHIP SPEED (KNOTS): 15
AIRCRAFT SPEED (KNOTS): 120
BUOY DEPTHS (FT): 1500

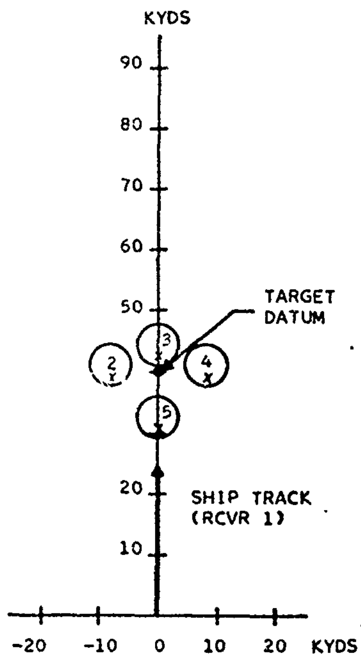

P_{MULT} = 1.00 M = 1.00

P_{BIST} = .65

P_{MONO} = 1.00

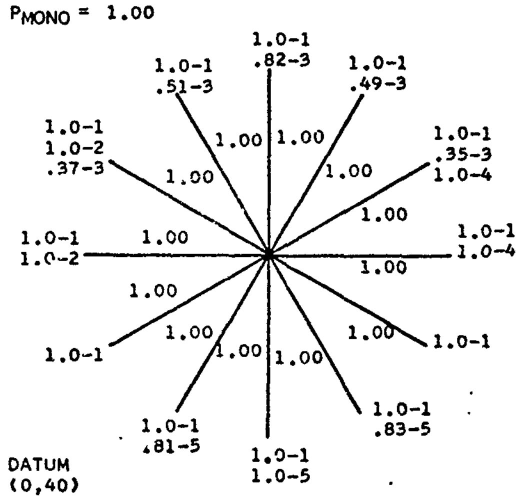

Figure A-63

ENVIRONMENT: MEDITERRANEAN
LAYER DEPTH (FT): 100
SYSTEM: SQS-26/41-X
XMTR MODE: BB/ODT
TARGET DEPTH (FT): 600
TARGET SPEED (KNOTS): 10
SHIP SPEED (KNOTS): 15
AIRCRAFT SPEED (KNOTS): 120
BUOY DEPTHS (FT): 60

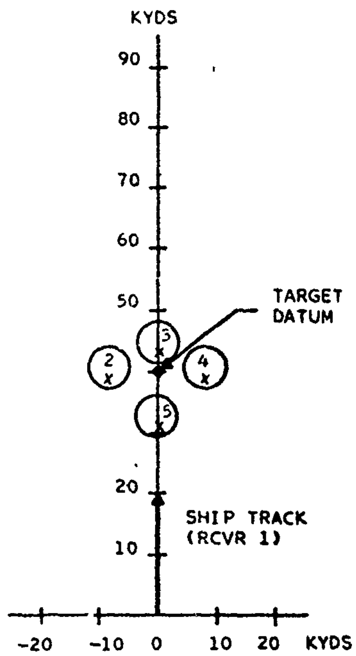

P_{MULT} = .99   M = .99

P_{BIST} = .90

P_{MONO} = .99

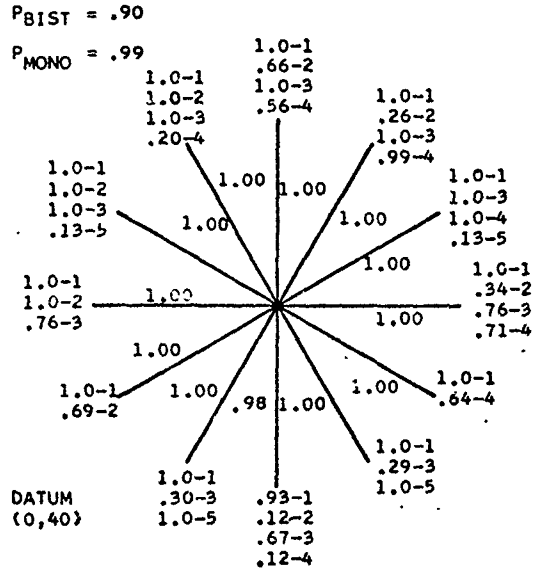

Hazeltine
Corporation

Figure A-64

ENVIRONMENT: MEDITERRANEAN
LAYER DEPTH (FT): 100
SYSTEM: SQS-26/41-X
XMTR MODE: BB/ODT
TARGET DEPTH (FT): 600
TARGET SPEED (KNOTS): 10
SHIP SPEED (KNOTS): 15
AIRCRAFT SPEED (KNOTS): 120
BUOY DEPTHS (FT): 1500

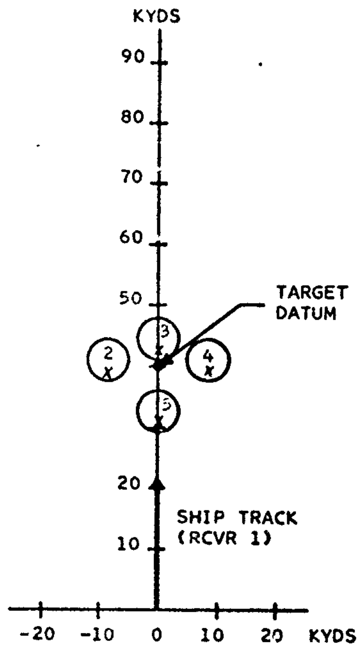

P_{MULT} = .99 M = 1.00

P_{BIST} = .81

P_{MONO} = .99

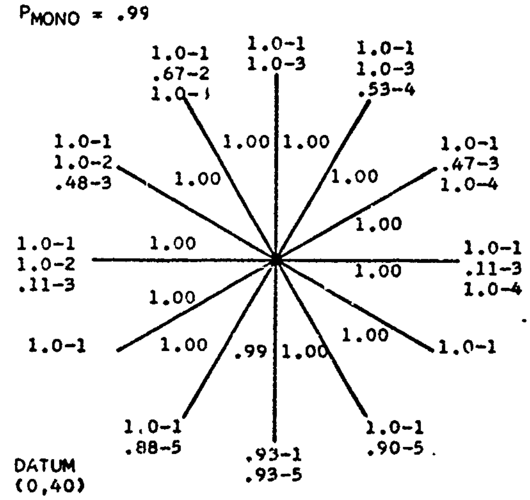

Hazeltine Corporation

Figure A-65

ENVIRONMENT: MEDITERRANEAN
LAYER DEPTH (FT): 100
SYSTEM: SQS-26/41-X
XMTR MODE: BB/ODT (2ND CZ)
TARGET DEPTH (FT): 300
TARGET SPEED (KNOTS): 10
SHIP SPEED (KNOTS): 15
AIRCRAFT SPEED (KNOTS): 120
BUOY DEPTHS (FT): 40

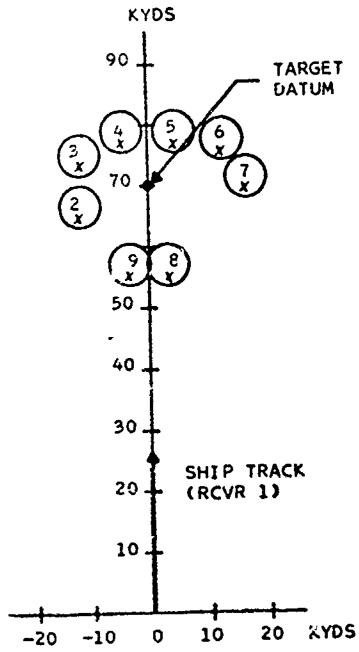

$P_{MULT} = .76$ M = .77

$P_{BIST} = .62$

$P_{MONO} = .60$

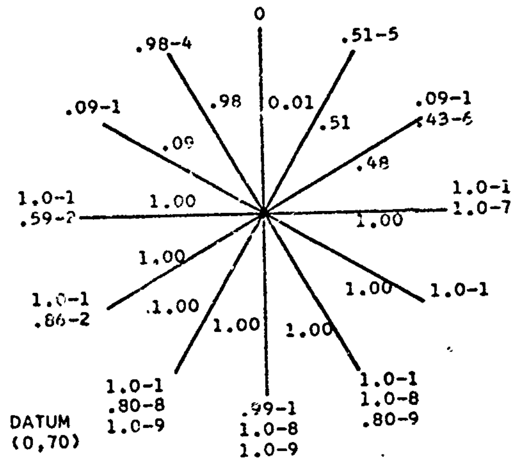

Figure A-66

ENVIRONMENT: MEDITERRANEAN
LAYER DEPTH (FT): 100
SYSTEM: SQS-26/41-X
XMTR MODE: BB/OUT (2ND CZ)
TARGET DEPTH (FT): 300
TARGET SPEED (KNOTS): 10
SHIP SPEED (KNOTS): 15
AIRCRAFT SPEED (KNOTS): 120
BUOY DEPTHS (FT): 1500

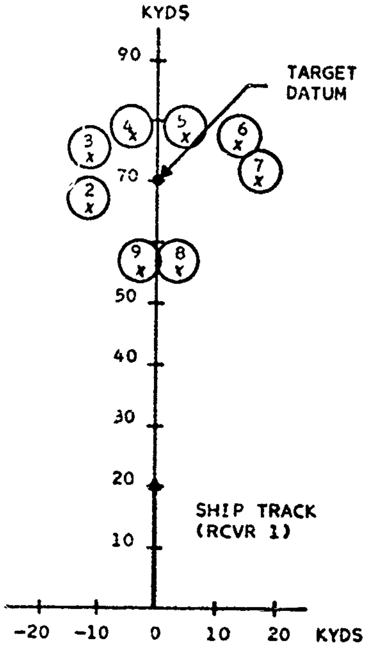

P_{MULT} = .77 M = .79

P_{BIST} = .77

P_{MONO} = .60

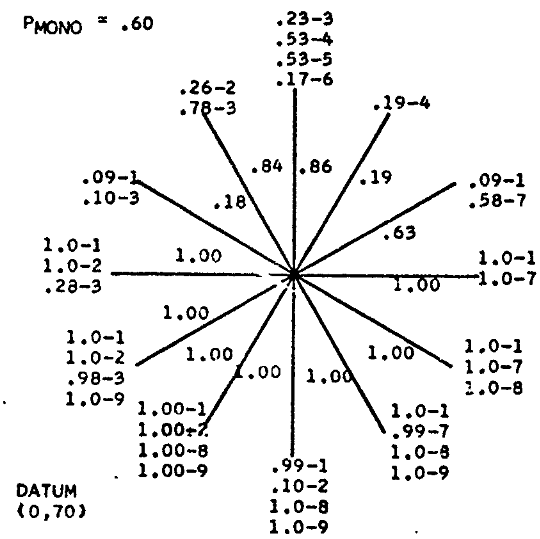

Hazeltine Corporation

Figure A-67

ENVIRONMENT: MEDITERRANEAN(DAY)
LAYER DEPTH (FT): 100
SYSTEM: SQS-26/41-X
XMTR MODE: BB/ODT
TARGET DEPTH (FT): 300
TARGET SPEED (KNOTS): 10
SHIP SPEED (KNOTS): 15
AIRCRAFT SPEED (KNOTS): 120
BUOY DEPTHS (FT): 60

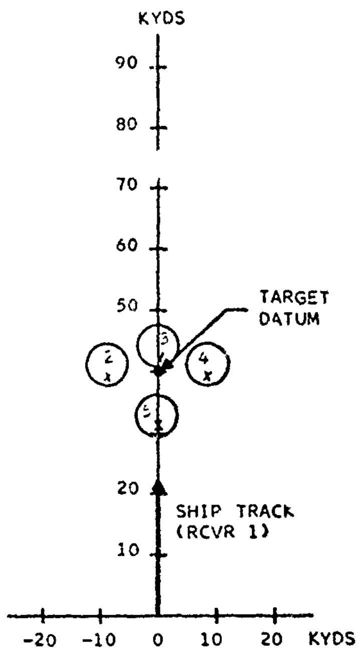

P_{MULT} = 1.00 M = 1.00

P_{BIST} = .81

P_{MONO} = 1.00

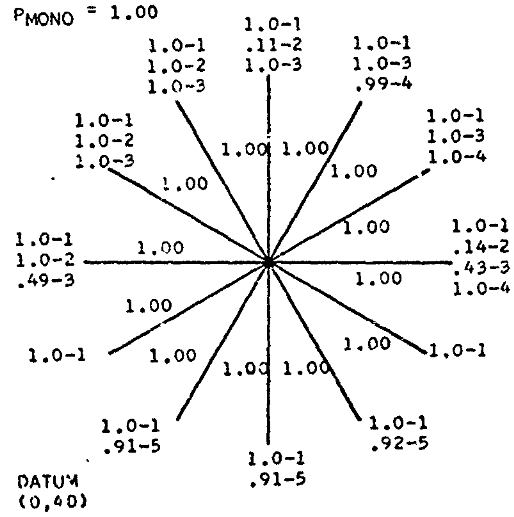

Hazeltine
Corporation

Figure A-68

ENVIRONMENT: MEDITERRANEAN
LAYER DEPTH (FT): (NO SURFACE DUCT)
SYSTEM: SQS-26/41-X
XMTR MODE: BB/ODT
TARGET DEPTH (FT): 55
TARGET SPEED (KNOTS): 10
SHIP SPEED (KNOTS): 15
AIRCRAFT SPEED (KNOTS): 120
BUOY DEPTHS (FT): 60

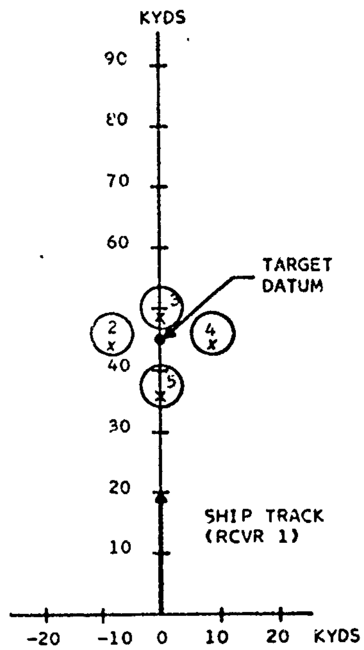

P_{MULT} = 1.00   M = 1.00

P_{BIST} = .58

P_{MONO} = 1.00

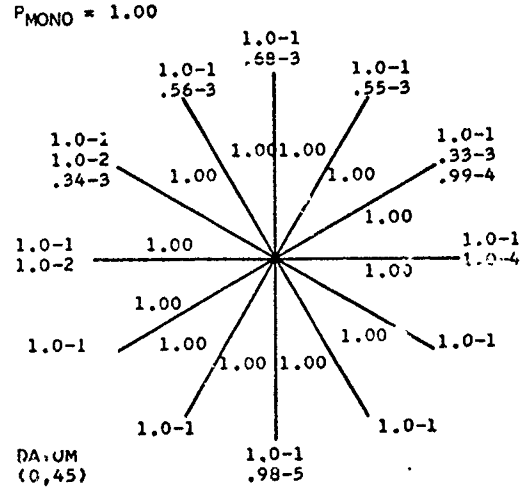

ENVIRONMENT: MEDITERRANEAN
LAYER DEPTH (FT): (NO SURFACE DUCT)
SYSTEM: SQS-26/41-X
XMTR MODE: BB/ODT
TARGET DEPTH (FT): 55
TARGET SPEED (KNOTS): 10
SHIP SPEED (KNOTS): 15
AIRCRAFT SPEED (KNOTS): 120
BUOY DEPTHS (FT): 1500

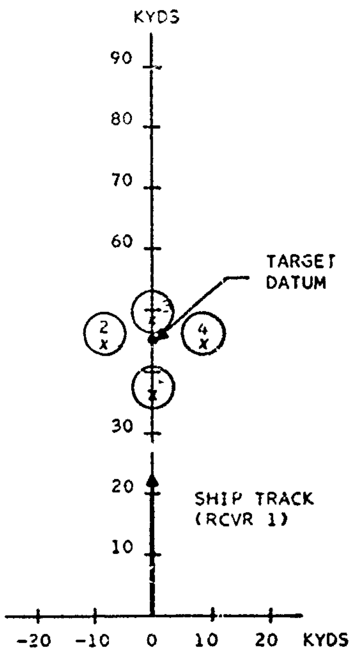

P_{MULT} = 1.00   M = 1.00

P_{BIST} = .46

P_{MONO} = 1.00

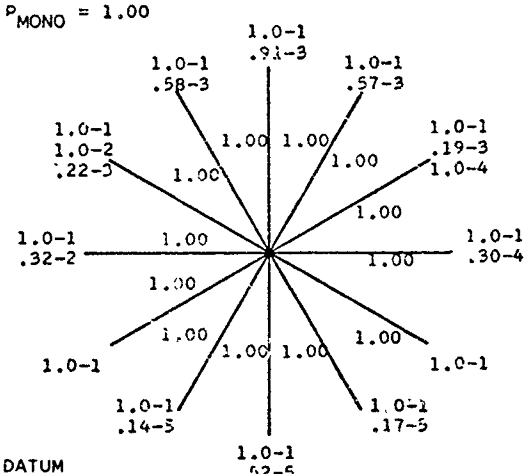

DATUM
(0,45)

Hazeltine
Corporation

Figure A-70

ENVIRONMENT: MEDITERRANEAN
LAYER DEPTH (FT): (NO SURFACE DUCT)
SYSTEM: SQS-26/41-X
XMTR MODE: BB/ODT
TARGET DEPTH (FT): 300
TARGET SPEED (KNOTS): 10
SHIP SPEED (KNOTS): 15
AIRCRAFT SPEED (KNOTS): 120
BUOY DEPTHS (FT): 60

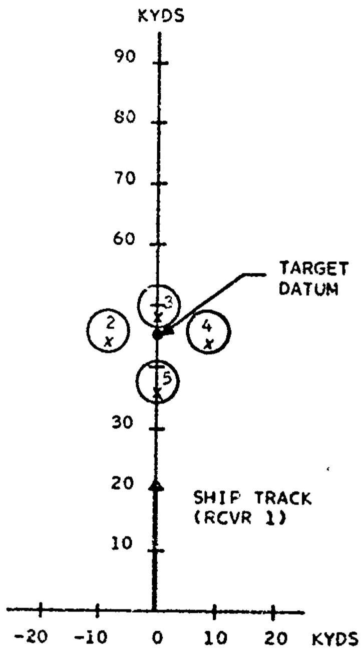

P_{MULT} = 1.00 M = 1.00

P_{BIST} = .39

P_{MONO} = 1.00

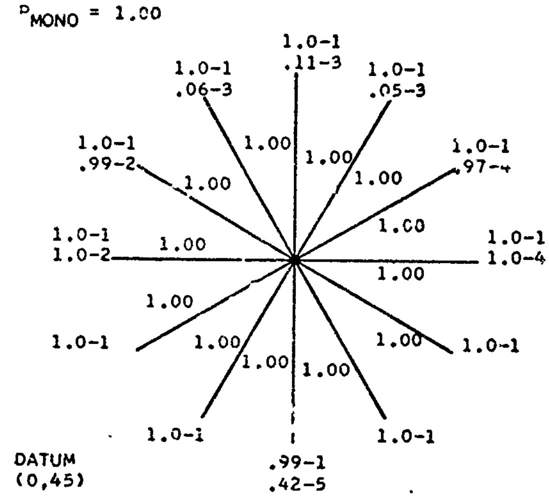

Hazeltine
Corporation

Figure A-71

ENVIRONMENT: MEDITERRANEAN
LAYER DEPTH (FT): (NO SURFACE DUCT)
SYSTEM: SQS-26/41-X
XMTR MODE: [illegible]/ODT
TARGET DEPTH (FT): 300
TARGET SPEED (KNOTS): 10
SHIP SPEED (KNOTS): 15
AIRCRAFT SPEED (KNOTS): 120
BUOY DEPTHS (FT): 1500

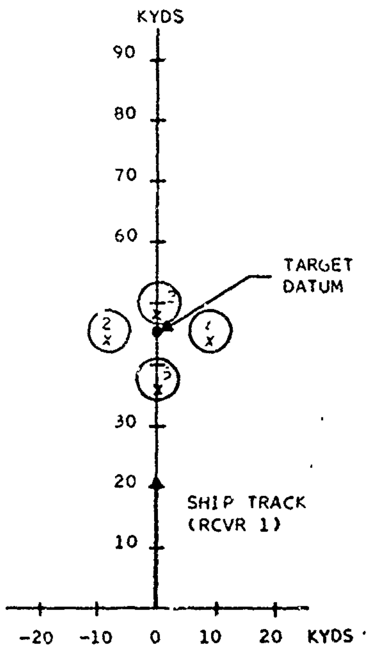

P_{MULT} = 1.00 M = 1.00

P_{BIST} = .93

P_{MONO} = 1.00

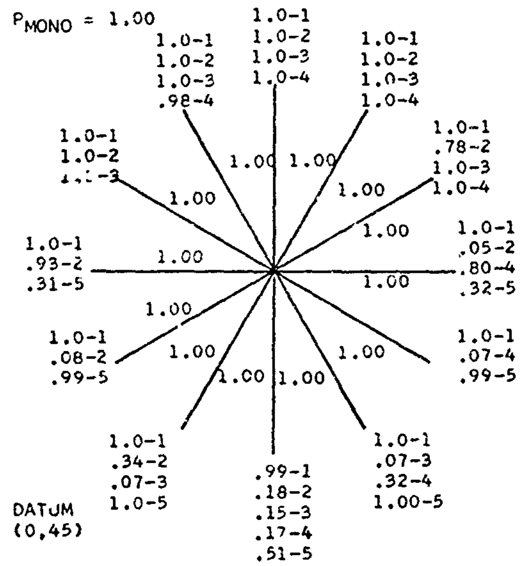

Hazeltine Corporation

Figure A-72

ENVIRONMENT: MEDITERRANEAN
LAYER DEPTH (FT): (NO SURFACE DUCT)
SYSTEM: SQS-26/41-X
XMTR MODE: BB/ODT
TARGET DEPTH (FT): 600
TARGET SPEED (KNOTS): 10
SHIP SPEED (KNOTS): 15
AIRCRAFT SPEED (KNOTS): 120
BUOY DEPTHS (FT): 60

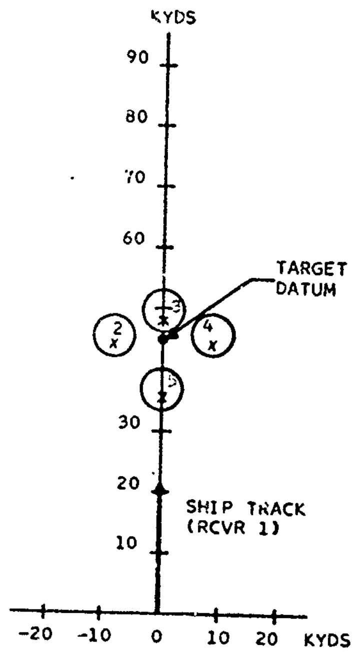

P_{MULT} = 1.00 M = 1.00

P_{BIST} = .43

P_{MONO} = 1.00

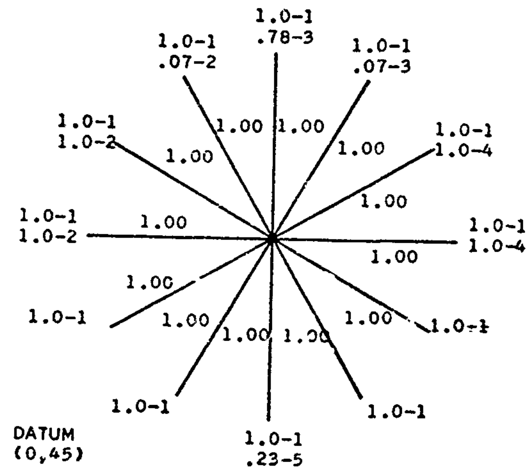

6165

Hazeltine Corporation

Figure A-73

ENVIRONMENT: MEDITERRANEAN
LAYER DEPTH (FT): (NO SURFACE DUCT)
SYSTEM: SQS-26/41-?
XMTR MODE: BB/ODT
TARGET DEPTH (FT): 600
TARGET SPEED (KNOTS): 10
SHIP SPEED (KNOTS): 15
AIRCRAFT SPEED (KNOTS): 120
BUOY DEPTHS (FT): 1500

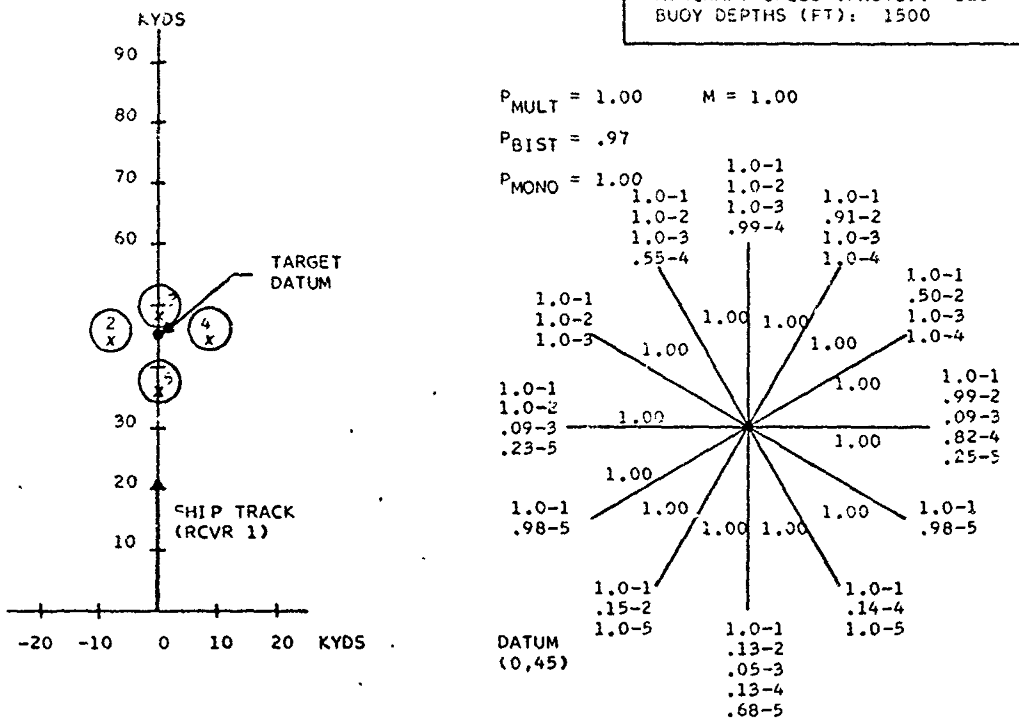

Hazeltine Corporation

Figure A-74

ENVIRONMENT: NORTH ATLANTIC
LAYER DEPTH (FT): 150
SYSTEM: CASS
XMTR MODE: BB/ODT
TARGET DEPTH (FT): 55
TARGET SPEED (KNOTS): 10
SHIP SPEED (KNOTS): 15
AIRCRAFT SPEED (KNOTS): 120
BUOY DEPTHS (FT): 1500

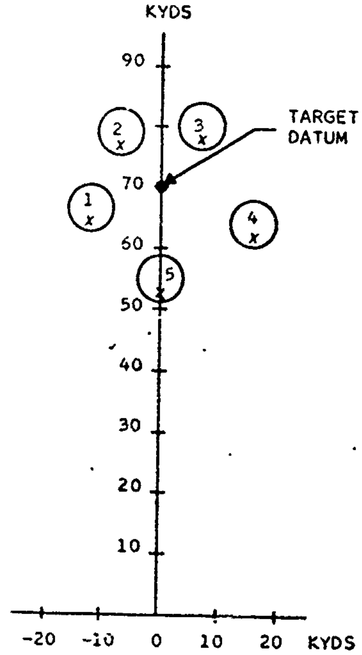

M = .59

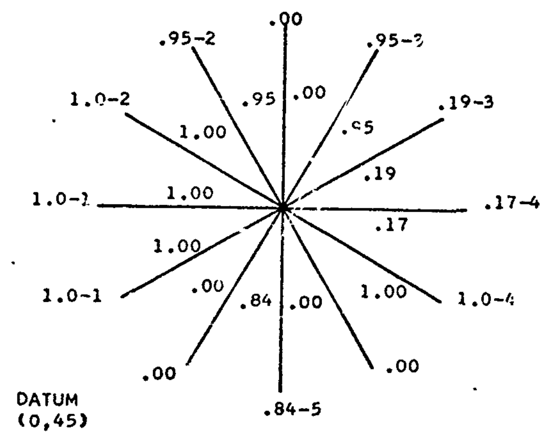

Figure A-75

ENVIRONMENT: NORTH ATLANTIC
LAYER DEPTH (FT): 150
SYSTEM: SQS-26/CASS
XMTR MODE: [illegible]/ODT, DP
TARGET DEPTH (FT): 300
TARGET SPEED (KNOTS): 10
SHIP SPEED (KNOTS): 15
AIRCRAFT SPEED (KNOTS): 120
BUOY DEPTHS (FT): 1500

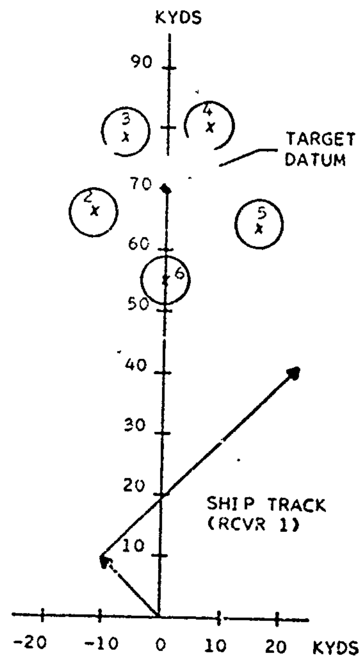

P_{MULT} = 1.00   M = 1.00

P_{CASS} = 1.00

P_{MONO} = .46

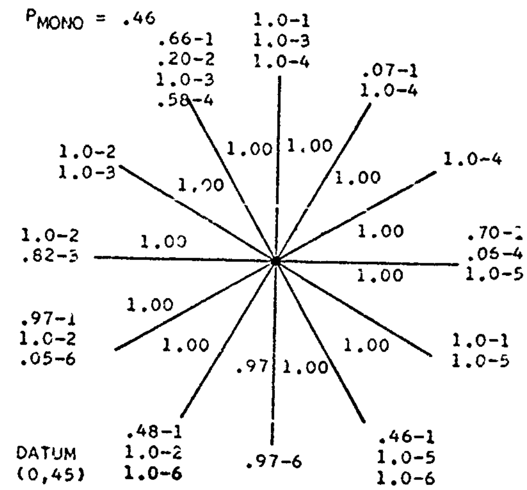

Figure A-76

ENVIRONMENT: NORTH ATLANTIC
LAYER DEPTH (FT): 150
SYSTEM: SQS-26/CASS
XMTR MODE: BB/ODT, DP
TARGET DEPTH (FT): 600
TARGET SPEED (KNOTS): 10
SHIP SPEED (KNOTS): 15
AIRCRAFT SPEED (KNOTS): 120
BUOY DEPTHS (FT): 1500

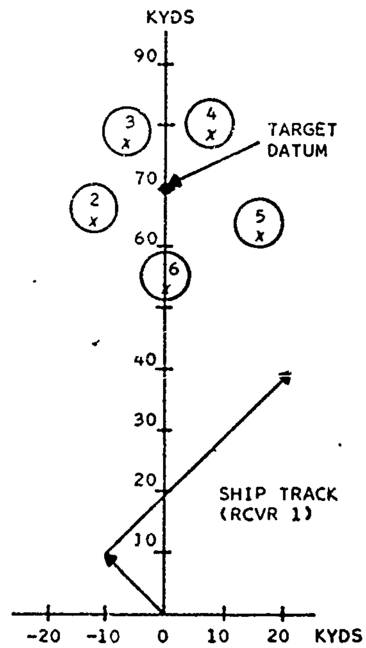

P_{MULT} = .99 M = .99

P_{CASS} = .99

P_{MONO} = .42

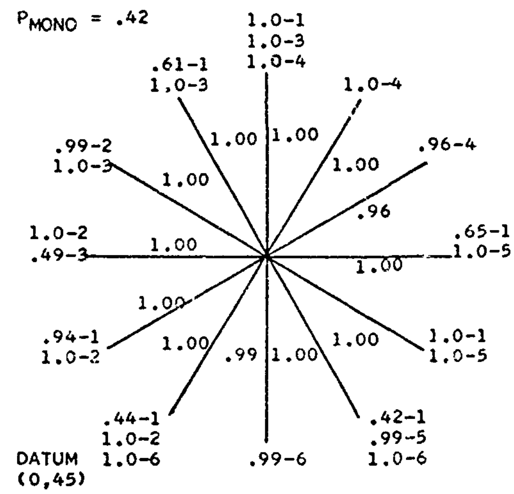

APPENDIX B (U)

SURFACE SCATTERING: INFLUENCE ON ACOUSTIC PROPAGATION LOSSES

A. INTRODUCTION

(U) The calculation of acoustic propagation losses in the ocean using ray tracing computer models leads to two surface related problems: 1) no energy is predicted in the shadow zone where ray paths do not exist; 2) a reasonable choice must be made for surface losses due to reflection in the specular direction.

(U) Energy in the shadow zone can be calculated from equations based on empirical data such as measured in the AMOS sea experiments. These data, however, are restricted in their applicability and therefore cannot be generalized for all environments and sonar (or target) depths.

(U) Empirical surface reflection data is not always available for environments and sea conditions of interest.

(U) The present discussion shows how a unified theory of surface phenomena including effects of scattering, bubble effects, and diffraction leads to more general and widely applicable solutions to these problems.

B. SCATTERING FROM A ROUGH SURFACE

(U) Our point of departure for developing a general function for surface scattering is the equation for scattering from a gaussian distributed rough surface as derived by Beckmann.[1] The general scattering equation can be written as:

$$S_s = e^{-g}\left(\rho_o^{\,2} + \frac{\pi\, T^2 F^2 \sin^2\theta_1}{\lambda^2} \sum_{m=1}^{\infty} \frac{g^m}{m!m} e^{-v_{xy}^{\,2}\, T^2/4m}\right) \tag{1}$$

where:

$$F = \frac{1 + \sin\theta_1 \sin\theta_2 - \cos\theta_1 \cos\theta_2 \cos\phi}{\sin^2\theta_1 + \sin\theta_1 \sin\theta_2} \tag{2}$$

$$v_{xy}^{\,2} = \frac{4\pi}{\lambda^2}\left(\cos^2\theta_1 - 2\cos\theta_1 \cos\theta_2 \cos\phi + \cos^2\theta_2\right) \tag{3}$$

$$g = \frac{4\pi^2\sigma^2}{\lambda^2}\,(\sin\theta_1 + \sin\theta_2)^2 \qquad (4)$$

and θ_1 and θ_2 are the incident and reflected grazing angles at the scatterer, $\emptyset$ is the azimuthal angle at the scatterer, T is the surface correlation length, σ is the rms wave height and λ is the acoustic wavelength. g is the acoustical roughness of the surface and depends on the scattering angles as well as on wave height. ρ_o is a function which is 1 in the specular direction ($\theta_1 = \theta_2$, $\emptyset = 0$) and 0 elsewhere.

(U) At this point, most authors restrict the value of g in order to use asymptotic expressions for equation (1). This, however, also restricts the generality of their solutions and, in many cases, asymptotic expressions are used outside their range of applicability.

(U) Since we are interested in scattering at all angles and for varying surface roughness, we will use equation (1) for our scattering function. We will utilize asymptotic expression found from (1), however, the values of g at which these expressions will be used are kept well within the limits of good approximations and cover all possible values of g. The three regions of g, which we consider and the expressions used are:

$$S_s = e^{-g}\left(\rho_o^2 + \frac{g\pi T^2 F^2 \sin^2\theta_1}{\lambda^2}\, e^{-v_{xy}^2 T^2/4m}\right);\ g \leq .1 \qquad (5)$$

$$S_s = e^{-g}\left(\rho_o^2 + \frac{\pi T^2 F^2 \sin^2\theta_1}{\lambda^2} \sum_{m=1}^{20} \frac{g^m}{m:m}\, e^{-v_{xy}^2 T^2/4m}\right).1 < g < 10 \qquad (6)$$

$$S_s = \frac{\pi F^2 T^2 \sin^2\theta_1}{\lambda^2 v_z^2 \sigma^2}\, e^{-v_{xy}^2 T^2/4 v_z^2 \sigma^2} \qquad g \geq 10 \qquad (7)$$

where:

$$v_z^2 = \frac{4\pi^2}{\lambda^2}\,(\sin\theta_1 + \sin\theta_2)^2 \qquad (8)$$

(U) The validity of these expressions when used in the regions of acoustical roughness as indicated is well illustrated in Figure 1 of a paper by Medwin.[2]

(U) In using these equations for calculating surface scattering correct values for the surface correlation length T, and the rms wave height σ must be found as a function of wind velocity. Following the approach used by Medwin[3] which assumes an isotropic gaussian distributed rough surface, we have a relation between T, σ, and the mean square surface slope Σ:

$$T = \frac{2\sigma^2}{\Sigma^2} \tag{9}$$

Σ is found from the generally accepted expression derived by Cox and Munk[4];

$$\Sigma^2 = 5.12 \times 10^{-5}\, W + 0.003 \tag{10}$$

where W is the wind velocity in cm/sec.

(U) The choice of the correct value for σ depends on the factor of sea surface roughness which contributes most strongly to surface scattering. While most authors choose a formula for the wave heights of a fully developed sea, we have used values of rms wave height as found empirically in a study of reverberation backscattering by Garrison et.al..[5] The values of σ found in their study range from about 1 to 7 inches for wind velocities from 6 to 17 knots. These values are considerably smaller than wave heights from a fully developed sea and indicate that the major contribution of scattering arises from small perturbations of the developed sea. It is probable that contributions from both effects, the developed sea waves and local facets should be included, but the second term seems to be dominant in scattering and leads to more reasonable values of specular surface reflection coefficients.

C. REFLECTION COEFFICIENT

1. Surface Scattering Effects

(U) The reflection coefficient for the surface cannot be assumed to consist of simply the specular term of equation (1) because for actual processors, energy arriving during a finite time period (10 ms in our study) is detected and therefore all energy arriving during this time must be accounted for in calculations. This means that the reflection in the specular direction will consist of the actual specular term from (1) plus all scattered energy arriving within 10 ms of this specular ray.

(U) A computer program was written which calculates reflection coefficient by integrating the energy scattered into the specular direction. This program is adaptive in both time and space; that is, it integrates energy arriving from points around ever increasing sized circles centered around the specular contact until either: 1) the contribution becomes negligibly small or 2) the ray travel time is outside the bounds of the processor integration period.

(U) Our approach to surface reflection also eliminates the problems which arise when trying to use closed form solutions for the reflection coefficient. If closed forms are used, the assumption must be made that the source and receiver are in the far field (Fraunhofer region). Tests of these types of solutions indicate that predicted losses are 5-20 dB too high and this is because all of the arriving energy is not accounted for.

(U) The adaptive integration utilizing the whole scattering function is equivalent to a Fresnel solution which has been deemed necessary by several authors.

(U) Because we have preserved the form of the scattering equations useful for all values of g, reflection coefficients can be calculated for all incident angles from 0 to 90°. The results for various wind velocities are shown in Figure 1. The negative surface losses found for small grazing angles are actually gains and this is reasonable both from a mathematical point of view and from similar experiments in optics. The fact that this is never seen in sea experiments is due to bubble losses which are always present in a rough sea. (If the sea surface were smooth, then there would be no bubbles but also no scattered energy and R would be 1.)

2. Bubble Effects

(U) Air bubbles near the sea surface have a two-fold effect on surface reflections: 1) absorption and scattering of energy from an acoustic ray and 2) refraction of the ray changing its angle of contact with the surface. This topic is discussed in detail in Medwin's paper[3] and the mathematics will not be presented here. The final results can be summarized here in the following equations.

(U) The surface loss in dB per bounce due to bubbles is given by:

$$A_b = 2 \int_L^o a_b \, dS \tag{11}$$

$$a_b = 3.27 \times 10^{-15} f_o^3 W (1 + 10^{-4} W^2) (1 + 0.1Z)^{-4} \tag{12}$$

Figure 1

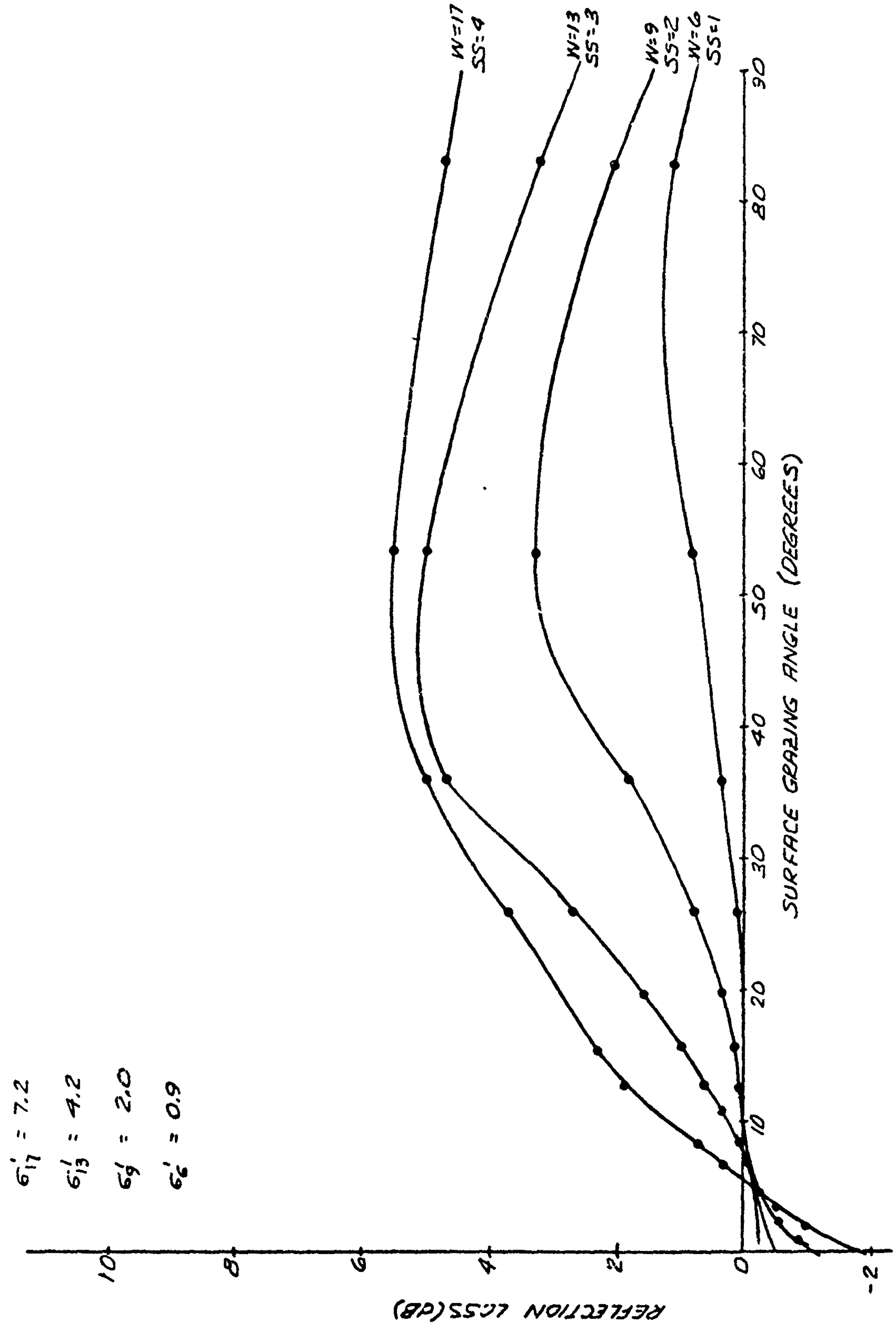
W=17
SS=4
W=13
SS=3
W=9
SS=2
W=6
SS=1
SURFACE GRAZING ANGLE (DEGREES)
REFLECTION LOSS (dB)
σ'17 = 7.2
σ'13 = 4.2
σ'9 = 2.0
σ'6 = 0.9

Z is the depth, W is the wind velocity in knots and f_o is the resonent frequency of the bubbles. The integration extends along the acoustic ray throughout the layer L where bubbles exist. This expression can be numerically integrated by using short straight line segments along the path.

(U) The angle of incidence at the surface can be computed from the no-bubble incident angle by using the equations:

$$C_s = C\,(1 - F_c) \qquad (13)$$

$$F_c = 9.74 \times 10^{-5}\, W\,(1 + 10^{-4}\, W^2) \qquad (14)$$

where C is the uncorrected acoustic velocity at the surface and W is wind velocity in knots. The incident angle is then found from Snells' law;

$$\frac{\cos \theta_s}{c_s} = \frac{\cos \theta_o}{c_o}$$

where C_o and θ_o are values found at the bottom of the bubble layer.

(U) We have found it reasonable to use a value of $f_o \sim 10000$ Hz which is considerably lower than that proposed by Medwin. This can be explained by the observation that bubbles tend to form in clusters and thus the average "bubble" size increases and the resonant frequency decreases.

(U) The bubble losses calculated using these values and a wind velocity of 17 knots are shown as curve 2 in Figure 2. The lower scales represent the uncorrected and bubble refraction corrected ( ) grazing angles. The reason the curve has a peak is that rays with shallower angles do not pass through the whole bubble layer.

(U) Also shown on this figure, is the loss due to surface roughness (curve 1) and finally the total surface loss per bounce for reflection in the specular direction (curve 3).

D. PROPAGATION IN THE SHADOW ZONE

(U) Energy propagated into the shadow zone was calculated using a technique similar to that of Schweitzer[6]. The basic geometry is illustrated in Figure 3. The fundamental operation used to calculate the propagation loss from target to receiver is:

Hazeltine Corporation

Figure 2

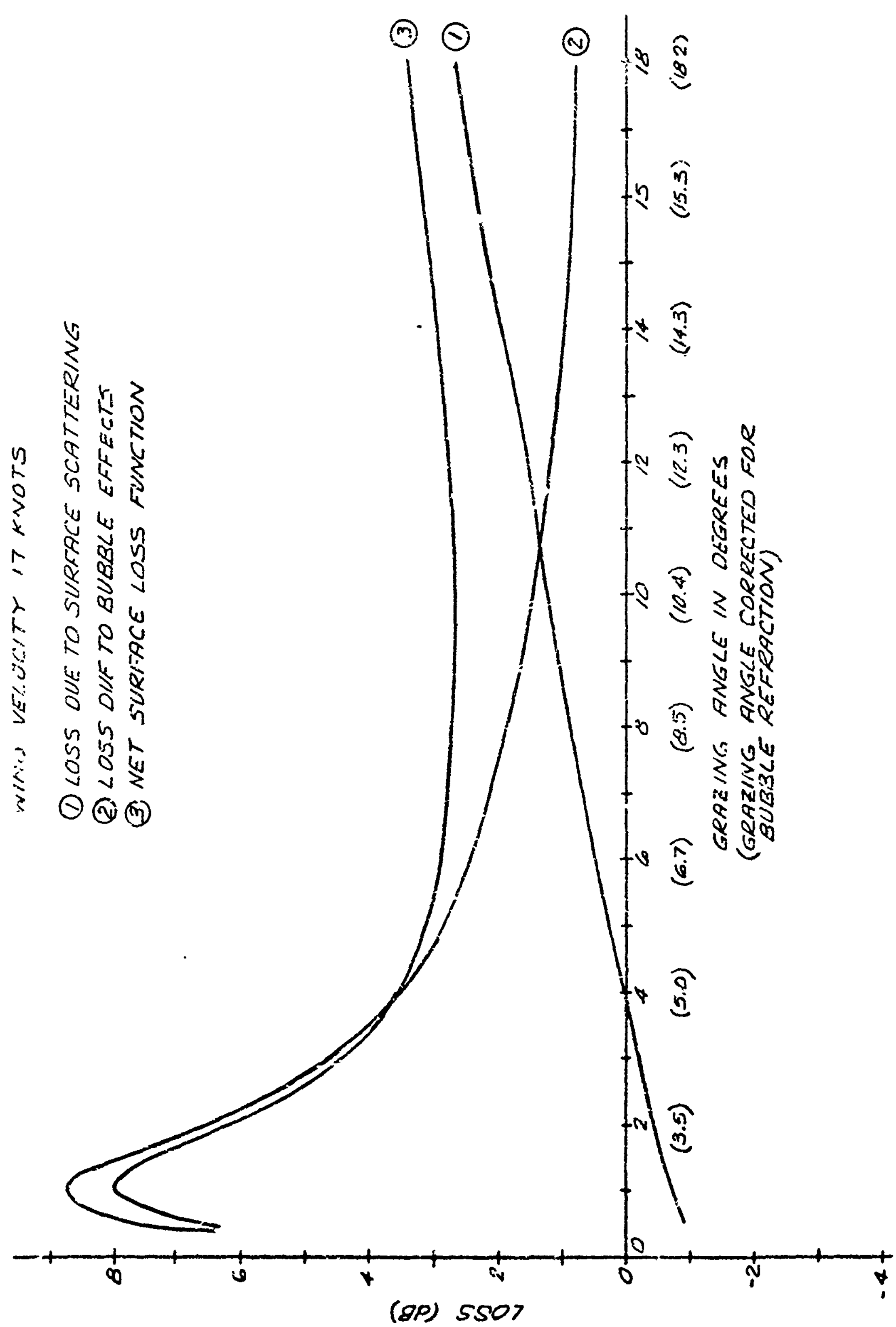

Figure 3

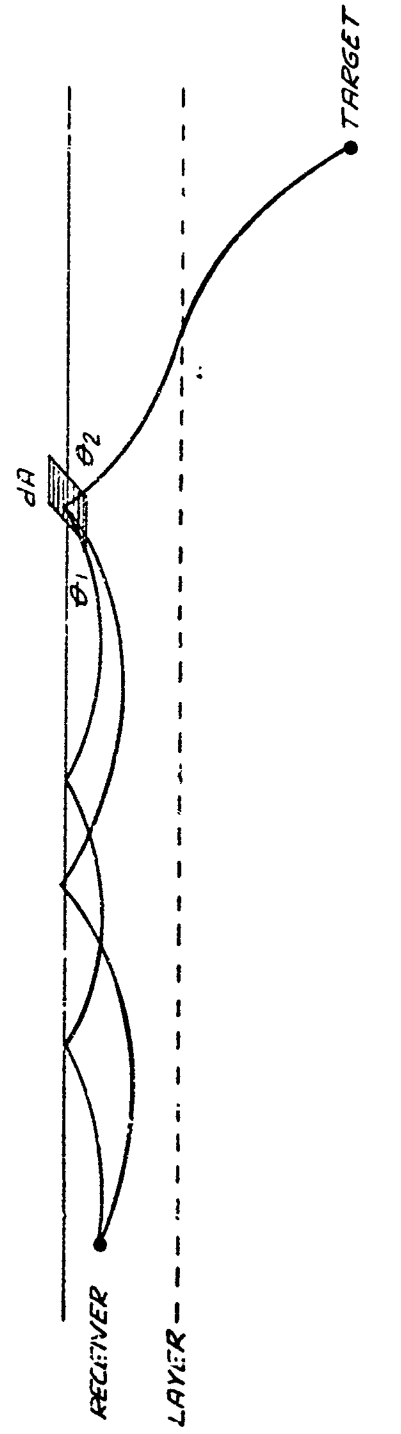

$$P = \iint P_1 S_s P_2 \, dA \qquad (15)$$

where P_1 is the propagation loss within the duct from the receiver to the area element dA, P_2 is the propagation loss from dA the below layer target and S_s is the surface scattering coefficient. We have again used the total scattering function of equation (1) and the integration is carried out by an adaptive computer program which sums contributions from circular annulae centered over the target. It is found that the major portion of energy arrives from a narrow strip between receiver and target and therefore our program integrates around a circle starting on the receiver-target axis and continues until the contributions are negligible. Then the next annulus is taken and the process is repeated until the on-axis contribution is also negligibly small. We have chosen 2^0 azimuthal integration steps and 50 yard range steps. The program is also time adaptive in that only the energy arriving within 10 ms of the peak is retained.

(U) In using the scattering function, it will be noted that there are several ray paths from the surface to the element dA. The angle θ_1, is thus not well defined but it has been shown that S_s is highly insensitive to angular variations up to about 3^0 which are typical of ducted rays.

(U) The actual computation then consists of: 1) calculating the surface "illumination" due to the receiver at 1000 yard intervals, 2) calculating the propagation losses from target to transmitter in 50 yard steps out to about 4000 yds, 3) carrying out the above described integration using actual propagation losses extrapolated from the tables generated in steps 1 and 2.

(U) Figure 4 illustrates the values of surface "illumination" (actually propagation losses from the receiver) and the resulting values of integrated shadow zone energy. These points were calculated using a detailed ray tracing program and thus show the wide variations due to surface "hot spots" or mini convergence zones.

(U) While these results are typical of a particular environment, it is more useful to have smoother curves to work with in acoustic prediction models. This was carried out by smoothing both the surface illumination tables and the resulting shadow zone propagation loss tables. In addition, a diffraction term was added to account for energy which "leaks" into the shadow zone from the limiting rays. The use of diffraction attenuation coefficients is discussed by Noble[7] and the value we used was 6 dB/kyd.

(U) Figure 5 shows the final results for smoothed shadow zone propagation losses including diffraction for a receiver at 60' and a target at 250'. This curve is in good agreement with the empirical AMOS curve for the same conditions. The advantage of our theory is that it will hold up in cases where AMOS data is not valid.

Figure 4

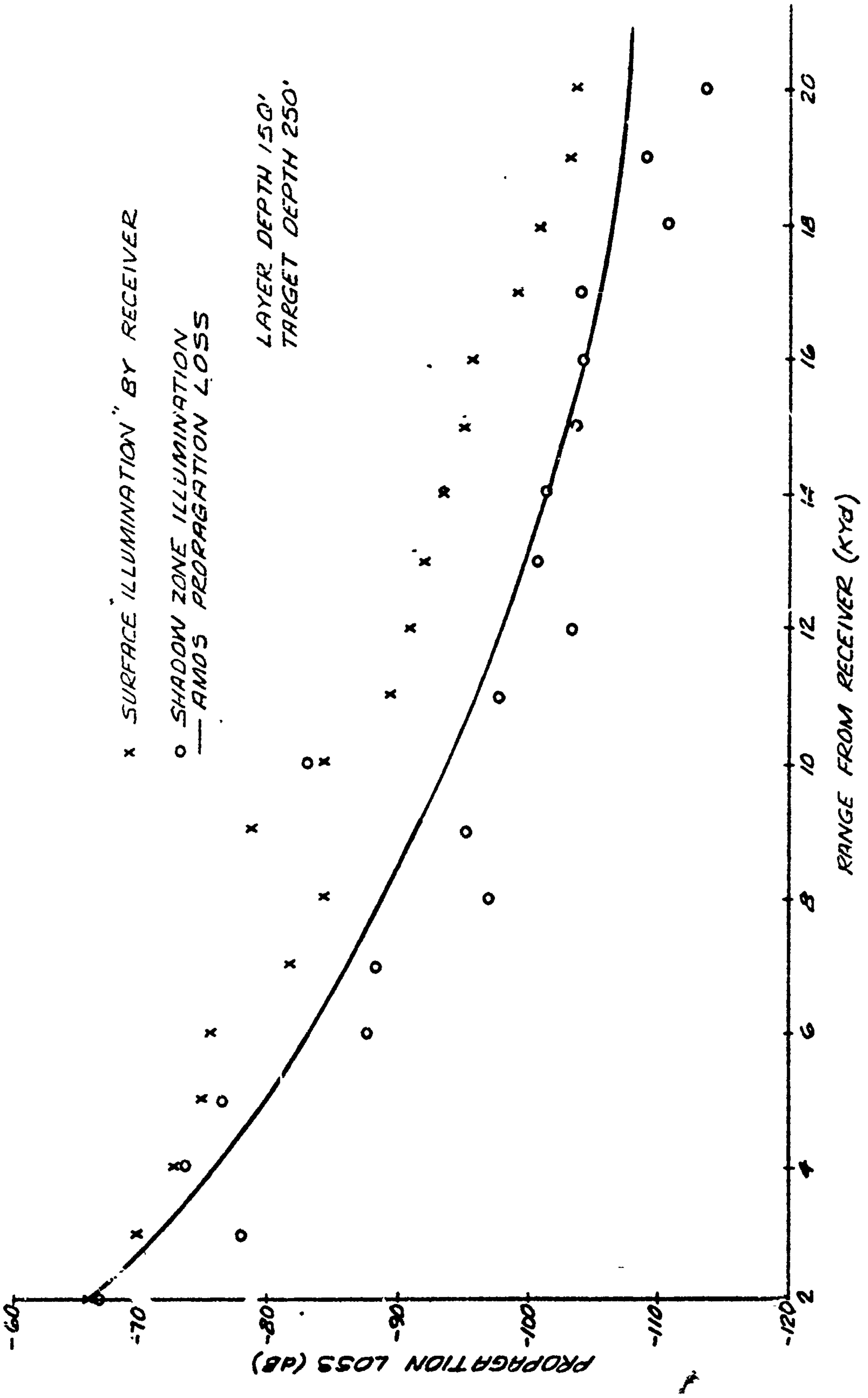
× SURFACE "ILLUMINATION" BY RECEIVER
○ SHADOW ZONE ILLUMINATION
— AMOS PROPAGATION LOSS
LAYER DEPTH 150'
TARGET DEPTH 250'
RANGE FROM RECEIVER (KYd)
2
4
6
8
10
12
14
16
18
20
PROPAGATION LOSS (dB)
-60
-70
-80
-90
-100
-110
-120

Figure 5

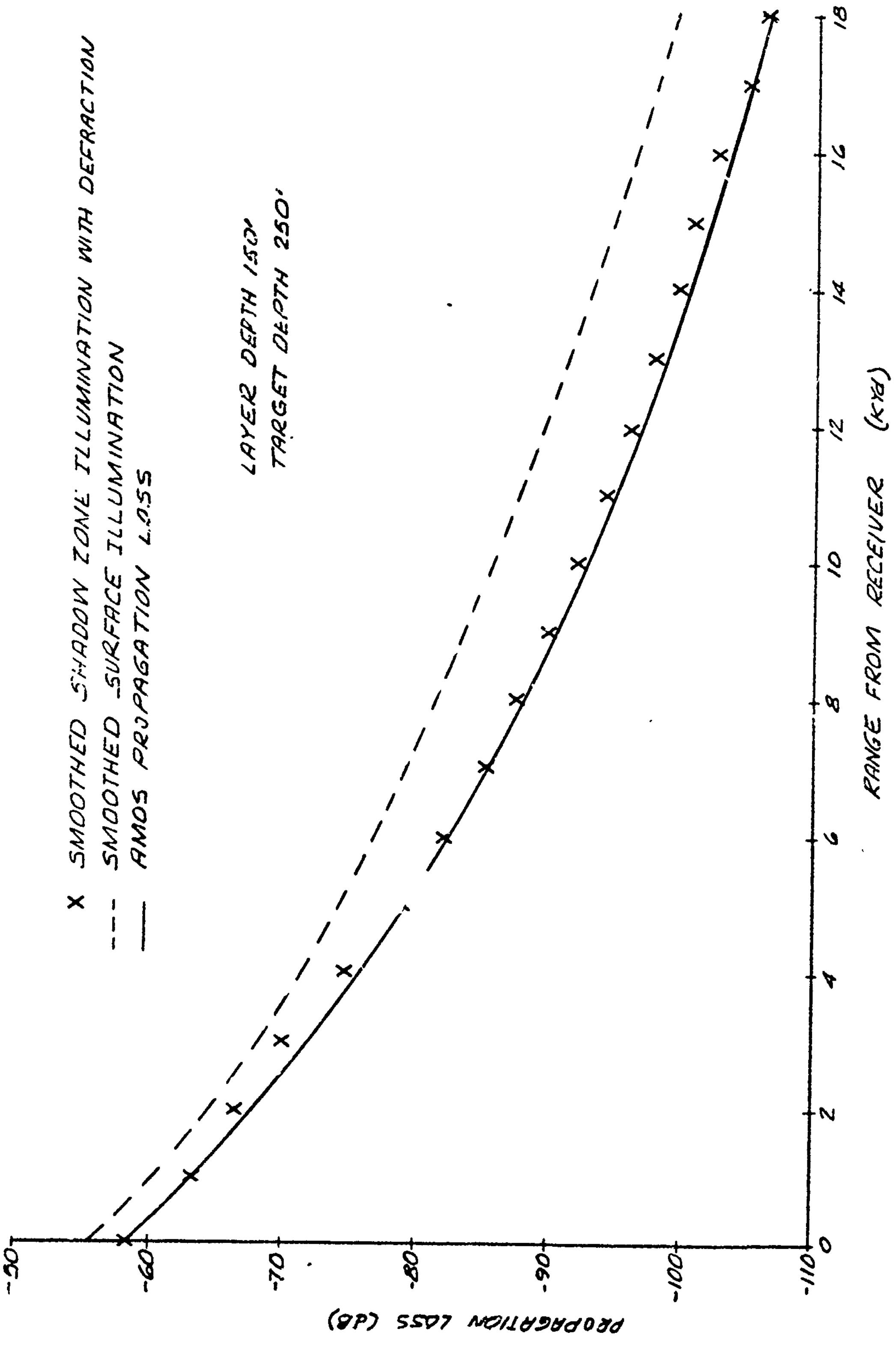
X SMOOTHED SHADOW ZONE ILLUMINATION WITH DEFRACTION
-- SMOOTHED SURFACE ILLUMINATION
— AMOS PROPAGATION LOSS
LAYER DEPTH 150'
TARGET DEPTH 250'
RANGE FROM RECEIVER (KYd)
PROPAGATION LOSS (dB)
0
2
4
6
8
10
12
14
16
18
-50
-60
-70
-80
-90
-100
-110

(U) Reversing the roles of receiver and target from those shown in Figure 3 will lead to entirely different results if the receiver is directional since most of the energy comes down from the surface at rather steep angles. This fact is important in the placement of vertically directional sonobuoys in environments where shadow zones exist.

(U) Another point of interest is the fact that if much of the energy arriving at a target in a shadow zone comes from above , then corrections should be made to the concept of target strength in these situations.

E. CONCLUSIONS

(U) A unified technique of applying scattering theory to shadow zone propagation and surface reflection has given results which agree with measured data but are much more widely applicable. The results are encouraging enough to merit further study, particularly in terms of experiments to measure the time spreading of surface reflections, the actual reflection coefficients calculated and the influence of the theory on target strength.

REFERENCES (U)

1. P. Beckmann and A. Spizzichino, "The Scattering of Electromagnetic Waves from Rough Surfaces," MacMillan Company, New York (1963).

2. H. Medwin, "Specular Scattering of Underwater Sound from a Wind Driven Surface," Journal of the Acoustical Society of America, Vol. 41, No. 6, (1967).

3. H. Medwin, "The Rough Surface and Bubble Effect on Sound Propagation in a Surface Duct," 28th Navy Symposium on Underwater Acoustics, November 17-18, 1970.

4. C. Cox and W. Munk, "Measurement of the Roughness of the Sea Surface from Photographs of the Sun's Glitter," J. Opt. Soc. Am., 44, 838-850, (1954).

5. G.R. Garrison, S.R. Murphy and D.S. Potter, "Measurements of the Backscattering of Underwater Sound from the a Surface," J. of the Acoust. Soc. of Am., Vol 32, No. 1, (1950).

6. B.J. Schweitzer, "Sound Scattering into the Shadow Zone below an Isomthermal Layer," J. of the Acoust. Soc. of Am., Vol. 44, No. 2, (1968).

7. W.J. Noble, "Theory of the Shadow Zone Diffraction of Underwater Sound," J. of the Acoust. Soc. of Am., Vol. 28, No. 6, (1956).

Hazeltine
Corporation

Appendix C (C)

DISTRIBUTION LIST

DISTRIBUTION LIST FOR
"OPERATIONS ANALYSIS OF A MULTISTATIC ECHO RANGING SYSTEM"

	No. of Copies
Director Defense Research and Engineering Department of Defense Washington, D.C. 20301	1
Assistant Secretary of Defense (Systems Analysis) Department of Defense Washington, D.C. 20350	1
Joint Chiefs of Staff Studies, Analyses, and Gaming Agency Washington, D.C. 20301	1
Assistant Secretary of the Navy (Research & Development) Department of the Navy Washington, D.C. 20350	1
Chief of Naval Research Department of the Navy Arlington, Virginia 22217	
(Code 461)	1
(Code 462)	2
(Code 466)	1
Chief of Naval Operations Department of the Navy Washington, D.C. 20350	
(Op-02)	1
(Op-03)	1
(Op-32)	1
(Op-05)	1
(Op-95)	1
(Op-952C)	1
(Op-96)	1

	No. of Copies
Chief of Naval Material Washington, D.C. 20360	
(Code ASW-141)	1
(Code ASW-142)	1
(Code ASW-22)	1
(Code NAIR-5031C)	1
(Code NAIR-APC256A)	1
(Code PM-15)	1
(Code PMS-380)	1
(Code EP-03)	1
COMASWFORLANT Norfolk, Virginia 23511	1
COMASWFORPAC FPO San Francisco 96601	1
COMASWFORSIXTHFLT FPO New York 09521	1
COMSUBDEVGRU 2 USN Submarine Base New London, Connecticut 06320	1
COMCRUDESLANT U.S. Naval Base Newport, Rhode Island 02840	1
COMCRUDESPAC FPO San Diego, California 92132	1
DESDEVGRU U.S. Naval Base Newport, Rhode Island 02840	2
(Mr. R. Johnson)	1
(Library)	1
COMFIRSTFLT FPO San Francisco 96601	1
Commanding Officer USS GLOVER (AGDE-1) FPO New York, New York 09501	1
Naval Academy Annapolis, Maryland 21402 (ATTN: Librarian)	1
Naval Postgraduate School Monterey, California 93940 (ATTN: Librarian)	1

Hazeltine
Corporation

	No. of Copies
Naval War College Newport, Rhode Island 02840 (Library)	2
Naval Research Laboratory Washington, D.C. 20390 (Code 7805)	1
(Code 2620)	2
Naval Air Development Center Johnsville, Pennsylvania 18974 (AETD)	1
(SDD)	1
(Library)	1
Naval Electronic Laboratory Center San Diego, California 92152 (Code 230)	1
(Library)	1
Naval Ship Research & Development Center Bethesda, Maryland 20034	1
Naval Undersea Research & Development Center San Diego, California 92152 (Dr. J. Stewart)	1
(Dr. G. Kinneson)	1
(Library)	1
Naval Underwater Systems Center New London Laboratory New London, Connecticut 06320	1
(Code 2130)	1
(Mr. J. Hanrahan)	1
Naval Underwater Systems Center Newport Laboratory Newport, Rhode Island 02840	1
Naval Weapons Center China Lake, California 93555 (Code 12)	1
(Library)	1
Naval Coastal Systems Laboratory Panama City, Florida 32402	1
Naval Ordnance Laboratory White Oak Silver Spring, Maryland 20910	1

	No. of Copies
Naval Weapons Laboratory Dahlgren, Virginia 22448 (ATTN: Library)	1
Applied Physics Laboratory John Hopkins University 8621 Georgia Avenue Silver Spring, Maryland 20904	1
Ketron, Incorporated 656 East Swedesford Road Wayne, Pennsylvania 19087 (Mr. J.D. Kettelie)	1
Arthur D. Little Acord Park Cambridge, Massachusetts 02139 (Dr. J.N. Dobbie)	1
Mathematics, Inc. 4905 DelRay Avenue Bethesda, Maryland 20014 (Dr. Saul Gass)	1
Operations Research, Inc. 1400 Spring Street Silver Spring, Maryland 20910 (Dr. E. Holmboe)	
Naval Warfare Research Center Menlo Park, California 94025 (Mr. Larry Low)	1
Tetra-Tech, Inc. 1911 Fort Myer Drive Arlington, Virginia 22209 (Mr. Klinkner)	1
Vector Research, Inc. P.O. Box 1506 Ann Arbor, Michigan 48106 (Dr. Seth Bonder)	1
Daniel H. Wagner Associates, Inc. Station Square One Paoli, Pennsylvania 19301	1
Institute for Defense Analyses 400 Army-Navy Drive Arlington, Virginia 22202	1
Defense Documentation Center Cameron Station Alexandria, Virginia 22314	2

(This page is unclassified)

Hazeltine
Corporation

	No. of Copies
NAVSEC Hyattsville, MD 20782 (Code 6112) (Mr. Dave Mandel)	1

(This page is unclassified)